Effect of Elevated Glucose on Primary Human Tenocytes and Implications for Diabetic Tendinopathy



Zuzana Kalivodova

Green Templeton College

Nuffield Department of Orthopaedics, Rheumatology and Musculoskeletal Sciences

University of Oxford

A thesis submitted for the degree of

Master of Science by Research in Musculoskeletal Sciences

Michaelmas Term 2016

In Loving Memory of

J.K.

1953 - 2015

Statement of length

This thesis contained 24,995 words at the time of printing; this is in compliance with Medical Sciences Graduate School directions [1].

[1] The thesis word limit for this research degree is 30,000 words, exclusive of bibliography, appendices, diagrams, tables and their legends/captions.

Acknowledgements

A large number of people helped me during my degree journey. I would like to thank all of them, and in particular to:

Assoc. Prof. Philippa Hulley for her continuous and neverending support and academic advice, patience, understanding, and for providing me with a sense of belonging to Botnar.

Assoc. Prof. Mark Thompson for making me feel welcome in his research group, and for his readiness to help whenever I needed.

Assoc. Prof. Afsie Sabokbar for being a great advisor when I needed to see some hope.

Prof. Donald Chambers for his regular scientific advice and constructive feedback.

Alison Franklin for being wonderful, and for listening to all of my worries.

Dr. Peter Cain for proof-reading the manuscript, for encouraging me along the way, for neverending help in the laboratory, and for being a fabulous friend in general.

Dr. Seint Lwin for helping me so much during my third year especially - your everyday presence in Botnar made a big difference to each of my days.

Dr. Kelly Rooke for the lovely chats we had, for our PhD room camaraderie, and our in-jokes about powerhouses. Kelly, you were missed greatly when you left.

Dr. Srinivasa Rao for being so knowledgeable about absolutely everything, and for being happy to share it. I wish I had your patience :-)

Dr. Ali Zarei for answering all of my very many questions, and never failing on helping me when I had an emergency experimental disaster.

Dr. Anneke Kramm for encouragement, inspiration, and the lovely times we had sitting side by side.

Dr. Maria Kuzma-Kuzniarska for all the assistance in the lab, and her friendly attitude.

NDORMS & Orthopaedic Research UK.

To ♡ Lucia ♡. You are my torch (I know that does not sound very romantic): held high, moving forward and showing me the road ahead, and that it's safe to walk on it. I said it before, and I will say it again and again: I want to marry you!

Ruby for all her love, and for motivating me and encouraging me all the way to the finish line (even 20 min before submission!). I could not have done this without you. Your presence lights up the PhD room & my world.

LaTeX wizard Wojtek for his never-ending support, love, understanding & patience. His LaTeX skills saved me every time there was an emergency crash.

Serena for all her love. You have inspired me so much, my dear. And also for all the coffee she has given me over the years (yes, we love the same brand). Just know I wear the butterfly necklace almost daily.

Mike for never failing when I needed his help - be it statistics or cheering up. Having you around Botnar was always a treat. And special thanks to a very special Christmas dinner.

Lenka for being a terrific graduate mentor to me from 'the other place', and for teaching me how to achieve my best 2k score ;-) I can't wait to live in the same country as you so we can finally catch up.

Siri for help first from Oxford, and then remotely. I have missed you in Oxford so much after you moved out. You are very special to me.

Martin M. for being a friend for a lifetime. I am so happy you are there. I will always be, too.

Charlie T. for being my fellow runner - those early morning were so worth it. I am still sad you moved to 'the other place'. GTC is not the same without you.

Charlotte K. for always keeping an eye on me even after she moved out of Oxford many years ago. I cannot wait to be reunited with you again! I have missed you so much.

Elizabeth for being my faithful library buddy. Together, we have been to so many Oxford libraries. I wish you only the very best, you deserve nothing less.

Chao for motivating me in our who-is-gonna-stay-later-in-the-PhD-office-tonight contest. We know who was winning most of the time ;-)

Anna M for all the love she has given me.

Mona for being a great advisor and mentor. You were so missed after you left Botnar.

My family: JK, MK, JM, MP & RP. Simply, for everything.

This thesis is dedicated to one specific person; they know who they are.

And finally, to all the baristas of Oxford that served me coffee; my favourite quote of all time is...

"You can do it." - coffee

Abstract

Diabetes mellitus (DM) is associated with a variety of musculoskeletal manifestations, including tendinopathy. The incidence of tendon disease in DM patients is increased compared to the general population, suggesting that tendon is a tissue sensitive to elevated blood glucose. Furthermore, it has been shown that chronic high blood glucose levels cause damage to cells in several ways, including increased oxidative stress. Therefore cellular responses of *in vitro* primary human tenocytes to a range of chronic glucose conditions (5, 17 and 30 mM) were investigated. Additionally, cells were also exposed to H_2O_2. Streptozotocin-induced type I diabetic (T1D) rats were used to evaluate *in vivo* changes.

First, tenocyte physiology exhibited changes in multiple aspects in response to elevated glucose concentration. Gene expression of collagen, asporin, biglycan and aggrecan was upregulated in 17 mM glucose condition. Data further indicated that SOD-2 was markedly increased in response to elevated glucose (12-fold increase in 17 mM glucose and 5-fold increase in 30 mM glucose, both compared to 5 mM glucose control). Immunohistochemistry on T1D rats indicated that skeletal muscle tissue was 3NT-positive to a high degree in diabetic condition compared to control.

Second, oxidative stress was induced in primary human tenocyes by H_2O_2 treatment. Extracellular glucose affected cellular response to H_2O_2: 1 mM H_2O_2-treated tenocytes in high glucose media had cell metabolic activity significantly decreased compared to identical H_2O_2 treatment in low glucose media. Furthermore, acute treatment with glucose identified that even short (72 h) bursts of elevated glucose can aggravate the response of cells to H_2O_2. A panel of protective agents was tested; N-acetylcysteine was the sole treatment that proved to be effective to a certain degree. Overall, negative effects of H_2O_2 were more pronounced under elevated glucose condition in primary human tenocytes. Findings of this thesis provide a necessary fundamental insight into diabetic tendon problems and may inform the development of new clinical treatments.

Contents

Abbreviations **iv**

1 Introduction **1**

1.1 Tendon biology . . . 2

1.1.1 Tendon structure . . . 2

1.1.2 Tendinopathy . . . 6

1.2 Diabetes mellitus . . . 9

1.2.1 Types of diabetes mellitus & treatment . . . 10

1.2.2 Glucose & its metabolic regulation . . . 11

1.2.3 Hyperglycemia . . . 11

1.3 Reactive oxygen species & oxidative stress . . . 13

1.3.1 What are reactive oxygen species & their significance . . . 13

1.3.2 Chemical structure of ROS . . . 13

1.3.3 ROS natural occurrence & its harmful effect . . . 13

1.3.4 Sites of ROS generation . . . 15

1.3.5 ROS defence mechanisms . . . 15

1.3.6 The role of ROS in hyperglycemia & DM . . . 15

1.4 Diabetes-associated musculoskeletal complications . . . 17

1.4.1 Diabetes-associated musculoskeletal complications in general . . . 17

1.4.2 Diabetic tendon . . . 19

1.5 Cellular senescence . . . 20

1.6 Aims of this project . . . 21

2 Materials & methods **23**

2.1 Human & animal samples . . . 23
2.2 Tendon cell culture . . . 24
2.3 Mannitol control of osmolarity . . . 25
2.4 Alamar Blue assay . . . 27
2.5 Chromogenic & fluorescence microscopy imaging . . . 27
2.6 Live/Dead cell viability assay . . . 27
2.7 EdU DNA incorporation assay . . . 28
2.8 TUNEL apoptosis assay . . . 28
2.9 RNA extraction . . . 28
2.10 cDNA synthesis & qPCR . . . 29
2.11 Soluble collagen Sircol assay . . . 30
2.12 Cell number determination . . . 30
2.13 Dimethylmethylene Blue assay . . . 32
2.14 Monolayer scratch assay . . . 32
2.15 Immunohistochemistry (IHC) staining . . . 33
2.16 Hydrogen peroxide (H_2O_2) treatment assay . . . 36
2.17 Protein isolation & Western blotting . . . 36
2.18 Statistical analysis . . . 38

3 Tendon cell and extracellular matrix phenotype in hyperglycemia **39**

3.1 Hypothesis & aims . . . 39
3.2 Experimental design . . . 40
3.3 Results . . . 41
3.3.1 Aim 1: to determine the effect of glucose concentration on tenocyte metabolism . . . 41
3.3.2 Aim 2: to determine the effect of glucose concentration on tenocyte total number and proliferation . . . 50
3.3.3 Aim 3: to explore the effect of glucose concentration on tenocyte senescence and death . . . 57
3.3.4 Aim 4: to determine the effect of glucose on tenocyte ECM synthesis and breakdown . . . 61

3.3.5 Aim 5: to determine the effect of glucose concentration on oxidative stress-responsive proteins in tenocytes . . . 66
3.3.6 Aim 6: to determine the effect of glucose concentration on cell migration & proliferation capacity of tenocytes . . . 68
3.3.7 Aim 7: to examine rat tail tissue for effects of STZ-induced uncontrolled T1D: Hematoxylin & Eosin stain highlights rat tail structures 72
3.3.8 Aim 7: to examine rat tail tissue for effects of STZ-induced uncontrolled T1D: 3-nitrotyrosine as indicator of nitroxidative stress . . . 75
3.3.9 Aim 7: to examine rat tail tissue for effects of STZ-induced uncontrolled T1D: evaluation of FOXO-1a levels in diabetic vs. healthy rats . . . 77
3.4 Discussion . . . 83

4 Effect of chronic glucose conditioning on hydrogen peroxide-induced oxidative stress response 88
4.1 Hypothesis & aims . . . 88
4.2 Experimental design . . . 89
4.3 Results . . . 90
4.3.1 Aim 1: to determine an appropriate H_2O_2 concentration range for experiments on tenocytes . . . 90
4.3.2 Aim 2: to assess the effect of glucose and acute H_2O_2 treatment on cell metabolic activity and viability . . . 93
4.3.3 Aim 3: to assess the effect of acute glucose and H_2O_2 treatment on tenocyte metabolic activity . . . 107
4.3.4 Aim 4: to quantify the effect of glucose and acute H_2O_2 on expression of selected genes . . . 109
4.3.5 Aim 5: to determine whether the glucose and H_2O_2-induced response can be attenuated by selected protective agents . . . 117
4.4 Discussion . . . 131

5 Discussion 138
5.1 Effect of glucose on tendon cells . . . 140
5.2 Effect of glucose on tendon ECM . . . 141

5.3 Oxidative stress 142
5.4 Animal model 143
5.5 Limitations of the study 143

Appendices **146**

A Conferences **147**

B Acquired training **149**

Bibliography **152**

List of abbreviations

3NT	3-nitrotyrosine
AA	ascorbic acid
ACAN	human aggrecan gene
ACTB	human β-actin gene
ADSCs	adipose-derived stem cells
AGEs	advanced glycation end products
ANOVA	analysis of variance
ASPN	human asporin gene
BCN	human biglycan gene
BMSCs	bone marrow stem cells
BrdU	5-bromodeoxyuridine
CAT	human catalase gene
CDKN1A	human cyclin dependent kinase inhibitor 1A gene, also known as P21
cDNA	complementary DNA
COL1A1	human collagen type I alpha 1 chain gene
COL1A2	human collagen type I alpha 2 chain gene
COL3A1	human collagen type III alpha 1 chain gene

CT	cycle threshold, in qPCR
Cu	copper
DAB	3,3'-diaminobenzidine
DAPI	4',6-diamidino-2-phenylindole
DCFDA	cellular reactive oxygen species detection assay
DCN	human decorin gene
ddH_2O	double-distilled H_2O
Dex	dexamethasone
DM	diabetes mellitus
DMB	dimethylmethylene blue
DMSO	dimethyl sulfoxide
DNA	deoxyribonucleic acid
DTT	dithiothreitol
E10	embryonic day 10 of development
ECM	extracellular matrix
EDTA	ethylenediaminetetraacetic acid
EdU	5-ethynyl-2'-deoxyuridine
ESWT	extracorporeal shock wave therapy
$FADH_2$	flavin adenine dinucleotide
FCS	fetal calf serum
FOXO	forkhead box O
FOXO1	human forkhead box O1 gene

GAG	glycosaminoglycan
H_2O_2	hydrogen peroxide
HRP	horseradish peroxidase
ICC	immunocytochemistry
IHC	immunohistochemistry
L/D	Live and dead cell stain
M	molar
MAP	mitogen-activated protein
mM	milli-molar
MMP	matrix metalloproteinase
MMP2	human matrix metalloproteinase 2 gene
Mn	manganese
mRNA	messenger ribonucleic acid
MSK	musculoskeletal
MTJ	myotendinous junction
n, *N*	number
NAC	N-acetylcysteine
NADH	reduced nicotinamide adenine dinucleotide
NaF	sodium fluoride
NFKB	nuclear factor kappa B
ns	not significant, in statistics
NSAIDs	non-steroidal anti-inflammatory drugs

OS	oxidative stress
OTJ	osteotendinous junction
PBS	phosphate-buffered saline
PG	proteoglycan
pH	power of hydrogen
PMSF	phenylmethanesulfonyl fluoride
PRP	platelet rich plasma
qPCR	quantitative polymerase chain reaction
RAGE	receptor for advanced glycation end products
RNA	ribonucleic acid
RNS	reactive nitrogen species
ROI	region of interest
ROS	reactive oxygen species
RT	reverse transcriptase
SD	standard deviation
SDS-PAGE	Sodium Dodecyl Sulfate PolyAcrylamide Gel Electrophoresis
SEM	standard error of the mean
SOD1	human superoxide dismutase 1 soluble gene
SOD2	human superoxide dismutase 2 mitochondrial gene
SOD3	human superoxide dismutase 3 extracellular gene
STZ	streptozotocin
T1D	type 1 diabetes mellitus

T2D	type 2 diabetes mellitus
TCA	tricarboxylic acid
TIMP	tissue inhibitor of metalloproteinase
TRS	target retrieval solution
TSCs	tendon stem cells
TUNEL	terminal deoxynucleotidyl transferase mediated deoxyuridine triphosphate nick end labeling
μM	micro-molar
UPR	unfolded protein response
WB	Western blot
Zn	zinc

1 Introduction

Diabetes mellitus (DM) has adverse effects on connective tissues (1), and has been associated with a variety of musculoskeletal (MSK) manifestations including tendinopathy (2). The incidence of tendon disease in DM patients is increased compared to the general population (2), suggesting that tendon is sensitive to high blood glucose. The most commonly affected body parts are the upper limbs, especially hand and shoulder (3), e.g. frozen shoulder and Dupuytrens contracture, among other. Diabetic tendons of the foot cause altered gait and have much greater risk of injury, foot ulcers and amputation. Diabetic tendinopathy aetiology has not yet been fully explained; the majority of available research is limited to acute glucose exposure and animal tissues. We know it is complex with various factors such as advanced glycation end products (AGEs), reactive oxygen species, inflammation, genetics and epigenetics (4). It has been shown that chronic high blood glucose levels cause damage to cells in several ways, including increased oxidative stress (5). Therefore I investigated the cellular responses to a range of chronic glucose conditions and to exposure of H_2O_2 in primary human tenocytes. This will provide a necessary fundamental insight into diabetic tendon problems as well as inform the development of new clinical treatments.

1.1 Tendon biology

Tendon is a highly organized fibrous connective tissue. Its primary function is to transmit tensile load from skeletal muscle to bone and in this way enable joint movement of the MSK system (6, 7, 8, 9, 10). CITE Tendon is also a joint stabilizer and a shock absorber, and in this manner can limit potential damage to muscle. The tissue is well adapted and specialized to resist high tensile forces (6). The classical view of tendon tissue and its extracellular matrix (ECM) has labelled it as inert and static, with 'low' metabolism as tendons are not vascularized to a high degree compared to other tissue types. However more recently tendon has been shown to be metabolically active and well responsive to external stimuli; it responds to mechanical loading by both structural and functional adaptation. Therefore it is now suggested that tendon is a lively structure with dynamic protein turnover and capacity to adapt greatly, whether to activity or inactivity (6).

1.1.1 Tendon structure

Approximately 55-70% of tendon is water, while the remaining percentage of the tissue (dry matter) is the collagenous and non-collagenous matrix. The most important type of collagen that is found in tendon is collagen type I, but other types are present (collagen II, III, IV and V)(11). Collagen is arranged within the tissue in a longitudinal manner (in parallel to its long axis) and is grouped as fibrils, fibers, fascicles and tendon itself (figure 1.1). Spaces between these hierarchical levels are filled with a small amount of non-collagenous matrix (12). A membrane called epitenon is surrounding the tendon (13). The non-collagenous matrix is a mixture of glycoproteins and other smaller molecules. Blood supply of tendons is mainly from muscle, and is divided into three regions (myotendinous junction, osteotendinous junction, paratenon/synovial sheath)(6, 14). Plexuses of nerve fibres can be found in paratenon; their branches penetrate the epitenon. The majority of the fibres do not penetrate the main tendon body, however instead terminate on its surface. Mechanoreceptors and nociceptors are both present to detect pressure, tension and pain (13, 15).

The two most important components of tendon tissue are tendon cells and the ECM. **Cellular composition** of tendon is comprised of tenoblasts and tenocytes (90-95% of the total cell population) and of other cell types such as chondrocytes, synovial cells, vascular

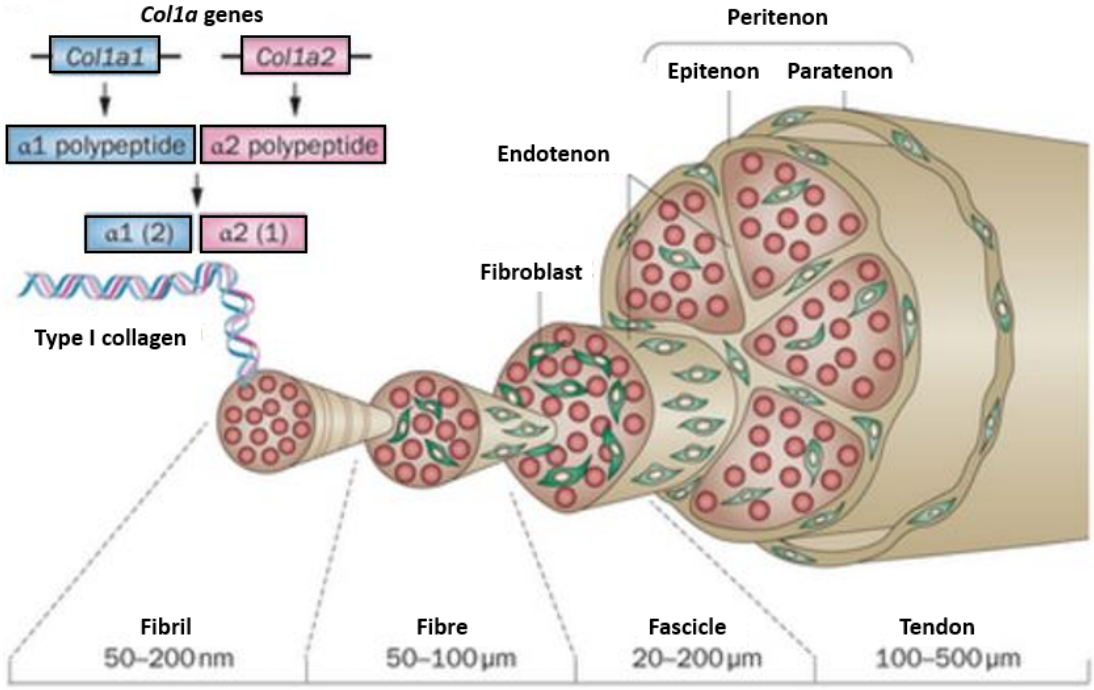

Figure 1.1: Tendon architecture. Adapted from (16).

endothelial cells and smooth muscle cells (the remaining 5-10%)(9, 13). In general, cells in tendon tissue are relatively sparse and occupy only a small proportion of it (11). The tenoblasts and tenocytes are specialized elongated fibroblasts that lie between the longitudinally arranged collagen fibres. Tenoblasts are immature tendon cells with high metabolic activity, i.e. they exhibit intense ECM synthesis (17). The size of a typical tenoblast is about 20-70 μm in length and 8-20 μm in width. Tenocytes are mature tendon cells with large cytoplasmic extensions which connect adjacent cells via gap junctions both longitudinally and laterally throughout the tissue (6, 18). Their elongated shape is spindle-like and often measures 80-300 μm in diameter (13). Tenocytes have a key role in both the biosynthesis of all ECM components and in homeostasis, adaptation and remodelling of the ECM (10, 13, 15, 17).

The extracellular matrix is a complex well-organized 3D structure that is exclusively secreted by the resident cells. The main function of the ECM is to provide physical support (is acts as a lattice for cell migration and proliferation) along with biochemical signals to the surrounding cells and tissue (19). The tissue integrity relies on the structural and mechanical integrity of the ECM network and its timely remodelling. The tendon ECM is predominantly composed of collagen, with collagen type I being the most

prevalent at about 95% (10, 20). Other types of collagen (types III, V, XI, XII and XIV) are present (10, 19, 21). Collagen type I is a heterotrimeric macromolecule composed of 3 polypeptide chains. Genes *col1a1* and *col1a2* produce pro-alpha1(I) and pro-alpha2(I) chains, respectively (6). These chains fold and assemble into a triple helical pro-collagen molecule which contains two alpha1(I) chains and one alpha2(I) chain (figure 1.2) (6, 22). The pro-collagen molecule is then secreted from the cell and assembles into collagen fibrils (figure 1.1).

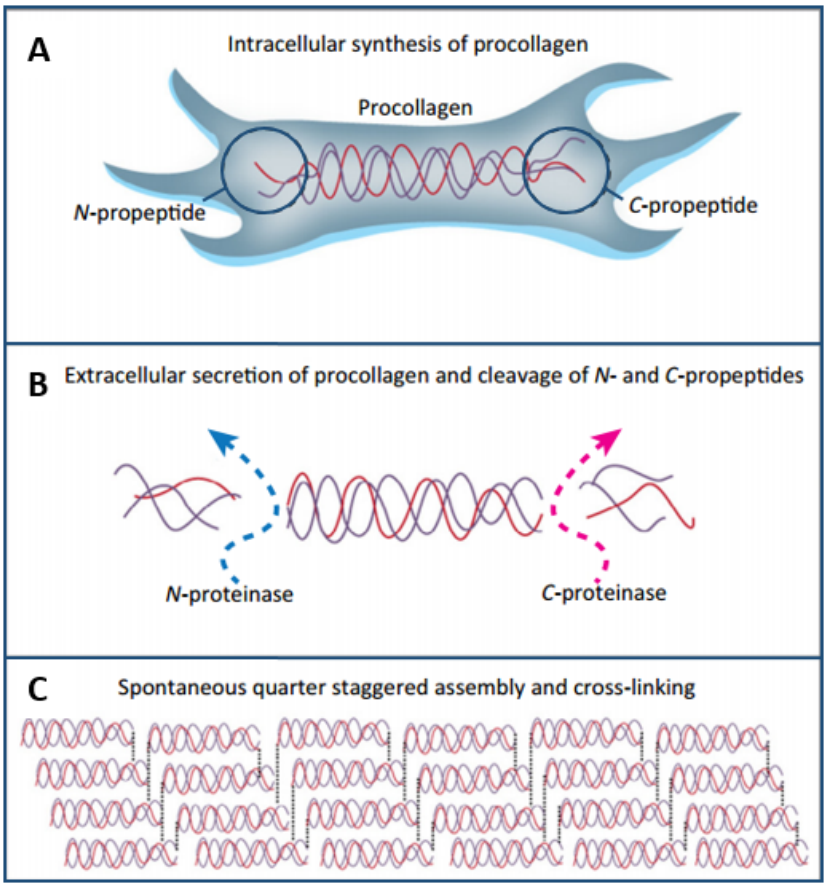

Figure 1.2: Collagen secretion and assembly. Collagen synthesis follows the regular pathway of secreted proteins. A) First, long precursors termed procollagens are formed. These consists of a 300-nm-long triple-helical structure which is flanked by a C-propeptide domain and a N-propeptide domain. Disulfide bonds in the sequence align the three chains; B) After the assembly of procollagen, it is secreted from the cell into the extracellular space by exocytosis. At this stage, procollagen peptidases cleave the N-terminal and C-terminal propeptides. The remaining protein is now termed tropocollagen; C) Collagen molecules spontaneously self-assemble into characteristic "quarter-staggered" fibrils. These fibrils are stabilized by covalent cross-linking (14, 23). Adapted from (19).

Furthermore, another overall component of the ECM is ground substance which is

a complex mixture of glycosaminoglycans, glycoproteins, proteoglycans, and other small molecules (13, 14). **Glycosaminoglycans (GAGs)** are molecules of long non-branched mucopolysaccharides that contain a repeating disaccharide regions of uronic acid and an amino sugar (24). They are located either on cell surface or in the ECM. Examples of the most physiologically important GAGs are hyaluronic acid, dermatan sulfate, chondroitin sulfate, heparin, heparan sulfate, and keratan sulfate. The majority of GAGs are linked to protein, thus forming a **proteoglycan (PG)**. The GAGs extend from the core structure in a brush-like manner. Most mammalian cells, including tenocytes, have the ability to synthesize PGs and to secrete them into the ECM, insert them into the plasma membrane or to store them in vesicles. The PGs in the ECM interact with other ECM components and help to maintain joint-fluid viscosity and thus provide resistance to compressive forces. Some PGs contain only one GAG chain (e.g. decorin), whereas others can have several hundred GAG chains (e.g. aggrecan)(6, 10, 25). GAGs can be classified in several ways but the most common is their degree of sulfation (24).

Extracellular degradation by **matrix metalloproteinases (MMPs)** is the primary mechanism in tendon to maintain, adapt, remodel and repair the tissue (11). A smaller proportion of degradation is achieved intracellularly by phagocytosis of matrix molecules. ECM degradation is part of normal physiological homeonstasis. MMPs are endogenous peptidases that digest collagen and other structural components of the ECM (9, 26, 27). ECM turnover needs to be executed in a timely and precise fashion. Therefore under normal physiological conditions MMPs are tightly regulated (28, 29). Inappropriate MMP upregulation can lead to alterations of normal ECM architecture which may ultimately hinder proper tissue functionality and may contribute to diseases such as arthritis, tumour cell metastasis and atherosclerosis (27, 30). MMPs are secreted as inactive zymogen precursors which are catalytically activated by cleavage (31). Endogenous inhibitors also play a role in MMP regulation: tissue inhibitors of matrix metalloproteinases (TIMPs) are the most significant (29, 32). The role of MMPs in tendinopathy has been long considered, and their dysregulation is one of the leading hypotheses of tendon pathology (33).

1.1.2 Tendinopathy

Tendon disease and injury is termed tendinopathy; technically it refers to a broad range of clinical tendon disorders (10). Tendinopathy accounts for about 30% - 50% of all MSK consultations (34, 35), is often under-reported, and is most common in athletes, manual workers and older individuals. It may render movement chronically painful and may lead to restricted range of motion, thus causing disability with socio-economic consequences (8, 36). Tendon injury can happen at any tendon, but the most common problems are: Achilles tendinopathy, patellar tendinopathy, tennis elbow, golfer's elbow, supraspinatus tendinopathy and chronic tendon pain (37). On the tissue level, tendinopathy often includes matrix degradation, neovascularisation and swelling (10).

Tendinopathy risk factors

The pathogenesis of tendinopathy is not fully understood (13). One of the main risk factors for tendon disease is age (35, 38); an association has been clearly revealed by epidemiological studies. It is generally assumed that native tendon properties decline with age, as tendon is a very common site of pain and discomfort in the older population group. A favoured hypothesis of aged tendon is that with age there is an imbalance between anabolism and catabolism (38, 39), in favor of catabolism. Another piece of the puzzle may be 'inflamm-aging' (35, 40) meaning a chronic molecular inflammation with elevated inflammatory cytokines. It has been for long accepted that increased inflammation does not play a contributing role in initiation of tendinopathy (41) however this view has been recently increasingly challenged (35, 42). Transcriptome analysis of a healthy aged human Achilles tendon revealed that genes that are differentially expressed in ageing are those associated with cellular function and growth (21). Therefore it is thought that cells in aged tendon loose their ability to respond correctly to mechanical and chemical cues (21). Some believe that tendinopathy (or its initiation) is the result of tissue overload, overuse, repetitive strain or microtrauma (10, 43). It is also hypothesized that the formation of collagen cross-links as the tissue progressively ages contributes to tissue stiffness and therefore an increased risk of tendinopathy. Prevention and treatment of tendinopathy remain important goals in musculoskeletal medicine.

Tendon healing

Tendon healing is a complex cascade of sequential but also overlapping stages that can altogether last more than a year (8, 13, 34, 44, 45). First, during inflammatory stage inflammatory cells migrate to the site of injury and phagocyte necrotic tissue. During the proliferative or repair stage, fibroblasts synthesize new ECM that is randomly organized at this stage. Functional repair and regeneration of tendon tissue requires the last, remodeling, phase (8). It is currently not exactly clear whether tendon healing is mediated by external cells that migrate to the site of injury from the surrounding sheath and synovium, or by the proliferation of resident remaining tenocytes. The accepted paradigm is that it can be mediated both intrinsically and extrinsically (13, 19, 37). It is well recognized that the tissue appears scar-like after healing, and that the mechanical properties of healed tendon never completely regain its native state prior to injury (8, 13, 34, 35, 36, 46).

Current tendinopathy treatments & management

The current therapies are numerous, but very few of them are truly effective or evidence-based as tendon diseases often respond poorly to treatment. As the precise mechanism behind tendinopathy is currently unknown, we are treating more of a consequence rather than a cause (6, 35). Latest research is focused on the development of biologics delivery and stem cell based therapy (16, 47). Perhaps the combination of pharmaceutical approaches and scaffold or tissue graft therapies will offer improved outcomes. The current most common therapies include:

- *Physical therapy*: usually involves stretching and strenghtening components. Can also involve eccentric strengthening protocols which might help restoring normal tissue structure. Controlled eccentric motion therapy is the treatment of choice especially for tendinopathy in the patellar, Achilles, and rotator cuff tendons (16). However overall there is mixed evidence of success to support eccentric exercise therapy (6, 9, 34, 48).

- *Local corticosteroid injections*: very common. They reduce inflammation and control pain short-term (i.e. under 6 weeks), however their long-term efficiency remains controversial as ruptures after injections have been reported (9, 34, 35, 48).

- *Non-steroidal anti-inflammatory drugs (NSAIDs)*: oral medication that treats pain and reduces inflammation. There is no evidence that these are effective long-term. Moreover, their long-term use is not recommended as there are too many complications associted with them (6, 9, 34, 48).

- *Surgical treatment*: tendon ruptures and lacerations are sutured together and this therapeutic modality remains the gold standard in clinics (6, 34). However re-tear rates are as high as 94%; some of the hypotheses behind re-tears include advanced patient age, muscle atrophy, fatty infiltration, smoking and large size of the original tear (35, 49).

- *Extracorporeal shock wave therapy (ESWT)*: consists of delivering several low-energy shock waves directly into the painful area in order to reduce pain. We currently do not understand the mechanism: perhaps there is stimulation of neovascularization or tenocytes release growth factors in response to shock waves and this in turns facilitates tendon healing. Mixed success outcomes remain (9, 34, 48).

- *Platelet-rich plasma injections*: have been introduced into clinical practice to treat tendinopathy and acute tendon injury. The injections have 3-4 higher concentration of platelets and contain growth factors. These exogenous growth factors promote matrix synthesis and tissue repair (9, 48). However platelet-rich plasma usage showed mixed success outcomes (35, 36).

- *Stem cell therapy*: this includes mesenchymal stem cells, bone marrow stem cells cells, adipose-derived stem cells and tendon stem cells to promote tendon healing (50). They have excellent promise but more research is required. For example, currently no study in large animal models have been done with tendon stem cells (51). Stem cells could be used in conjunction with scaffolds (as long as there is good cell-scaffold interaction) (34, 52).

- *Scaffolds*: are patches for tendon repair; they serve to reinforce the strength of the repaired area (very popular with rotator cuff repair, for example). They can also be used as a vehicle for delivery of cells and growth factors (34, 36). They are either natural or biodegradable synthetic (46, 52); both of these categories reported

an increase ECM deposition compared to controls (52). Nanoarchitecture of the scaffold important for ECM deposition (8, 50) hence choice of material and its processing technique remain important.

Other current therapies include immobilization, gene therapy, cryotherapy, heat treatment, low-level laser therapy, and therapeutic ultrasound (8, 9, 34).

1.2 Diabetes mellitus

Diabetes mellitus (DM) is an endocrine disorder characterized by sustained high blood glucose levels. Incidence of T2D has been sharply rising in the last decades (53), and this trend is also predicted for the future. Globally, 415 million adults (of which 60 million in Europe) between the ages of 20 and 70 have been estimated to suffer from diabetes in 2015 (54). In the UK alone, there are currently 3.5 million people diagnosed with diabetes and an estimated 549,000 people undiagnozed (55). Actually, it is estimated that 1 in 2 adults worldwide with T2D are undiagnosed (54). In the surveys, diabetes is defined as having a fasting plasma glucose level equal to or greater than 7.0 mM, or being on medication for diabetes or raised blood glucose (56). Blood glucose levels chronically exceeding 7 mM can cause damage to internal organs, however with T2D it can take years to manifest symptoms. This raises the point that elevated levels of plasma glucose circulating in the body may cause progressive cumulative damage which might be irreversible. Early intervention with tight glucose control is therefore of paramount importance. Diabetes erodes quality of life of the patient and with time causes major health complications. DM increases the risk of cardiovascular disease 3- to 8-fold (57) leading to heart attacks and strokes, as well as being the leading cause of blindness, renal failure and lower limb amputation (4, 56, 58). Risk factors for T2D include age, genetics, obesity, sedentary lifestyle, high blood pressure, high cholesterol, high fat diet and notably high saccharide diet. Once DM develops in the body the amount of glucose in the blood will remain too high because the body cannot use it properly. Epidemiological and experimental studies suggest that it is the glucose *per se* that is the main contributing factor in the development of diabetic complications (59, 60). Last but not least, DM places a severe economic burden on society: in 2012 the UK spent approximately 10% of the NHS budget

on DM (61), and in 2015 approximately 12% percent of global health expenditure was spent on DM (62).

1.2.1 Types of diabetes mellitus & treatment

Type 1 diabetes mellitus (T1D)

T1D accounts for about 5-10% of all diabetic cases, and is characterized as pancreatic dysfunction where insulin-producing pancreatic islet β-cells are progressively destroyed by the immune system. Eventually this leads to a partial or absolute insulin deficiency and patients must therefore take exogenous insulin as part of therapy (63). This is the diabetes type that is currently prevalent in children. This type of diabetes has a genetic predisposition with a complex genetic pattern.

Type 2 diabetes mellitus (T2D)

T2D is a multifactorial metabolic disorder that accounts for the remaining 90-95% of diabetes cases. Cells develop insulin resistance and become unable to manage glucose load due to chronic exposure to hyperglycemia; patients may require to take additional insulin because of resulting islet burn-out. T2D progresses for a while before symptoms can be seen, and hence it is generally diagnozed later than T1D. Patients may have had mild T2D or glucose intolerance for some time before being diagnozed clinically (64, 65). Data confirms that risk of diabetic complications commences many years before the onset of clinical diabetes. T2D is strongly associated with sedentary lifestyle and obesity, and accounts for the wordwide diabetes epidemic, in both developed and developing nations. T2D is also increasingly common in children.

Current diabetic treatments

The most effective treatment for diabetes has been proven to be a combination of approaches: therapeutics (insulin and oral hypoglycemic drugs), exercise regimen and a balanced low-glucose diet. The oral hypoglycemic drugs that are used to treat T2D are for example sulfonylureas, metformin, thiazolidinediones and alpha-glucosidase inhibitors. Depending on the class, they either stimulate insulin secretion, increase insulin action, act on tissues to increase glucose uptake, or slow down the absorption of glucose. With DM, prevention is more important than cure; it is believed that change of dietary habits and physical activity will help to decrease the wordwide incidence of diabetes (64).

1.2.2 Glucose & its metabolic regulation

Glucose is a six-carbon monosaccharide that is the primary metabolic fuel of most cells in both unicellular and multicellular organisms. The large glucose polymers, glycogen and starch, are used to store energy in animal cells and plant cells, respectively. Insulin activates glucose uptake by binding to its transmembrane receptor and signaling for glucose transporter proteins (GLUTs) to be inserted into the cell membrane. Glucose is transported into the cell once it binds to GLUT proteins. Glucose uptake can therefore be limited by abundance of GLUTs as well as by sensitivity of the insulin signaling pathway. Once glucose gets into the cell, it is oxidized (figure 1.3). Glucose is a source of ATP generation; ATP transports energy within cells.

1.2.3 Hyperglycemia

Hyperglycemia, also termed impaired glucose tolerance, is a sustained increase in blood (plasma) glucose level. By definition, hyperglycemia is when glucose values are between intermediate normal and diabetic following a glucose load. If hyperglycemia is prolonged it can lead to many health complications, including DM (68). Hyperglycemia seems to cause more damage in some tissues of the body than in other: it is in particular the retinal tissue, neural tissue (leading to loss of peripheral sensation), kidney tissue (leading to end-stage renal failure via glomerular hyperfiltration) and vascular tissue that are severely affected by hyperglycemia (69). One of the most vulnerable tissues to hyperglycemia (and hence widely studied) is vascular endothelium. One of the current hypotheses is that cells that are most damaged from hyperglycemia do not downregulate their glucose transport rate across the cell membrane flexibly enough: if glucose is high extracellularly, it will also be high intracellularly. In contrast, cells that resist hyperglycemic damage better seem to be able to downregulate their glucose uptake (57). Furthermore, in the tissues that become damaged from hyperglycemia there are primarily two mechanisms how glucose exerts its negative effect. First, by the toxic effect of hyperglycemia derivatives (AGEs, and since hyperglycemia induces mitochondrial superoxide production therefore also intracellular ROS (59)). Second, by sustained alterations in cellular signaling pathways. Overall, diabetes-associated complications are the main cause of both diabetic morbidity and mortality worldwide.

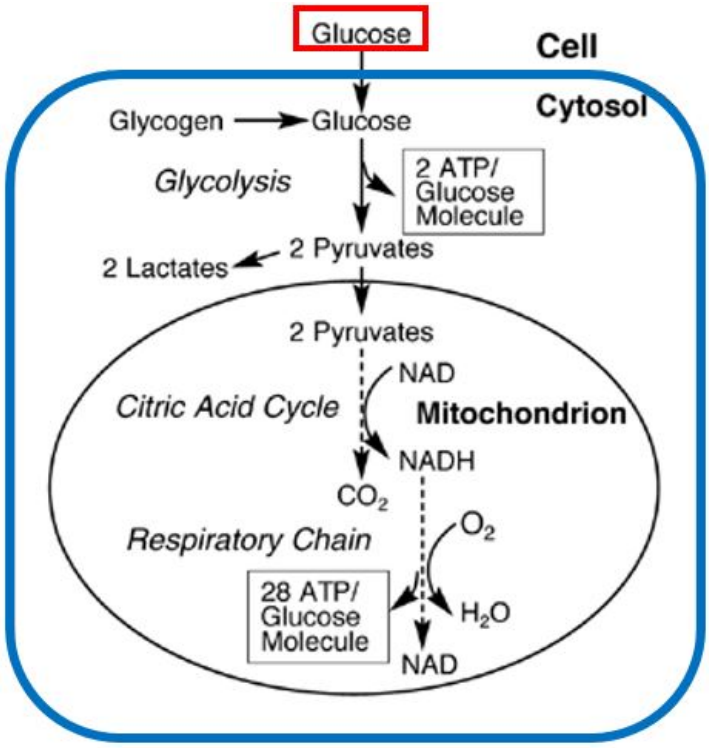

Figure 1.3: Overview of glucose metabolism. Extracellular glucose enters the cell from the blood stream or, alternatively, glycogen that is already present in the cell is broken down. Glucose oxidation begins with glycolysis that takes place in the cytosol, and the end results are pyruvate, reduced nicotinamide adenine dinucleotide (NADH) and 2 molecules of ATP (not all in figure). Based on the intracellular oxygen conditions, cytosolic NADH can then donate reducing equivalents to the respiratory chain or it can reduce pyruvate to lactate (which will serve as a substrate for hepatic gluconeogenesis). Pyruvate can be transported into mitochondria for oxidization in the tricarboxylic acid (TCA) cycle, also termed citric acid cycle. This produces CO_2, H_2O, 4x NADH and flavin adenine dinucleotide ($FADH_2$)(not all in figure). These NADH and $FADH_2$ provide energy for ATP generation through oxidative phosphorylation by the respiratory chain, also termed the mitochondrial electron transport chain. The respiratory chain, that electrons flow through, is composed of 4 inner-membrane-associated enzyme complexes, cytochrome c and ubiquinone (not in figure)(5, 66). In this system, electrons are donated from NADH and are passed through the enzyme complexes in the chain. As a result, H_2O and additional molecules of ATP are generated using the energy that was released through the successive electron transfers. The respiratory chain yields more ATP molecules than glycolysis alone (28 ATP molecules per one glucose molecule). Adapted from (67).

1.3 Reactive oxygen species & oxidative stress

1.3.1 What are reactive oxygen species & their significance

Reactive oxygen species (ROS) are produced as a natural by-product of the mitochondrial electron transport chain under aerobic conditions. They are cleared out by the organism to a large extend, but certain acummulation is inevitable. This is also the basis of the oxidative stress aging theory, proposed by Denham Harman in 1957 where he proposed that due to oxygen metabolism ROS are generated and are responsible for aging and age-related diseases (70, 71, 72, 73). Physiological concentrations of ROS are beneficial as they involve cell signaling pathways and survival from invading pathogens. Pathological oxidative stress (OS) is caused when the balance between formation of reactive oxygen and nitrogen species (table 1.1 identifies some of the most common ones) and their removal is disturbed (74). An elevated, unbalanced ROS concentration is thought to contribute to the development of many chronic or late-onset diseases such as diabetes, cancer, hypertension, atherosclerosis, inflammation, asthma, Alzheimer's disease, systemic lupus erythematosus, rheumatoid arthritis and premature aging (75).

1.3.2 Chemical structure of ROS

Reactive oxygen species are metabolites of molecular oxygen (figure 1.4). Common ROS include hydrogen peroxide, hydroxyl radical, hypochlorous acid, nitric oxide, peroxyl radical, peroxynitrite anion, singlet oxygen and superoxide anion. Hydrogen peroxide (H_2O_2) is used in this project; it is freely diffusible and relatively long-lived, and is a central player in stress signal transduction pathways.

1.3.3 ROS natural occurrence & its harmful effect

There is a growing evidence that many ROS are regulatory agents in a range of biological functions, such as signaling (78, 79). Therefore not all free radicals are 'bad'. However, overproduction or insufficient removal of ROS may result in inappropriate oxidation of macromolecules and cell structures such as proteins, membrane lipids and nucleic acids, potentially causing their dysfunctionality (68, 80, 81). In this way, OS can compromise cell viability and even trigger apoptosis (82, 83). Furthermore, OS can also lead to

Nomenclature of reactive species	
Free radicals	*Nonradicals*
Reactive oxygen species (ROS)	
Superoxide, $O_2^{\bullet -}$	Hydrogen peroxide, H_2O_2
Hydroxyl, $OH^{\bullet}$	Hypobromous acid, HOBr
Hydroperoxyl, $HO_2^{\bullet}$	Hypochlorous acid, HOCl
	Ozone O_3
Peroxyl, $RO_2^{\bullet}$	Singlet oxygen ($O_2^1\Delta g$)
Alkoxyl, $RO^{\bullet}$	Organic peroxides, ROOH
Carbonate, $CO_3^{\bullet -}$	Peroxynitrite, ONOO
Carbon dioxide, $CO_2^{\bullet -}$	Peroxynitrous acid, ONOOH
Reactive chlorine species (RCS)	
Atomic chlorine, $Cl^{\bullet}$	Hypochlorous acid, HOCl
	Nitryl (nitronium) chloride, NO_2Cl
	Chloramines
	Chlorine gas (Cl_2)
Reactive nitrogen species (RNS)	
Nitric oxide, $NO^{\bullet}$	Nitrous acid, HNO_2
Nitrogen dioxide, $NO_2^{\bullet}$	Nitrosyl cation, NO^+
	Nitroxyl anion, NO^-
	Dinitrogen tetroxide, N_2O_4
	Dinitrogen trioxide, N_2O_3
	Peroxynitrite, $ONOO^-$
	Peroxynitrous acid, ONOOH
	Nitronium (nitryl) cation, NO_2^+
	Alkyl peroxynitrites, ROONO
	Nitryl (nitronium) chloride, NO_2Cl

Table 1.1: Summary of reactive species. Adapted from (76).

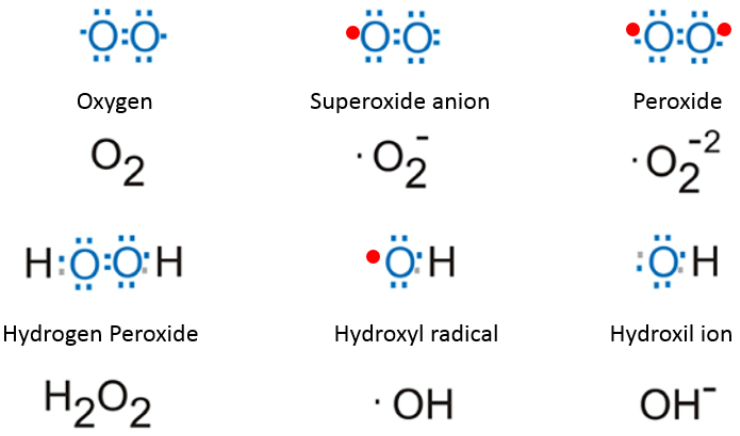

Figure 1.4: Electron and chemical structures of the most common ROS. Red dots represent an unpaired electron. Adapted from (77).

deregulation of signaling pathways, such as activation of advanced glycation pathway (leading to generation of AGEs), and to increased expression of receptor for advanced glycation end products (RAGE) (57). Last but not least, it has been suggested that oxidative stress is also an important modulator of telomere loss (84). Telomeres in human cells shorten with each round of DNA replication; it now seems that OS accelerates telomere loss, while antioxidants decelerate it.

1.3.4 Sites of ROS generation

ROS are naturally generated by the energy metabolism of the cell during the mitochondrial electron transport chain. Mitochondria are not only the location of OS generation but also a key location of its neutralization.

1.3.5 ROS defence mechanisms

The antioxidant defence system is sophisticated and serves for counteracting and regulating overall ROS levels in order to maintain physiological homeostasis. It can be divided as enzymatic and non-enzymatic. The enzymatic system includes catalase (CAT), superoxide dismutase (SOD) and glutathione peroxidase (GPx) (71, 72). SODs are metal-containing enzymes that are one of the most important lines of the defense system against ROS; they scavenge in the mitochondrion, nucleus, cytoplasm and extracellular spaces (85). SODs are particularly effective against superoxide anion radicals as they catalyze their dismutation (75). To date, three mammalian highly compartmentalized SOD isoforms have been identified and described: SOD-1, -2 and -3 (figure 1.5). SOD-1 is dimeric while SOD-2 and -3 are tetrameric. The most abundant human SOD is the cytosolic SOD-1 (85). The non-enzymatic ROS defence systems include glutathione and nutrients such as vitamins A, C and E (71).

1.3.6 The role of ROS in hyperglycemia & DM

Increasingly more research is providing evidence that hyperglycemia severely upregulates production of ROS via mitochondrial electron transport chain (66). For example, it increases the production of ROS in bovine aortic endothelial cells (86). Elevation of ROS then leads to OS and contributes in a major manner to the development and progression

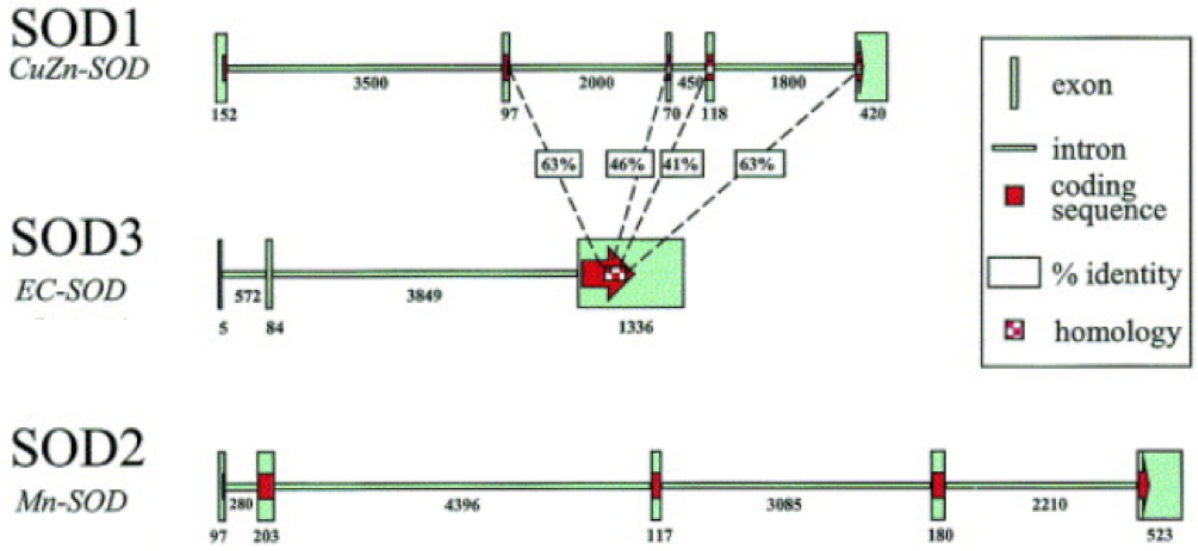

Figure 1.5: Human superoxide dismutase gene family. Both SOD-1 and SOD-3 have copper (Cu) and zinc (Zn) in their catalytic center. SOD-1 is localized to intracellular cytoplasmic compartments, and also termed CuZn-SOD. SOD-3 is localized to extracellular spaces, and is termed EC-SOD. SOD-2 has manganese (Mn) as a cofactor, is localized to mitochondria of aerobic cells, and is termed Mn-SOD. Size of exons and introns is indicated in this figure in base pairs. SOD-1 and SOD-3 share amino acid sequence homology, while SOD-2 has no significant homology with either of them. Adapted from (75).

of DM and its associated complications (58, 81, 87). For this reason, elevated OS is currently the leading hypothesis for the explanation of diabetes-induced complications: in 'diabetic cells' more pyruvate is available as a result of increased glycolysis, and hence more electron donors are available for the electron transport chain. ROS can render the signaling between insulin and glucose transport inactive and in this way lead to insulin resistance onset in T2D (88). Increasing the clearance rate of ROS by providing cells with mitochondrial antioxidants (e.g. idebenone) has been shown to exert an alleviating effect (87). The strategy of inhibiting OS has also been confirmed as successful in other preliminary studies (89).

1.4 Diabetes-associated musculoskeletal complications

1.4.1 Diabetes-associated musculoskeletal complications in general

In DM the tissues of the body are exposed to physiologically very high glucose concentrations. Strikingly, some tissue types (e.g. epithelium, kidney, retina and neural tissue) appear to be more susceptible to damage by hyperglycemia than others. Indeed, diabetic complications target mostly the feet, cardiovascular (CV) system, the retina, neural system and the kidneys. However, DM also exerts adverse effects on connective tissues (1), and has been associated with a variety of MSK manifestations (2). Although MSK complications are less 'high profile' than for example the vascular complications, they significantly compromise the quality of life of patients. Since the worldwide incidence of DM has sharply increased, and since the life expectancy of diabetic patients has also increased, this has resulted in an sharply rising clinical significance of these MSK changes (2). The most commonly affected MSK body parts are the upper limbs, especially hand and shoulder (3, 90). The overall list of MSK complications includes the following (2, 65, 91, 92):

- Dupuytren's contracture (the most frequent diabetic MSK complication, involves thickening of the palmar aponeurosis and contraction deformity of the fingers (3, 92));
- Carpal tunnel syndrome (causes paraesthesia over the cutaneous distribution of the mediam nerve on the fingers);
- palmax flexor tenosynovitis (also known as 'trigger finger'/flexor tenosynovitis/stenositing tenovaginitis, caused by fibrous tissue proliferating in the tendon sheath, limits tendon movement);
- stiff hand syndrome;
- rotator cuff tear;
- shoulder adhesive capsulitis (also known as 'frozen shoulder'/shoulder periarthritis/obliterative bursitis, renders shoulder movement painful and difficult);
- calcific periarthritis of the shoulder;

- foot ulcers;
- Charcots arthropathy (also known as neuropathic Charcots joint/Charcots disease, is a result of diabetic peripheral neuropathy, leads to painless progressive joint destruction (3, 92));
- diabetic cheiroartropathy (also known as limited joint mobility, up to 50% of diabetics suffer from this, most commonly affects the hand, causes pain and restricted mobility of joints (3, 92, 93));
- Sudecks atrophy (also known as reflex sympathetic dystrophy/algodystrophy/chronic regional pain syndrome, causes pain, swelling and impaired mobility);
- diabetic amyotrophy (rare neuropathic atrophy of proximal muscles, is the cause of muscle weakness and wasting, and muscle pain (3, 92));
- muscular infarction;
- diffuse idiopathic skeletal hyperostosis (also known as ankylosing hyperostosis/Forestiers disease, is characterized by new bone formation, particularly in the spine region);
- osteomyelitis (infection or inflammation of the bone or bonne marrow (3)).

Additional complications include crystal arthritides, infections, osteoporosis, osteoarthritis, ischemia and gangrene (2, 65, 91, 92). Diabetes is the most common cause of non-traumatic limb amputations, e.g. amputations of toes, foot or leg as a result of neuropathy. Sensory neuropathy develops first which then initiates ulceration and infections, and in this manner amputation becomes inevitable (91). Mortality rates after diabetic foot ulceration and amputation are high, with up to 70% of patients dying within 5 years of having an amputation (94). Overall, classifying the MSK manifestations of DM remains challenging, since most of the pathophysiological mechanisms remain currently obscure. It has been hypothesized that perhaps an excessive glycosylation of collagen and/or less remodelling in the MSK tissues may be responsible. The associations between DM and MSK manifestations have been supported by epidemiological studies (2). The treatment of diabetes-associated health complications brings an enormous economic burden, and this is predicted to rise together with the increase in DM incidence (4).

1.4.2 Diabetic tendon

Tendinopathy commonly leads to chronic pain, tendon rupture and disability with considerable socio-economic consequences. The incidence of tendon disease in DM patients is increased compared to the general population (2), suggesting that this tissue is sensitive to high blood glucose. Normal glucose level (but that of the upper range) constitutes a risk factor for tendinopathy, namely for rotator cuff tear (95). Patellar and Achilles tendon of diabetic rats present altered mechanical properties compared to control animals (96, 97). Furthermore, it has been demonstrated that tendon healing is impaired in diabetic animal models (1, 98, 99). Experiments on streptozotocin (STZ)-induced diabetic mice have shown impaired healing at the tendon-bone interface: this was demonstrated by less fibrocartilage and less organized (and decreased content of) collagen, and an increased presence of AGEs (23, 99, 100). Similarly, impairement in healing was shown in a T2D rat model of healing of Achilles tendon: reduced expression of collagen I, III and MMP-3 (compared to control intact Achilles tendon) was responsible for less degradation of matrix proteins and impaired subsequent tissue remodelling (1). Diabetic rats also exhibited less fibroblast proliferation and lymphocyte infiltration in transected Achilles tendon compared to control rats (101). Undeniably, diabetic patients present problems with tendon healing following surgery: for example they exhibit a restricted range of shoulder motion, and experience more re-ruptures (65). Thus there is a need for early diabetes diagnosis as soft tissue repair patients with uncontrolled DM are likely to have different success outcomes in comparison to general population. Diabetic tendinopathy aetiology has not yet been fully explained; the majority of available research is limited to acute glucose exposure and animal tissues (100, 102). We know it is complex with various factors such as AGEs, ROS, inflammation, genetics and epigenetics.

It is confirmed that part of the diabetic damage to tendon comes from AGEs that have accumulated in the tissue (6). AGEs naturally accumulate over a lifetime, however this process is much accelerated in DM due to excess glucose. AGEs are responsible for collagen cross-linking and in this manner for decrease in the biological and mechanical function of the tissue. In terms of the structure, on the macroscopic level thickening or thinning of tendon, stiff tendon and tendon calcification have been observed in diabetic patients (102, 103). An example is the volume of supraspinatus and biceps tendons that increased

in diabetics (104), or compromised structure of the mid-portion of Achilles tendon in T2D patients (105). On the microscopic level, structural reorganization in diabetic tendon has been described. A comparison by electron microscopy of Achilles tendon from healthy vs. long-term diabetic patients revealed that diabetics had increased packing density of collagen fibrils, decreased fibrillar diameter and abnormal fibril morphology (91). Other literature supports the notion of disorientation of collagen fibrils as common in DM (104, 106). Lastly, a large body of evidence from cell culture and animal experiments identified glucose-induced persistent epigenetic alterations in vascular endothelium (1, 107) which may be of relevance to tendon tissue as well.

1.5 Cellular senescence

Cellular senescence refers to a permanent cell cycle arrest with the development of aberrant gene expression, abnormal paracrine signaling and proinflammatory behavior (108, 109). Cells remain metabolically active and adopt characteristic phenotypic changes. Senescent cells often appear multinucleated, large and extended, and exhibit spindle and vacuolization features. There are two forms of cellular senescence: replicative senescence and stress-induced premature senescence. Markers currently utilized to detect senescent cells are limited and lack specificity. Commonly, p16 an important regulator of senescence is now used to identify senescent cells (110). In the context of organismal ageing, individual cells experience multiple cellular pressures, i.e. combinations of diverse senescence-promoting stressors. It is evident that oxidative stress is a central process involved in the induction and maintenance of cellular senescence (111). The relevance of the senescence topic in tendon biology is apparent as tendon is prone to early degeneration. Furthermore, as senescence may cause aberrant tissue architecture facilitated by ECM degradation and tissue fibrosis (112), it bears importance to tendon which is a tissue very much reliant on its correct ECM structure.

1.6 Aims of this project

Main objective

Gaps remain in our current tendon knowledge, especially regarding diabetic tendinopathy aetiology and the role of high glucose in diabetic tendon pathology. This thesis aims to investigate the cellular processes underlying diabetic tendinopathy. More concretely, our research is using chronic glucose exposure on primary human tendon-derived cells. The goal of this research is to identify induced effects on the tenocyte transcriptome and proteome of chronic high glucose exposure on tenocytes and to explore the mechanisms that mediate these effects.

Thus in this thesis experiments were conducted where human primary tendon cells were subjected to high pathological concentrations of glucose and hydrogen peroxide-induced oxidative stress in order to examine (i) firstly the direct effect of chronic high glucose exposure alone on tenocyte function, and (ii) secondly if elevated glucose contributed to the activation of the same pathway that feeds into ROS-induced signaling in tendon. The aim was to identify tenocyte specific problems arising in DM.

Hypothesis

In the first part, null hypotheses are as follows: *Glucose concentration in cell culture medium has no effect on tenocyte physiology. STZ-induced diabetic rats show no differences in tail physiology compared to healthy (control) rats.*

These hypotheses will be answered by performing aim 1-7:

Aim 1: to determine the effect of glucose concentration on tenocyte metabolism;

Aim 2: to determine the effect of glucose concentration on tenocyte number and proliferation;

Aim 3: to explore the effect of glucose concentration on tenocyte senescence and death;

Aim 4: to determine the effect of glucose concentration on tenocyte ECM synthesis and breakdown;

Aim 5: to determine the effect of glucose concentration on oxidative stress-responsive enzymes in tenocytes;

Aim 6: to determine the effect of glucose concentration on cell migration & proliferation capacity of tenocytes;

Aim 7: to examine rat tail tissue for effects of STZ-induced T1D.

In the second part, null hypothesis is as follows: *Glucose concentration in cell culture medium exerts no effect on the response of tenocytes to hydrogen peroxide (H_2O_2)-induced oxidative stress.*

This hypothesis will be answered by performing aim 1-6:

Aim 1: to determine an appropriate H_2O_2 concentration range for experiments on tenocytes;

Aim 2: to assess the effect of glucose and acute H_2O_2 treatment on tenocyte metabolic activity and viability;

Aim 3: to assess the effect of acute glucose and H_2O_2 treatment on tenocyte metabolic activity;

Aim 4: to quantify the effect of glucose and acute H_2O_2 on expression of selected genes;

Aim 5: to determine whether the glucose and H_2O_2-induced response can be attenuated by selected protective agents.

2
Materials & methods

2.1 Human & animal samples

To address the hypotheses that were given in Introduction, I used human tendon cells and rat tail samples.

In the first phase, human tendon cells were used. Healthy human hamstring tendon tissue was obtained from the Oxford Musculoskeletal Bank with full patient consent in compliance with National and Institutional ethical requirements, the United Kingdom Human Tissue Act, and the Declaration of Helsinki. In total 10 donors were used; 9 males (age 19 - 49 years, mean value 27.4 years) and 1 female (age 20). All donors were undergoing ACL reconstruction. It was confirmed that none of them had previous history of diabetes or metabolic syndrome. Primary tenocytes were derived from the tendon samples in two ways. The first method was monolayer explant, i.e. outgrowth of migrating cells from a piece of tissue (113). Alternatively, cells were obtained by collagenase method which is disaggregation of the tissue by enzymatic means (Collagenase from Clostridium histolyticum, Sigma, Poole, UK).

In the second phase, rat tail samples were used. Rat tails were obtained in collaboration with the University of Manchester, UK, where rats were sacrificed and their tails

removed. Two groups of samples were obtained: from control animals and from 16-week diabetic rats. T1D was induced in the diabetic rats by a well-validated STZ induction method. 6 control and 6 diabetic rats were used, both whole tail cross-sections and longitudinal sections from isolated tendon fascicles were available from each rat. At time of sacrifice the control group had a mean blood glucose level of 9.0 mM (n=6), while the untreated diabetic group had a mean of 27.5 mM (n=6). Tail cross sections and isolated tendon fascicles have been fixed in 10% neutral buffered formalin (tail pieces for cross sections also decalcified in 0.5% formic acid), embedded in paraffin and all samples sectioned to 5 μm by the Kennedy Institute of Rheumatology Histology unit.

2.2 Tendon cell culture

Primary human tenocytes were cultured in monolayer and passaged at 70-80% confluency from P0 $\rightarrow$ P5. No indication of overall phenotypic drift of tendon cell markers has been shown in our laboratory previously up to passage P5 (114). When cells were not employed immediately for experiments, they were cryo-banked in liquid nitrogen at -196 °C for long-term storage.

Chronic glucose culture was established from cell passage P1 onwards; they were cultured in medium containing different concentrations of glucose (D configuration, Fisher brand). Three glucose concentrations were chosen: 7.7 mM, 17.2 mM and 37.8 mM. Therefore cells were cultured in a 50:50 mixture of DMEM (cat.no. BE12-708F) and Ham's F-12 (cat.no. BE12-615F) medium to achieve final glucose concentration of 7.7 mM. Cells were also cultured in DMEM/F12 medium (cat.no. BE12-719F) which contains 17.2 mM glucose. Finally, for the third group of cells 0.5 M glucose stock was added to DMEM/F12 medium thus creating 37.8 mM glucose concentration. DMEM medium was supplemented with 5 mM Glutamax (Life Technologies, Paisley, UK) to achieve identical formulation. All culture media were obtained from Lonza (Lonza, Slough, UK). To optimize glucose concentrations after *transfer report* feedback, Biosera medium (Biosera, Nouaille, France) was employed to achieve the following concentrations: 5.0 mM, 17.5 mM and 30.0 mM. Therefore, all glucose concentrations in culture medium used throughout this project could be classified as **low (5.0 and 7.7 mM), medium (17.2 and 17.5 mM) and high (30.0 and 37.8 mM) glucose**. Throughout the text of this project,

glucose concentrations will be referred to as 5, 8, 17, 30 and 38 mM in order to avoid decimal numbers. In order to create 0.5 l of ready-to-use Biosera medium, Biosera medium was supplemented with 7.46 ml of Hepes (Sigma, Poole, UK), 5 ml of Glutamax (Life Technologies, Paisley, UK), 25 ml of fetal calf serum (FCS)(Biosera, Boussens, France) to create a final concentration of 5 % FCS, and adequate amount of glucose to create the 5-17-30 mM glucose conditions. In this manner, the final formulation of Biosera medium was identical to the previously employed Lonza medium, with the exception of sodium pyruvate as discovered subsequently in this project [1]. All media were supplemented with 5% FCS (Biosera, Boussens, France). Following occasional tissue culture incubator infections, Penicillin-Streptomycin solution (Sigma, Poole, UK) was added as a prevention; concentration of 1% in culture medium was used. In order to create "pro-collagen" medium proline and L-ascorbic acid-2-P (Sigma, Poole, UK) were added to medium to achieve a final concentration of 50 μg/ml for both. Mycoplasma screening was performed to ensure absence of contamination in cell cultures.

I aimed to achieve a diabetic model hence the 5 mM glucose condition was considered to be the control concentration [2]. Rat tissue was type I diabetic for a period of 16 weeks (conducted in Manchester, UK) which is an extensive time point of tissues being subjected to elevated glucose levels in comparison to my chronic glucose cell culture P0 $\rightarrow$ P4.

2.3 Mannitol control of osmolarity

To ensure that observed differences across glucose conditions were not due to changes in osmolarity, a mannitol control was performed. Mannitol (Sigma, Poole, UK) is commonly used as an osmolarity control for high glucose media. Live and dead (L/D) cell stain was used for 5 mM glucose, 30 mM mannitol and 30 mM glucose medium. Results (figure 2.1) indicate that especially in the dead stain the low glucose and mannitol control are remarkably similar unlike the high glucose, which was expected.

[1] For more details see chapter 4, aim 2.

[2] Normal fasting plasma glucose level is between 4.0 to 6.0 mM, and up to 7.8 mM after a meal. Prediabetes is 6.1 to 6.9 mM glucose when fasting, and 7.8 to 11.0 mM glucose 2 h after a meal. DM is defined as having fasting plasma glucose levels higher than 7.0 mM, or higher than 11.1 mM 2 h after ingestion of 75 g oral glucose load (115, 116).

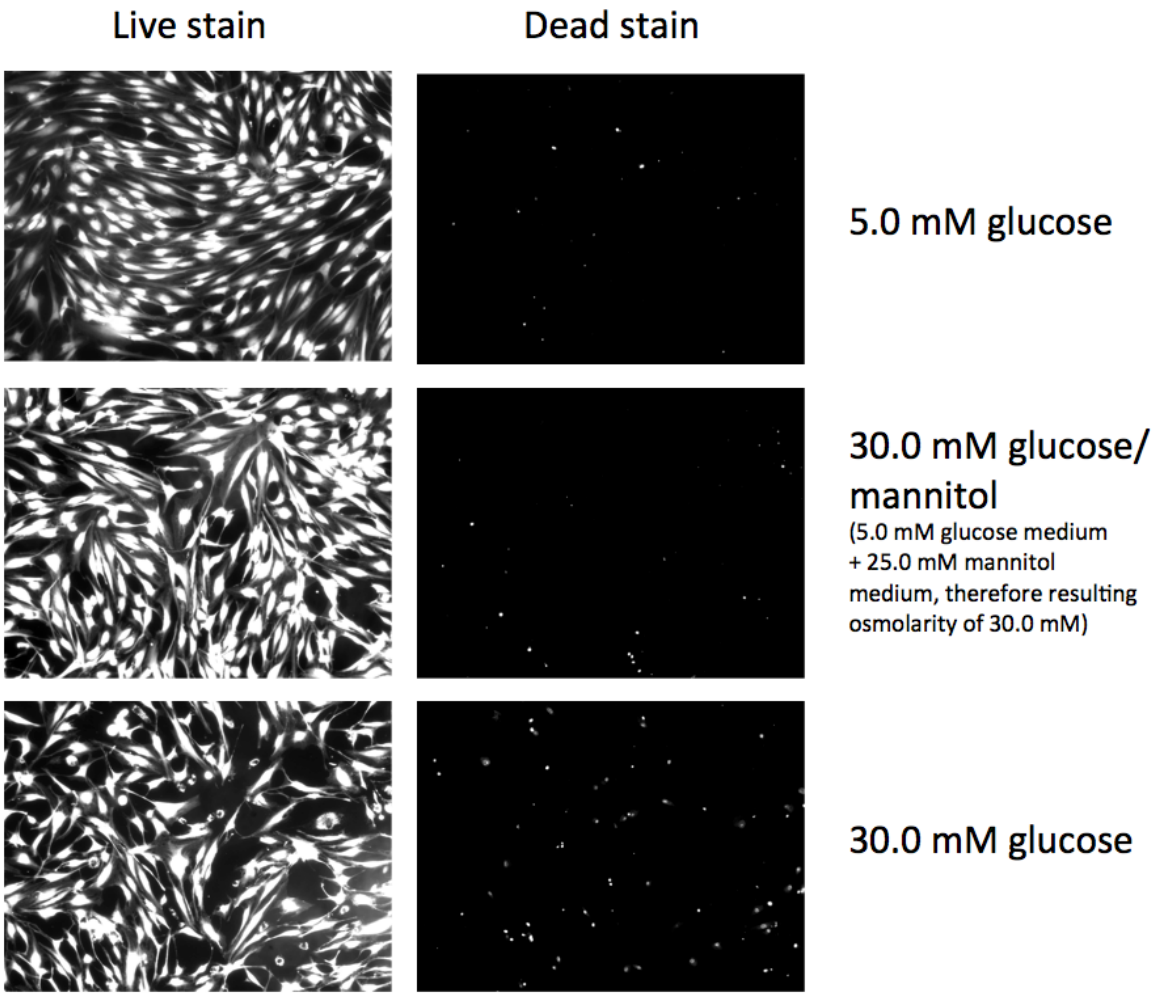

Figure 2.1: Mannitol control of medium osmolarity, as determined by L/D cellular stain on primary human tenocytes. All images were enhanced for brightness using ImageJ software.

2.4 Alamar Blue assay

Metabolic activity/viability of cultured tenocytes *in vitro* was determined using alamarBlue® assay (Invitrogen, Paisley, UK). Reagent was added to cells at a ratio of 1:10 with respect to the volume of culture medium, e.g. 10 μl of Alamar Blue reagent were added to 100 μl of medium of each well on 96-well plates. Cells were then incubated in the humidified CO_2 incubator at 37 °C for 3-4 h before analyzing fluorescence using 544 nm excitation and 590 nm emission on a fluorimeter (Fluostar Optima plate reader, BMG Labtech GmbH). When available, raw fluorescence values from wells with medium alone (i.e. culture medium with Alamar Blue without cells, blank control) were substracted to elimitate background fluorescence. It was confirmed that the addition of H_2O_2 (when required for experiment) did not change medium background values.

2.5 Chromogenic & fluorescence microscopy imaging

In order to evaluate cell monolayer or cross sections of tissue, chromogenic brightfield microscopy was used with immunostaining (e.g. DAB), while immunofluorescence was used with DAPI, L/D and fluorescence antibodies. The following microscopes were utilised: Olympus BX40 microscope with Olympus U-CMAD3 camera (Olympus, Southend-on-Sea, UK), Zeiss LSM 710/Axio Observer.Z1, and Nikon Eclipse Te300 microscope with a QImaging Retiga 2000R Fast 1394 camera (Nikon Corporation, Tokyo, Japan). Magnification from 40x to 600x was used. Quantitative data analysis was performed using ImageJ software (NIH).

2.6 Live/Dead cell viability assay

LIVE/DEAD^{TM} stain assay (Sigma, Poole, UK) which consists of calcein acetoxymethylester (AM) and ethidium homodimer-1 was used to visualize the ratio of live vs. dead tenocytes in monolayer. Briefly, the optimized procedure consisted of adding 2 μl of live and 2 μl of dead stain to 1 ml of serum-free colorless medium of each well on a 96-well plate. Cultured cells were then kept in humidified CO_2 incubator at 37 °C for 15 min before removing the reagents. Cells were kept in standard culture medium during analysis on selected fluorescence microscope.

2.7 EdU DNA incorporation assay

Click-it EdU AlexaFluor-555 Imaging Kit (Molecular probes, Eugene, Oregon, USA) was used to evaluate the proliferative capacity of tenocytes under different glucose conditions. EdU (5-ethynyl-2'-deoxyuridine) is a nucleoside analog of thymidine and is incorporated into DNA during active DNA synthesis.

Tenocytes were cultured on 13 mm diameter plastic coverslips in 24-well dishes and treated as appropriate for individual experiments. Cells were then incubated with 10 μM EdU solution and kept in humidified CO_2 incubator at 37 °C for 24 h. Fixation step followed using 3.7% formaldehyde in phosphate-buffered saline (PBS). Subsequently, cells were permeabilized by 0.5% Triton X solution. EdU that incorporated into DNA of the proliferating cells was fluorescently labelled: 200 μl of Click-iT® reaction cocktail (containing Alexa Fluor azide) was added to each well containing a coverslip. The plate was incubated at room temperature, protected from light. After 30 min, each well was washed with PBS. In order to enable determination of total cell number nuclear staining was subsequently performed using Hoechst 33342 (solution 1:2,000 in PBS to obtain a final concentration of 5 μg/ml), protected from light. After incubation for 30 min at room temperature, wells were washed with PBS, and cover slips mounted on microscope glass slides. Images were captured using a fluorescent microscope. The percentage of EdU-positive cells against total cell number was determined by automated counting in ImageJ 1.45 (NIH) software.

2.8 TUNEL apoptosis assay

Cell apoptosis was quantified using Terminal deoxynucleotidyl transferase (TdT) dUTP Nick-End Labeling 594 (TUNEL) assay (Molecular probes, Eugene, Oregon) which detects apoptotic cells with fragmented DNA. Manufacturer's protocol was followed.

2.9 RNA extraction

Tenocytes were cultured in 6-well plates and treated as appropriate for individual experiments. For tenocytes, I determined that the 6-well plate format was most suitable for optimal RNA yield. Total RNA was isolated from adherent cultured cells first using

Qiazol cell lysis buffer (Qiagen, GmbH) followed by purification columns (Zymo Research, Freiburg, Germany). Manufacturers protocol was followed. RNA was treated with DNase I to eliminate any contaminating genomic DNA. At end of the protocol, harvested RNA pellet was dissolved in 20 μl of nuclease-free water. Quality and amount of isolated RNA was assessed using Nanodrop spectrophotometer: purity was measured by UV absorbance at 260 and 280 nm. Absorbance ratios A260/A280 and A260/A230 were calculated. When possible, ratios greater than 1.8 were considered suitable for further step, however some exceptions were made and are indicated in corresponding figure legends. TapeStation system (Waldbronn, Germany) was used to control for quality of RNA structural integrity of a few selected samples. RNA was stored at -80 °C.

2.10 cDNA synthesis & qPCR

RNA that has been previously quantified at end of RNA extraction was defrosted on ice from -80 °C. cDNA synthesis was performed in two steps in order to reverse transcribe the RNA. Reagents used for the two steps were random hexamer oligonucleotides, dNTP mix, RNAse-free water, first strand buffer, DTT, and superscript RT. Controls for cDNA synthesis were created: no RT enzyme (no reverse transcriptase added) and no RNA template. After the cycle cDNA was aliquoted into a master stock and a more diluted ready-to-use concentration, then stored at -20 °C. Quantitative real-time polymerase chain reaction (qPCR) was performed on cDNA samples using either SYBR Green protocol or TaqMan protocol, depending on targets [1]. Therefore, either Quantitect real-time PCR primers (Qiagen) or TaqMan MGB FAM probes were employed with their corresponding master mix: Fast SYBRgreen master mix (Qiagen, Hilden, Germany) or TaqMan Fast Advanced Master Mix (Applied Biosystems, ThermoFisher Scientific). cDNA was appropriately diluted (2 ng per reaction well was determined as optimal amount) and used in qPCR reaction. A number of reference housekeeping genes were tested. 18S and TBP were not optimal as they seemed to fluctuate in response to set experimental conditions. β-actin was selected as the most stable endogenous control gene (note it was not validated on H_2O_2 samples, only on glucose samples). For the qPCR reaction no template control

[1] Refer to corresponding figure captions in Chapter 3 & 4 for details which of the two methods was used for specific genes.

(NTC) and samples previously synthesized from 'no RT control' were included for each tested gene. Each reaction mixture had a total volume of 10 μl, and was run in technical triplicate on a 384-well plate. Q-PCR was performed on ViiA^{TM} 7 Real-Time PCR System (Applied Biosystems). Expression of genes was calculated using the 2-deltaCt method (117).

2.11 Soluble collagen Sircol assay

The aim was to quantify collagen that was secreted by tenocytes into culture medium. For this purpose the Sircol assay kit (Biocolor Ltd., UK) was chosen. It contains a colorimetric picrosirius-red dye that binds to collagen structures. Manufacturer's protocol was followed. 1 ml of culture medium was aspirated from each well. Reagents used were in the following order: isolation concentration reagent, picrosirius-red dye, acid-salt wash reagent, and alkali reagent. At end of protocol, 200 μl of alkali reagent containing bound collagen were transferred to a 96-well plate for absorbance measurement. Wavelength of 540 nm was used on a SpectraMax 384 Plus plate reader (Molecular Devices LLC, California, USA) to obtain sample values. Quantification of collagen content was achieved using a linear absorbance standard curve. Reference stock of collagen type I was provided by manufacturer and was used to create dilutions which followed the same procedure as samples of interest.

2.12 Cell number determination

In a number of assays, determination of cell number was important in order to report normalized data.

Cell number was determined using one of the following methods [1]:

- PicoGreen Assay.

  Double-stranded DNA content was quantified using the Quant-iT PicoGreen assay kit (Invitrogen Molecular Probes, Paisley, UK) which contains a fluorescent nucleic acid stain. Manufacturer's protocol was followed. Reagents used were Pico Green

[1] Please refer to individual experiments in Chapter 3 & 4 to see which method was used.

dye, TE buffer, and DNA standard (supplied stock of 100 μg/ml). Alongside experimental samples a standard curve of 5 points was created. At end of protocol, a 96-well plate with samples of total volume 100 μl in each well was analyzed for fluorescence, with excitation 480 nm and emission 520 nm, on a spectrofluorometer Fluostar Optima (BMG Labtech GmbH, Allmendgruen, Germany). Fluorescence values from standards were plotted; a linear trend relationship was used to quantify DNA content of samples of interest.

- Hoechst stain.

  Culture medium was aspirated from wells with adherent cell cultures. Hoechst dye (Invitrogen, Paisley, UK) was diluted 1:10,000 in Phenol-red-free medium (Invitrogen, Paisley, UK), and solution was added to desired wells. Cells were then incubated in the humidified CO_2 incubator at 37 °C for 20-30 min. Subsequently the solution was removed and replaced with Phenol-red-free medium only. Cells were analyzed under fluorescent microscope, and images of interest captured. Total cell number was determined by automated count in ImageJ 1.45 (NIH) software.

- DAPI stain.

  4'6-diamidino-2-phenylindole dichloride dye (Sigma, Poole, UK), commonly known as DAPI, was diluted 1:500 in ddH_2O and solution added to plate wells or cover slips of interest. Samples were incubated for 5-15 min and protected from light. After incubation, samples were rinsed 3 times in ddH_2O for 1 min and in the case of coverslips mounted in Fluorsave (Calbiochem, San Diego, CA, USA). Cells were analyzed under fluorescent microscope, and images of interest captured. Total cell number was determined by automated cell count in ImageJ 1.45 (NIH) software.

- Trypan blue.

  Trypan blue count was performed in one of two ways: either manual count using plastic disposable counting slides, or automated count using specific machine counting slides. First, adherent cell monolayer was digested with Trypsin for about 3 min (until confirmed under light microscopy) in the humidified CO_2 incubator at 37 °C. Trypsin solution was then de-activated by addition of FCS-containing cell culture medium. Mixture was collected into Eppendorf tubes and centrifuged at 1400

g. Supernatant was carefully discarded and precipitate that contained cells was re-suspended in 100 μl of cell culture medium. 100 μl of Trypan blue (Gibco, Carlsbad, CA, USA) was added and well mixed. For manual count 9 μl for measurement on counting slides were used. Live cells were counted using tissue culture bright field microscope; dead blue cells were omitted from count. Cell Counter (Bio-Rad) was used for automated cell count.

2.13 Dimethylmethylene Blue assay

Dimethylmethylene Blue (DMB)-based spectrophotometry assay was used to quantify the amount of GAGs in samples. This assay was developed from work by Farndale *et al.* (118, 119) who researched cartilage cultures.

Medium was aspirated from wells with adherent cell culture, and cell layer was gently washed twice with PBS. Papain digestion buffer was added to wells. Cells were then incubated in the humidified CO_2 incubator at 37 °C for 30 min, then scraped and collected in an Eppendorf tube. Tubes were then incubated at 60 °C in water bath for 90 min, mixing occasionally. Chondroitin sulphate standard curve was prepared: 0, 1, 5, 7 and 10 μg/ml of chondroitin sulphate (Sigma C9819) in papain digestion buffer. 40 μl of each sample was added to a 96-well plate, followed by 100 μl of colour reagent. Absorbance of samples was analyzed at 520 nm on SpectraMax 384 Plus plate reader. GAG content was calculated using a linear absorbance chondroitin sulphate standard curve.

2.14 Monolayer scratch assay

In vitro scratch assay was employed to evaluate effect of glucose on migration capacity of cells. Tenocytes were chronically cultured in 8, 17 and 38 mM glucose medium in 96-well plates. Two treatment options (control and additional FCS) were used within each glucose condition. Confluent cell monolayer was scratched using a P200 pipette tip. Cell migration and proliferation were then imaged 1, 2, 3 and 4 days after the initial scratch. Cells were visualized using Live stain from L/D kit. Fluorescence microscopy was used to image 4 wells per treatment with 2 low power shots per well. ImageJ 1.45 (NIH) was used to quantify the surface area covered by cells.

Figure 2.2 illustrates the analysis sequence.

In IMAGE J: 1. Microscopy picture was opened (A in figure). 2. The most appropriate macro was selected out of the three macros which were created based on brightness of pictures (B in figure). 3. The most appropriate ROI shape was applied out of the two that were created, and positioned in such a manner that it best covered the scratch area. The ROI was adjusted if required as long as surface area was close to identical (C in figure). 4. Data value was obtained using the 'analyze → measure' tool in ImageJ, which quantified percentage area that was covered within the ROI. The value was copied into Microsoft Excel (D in figure).

In MICROSOFT EXCEL: 5. Raw value was divided by UU (i.e. unscratched untreated) value. 8 data values were calculated for each experimental condition, then mean and standard deviation (SD) were calculated.

In PRISM: 6. Graphs were plotted.

2.15 Immunohistochemistry (IHC) staining

Fixed tissue of interest was embedded in paraffin, and sectioned as described earlier.

Manual IHC protocol.

For Hematoxylin and Eosin stain tissue sections were de-paraffinized through a series of washes with Clearene and graded ethanol. Hematoxylin (Vector Labs, Burlingame, USA) and Eosin (Sigma, Poole, UK) stains were used. Subsequently, tissue sections were destained using ethanol and Clearene in reverse order, mounting medium added, and coverslips applied.

For staining with specific antibodies tissue sections were de-paraffinized through a series of washes with Clearene and graded ethanol. Antigen retrieval was performed overnight at 60 °C using citrate antigen retrieval buffer (Vector Labs, Burlingame, USA). 3% peroxidase block (hydrogen peroxide + methanol) was performed in order to block endogenous proteases, then rehydration of sections was continued. Sections were washed with PBS and permeabilized in 0.5% Triton X (Triton X + PBS) before being washed again. Blocking step with 3% Horse Serum (Horse serum + PBS) was applied for 1 h in order to block non-specific binding sites. Sections were incubated overnight with a primary antibody of choice at 4 °C in a humidified chamber. The following day, sections were

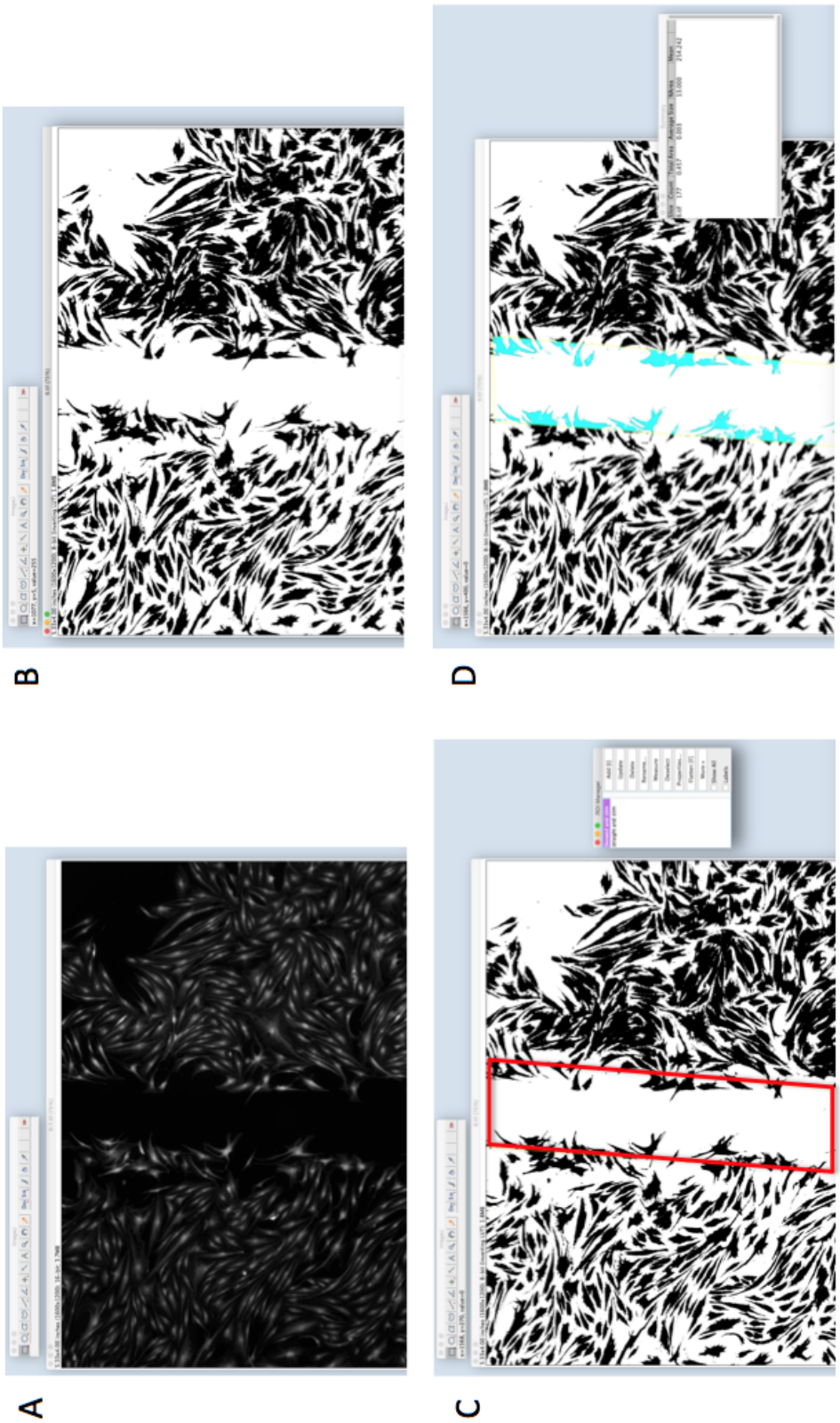

Figure 2.2: Analysis method for scratch assay. A) opened scratch microscopy image. B) macro was applied. C) selected region of interest (ROI) was positioned over scratch. D) 'analyze → measure' tool in ImageJ.

washed in PBS before using Vectastain Universal Elite ABC kit (Vectorlab, Peterborough, UK). A universal secondary antibody (contained within the kit) was applied for 30 min. AB reagent (A + B + PBS) was then applied to sections for 30 min. After washes with PBS, cells contained within the sections were stained with DAPI nuclear stain. Indicator Immpact DAB SK-4105 (Vector Labs, Burlingame, USA) was applied to sections (consisting of DAB concentrate + DAB diluent) until brown color developed, usually in 5-8 min. Sections were then washed in water, mounting medium Fluorsave (Calbiochem, San Diego, CA, USA) added and a coverslips applied. Immunostained sections were evaluated for the presence of desired components using microscopy, and images at different magnifications were captured.

Automated IHC protocol.

Machine Dako Autostainer Link 48 (Dako, Agilent Technologies, Santa Clara, CA, USA) was used in this protocol. Slides were baked for 1 h at 60 °C in order to increase tissue adherence. Heat-mediated high power of hydrogen (pH) antigen retrieval step was performed on PT links machine in FLEX Target Retrieval Solution (TRS) antigen retrieval fluid (Dako, Agilent Technologies, Santa Clara, CA, USA) where each chamber held 30 ml of 50x concentrated FLEX TRS and 1470 ml of dH_2O. Slides were then placed into wash buffer solution (75 ml wash buffer 20x Dako Envision Flex + 1425 ml dH_2O) for 5 min. Reagents used for automated staining were: peroxidase blocker, FLEX Horseradish Peroxidase (HRP), rabbit universal negative isotype control, and substrate buffer containing 20 drops of 3,3'-diaminobenzidine (DAB) chromogen. Antibody of choice was diluted in antibody diluent (Dako, Agilent Technologies, Santa Clara, CA, USA) to reach desired concentration. After staining slides were placed in dH_2O. From dH2O slides were put through ethanol dilutions and xylene before being mounted in Pertex and covered with coverslips. Image acquisition was performed on microscope the following day to enable Pertex drying sufficiently.

List of used antibodies:

- MMP-13 mouse monoclonal anti-human pro MMP-13 antibody (R&D Systems, Minneapolis, MN, USA), dilution 1:500 in PBS-Tween;
- 3-NT mouse monoclonal antibody Alexis biochemicals ALX-804-505, 39B6 (Axxora, Farmingdale, USA), dilution 1:100;

- FOXO1a rabbit monoclonal Abcam EP927Y ab52857 IgG isotype antibody (Abcam, Cambridge, UK), recognizes both phosphorylated and unphosphorylated FOXO1a, dilution 1:100;

- HRP-conjugated secondary mouse antibody 1858413 (Pierce, Rockford, IL, USA), dilution 1:25,000 in PBS-Tween, and Universal secondary antibody for rabbit primary (Vector Universal ABC kit ,Vector Labs, Burlingame, USA), dilution 1:50,000 in PBS-Tween.

2.16 Hydrogen peroxide (H_2O_2) treatment assay

Cells were subjected to H_2O_2 to induce oxidative stress. 30% H_2O_2 (Sigma, Poole, UK) was diluted to desired concentration in the range of 0-2,000 μM in culture medium. Solution was added to adherent cells in 96-well plates, and incubated for 3, 18 or 24 h in the humidified CO_2 incubator at 37 °C. For the last 3 h of the incubation alamarBlue® reagent was added (using the protocol described earlier) and fluorescence analyzed at end of total incubation time. L/D stain and RNA extraction were performed at end of total incubation time using the protocols described earlier. Cell protein content was isolated at end of total incubation time (please refer to next section). Selected protective agents N-acetylcysteine (NAC), ascorbic acid (AA) and resveratrol were all from Sigma, Poole, UK.

2.17 Protein isolation & Western blotting

I. Preparation of lysate from cell culture

Cells were lysed in order to release proteins of interest. 10 cm Petri plates with adherent tenocytes (already treated for experiment as desired) were placed on ice and medium was aspirated from wells. Cells were then washed in order to remove residual growth medium, and lysis reagent was added to each plate. Lysis reagent consisted of 50 ml of phosphate-buffered saline (PBS) + 500 μl of 100 mM phenylmethanesulfonyl fluoride (PMSF) + 500 μl of 100 mM ethylenediaminetetraacetic acid (EDTA) + 500 μl of 100 mM sodium fluoride (NaF) + 500 μl of 10 mM sodium orthovanadate. Cell layer was scraped off the dish using a plastic disposable cell scraper, and cell suspension

was collected into an Eppendorf tube. Samples were sonicated (Sonicator W-225, Heat Systems-Ultrasonics Inc., USA) on ice for 15-20 s to disrupt cells. Cell lysates were then centrifuged to pellet the cell debris, and supernatant was gently aspirated and transferred into a fresh tube which was kept on ice (tubes with pellet were discarded).

II. Determination of protein concentration

The concentration of protein in samples was quantified using a Pierce bicinchonic acid (BCA) assay kit (Pierce, Rockford, IL, USA). Serial dilutions of bovine serum albumin (BSA) were used to create a protein standard: stock of BSA (BioRad, Hemel Hempstead, UK) of concentration of 2 mg/ml was used to create 6 values on the curve. Subsequently, 150 μl of PROD22660 dye were added to 10 μl of each sample; lysis buffer alone was used for blank reading. This colorimetric reaction was analyzed on a plate reader at 660 nm wavelength and protein concentrations were calculated using the standard curve. Based on results, protein content was adjusted to be homogenous across all samples. Loading dye was prepared in a 9:1 ratio with dithiothreitol (DTT), e.g. 450 μl BIORAD dye + 50 μl DTT. Once the loading dye was prepared, it was added to samples in a 1:2 ratio, e.g. 150 μl of dye + 300 μl of sample. Total protein samples were denatured by immersion in 95 °C water on a hotplate for 5 min, and subsequently stored at -20 °C.

III. SDS-PAGE electrophoresis

Preparation of polyacrylamide gels consisted of making gradient sodium dodecyl sulphate polyacrylamide gels ('lower' and 'upper'); gel percentage was selected in respect to expected protein size. 25 μl of each sample, including a molecular weight marker (Precision Plus Mwt marker, BioRad, Hemel Hempstead, UK) was loaded into gel using gel loading tips. To achieve protein separation according to size the gel was run at 170 V for 45-60 min in running buffer.

IV. Western blotting

Proteins were transferred onto a blotting membrane using a wet transfer system. Transfer tank was filled with transfer buffer and samples run at 200 mA for 60-90 min to ensure complete protein transfer. Membrane was blocked in order to prevent non-specific background binding of the primary and/or secondary antibodies: this was achieved using milk. Skimmed milk powder solution (5% in PBS-Tween 0.1%) was stirred on a beaker until homogenous. Membrane was then blocked with the solution for 1 h on shaker. It

was then incubated with primary antibody of choice overnight at 4 °C under agitation. The following day, membrane was washed with PBS Tween and incubated with secondary antibody at room temperature for 45 min under agitation. In order to develop the membrane it was washed with PBS Tween and SuperSignal West Dura or ECL were applied. Membrane was exposed and chemiluminescence emanating was captured in digital images using a dark box camera system. Membrane was then stripped of antibodies, and blotted with primary antibody of a housekeeping gene which was diluted at a required concentration. Incubation with secondary antibody followed, for 45 min. Substrate and camera were used in identical manner as previously. Intensity of protein bands was measured in ImageJ software, using the 'analyze → measure' tool in the package.

2.18 Statistical analysis

Statistical analysis was performed in GraphPad Prism 6 (GraphPad Software Inc., La Jolla, USA). Values are presented as mean +/- standard deviation (SD) or standard error of the mean (SEM)(as indicated in corresponding figure captions). Definitions of SD and SEM were adopted from (120). Normality of data was tested using D'Agostino & Pearson and/or Shapiro-Wilk normality test. Comparison between two groups of data were performed using two-tailed T-test, however the majority of data within this thesis contained more than two experimental groups. Thus either parametric one-way/two-way analysis of variance (ANOVA) was used with Tukeys or Bonferroni *post-hoc* tests, or non-parametric Kruskal-Wallis test with Dunns *post-hoc* test were used. In figures statistical significance is indicated in comparison to control group unless indicated otherwise. Prism significance intervals are defined as: not significant (ns) $P > 0.05$; * $P \leq 0.05$; ** $P \leq 0.01$; *** $P \leq 0.001$.

3

Tendon cell and extracellular matrix phenotype in hyperglycemia

3.1 Hypothesis & aims

Null hypotheses are as follows: *Glucose concentration in cell culture medium has no effect on tenocyte physiology. STZ-induced diabetic rats show no differences in tail physiology compared to healthy (control) rats.*

These hypotheses will be tested by addressing aims 1-7:

Aim 1: to determine the effect of glucose concentration on tenocyte metabolism;

Aim 2: to determine the effect of glucose concentration on tenocyte total number and proliferation;

Aim 3: to explore the effect of glucose concentration on tenocyte senescence and death;

Aim 4: to determine the effect of glucose concentration on tenocyte ECM synthesis and breakdown;

Aim 5: to determine the effect of glucose concentration on oxidative stress-responsive proteins in tenocytes;

Aim 6: to determine the effect of glucose concentration on cell migration & proliferation capacity of tenocytes;

Aim 7: to examine rat tail tissue for effects of STZ-induced uncontrolled T1D.

3.2 Experimental design

The overall research objective in this chapter was to assess how tendon tissue responds to elevated glucose level, as would be the case for a diabetic individual.

In order to address the aims described above an *in vitro* model of human diabetic tendinopathy was generated using tendon hamstring samples from healthy individuals which were obtained from the Nuffield Orthopaedic Centre (Oxford Musculoskeletal Bank), Oxford. Primary cells were derived by explant or collagenase culture. Afterwards, cells were chronically cultured (i.e. cultured through multiple passages, P0 $\rightarrow$ P4) in different glucose media of 5, 8, 17, 30 and 38 mM glucose. These glucose concentrations were chosen to illustrate concrete points. Both the 5 mM and 8 mM glucose media were used to mimic a physiological level of glucose in the blood of a healthy individual. 5 mM is normoglycemic, while 8 mM is normal post feeding but abnormal under fasting conditions. The 17 mM level was used to mimic the standard tissue culture conditions: it is the glucose level in regular Ham's-F12 medium [1]. It must be noted, however, that 17 mM glucose corresponds to diabetic levels in a human. The 30 mM and 38 mM glucose media were chosen to represent a severely diabetic level of glucose which would be expected to be detrimental to both *in vitro* experimental cells and to humans. The 5 mM glucose condition is considered the control condition in this thesis.

In this project the effects of glucose on both the cells and the ECM components were examined, as well as on the tendon tissue as a whole (see IHC experiments, Aim 7). The cell culture was entirely derived from clinical samples (as described above), while the samples for IHC were derived from a rat animal model. One of the advantages of this approach is that it breaks the complex tendon environment down into its constituent cells and studies these cells in an isolated manner. As the tenocytes are isolated neither blood supply nor nerves are present, therefore the direct effect of elevated glucose concentration

[1] Typical 'low' glucose medium is 1 g/L = 5.6 mM.

on the cells is exposed. On the other hand, this may also constitute a disadvantage as the isolated cells will behave differently compared to their natural milieu.

3.3 Results

3.3.1 Aim 1: to determine the effect of glucose concentration on tenocyte metabolism

Metabolic activity is sensitive to extracellular glucose, as measured at one time point

Metabolic activity was determined by Alamar Blue assay: figures 3.1 and 3.3 show the effect of different glucose concentrations on tenocyte metabolic activity and tenocyte number. As total metabolic activity of a tenocyte population is influenced by its cell number, Hoechst stain was used for normalization (A and B in figure 3.1). In this experiment from a single donor, cell number is increased in 38 mM glucose compared to all other conditions (B in figure 3.1). This is not in agreement with the proliferation data from 2 different patients described below in figures 3.16 and 3.18. Once absolute Alamar values were normalized it can be seen that tenocytes in 17 mM and 38 mM glucose were both more metabolically active than tenocytes in 5 mM and 8 mM glucose (figure 3.2). In a consistent manner, the metabolic activity is higher in the 17 mM and 38 mM glucose conditions compared to 8 mM glucose (figure 3.3).

Metabolic activity is sensitive to extracellular glucose, as measured over time

The aim of this section was to look at metabolic activity of tenocytes (assessed by Alamar Blue assay, as previously) over time of the culture in different glucose conditions. It was vital to understand whether cell number changes in the glucose conditions throughout time. Figures 3.4, 3.5 and 3.6 show that once the absolute Alamar blue values are normalized metabolic activity per cell is increasing in all conditions over time. Perhaps this increase over time per cell suggests a metabolic adaptation, or increase in cell size. Interestingly, in figure 3.4 the metabolic activity of 8 and 17 mM glucose-exposed cells is increasing over time, while it is decreasing in the 38 mM glucose-exposed cells. The contact inhibition phenomenon (i.e. cells ceasing to migrate in the same direction after contact with other cells (121, 122)) is not expected to be responsible for this observation,

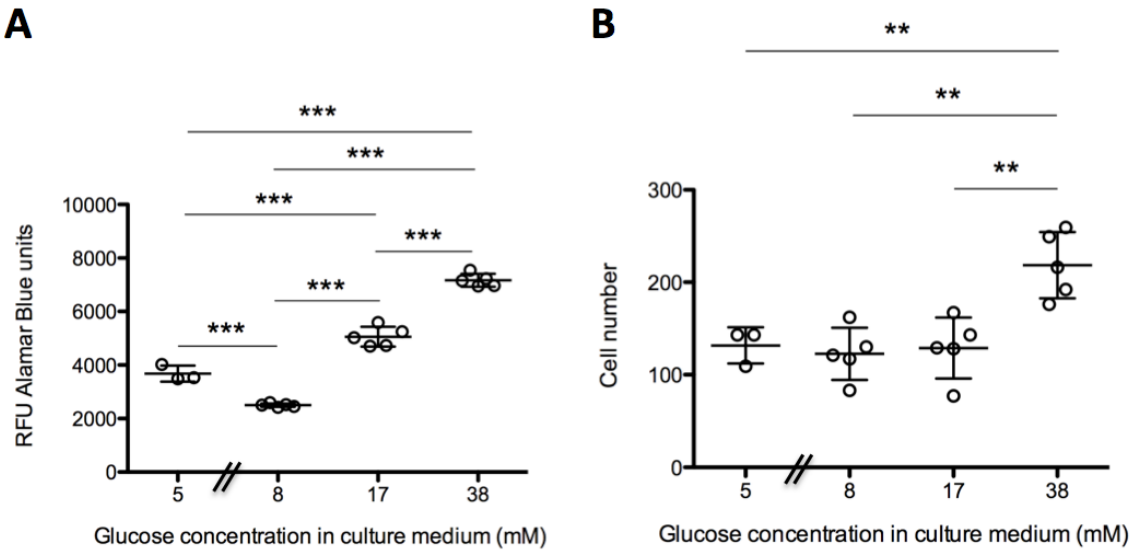

Figure 3.1: Tenocyte metabolic activity and cell number following culture in different glucose conditions. A) non-normalized Alamar values; B) total cell number based on Hoechst stain data. Data from 1 patient. Error bars represent SD. Note that 8, 17 and 38 mM medium was Lonza brand, however 5 mM medium was Biosera brand. Furthermore, the 5 mM glucose data was obtained at a different time but from the identical patient (see axis break), and this must be noted when interpreting the figure. One-way ANOVA and Tukey as *post-hoc* test.

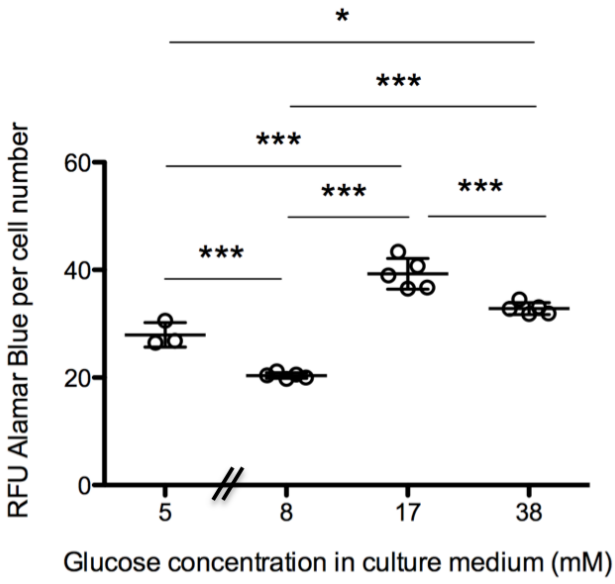

Figure 3.2: Tenocyte metabolic activity following culture in different glucose conditions, normalized to cell number. Data from 1 patient. Error bars represent SD. 8, 17 and 38 mM medium was Lonza brand, however 5 mM medium was Biosera brand. Furthermore, the 5 mM glucose data was obtained at a different time but from the identical patient (see axis break), and this must be noted when interpreting the figure. One-way ANOVA and Tukey as *post-hoc* test.

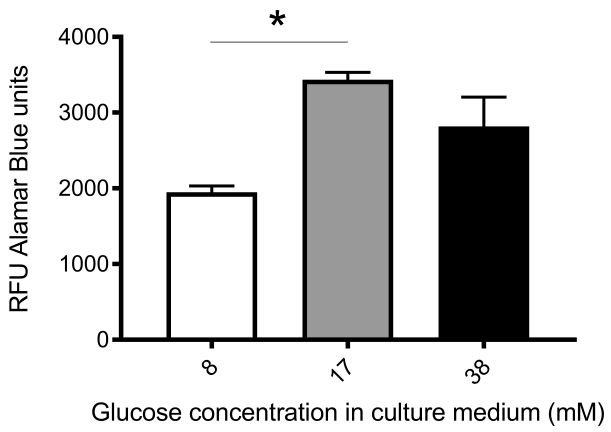

Figure 3.3: Tenocyte metabolic activity following culture in 8, 17 and 38 mM glucose media. Data from 3 patients. Data not normalized to cell number. N too small to determine normality (D'Agostino-Pearson). One-way ANOVA (p=0.0120) and Tukey as *post-hoc* test. N=3 for each bar. Error bars represent SEM.

as figure 3.5 indicates that the cell number in the 38 mM glucose condition was decreasing, and hence a decrease in the total metabolic activity of the 38 mM glucose cell population would not be of concern. In more detail, the figure 3.5 shows that cell number is decreasing over time in both 8 mM and 38 mM glucose conditions, while the population of 17 mM cells remains constant. An overall lower cell number in the 17 mM glucose condition was observed despite identical seeding density at origin of the experiment, and was of concern (therefore the experiment was repeated, as the following figures 3.7, 3.8 and 3.9 show).

A repeat of this experiment (with marginally different glucose concentrations) of a different patient is in figures 3.7, 3.8 and 3.9. The normalized data (figure 3.9) show that 5 mM glucose cells have increasing metabolic activity per cell over time, followed by the 17 mM glucose cells. The 30 mM glucose cells have very low metabolic activity throughout the entire experiment. It is more appropriate to look at figure 3.7 as cell number data is absent for Day 1 and Day 3 due to technical issue (the automated cell counter has a threshold below which it will not give a reading - the cell number was below this threshold on Day 1 and Day 3). Here it can be seen that both 5 and 17 mM glucose cells are increasing in metabolic activity over time and, most importantly perhaps, 30 mM glucose response is debatable. Unfortunately in this repeat of experiment there was a seeding issue. The 30 mM cells were extremely low in cell count: only about 10% of

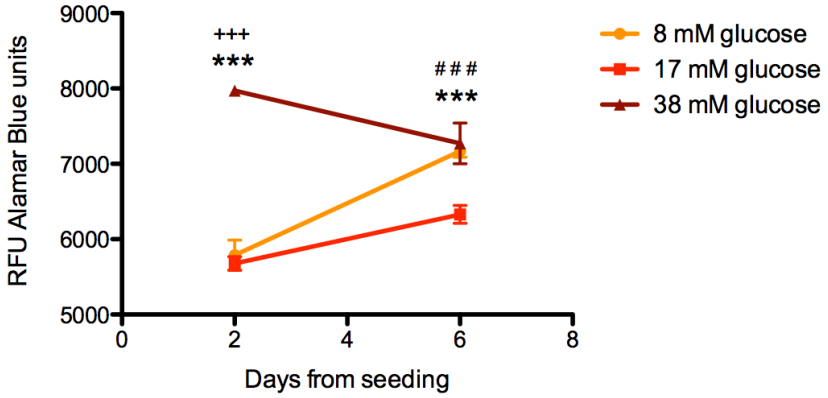

Figure 3.4: Metabolic activity of tenocytes cultured in 8, 17 and 38 mM glucose media over the course of 6 days. Day=0 is seeding into 96-well dishes. Data from 1 patient, Alamar incubation 3 h, values non-normalized. Data for Day 4 not available due to technical issue. Error bars represent SD; SD is indicated but at times not visible due to its small size. Two-way repeated measure ANOVA with Bonferroni as *post-hoc* test, # is 8 vs. 17 mM, + is 8 vs. 38 mM, $*$ is 17 vs. 38 mM.

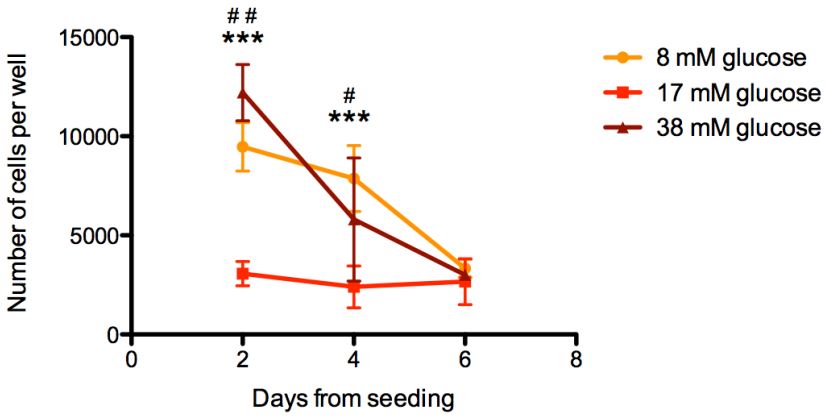

Figure 3.5: Tenocyte number over time in different glucose conditions (96-well plates). Data obtained from manual Trypan Blue count. Data from 1 patient. Error bars represent SD; SD is indicated but at times not visible due to its small size. Two-way repeated measure ANOVA with Bonferroni as *post-hoc* test, $*$ is 8 vs. 17 mM, # is 17 vs. 38 mM.

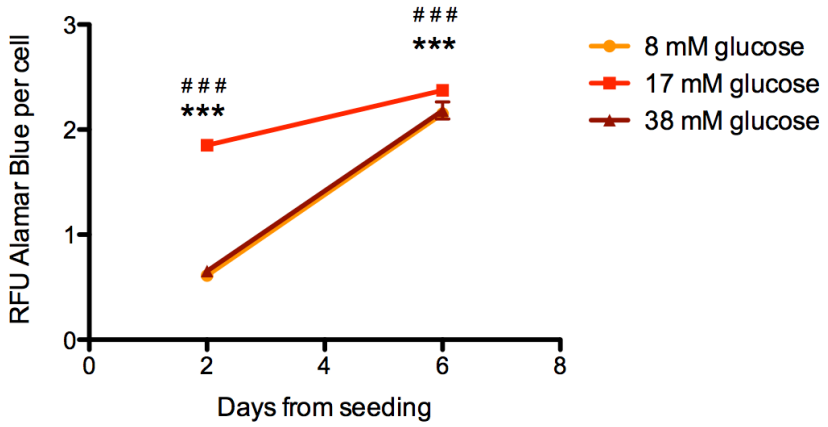

Figure 3.6: Normalized metabolic activity of tenocytes cultured in 8, 17 and 38 mM glucose media over the course of 6 days. Day=0 is seeding into 96-well dishes. Graph generated from data of the 2 previous graphs. Data from 1 patient. Error bars represent SD; SD is indicated but at times not visible due to its small size. Two-way repeated measure ANOVA with Bonferroni as *post-hoc* test, $*$ is 8 vs. 17 mM, # is 17 vs. 38 mM.

them were alive, as opposed to 80%+ in 5 mM and 17 mM cells. Therefore, the 5 mM and 17 mM cells were seeded at the same (high) density, while all the available cells for 30 mM were seeded. This and other ongoing problems with culturing the chronically 30 mM glucose-treated cells suggested that the cells might be undergoing senescence in 30 mM glucose. I aimed to repeat the exact time points of the previous experimental repeat, however the cells grew much slower this time. For this reason, the cells were maintained for 25 days (as opposed to 6 days previously), and monitored closely every day under the tissue culture microscope. In order to have quantitative information (in addition to the automated cell count) notes were taken during the experiment on cell confluency, as assessed under the microscope. On Day 1 (no cell number data available) the monolayer confluency was 30% for 5 mM and 17 mM glucose cells, and only 10% for 30 mM cells. On Day 3 (no cell number data available), the confluency was 40% for 5 mM cells, 30% for 17 mM cells, and only 15% for 30 mM cells. On Day 16 the confluency was 60, 60 and 20% for 5, 17 and 30 mM cells respectively; it must be noted that in general the cells have not grown much. This is partially due to their primary nature, and to being kept in 5% FCS. On Day 25 the confluency was 90%, 80% and 5% for 5, 17 and 30 mM cells respectively.

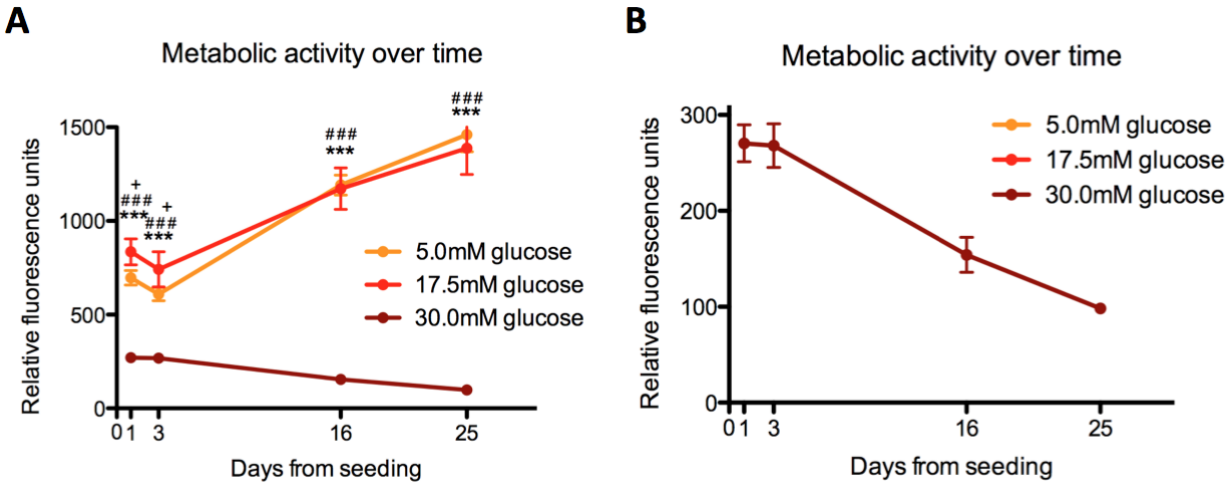

Figure 3.7: Metabolic activity of tenocytes cultured in different glucose conditions over the course of 25 days (48-well format). Alamar incubation 4 h, non-normalized values. A) view of entire data, B) close-up of 30 mM glucose data. Data from 1 patient. Values represent mean of 5 readings with error bars representing SD. SD is indicated but at times not visible due to its small size. Two-way repeated measure ANOVA with Bonferroni as *post-hoc* test, + is 5 vs. 17 mM, ∗ is 5 vs. 30 mM, # is 17 vs. 30 mM.

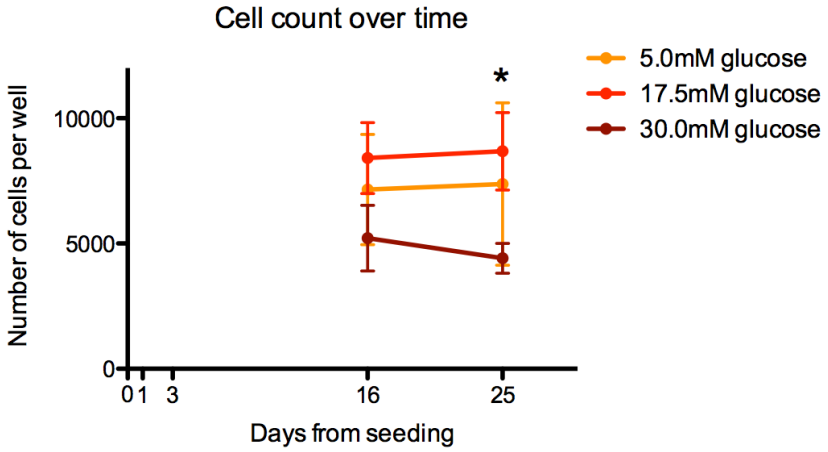

Figure 3.8: Tenocyte number in different glucose conditions over the course of 25 days (48-well format). Data from 1 patient. Data was not obtained for Day 1 and Day 3 due to technical issue (the automated cell counter has a threshold below which it will not give a reading - the cell number was below this threshold on Day 1 and Day 3). Trypan Blue data obtained using automated cell counter. Values represent mean of 5 readings with error bars representing SD. Two-way repeated measure ANOVA with Bonferroni as *post-hoc* test, ∗ is 17 vs. 30 mM.

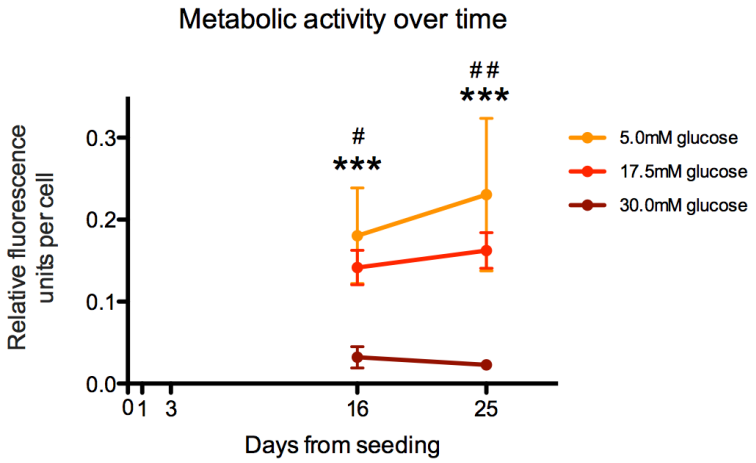

Figure 3.9: Normalized metabolic activity of tenocytes cultured in 5, 17 and 30 mM glucose over the course of 25 days. Day=0 was seeding into experimental dishes. Graph generated from data of 2 previous graphs. Data from 1 patient. Error bars represent SD; SD is indicated but at times not visible due to its small size. Two-way repeated measure ANOVA with Bonferroni as *post-hoc* test, $*$ is 5 vs. 30 mM, # is 17 vs. 30 mM.

Metabolic activity of 5 mM glucose-treated tenocytes does not respond to acute treatment with 17 mM nor 30 mM glucose

It was hypothesized that an acute insult with elevated levels of glucose may have an effect on cells that were chronically cultured in 5 mM glucose. For this purpose 5 mM cells were treated with 17 and 30 mM glucose for 24, 48 and 72 h. The metabolic activity of cells was unchanged, as measured by the Alamar Blue assay (figure 3.10). Cell number normalization of these Alamar values was desirable therefore DAPI images for all conditions were prepared. Preliminary cell count (figure 3.11) however showed little differences in cell density, and therefore the normalization step was omitted.

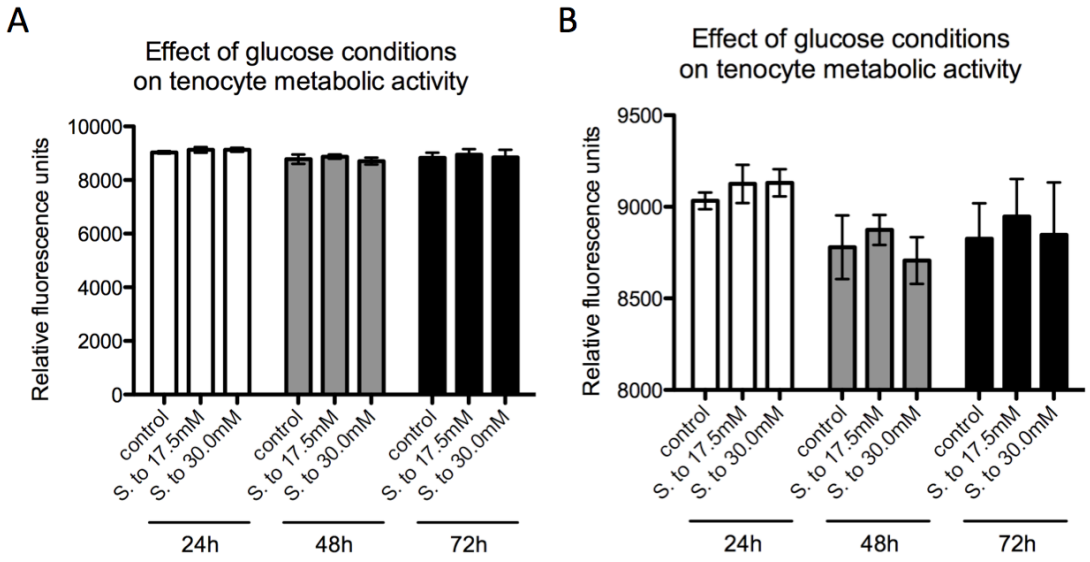

Figure 3.10: Metabolic activity of 5 mM cells after 24, 48 and 72 h of treatement with 17 and 30 mM glucose. Alamar Blue incubation 4 h, values not normalized. Control was switched from 5 mM to 5 mM, i.e. fresh medium. "S." = switched. Data from 1 patient. A) original graph, B) magnified section of graph. Columns represent a mean value of 5 data points, error bars represent SD. Repeated measures two-way ANOVA. p value for switching conditions 'ns', p value for time points ***.

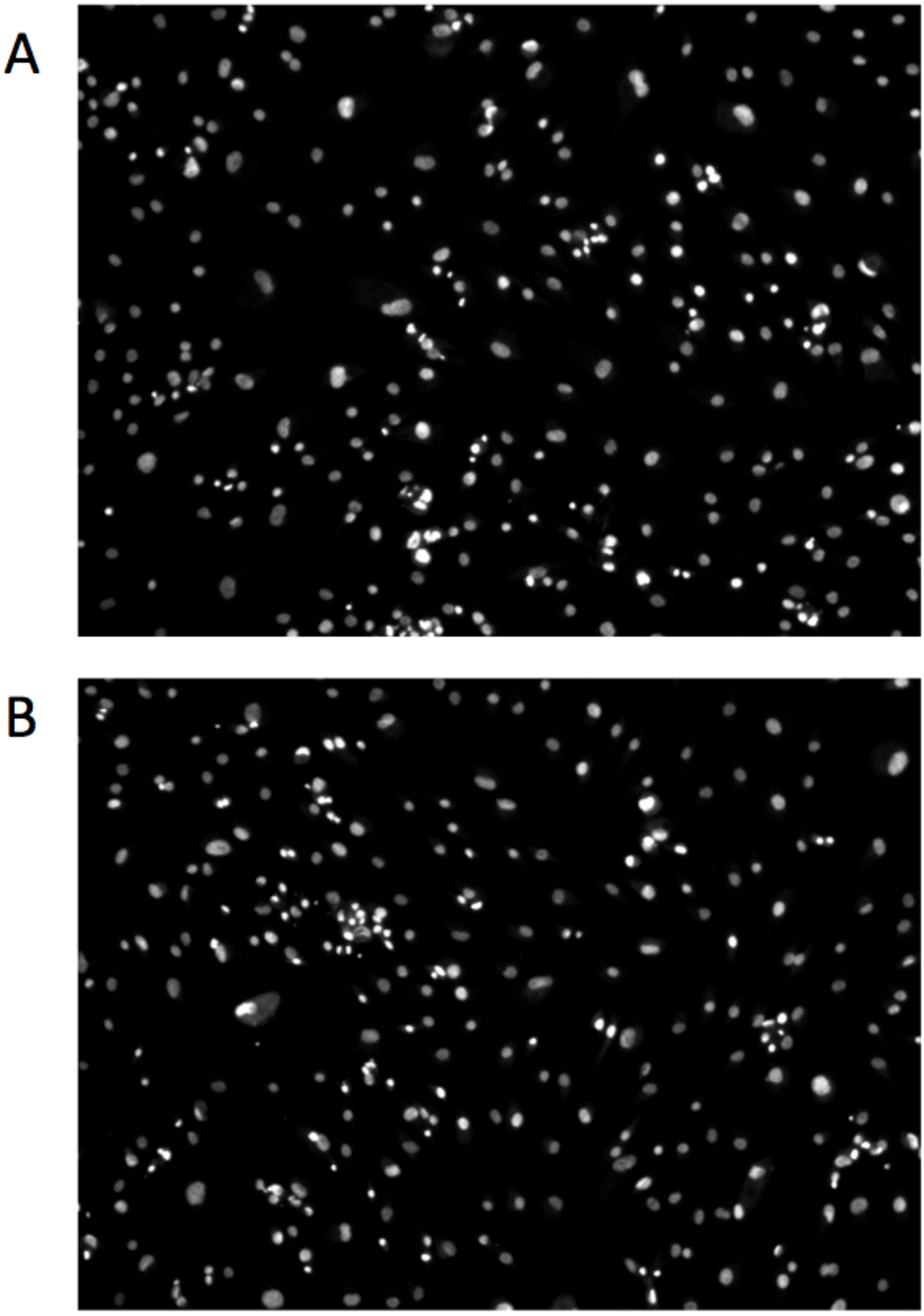

Figure 3.11: Cell nuclei visualized with DAPI stain to estimate tenocyte total number. A = 5 mM, B = 30mM glucose cells (17 mM glucose not analyzed in ImageJ, as difference - if any - would be expected between the lowest and highest concentrations). Images are the 72 h time point (selected as the most dramatic differences - if any - would be expected to be witnessed after the longest glucose exposure). Data from 1 patient. Magnification x100. Cell number was counted in ImageJ: mean was 306 ± 12 cells and 302 ± 4 cells for 5 mM and 30 mM cells, respectively. No statistical difference ($p = 0.811$) based on two-tailed T-test.

3.3.2 Aim 2: to determine the effect of glucose concentration on tenocyte total number and proliferation

Extracellular glucose affects tenocyte monolayer density

Tenocytes were chronically cultured in 5, 17 and 30 mM glucose medium and stained with Live stain to assess cell monolayer density. The results illustrate that the overall density depends on the glucose condition: the density was highest in 17 mM and lowest in 30 mM, as assessed by microscopy (figure 3.12). A repeat of this experiment (figure 3.13), this time conducted in an additional type of medium (pro-collagen medium, supplemented with 50 μg/ml AA and 50 μg/ml proline), confirms that cells are most confluent under 17 mM glucose concentration, while they are least confluent under 30 mM glucose concentration.

Tenocytes display increased proliferation rate in 38 mM glucose

The EdU incorporation assay that quantifies DNA synthesis was used to assess the rate of cell proliferation under different glucose conditions. Representation of the assay is in figure 3.14. Three FCS concentrations were used in this assay: 0, 5 and 20% FCS. 5% FCS is the standard culturing concentration used throughout this project. 0% FCS served as negative control (cells were not expected to proliferate much in this condition), while 20% FCS served as positive control (cells should proliferate considerably more than under 5% FCS).

Data are derived from 2 different patient donors. In patient 1, the assay revealed that tenocytes chronically cultured in 8 mM, 17 mM and 38 mM glucose proliferate significantly faster in 38 mM glucose (under 5% and 20% FCS), as seen in figure 3.15. No difference was observed under 0% FCS (figure 3.15). Intriguingly the resulting total cell number was the lowest in 38 mM glucose, whereas it was the highest in 17 mM glucose, regardless of the FCS concentration and equal cell seeding densities at origin of experiment (figure 3.16). Cell loss, perhaps due to detachment or death, may be higher in 38 mM glucose, resulting in net population decrease. The resulting total cell number data is consistent with the Live stain data in the previous figures 3.12 and 3.13.

In patient 2, 17 mM data was unfortunately lost but there are no differences in cell proliferation rate in 8 vs. 38 mM glucose (figure 3.17). However the pattern of figure 3.18 is in agreement with patient 1 data (figure 3.16) and indicates that cells are being lost

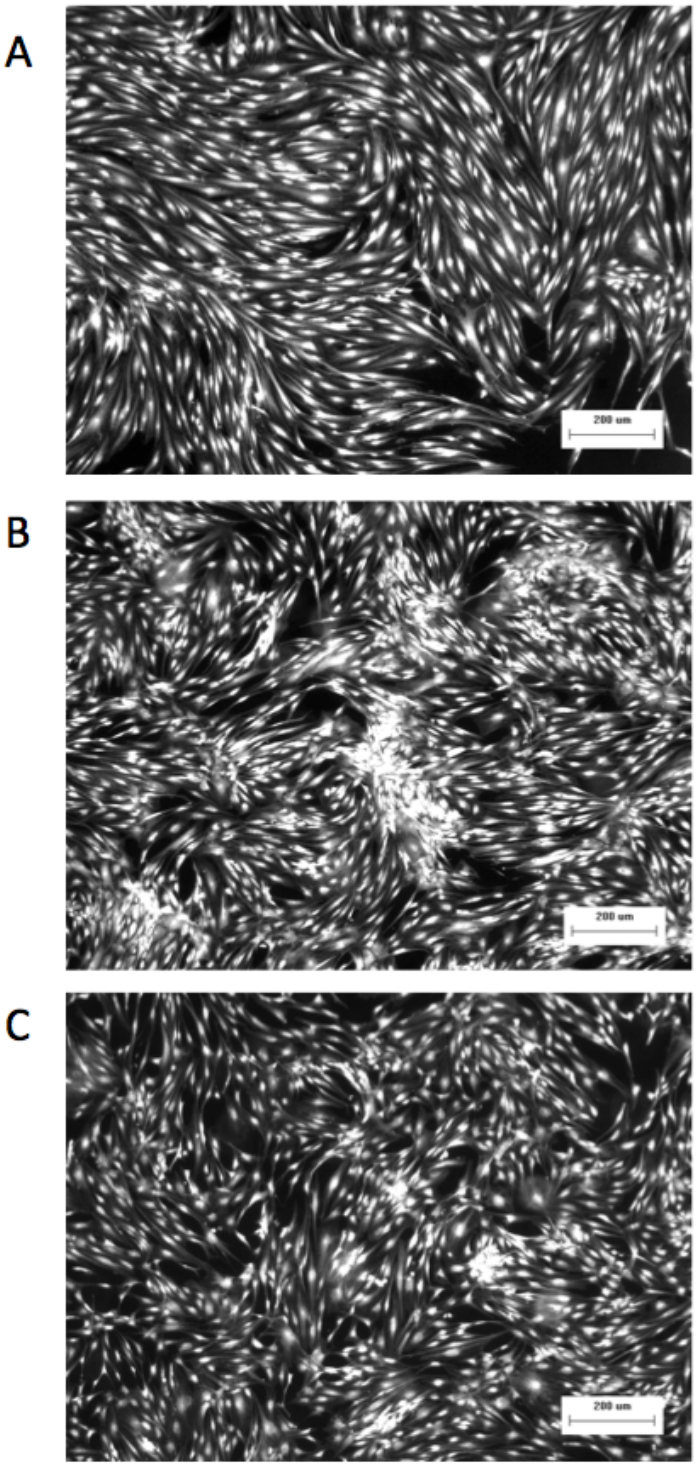

Figure 3.12: Tenocyte monolayer density as visualized by Live stain. A) 8 mM, B) 17 mM, C) 38 mM glucose condition. Data from 1 patient, cell passage P2, 5% FCS. Scale bar indicated is 200 μm.

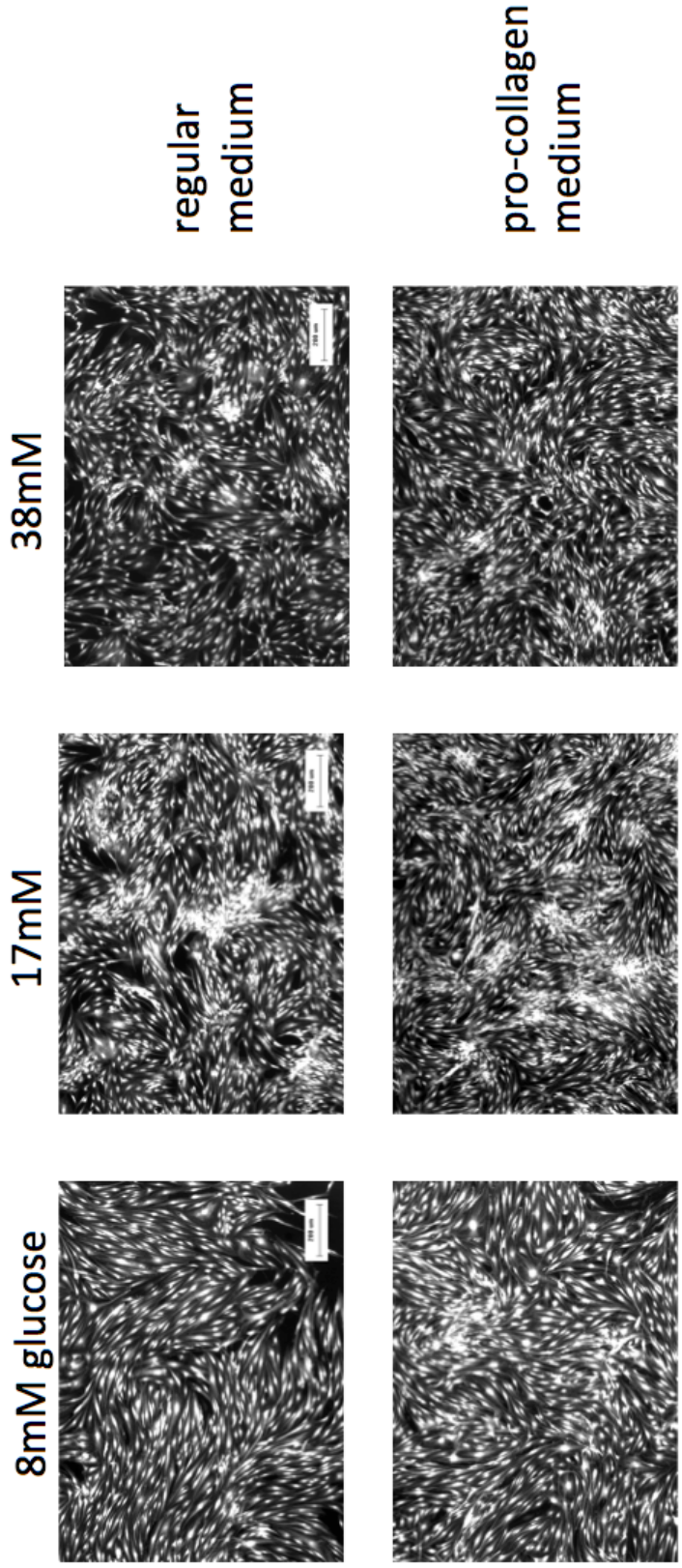

Figure 3.13: Tenocyte monolayer density as visualized by Live stain in 8, 17 and 38 mM glucose condition. Regular and pro-collagen media. Data from 1 patient. All images are same magnification: scale bar indicated is 200 μm.

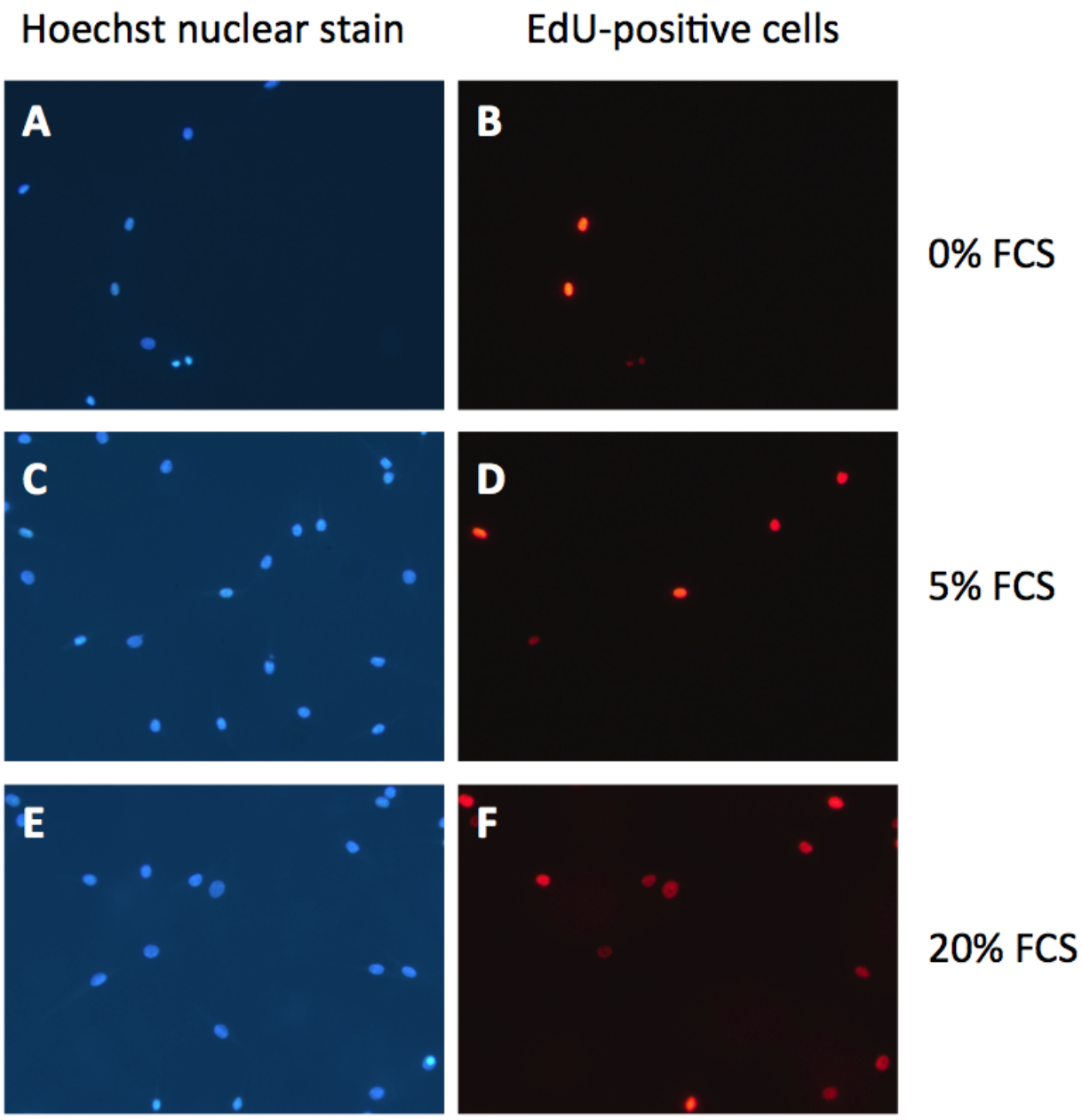

Figure 3.14: Representative images of the employed EdU assay. Data from patient number 2, 38 mM glucose condition. Magnification x200.

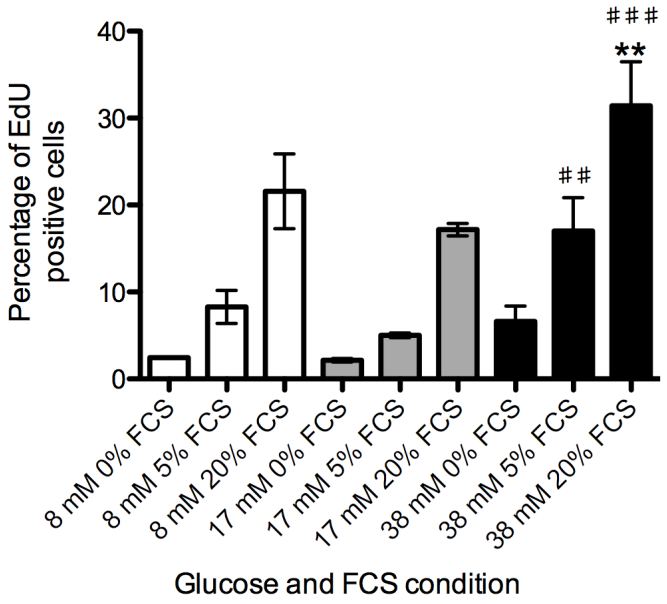

Figure 3.15: Tenocyte proliferative profile following culture in varying glucose media. Data from patient number 1. 8 mM 5% FCS was considered the baseline in this experiment, 0% FCS represents negative control, 20% FCS represents positive control. Columns represent a mean value of 3 data points with error bars representing SD. One-way ANOVA and Tukey *post-hoc* test. * vs. 8 mM, # vs vs. 17 mM.

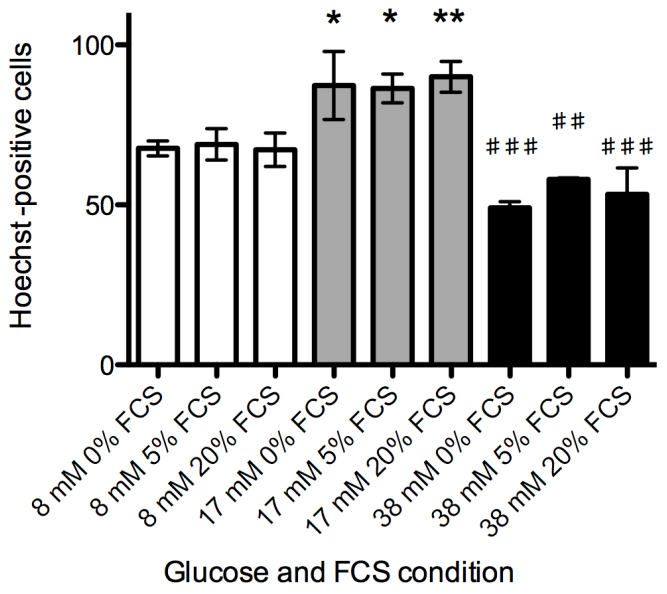

Figure 3.16: Total tenocyte number following culture in varying glucose conditions, as visualized by DAPI nuclear stain. Data from patient number 1. Columns represent a mean value of 3 data points with error bars representing SD. One-way ANOVA and Tukey *post-hoc test.* * is vs. 8 mM, # is vs. 17 mM.

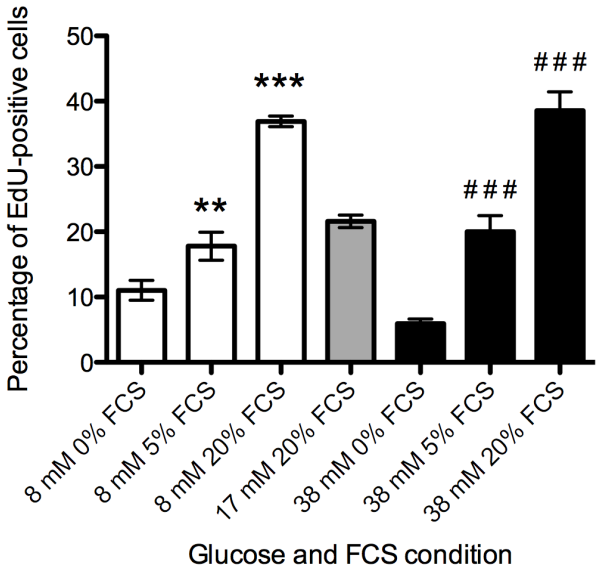

Figure 3.17: Tenocyte proliferative profile following culture in varying glucose concentrations. Data from patient number 2. Columns represent a mean value of 3 data points with error bars representing SD. *N* number too small to test for normality of data (Shapiro-Wilk test, D'Agostino & Pearson test). One-way ANOVA and Tukey *post-hoc* test. * is vs. 8 mM 0% FCS, # is vs. 38 mM 0% FCS. Only statistical significance of interest is indicated in graph.

at a higher rate in 38 mM glucose, either by increased death (reduced cell lifespan) or detachment.

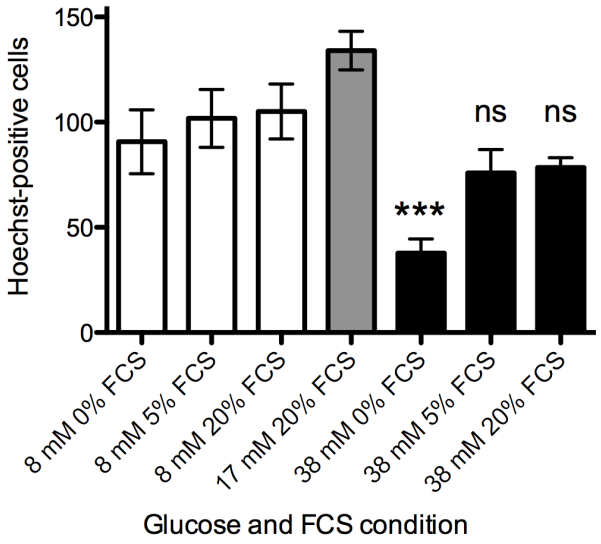

Figure 3.18: Total tenocyte number following culture in varying glucose conditions, as visualized by DAPI nuclear stain. Data from patient number 2. Columns represent a mean value of 3 data points with error bars representing SD. *N* number too small to test for normality of data (Shapiro-Wilk test, D'Agostino & Pearson test). One-way ANOVA and Tukey *post-hoc* test. Shown statistics is vs. 8 mM 5% FCS (control condition). Only statistical significance of interest is indicated in graph.

3.3.3 Aim 3: to explore the effect of glucose concentration on tenocyte senescence and death

Elevated levels of extracellular glucose may promote cell senescence

Cellular senescence is a state of irreversible growth arrest which can be induced by a variety of stresses, for example by ROS (112). Senescent cells remain metabolically active and do not turn into apoptotic cells immediately. They change in morphology instead, often becoming bigger in size. Senescent cells upregulate expression of p21, p16 or both (depending on the type and level of stress the p21 pathway can either antagonize or synergize with p16), which are not commonly expressed by quiescent or terminally differentiated cells (112).

The cell culture studies in this project provide initial findings of dose-dependent morphological senescence in human tenocytes with increasing glucose concentration (figures 3.19 and 3.20, taken at Day=0 and Day=5). 30 mM glucose cells exhibit the highest ratio of morphologically senescent cells, followed by 17 mM glucose cells, as assessed by fluorescent microscopy. However the 30 mM glucose cells were seeded at a lower density in this experiment since not enough cells could have been obtained. It remains important to notice that 17 mM cells show progressive senescence compared to 5 mM cells and this finding is trustworthy as these 2 conditions were seeded at the same seeding density at origin of experiment. These findings seem to be patient-specific or cell batch specific (processing each patient inevitably varies slightly), as can be seen when comparing figure 3.12 where 30 mM glucose cells display less senescence than in figures 3.19 and 3.20. It is possible that in figures 3.19 and 3.20 the 30 mM cells hit their replication limit, i.e. the total number of divisions a human cell can undergo in its lifespan. Equally, the senescence may be induced by a stressor which might be the elevated glucose level. A qPCR marker study was performed in order to establish which route, p21 vs. p16, is taken to senescence (see Chapter 4, Aim 5).

Effect of glucose on tenocyte apoptosis

Based on the above finding of decreased total cell number in the 38 mM glucose condition, cells are either being detached at a higher rate, entering senescence and failing to grow or becoming apoptotic in the 38 mM glucose condition. Apoptosis, also known as programmed cell death, is a tightly regulated cell suicide process which can be activated

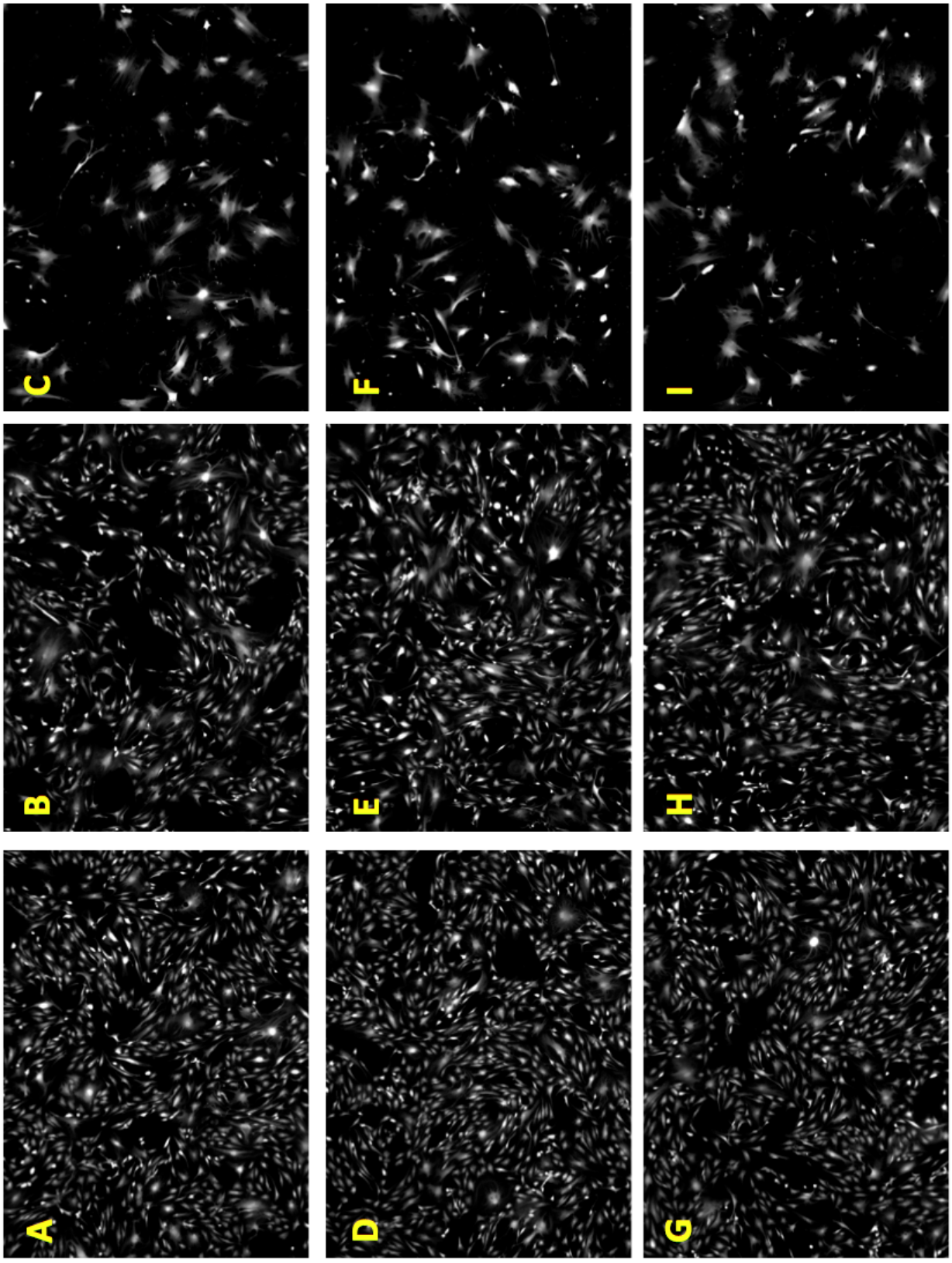

Figure 3.19: Tenocyte monolayer visualized with Live stain, Day=0. Data from 1 patient, cell passage P3. Magnification x400. A-D-G are 5 mM, B-E-H are 17 mM, C-F-I are 30 mM glucose cells.

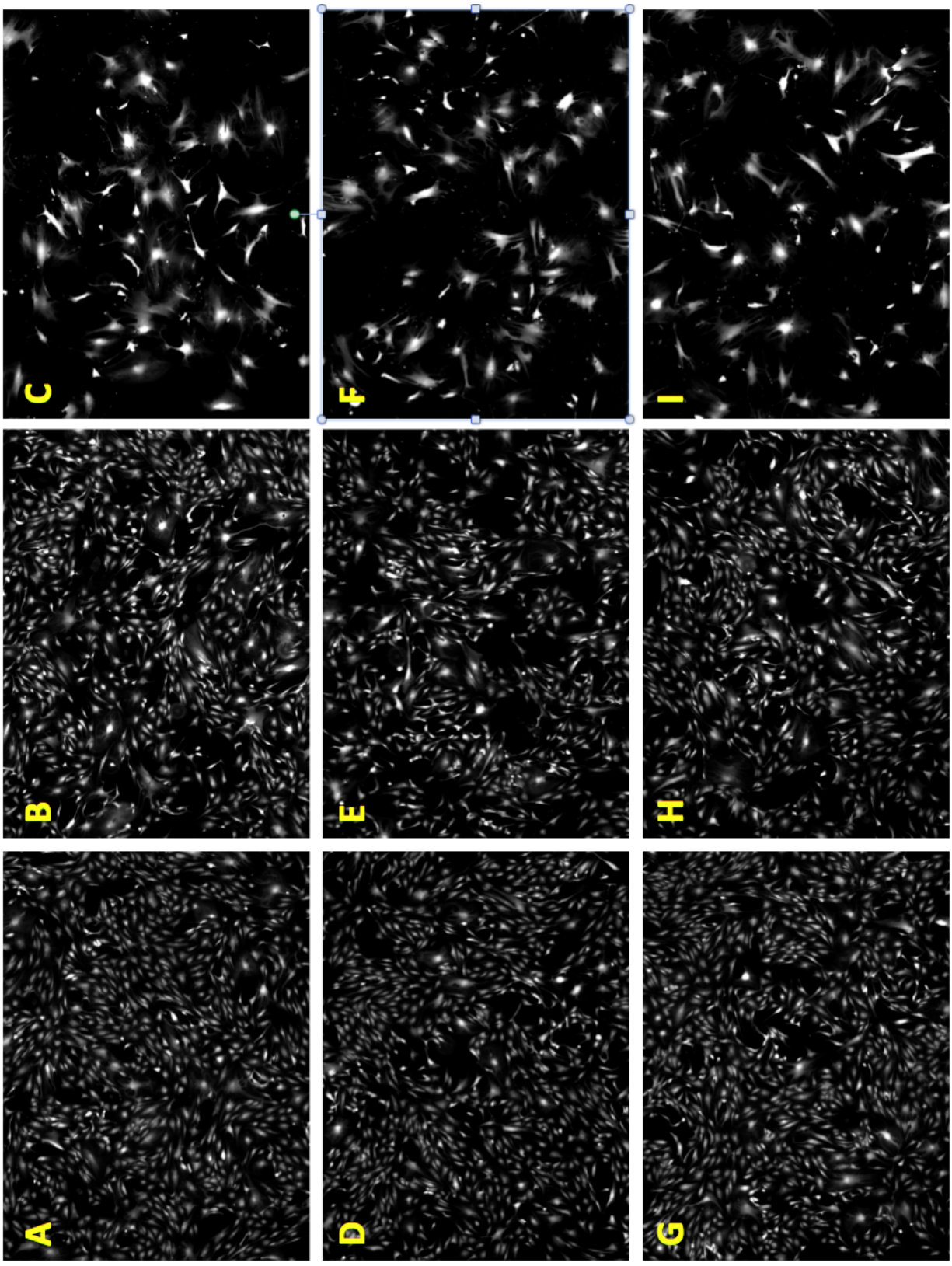

Figure 3.20: Tenocyte monolayer visualized with Live stain, Day=5. Data from 1 patient, cell passage P3. Magnification x400. A-D-G are 5 mM, B-E-H are 17 mM, C-F-I are 30 mM glucose cells.

by extracellular or intracellular signals. In this project I aimed to determine the levels of apoptosis in different glucose concentrations by the TUNEL assay. The assay was optimized and data for 2 patients collected. Preliminary analysis did not uncover any striking differences between the 8 and 38 mM glucose conditions. Full analysis was not achieved in time of this project submission: while total cell count can be automated, TUNEL-stained cells need to be manually assessed.

3.3.4 Aim 4: to determine the effect of glucose on tenocyte ECM synthesis and breakdown

Expression of *COL1A1* and *COL3A1* is upregulated in both 17 mM and 30 mM glucose

The most abundant collagen in tenton tissue (type I) and the fibrillar collagen III, encoded by *COL1A1* and *COL3A1* respectively, are both significantly upregulated in response to 17 mM and 30 mM glucose at the mRNA level (figure 3.21).

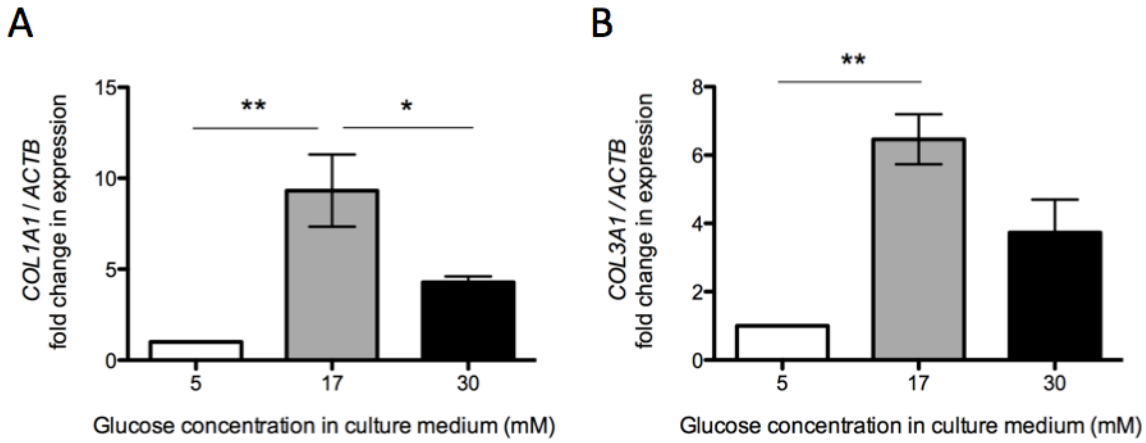

Figure 3.21: Collagen mRNA expression following culture in different glucose media (3 patients). A) collagen type I alpha 1 chain, B) collagen type III alpha 1 chain. Tenocytes were cultured in 5, 17 and 30 mM glucose medium, all were cell passage P4. RNA was extracted, converted to cDNA and qPCR quantified using SYBR Green. β-actin (*ACTB*) served as housekeeper gene. Error bars represent SEM. 5 mM n=2 patients, 17 mM n=2 patients, 30 mM n=3 patients. N too small to determine data normality. One-way ANOVA and Tukey as *post-hoc* test. A) ANOVA p value = 0.0026, B) p = 0.0096.

Soluble collagen is decreased in 38 mM glucose at the protein level

Data from 3 patients suggest that 2 out of 3 patients had equivalent levels of secreted collagen in 8 and 17 mM glucose but a decrease in 38 mM glucose medium. The third patient showed an increase at both 17 and 38 mM glucose however this increase was less at 38 mM, as determined by Sircol assay (figure 3.22).

Proteoglycans are upregulated on the mRNA level following culture in high glucose

In this project, the gene expression of four proteoglycans (PGs) was measured to assess the extent to which these key ECM components are modulated by elevated glucose levels.

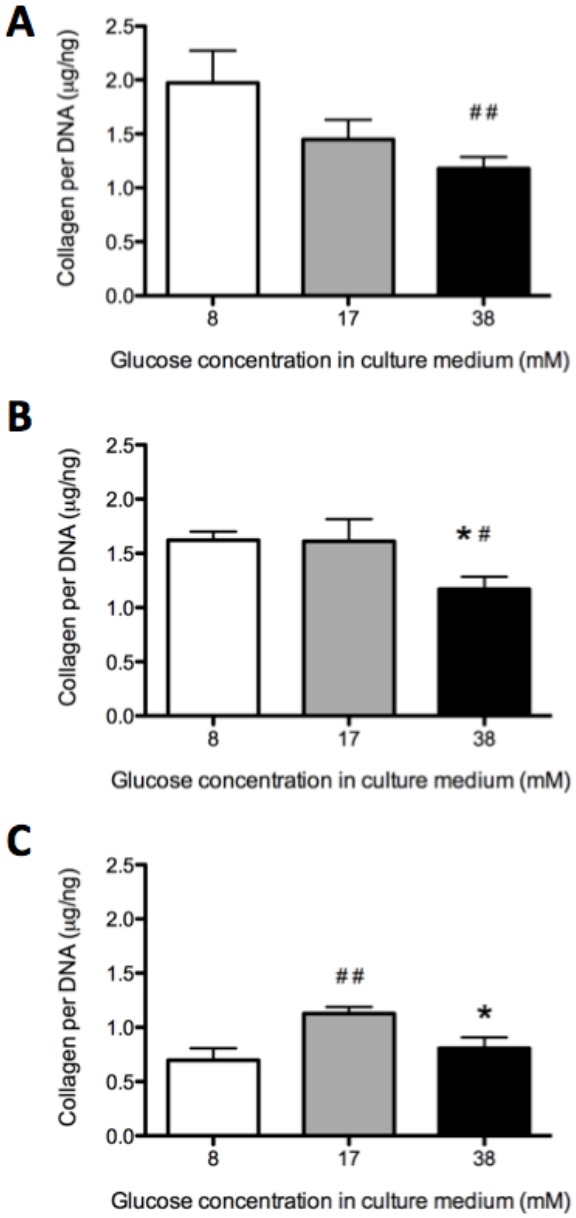

Figure 3.22: Glucose effect on soluble collagen output in human primary tenocytes, as determined by colorimetric Sircol assay. A) Patient 1, B) Patient 2, C) Patient 3. Cells grown on 12-well plates in medium that was supplemented with proline (50 g/ml) and L-ascorbic acid-2-P (50 g/ml). Culture medium collected after 4 days and after further 3 days, and combined together. Assayed as per manufacturer's instructions; resulting absorbency measured at 540 nm. Collagen values normalized to cell number using PicoGreen DNA measurement from cell layer of corresponding samples. Columns represent a mean value of 3 data points. D'Agostino-Pearson test for normality (n too small to determine), one-way ANOVA and Tukey *post-hoc* test. Statistical significance indicated: * is vs. 17 mM; # is vs. 8 mM. Error bars represent SD.

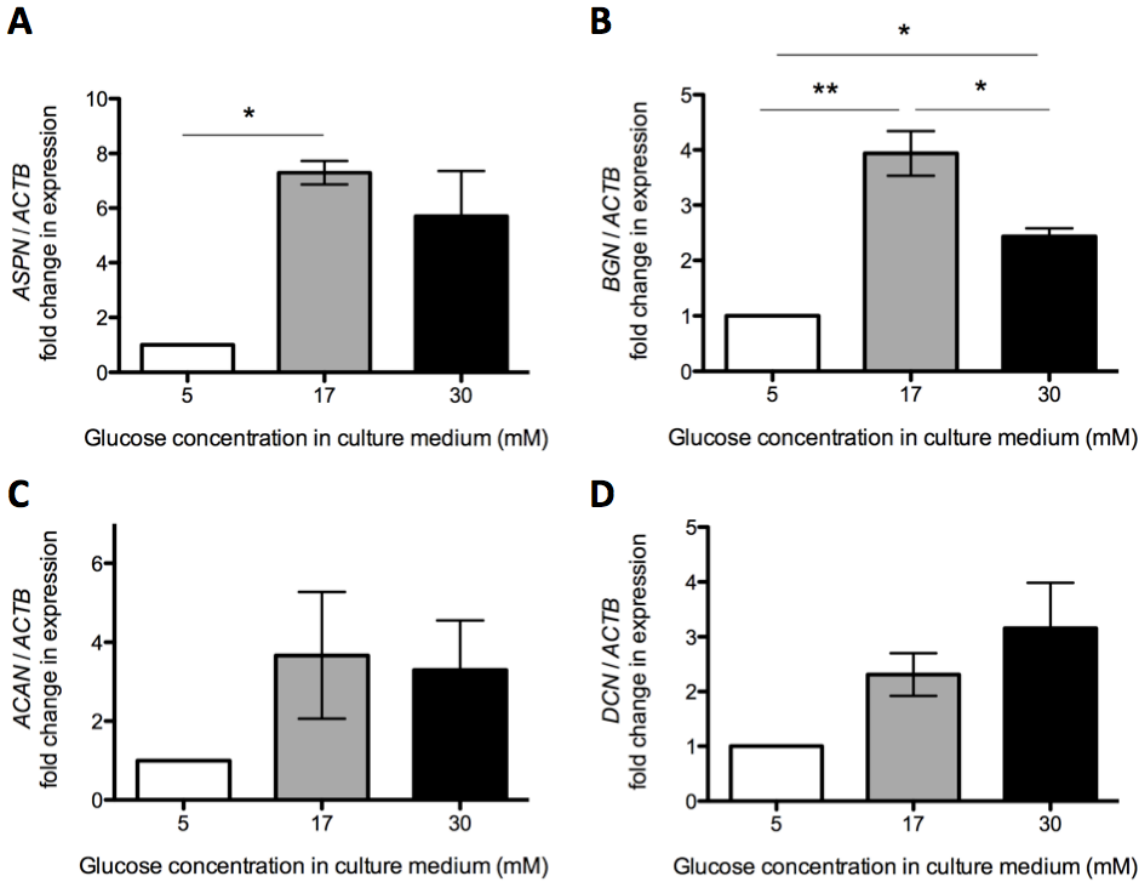

Figure 3.23: PGs expression following culture in different glucose media. A) Asporin *ASPN*, B) biglycan *BGN*, C) aggrecan ACAN, and D) decorin DCN. Tenocytes were cultured in 5, 17 and 30 mM glucose medium, all were cell passage P4. RNA was extracted, converted to cDNA and qPCR quantified using SYBR Green. β-actin (*ACTB*) served as housekeeper gene. 5 mM n=2 patients, 17 mM n=2 patients, 30 mM glucose n=3 patients. N too small to determine normality (D'Agostino & Pearson, and Shapiro-Wilk normality tests). One-way ANOVA and Tukey *post-hoc* test. A) ANOVA p value = 0.0256, B) p value = 0.0025, C) p value = 0.3909, D) p value = 0.1964. Error bars represent SEM.

Asporin (core protein encoded by *ASPN*) is a leucine-rich repeat PG. It competes with decorin for collagen I binding (123), and belongs to the same sub-family of small leucine-rich proteoglycans as for example biglycan and decorin (124). Asporin has been shown to play an important role in cartilage homeostasis and OA pathogenesis (124, 125), and was selected as target due to availability of primers in our laboratory. Biglycan (protein *BGN*) is a leucine-rich repeat PG that contains 2 GAG chains. Aggrecan (protein *ACAN*) is a chondroitin sulfate PG. Decorin (protein *DCN*) is a leucine-rich PG that binds to type I collagen fibrils. All 4 were found to be upregulated in response to 17 and 30 mM glucose (figure 3.23).

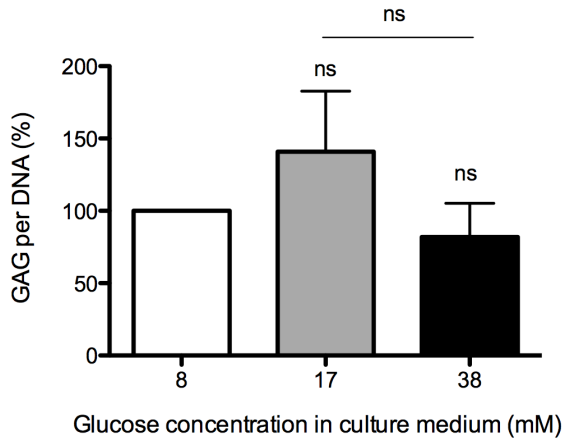

Figure 3.24: GAG secretion by human primary tenocytes following culture in varying glucose conditions (data from 3 patients). GAGs were quantified from cell layer of 12-well plates. Results were normalized to DNA content using PicoGreen measurement. 8 mM glucose condition was set as 100% in order to combine absolute values of 3 patients. Columns represent a mean value of 3 data points. *N* too small to determine normality (D'Agostino & Pearson, and Shapiro-Wilk normality tests), one-way ANOVA and Tukey *post-hoc* test. Error bars represent SEM.

Secreted GAGs remain unaltered at the protein level

The output of total sulphated GAGs is stable across the entire range of glucose conditions, as determined by the DMB assay (figure 3.24).

MMP2 expression in glucose-treated cells

Matrix metalloproteinases (MMPs) are enzymes responsible for breakdown of collagen and other ECM molecules. MMP-1, -2, -8, -13 and -14 possess enzymatic activity against fibrillar collagen (9). Increased MMP levels and their activity could lead to enhanced collagen degradation. In this project MMP-2, -9 and -13 were investigated at the mRNA level as these were expected to be the most glucose-sensitive based on the literature (126, 127, 128, 129, 130). Based on data from 3 patients, the expression of MMP-2 is indicating upregulation in 30 mM glucose compared to 5 mM glucose, although not statistically significant (figure 3.25). Expression of MMP-9 and MMP-13 was tested without success. Since these two MMPs have been detected in tendon by other researchers we assumed that the primers failed; a positive qPCR control was not available to check.

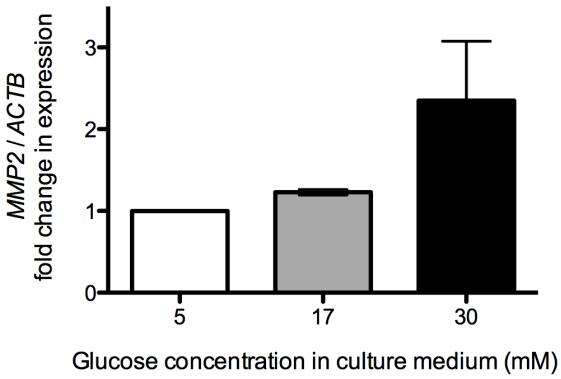

Figure 3.25: Effect of glucose on *MMP2* expression in primary human tenocytes (3 patients). Tenocytes were cultured in 5, 17 and 30 mM glucose medium, all cells were passage P4. RNA was extracted, converted to cDNA and qPCR quantified using TaqMan. β-actin (*ACTB*) served as housekeeper gene. 5 mM n=2 patients, 17 mM n=2 patients, 30 mM n=3 patients. Error bars represent SEM. N too small to determine normality (D'Agostino & Pearson, and Shapiro-Wilk normality tests). One-way ANOVA (p value = 0.2953) and Tukey *post-hoc* test. Note that negative RT control failed for both MMP-2 and β-actin: observed amplification in controls that had similar CT values as samples.

3.3.5 Aim 5: to determine the effect of glucose concentration on oxidative stress-responsive proteins in tenocytes

Response of the superoxide dismutase multigene family and catalase to 17 mM and 30 mM glucose on mRNA level

The family of superoxide dismutases (SODs) constitutes the first and most important line of an effective defense system against reactive oxygen species (ROS) that are a natural by-product of single electron reductions of molecular oxygen. SODs function by catalyzing the dismutation of superoxide anions. Three unique mammalian superoxide dismutases have been identified to date: superoxide dismutase SOD-1, SOD-2, and SOD-3 (figure 1.5)(75).

Furthermore, catalase is another key antioxidant enzyme which is implicated in oxidative stress defence. It converts the ROS H_2O_2 into water and oxygen and in this manner helps to diminish the harmful effects of H_2O_2.

In this project, all three SODs and catalase were examined (figure 3.26). The figure shows that SOD-1 gene expression did not change in response to glucose. SOD-2 is the gene that demonstrated the most responsiveness to glucose, as it was significantly upregulated ($\sim$ 12-fold) in 17 mM glucose and $\sim$ 5-fold in 30 mM glucose, both compared to 5 mM control glucose. SOD-3 demonstrated $\sim$ 2.5-fold upregulation in 30 mM glucose condition compared to control, while catalase showed $\sim$ 3-fold increase in 17 mM glucose, and $\sim$ 2-fold increase in 30 mM glucose compared to control.

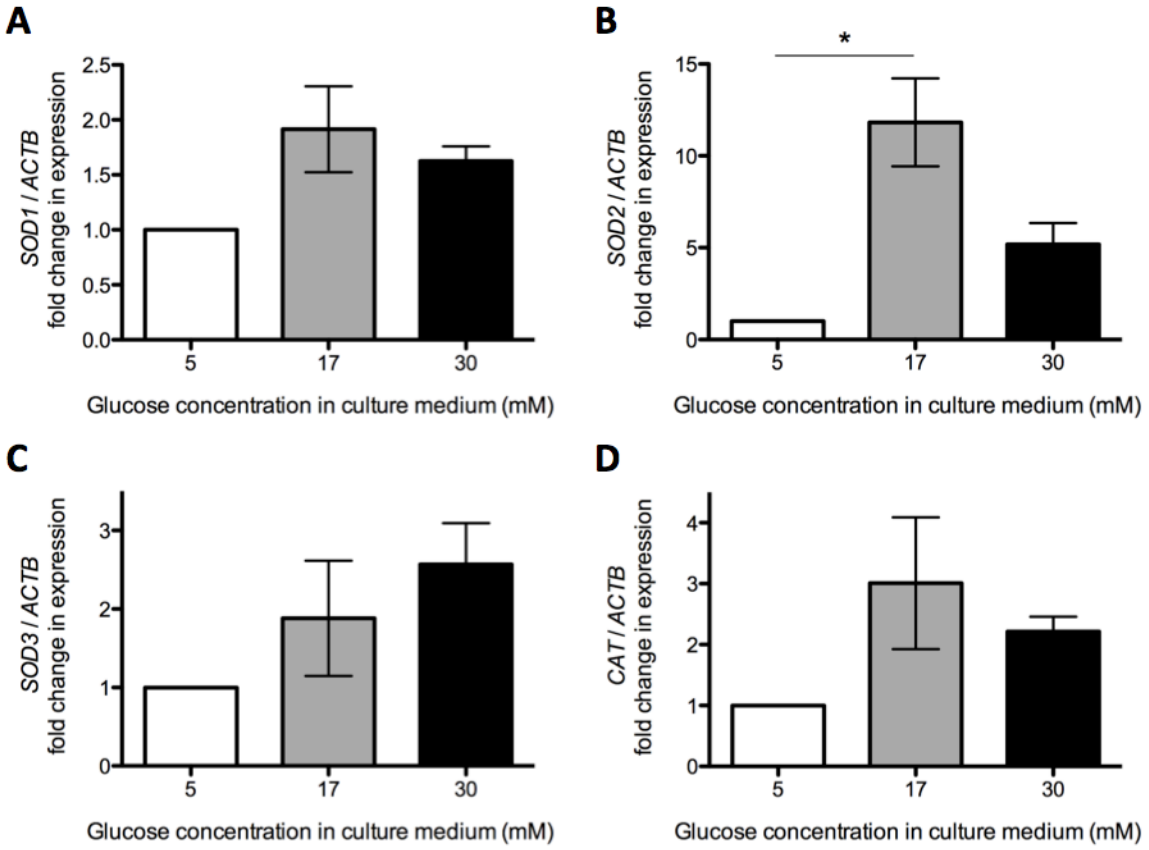

Figure 3.26: SOD-1, SOD-2, SOD-3 and catalase mRNA expression following culture in different glucose media. A) *SOD1*, B) *SOD2*, C) *SOD3*, D) *CAT*. Tenocytes were cultured in 5, 17 and 30 mM glucose media. All cells were passage P4. RNA was extracted, converted to cDNA and qPCR quantified using SYBR Green. β-actin (*ACTB*) served as housekeeper gene. 5 mM n=2 patients, 17 mM n=2 patients, 30mM n=3 patients. All graphs: n too small to determine normality (D'Agostino & Pearson, and Shapiro-Wilk normality tests). Error bars represent SEM. One-way ANOVA and Tukey *post-hoc* test. A) ANOVA p value = 0.1008, B) p value = 0.0196, C) p value = 0.2312, D) p value = 0.1571.

3.3.6 Aim 6: to determine the effect of glucose concentration on cell migration & proliferation capacity of tenocytes

Migration rate of tenocytes following scratch decreases both with glucose dose and dose duration

Delayed wound healing is one of the known complications of DM, currently affecting about 15% of DM patients (131). In general, skin wound healing requires coordination of several cell types, and consists a number of processes that include fibroblast proliferation and migration, collagen deposition and remodelling, wound contraction, and angiogenesis. It has been demonstrated that 30 mM glucose delays cell migration in human foreskin primary fibroblasts (131). Also, tendon remodelling and healing has been shown to be impaired in diabetic rats following injury. This was concluded from reduction in inflammatory cell numbers, less newly-formed blood vessels, and less proliferating cells in diabetic rats compared with either normal rats or insulin-treated rats (98).

Here I looked at the effect of chronic glucose treatment on human tenocyte migration and proliferation (often termed 'scratch assay'). Figure 3.27 provides a representation of Live-stained cells during the experiment.

In this experiment, cell migration is represented by the cells growing (i.e. proliferating and/or migrating) into the scratch area after 24, 48 and 72 h following scratch. Data of patient 1 (figure 3.28) suggest inhibition of 20% FCS-enhanced cell migration in 38 mM glucose. The 24 h and 48 h time points do not display any difference between 8 mM and 38 mM condition. As the time progresses, in the 72 h time point it is apparent that the cell migration rate in 38 mM glucose is lowered overall and, moreover, the ability of 20% FCS to stimulate the cells is lost in this glucose condition, compared to both 8 and 17 mM glucose conditions.

Data of patient 2 (figure 3.29) confirms the results of patient 1. In the 24 h time point, there is little difference apparent across the glucose conditions. The 48 h time point shows dramatic decrease of cell migration in both 17 and 38 mM glucose, while the 72 h time point clearly indicates the harmful effects of elevated glucose to the monolayer.

Data for a third patient were collected (360 microscopy images) however a preliminary analysis of the 72 h time point showed that positive control likely failed thus no more analysis was performed.

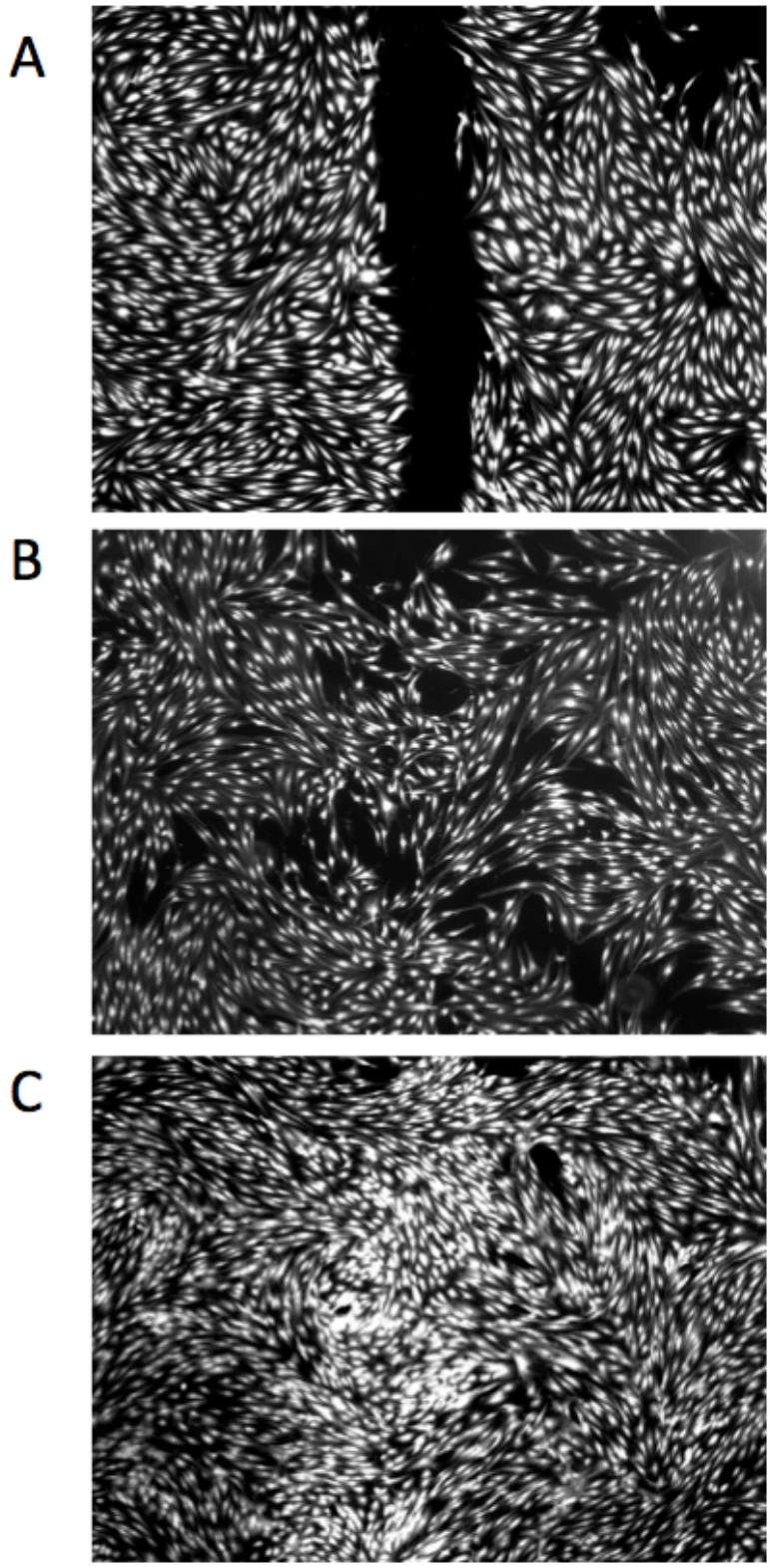

Figure 3.27: Representation of the scratch assay; tenocytes visualized by Live stain. A) tenocyte monolayer immediately following scratch, 5% FCS 38 mM glucose condition, B) untreated tenocyte monolayer 48 h after scratch, 5% FCS 38 mM glucose, C) 20% FCS-treated tenocyte monolayer 48 h after scratch, 20% FCS 38 mM glucose. 20% FCS-stimulated cells (positive control) migrate at a faster rate than untreated cells, as expected.

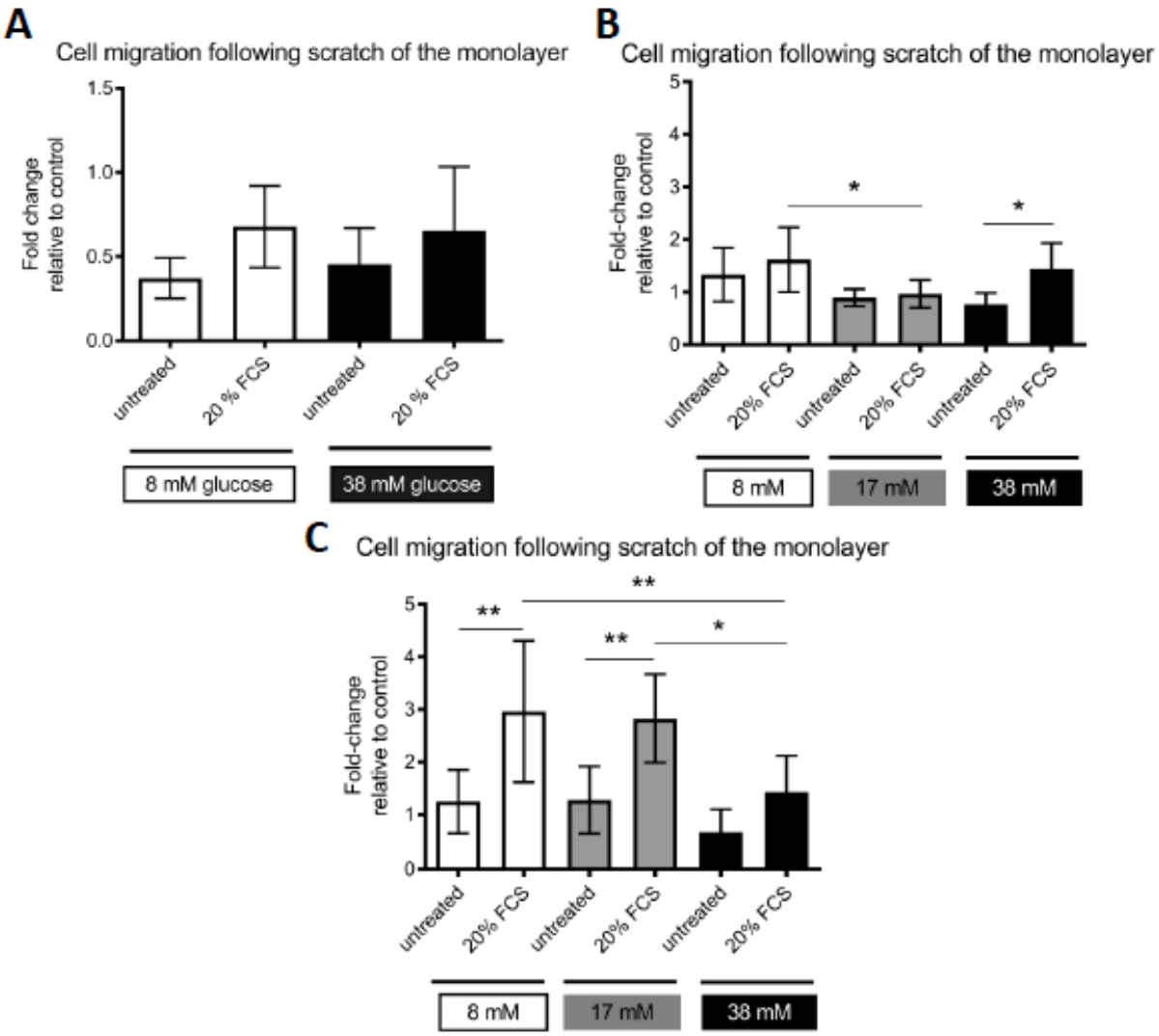

Figure 3.28: Effect of varying glucose concentration on migration of human tenocytes (patient 1). A) 24 h after scratch, B) 48 h after scratch, C) 72 h after scratch. Tenocytes chronically cultured in 8, 17 and 38 mM glucose media. Two treatment options (none and additional FCS) were used within each glucose condition. 20% FCS served as positive control. Cell migration is represented by the cells growing into the scratch area following scratch. Quantified as surface area covered with cells, then expressed as ratio of surface area entirely covered with cells if never scratched (of "unscratched untreated" = control). All normalized to unscratched untreated. Each column represents a mean value of 8 data points. All one-way ANOVA and Tukey. Error bars represent SD. "Untreated" = scratched but untreated cell migration, FCS = 20% fetal calf serum. Note that A was performed during a different repeat than B and C, but still on same patient. A) Two groups within this data are non-normally distributed (D'Agostino & Pearson normality test). All statistics was 'ns'. B) Data normally distributed (D'Agostino & Pearson normality test). Only statistics of interest is indicated in graph. C) Two groups within this data are non-normally distributed (D'Agostino & Pearson normality test). Only statistics of interest is indicated in graph.

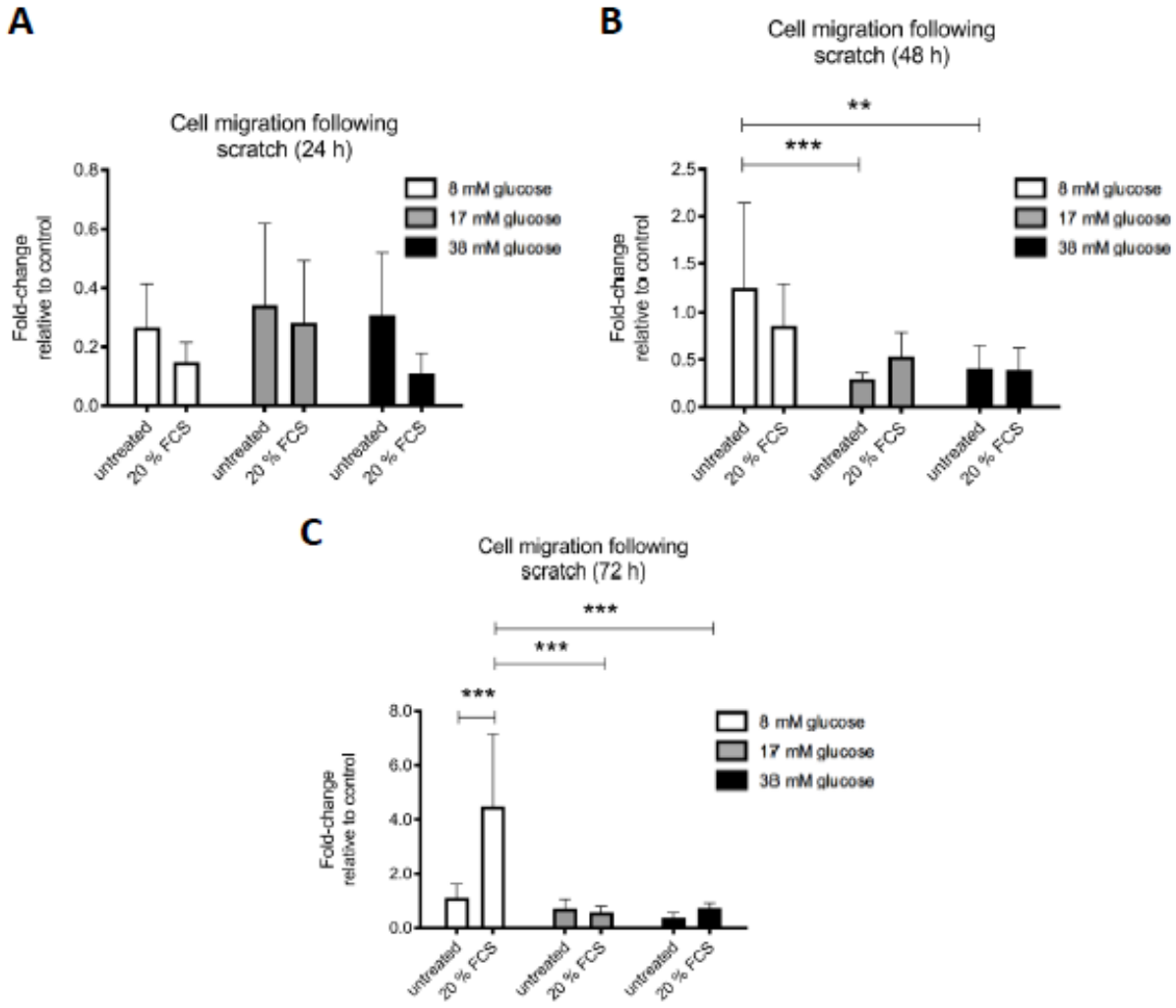

Figure 3.29: Effect of varying glucose concentration on migration of human tenocytes (patient 2). A) 24 h after scratch, B) 48 h after scratch, C) 72 h after scratch. Tenocytes chronically cultured in 8, 17 and 38 mM glucose media. Two compound options (none and additional FCS) within each glucose condition. 20% FCS served as positive control. Cell migration is represented by the cells growing into the scratch area following scratch. Quantified as surface area covered with cells, then expressed as ratio of surface area entirely covered with cells if never scratched (of "unscratched untreated" = control). All normalized to unscratched untreated. "Untreated" = scratched but untreated cell migration, FCS = 20% fetal calf serum. Each column represents a mean value of 8 data points. All one-way ANOVA and Tukey. Error bars represent SD. A) One group within this data is non-normally distributed (D'Agostino & Pearson normality test). All statistics of interest was 'ns'. B) One group within this data is non-normally distributed (D'Agostino & Pearson normality test). Only statistics of interest is indicated in graph. C) One group within this data is non-normally distributed (D'Agostino & Pearson normality test). Only statistics of interest is indicated in graph.

3.3.7 Aim 7: to examine rat tail tissue for effects of STZ-induced uncontrolled T1D: Hematoxylin & Eosin stain highlights rat tail structures

The previous part of this research project has been performed *in vitro* on primary human tenocytes. This next section of the project are pilot experiments on rat tissue examining some of the targets of interest. The tissue was from T1D rats which unlike my cell cultures had no insulin present. However they experienced 16 weeks of uncontrolled diabetes, presenting similar glucose levels [1] and even longer time of exposure than my cell cultures. Immunohistochemistry (IHC) was performed on cross sections of rat tails and on tendon fascicles, both from STZ-induced type 1 diabetic rats and control rats. Using STZ to induce experimental T1D in animals is a widely accepted method. The technique leads to selective destruction of β-cells in pancreatic islets.

General tail and tendon structures were assessed by Hematoxylin & Eosin (H & E) stain. **Tail cross sections** and isolated **tendon fascicles** from the tails were both examined. Figure 3.30 shows tendon tissue (A, D), isolated tendon fascicles (B, E), and muscle tissue (C, F). Figure 3.31 illustrates bone and cartilage (A, D), nerve (B, E), and skin structures (C, F). Overall, the histology of all displayed tissues appears to be normal.

[1] Refer to Human & animal samples section in Chapter 2 for precise glucose values.

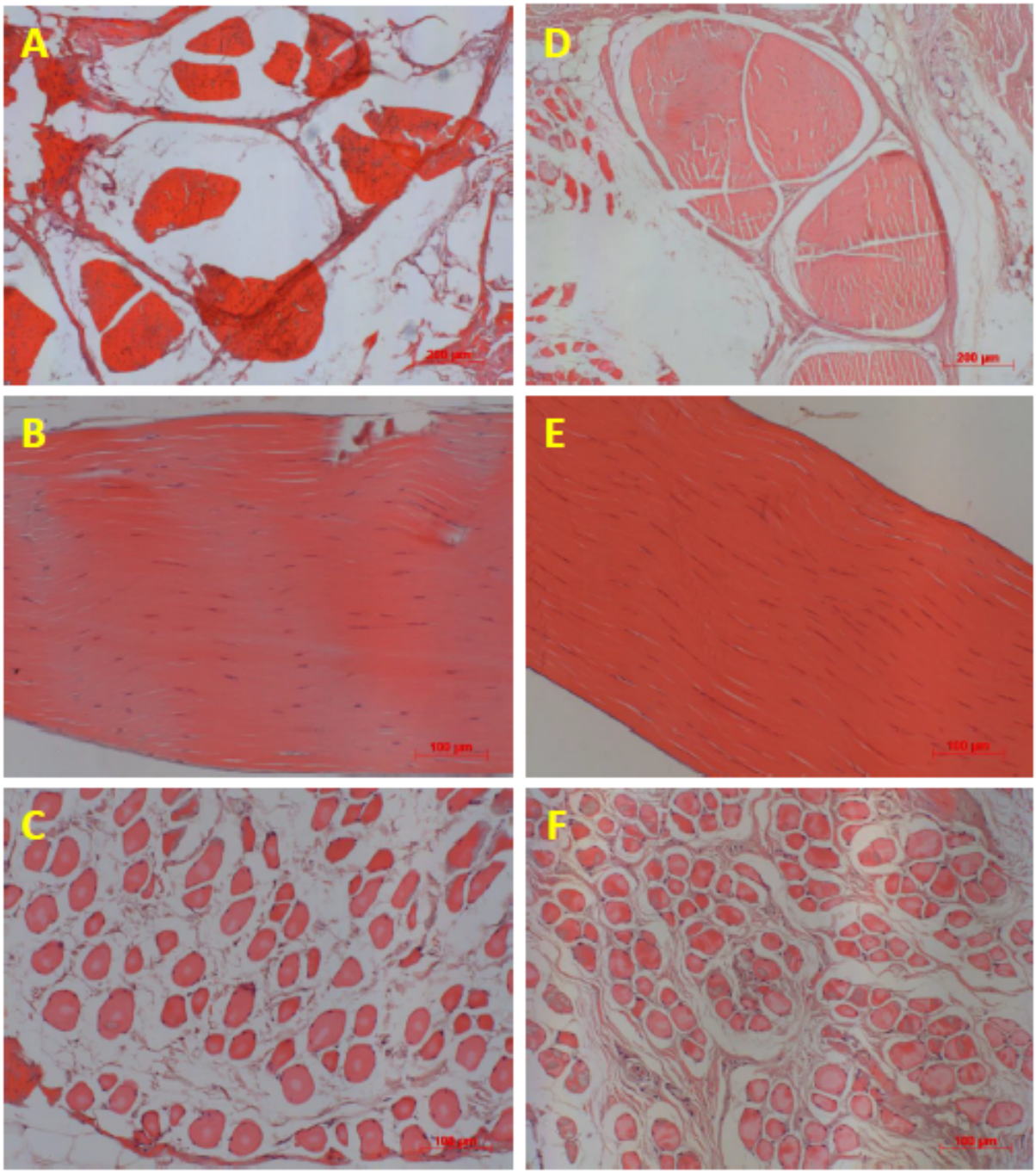

Figure 3.30: IHC images of rat tail cross sections (A, C, D, F) or rat tail tendon fascicles (B, E). Structures are highlighted by H & E stain. Control tissue (A-C), diabetic tissue (D-F). A) tendon, magnification x100. B) longitudinal section, magnification x200. C) skeletal muscle, magnification x200. D) tendon, magnification x100. E) longitudinal section, magnification x200. F) skeletal muscle, magnification x200.

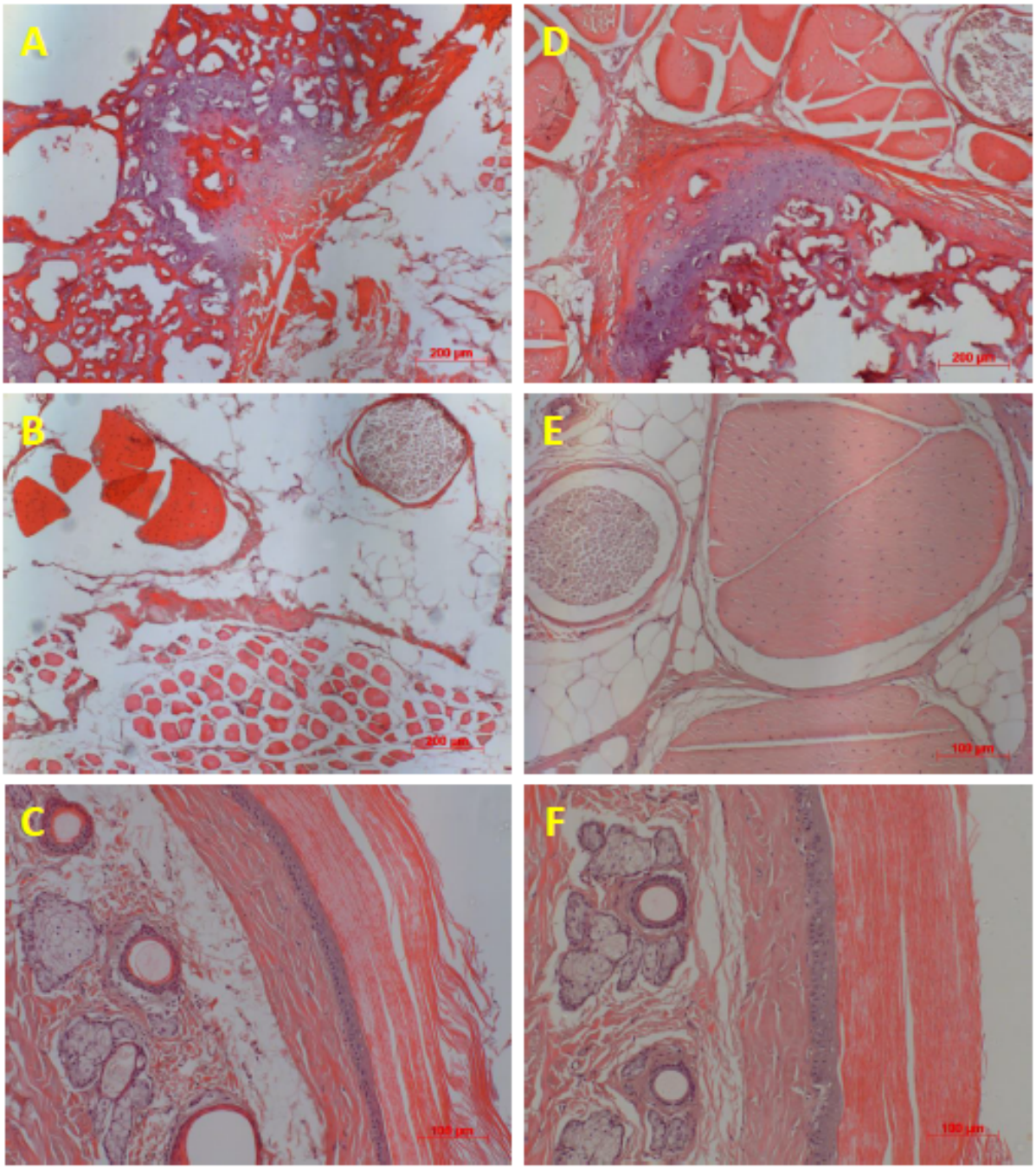

Figure 3.31: IHC images of rat tail cross sections. Structures are highlighted by H & E stain. Control tissue (A-C), diabetic tissue (D-F). A) bone and cartilage, magnification x100. B) nerve, tendon and skeletal muscle, magnification x100. C) epidermis, dermis and subcutaneous layer, magnification x200. D) bone, cartilage and tendon, magnification x100. E) nerve and tendon, magnification x200. F) epidermis, dermis and subcutaneous layer, magnification x200.

3.3.8 Aim 7: to examine rat tail tissue for effects of STZ-induced uncontrolled T1D: 3-nitrotyrosine as indicator of nitroxidative stress

The following sections give data of pilot experiments that suggest the role of elevated glucose in 3-nitrotyrosine (3NT) and Forkhead box protein O1 (FOXO-1a) upregulation. Hyperglycamia is believed to be closely associated with both increased oxidative and nitrative stress; reactive oxygen and nitrogen species (ROS and RNS) are generated in excess under hyperglycemia. Accumulating evidence shows that both of these have a pathogenic role in the development of diabetes-associated complications (132, 133). Reactive nitrogen species are nitric oxide (NO) and NO-related molecules, and include 3NT, nitrogen dioxide and peroxynitrite. Once RNS are formed they can cause oxidation, nitrosation, and nitration of their targets, i.e. causing nitroxidative, nitrosative, and nitrative stress. It has been shown that there is a dominance of oxidative processes caused by RNS (as opposed to nitrosative or nitrative), and therefore the term 'nitroxidative' stress is preferred (134). One study reported the presence of 3NT in the plasma of all tested diabetic patients, whereas 3NT was not detectable in the plasma of healthy controls (135). Other researchers suggest that increased presence of 3NT proteins in tissues of diabetic patients is associated with diabetes-induced complications (136). 3NT was used in this project as a standard indicator of nitroxidative stress. Figure 3.32 shows that 3NT is upregulated in three diabetic rat tail tissues compared to the healthy control tissue. It is especially the muscle (D in the figure) where significant increase in 3NT can be seen, as well as in the diabetic skin (E) and tendon (F). These findings remain preliminary: specimens (i.e. microscopy slides with adherent rat cross sections) from one diabetic and one control rat were used for this 3-nitrotyrosine experiment.

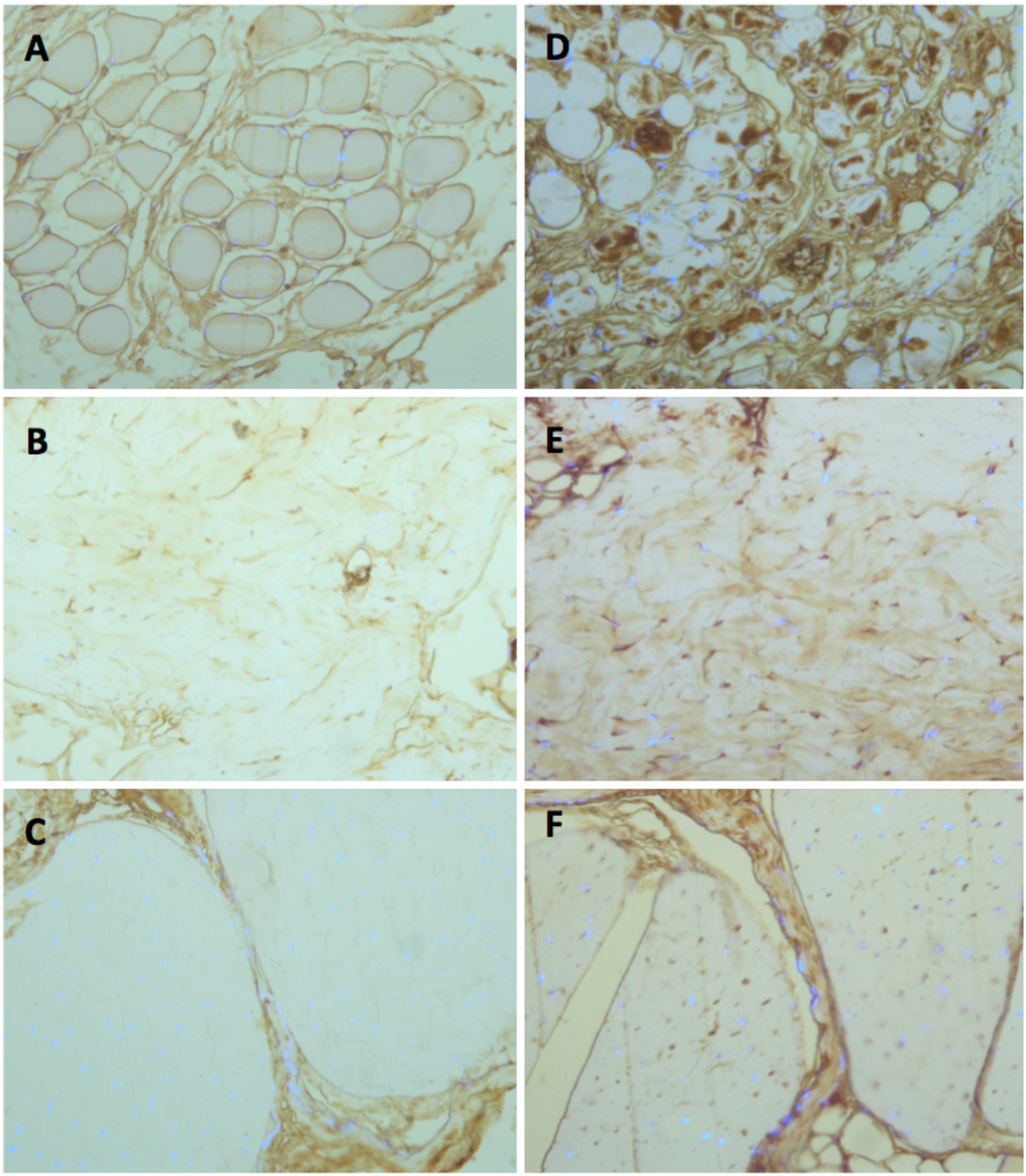

Figure 3.32: Immunolocalization of 3-nitrotyrosine as indicator of nitroxidative stress in healthy (A-C) and 16 week diabetic (D-F) rat tail tissue cross sections. Muscle A, D. Skin B, E. Tendon C, F. Primary antibody 3NT detected with DAB; DAPI are cell nuclei. Magnification 200x. Negative control not available. Photography courtesy of Assoc Prof Philippa Hulley.

3.3.9 Aim 7: to examine rat tail tissue for effects of STZ-induced uncontrolled T1D: evaluation of FOXO-1a levels in diabetic vs. healthy rats

Forkhead box O (FOXO) is a family of transcription factors that affect a wide range of cellular processes, for example metabolism, cell cycle regulation, apoptosis, cell survival and stress response; in this manner they play a far-reaching role in organismal tumour suppresion and longevity. More concretely, FOXOs translate a variety of environmental stimuli into specific gene-expression programmes (137). It has been shown that FOXOs are activated in response to OS. Under high ROS conditions, FOXOs translocate into the nucleus (they normally shuttle between the cytosol and nucleus) where they display an increased transcriptional activity. OS activates JNK kinase and JNK may phosphorylate FOXOs (138). However, FOXOs can also be (de-)acetylated and (de-)ubiquitinated in response to OS by other enzymes (73), as they are regulated by a combination of post-translational modifications (137). Target genes of FOXOs include SOD-2 and catalase (139).

FOXO1, sometimes termed FKHR, is one of the four members of the family; it is the marker that I studied in the rat tissues. Our research group previously confirmed the involvement of FOXO1 in oxidative stress response under 5 mM versus 17.5 mM glucose medium in cultured tendon cells (140). I aimed at taking these findings further by examining the animal tissues. In total, 6 control and 6 diabetic rats were used; 9 control and 9 diabetic specimens were used from these animals in this section.

Manual staining

Rat tissue was processed both manually and in an automated manner using Dako Autostainer Link 48. Figure 3.33 illustrates that rat tendon tissue does not show any apparent differences in FOXO1 levels. However in the same figure skeletal muscle is much more FOXO1-positive in T1D rats (the antibody employed recognizes both phosphorylated and unphosphorylated FOXO1A). The nerve tissue seems also very susceptible to elevated FOXO1 levels, as staining is much darker in T1D rat (figure 3.33).

In figure 3.34 the skeletal muscle diabetic morphology is visible, with diabetic tissue being more FOXO1-positive under both image magnifications. In figure 3.35 skin and sebaceous gland staining is equal (very dark) in both experimental and control samples,

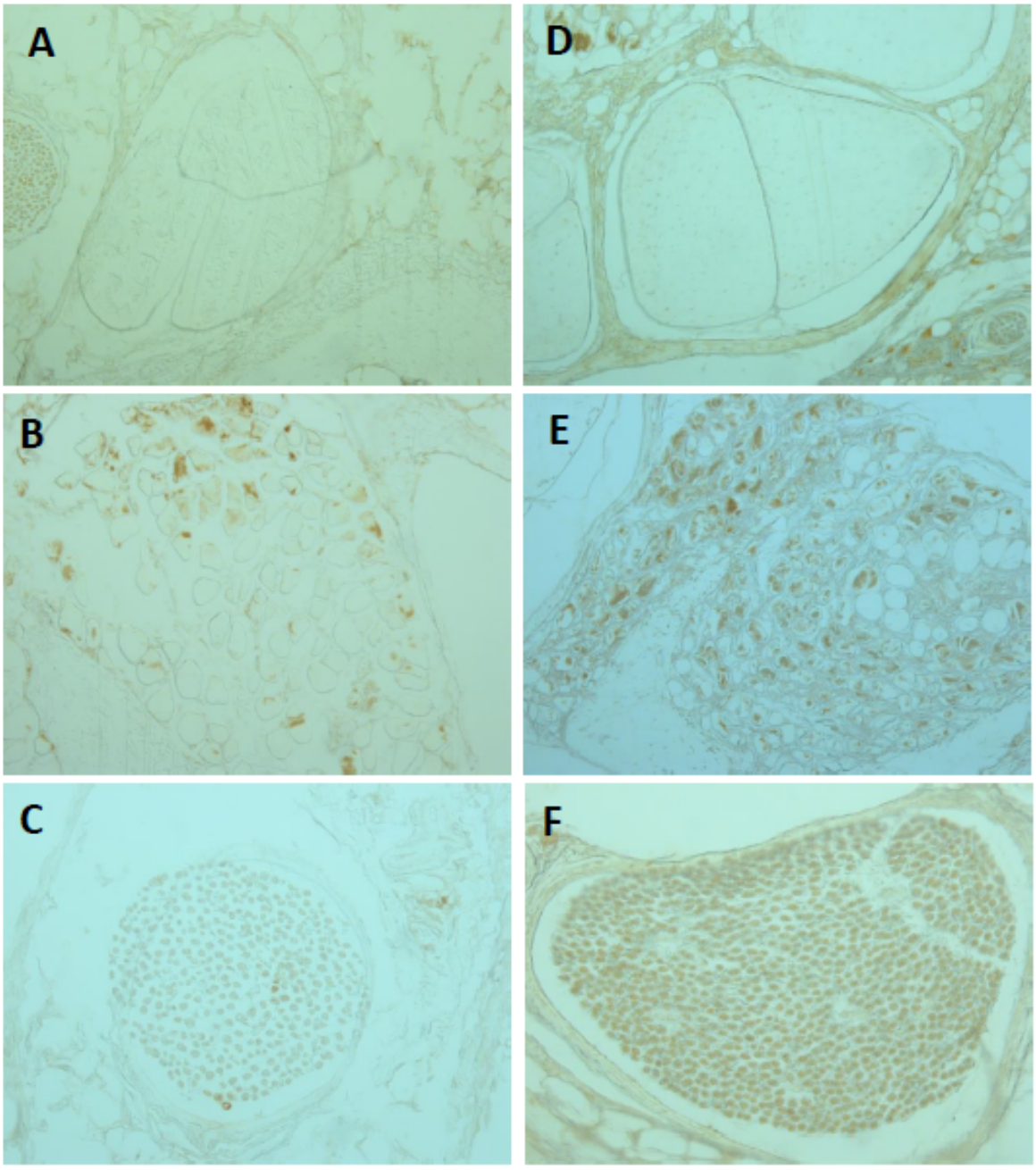

Figure 3.33: FOXO1A levels in diabetic vs. control rat tail tissue cross sections. Control (A-C) and 16 week diabetic (D-F) rat tail tissue. Tendon A, D. Skeletal muscle B, E. Nerve C, F. Primary antibody FOXO1A was detected with DAB stain. Magnification 100x (A, B, D, E), 200x (C, F).

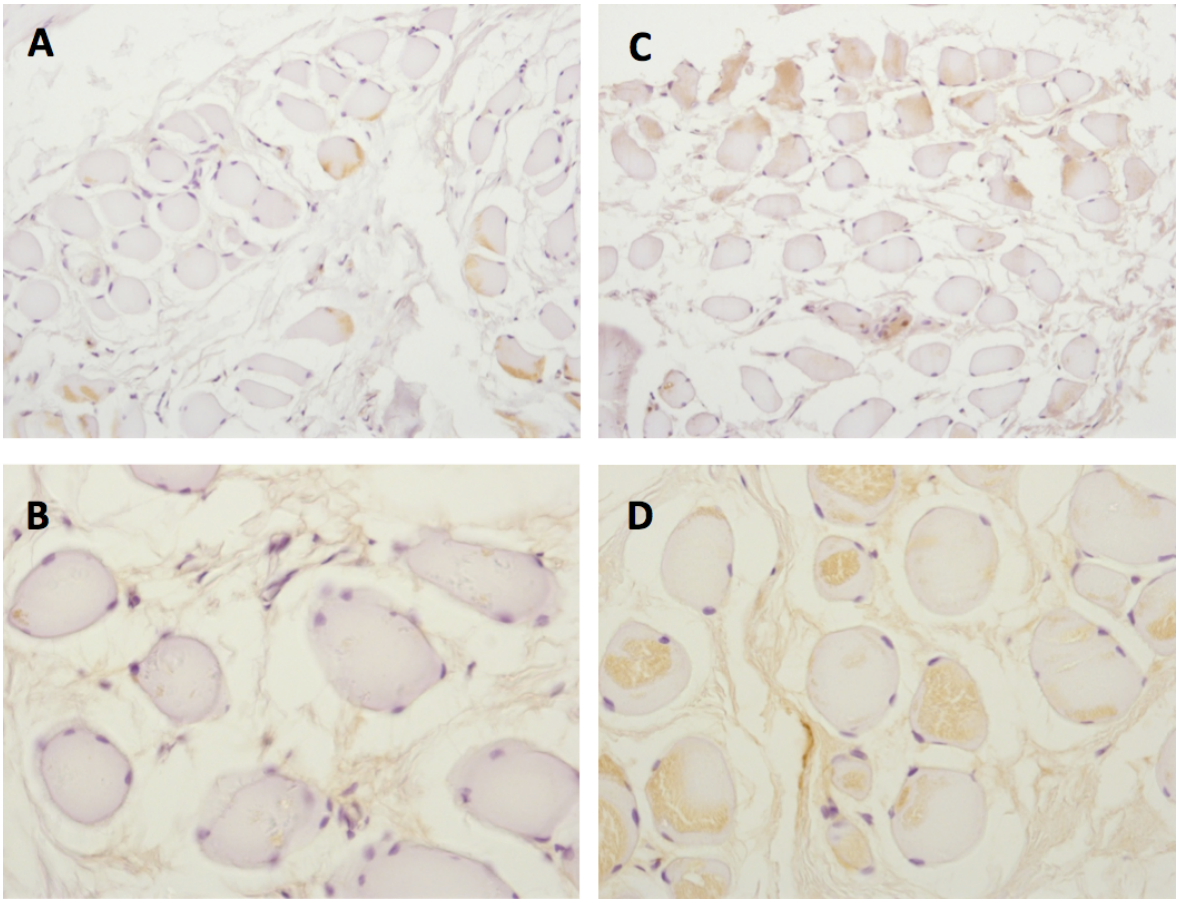

Figure 3.34: FOXO1A levels in diabetic vs. control rat skeletal muscle tissue cross sections. Control (A, B) and 16 week diabetic (C, D) rat tail tissue. Primary antibody FOXO1A was detected with DAB stain, while nuclear stain used was Hematoxylin. Magnification A, C 200x, B, D 400x. Photography courtesy of Assoc Prof Philippa Hulley.

while nerve bundles and tendon sheath are similarly stained across tested conditions. In high magnification tendon figures (3.36 and 3.37) it can be seen that tendon is similar across both conditions with overall very scarce FOXO1 stain. In figure 3.37 arrows indicate cells with more intense FOXO1 stain.

Automated staining

In figure 3.38 it can be seen that skeletal muscle is more FOXO1-positive in the diabetic samples (C) than in control (A); this confirms the previous findings. The skin seems to be very FOXO-positive in both diabetic and control (and even more so in the diabetic), which confirms previous findings. Lastly, the isotype control (figure 3.39) did not present any brown-coloured DAB stain, as expected.

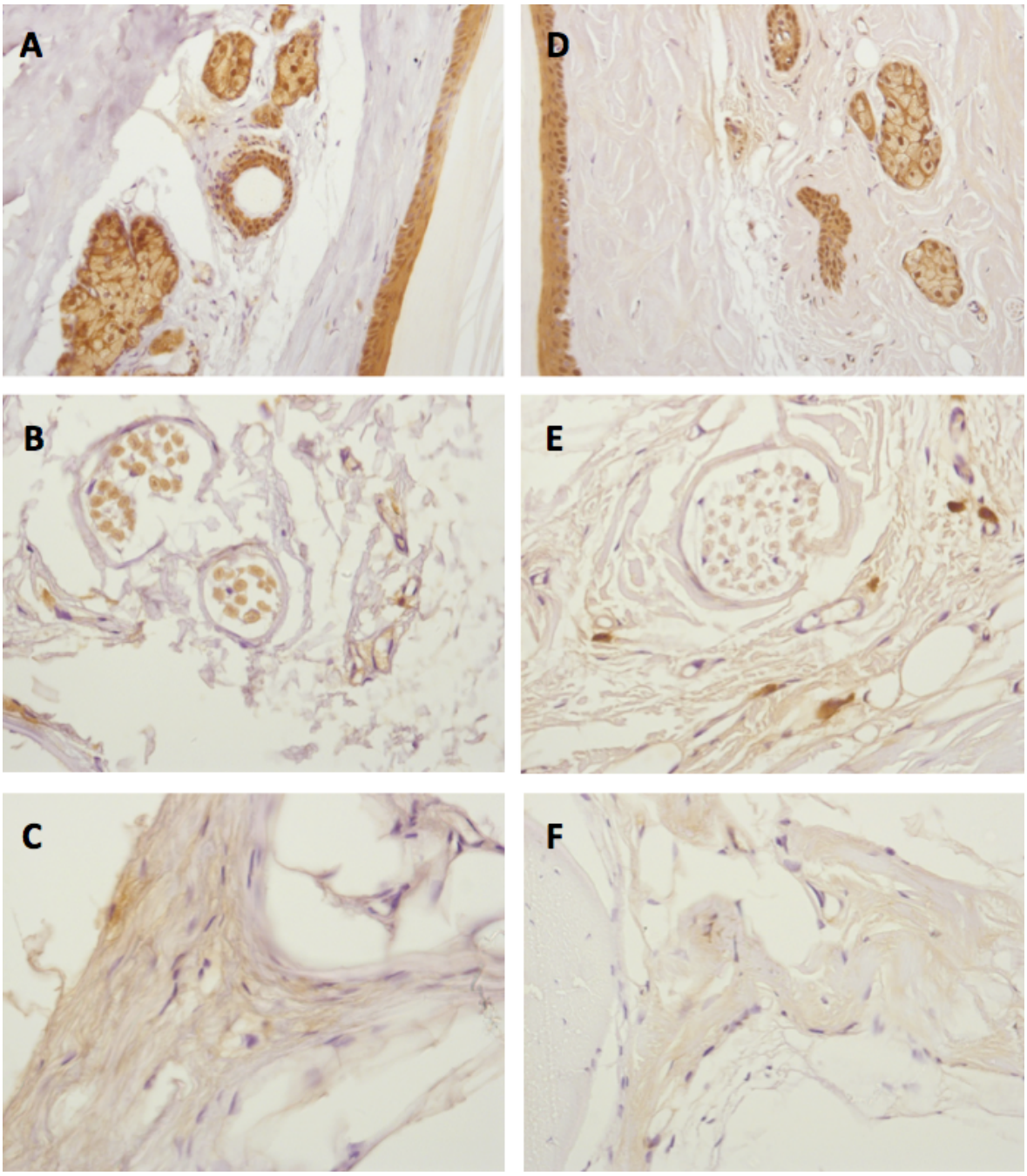

Figure 3.35: FOXO1A levels in diabetic vs. control rat tissue cross sections. Control (A-C) and 16 week diabetic (D-F) rat tail tissue. Skin A, D, nerve B, E, tendon sheath C, F. Primary antibody FOXO1A was detected with DAB stain, while nuclear stain used was Hematoxylin. Magnification A, B, D, E 200x, C, F 400x. Photography courtesy of Assoc Prof Philippa Hulley.

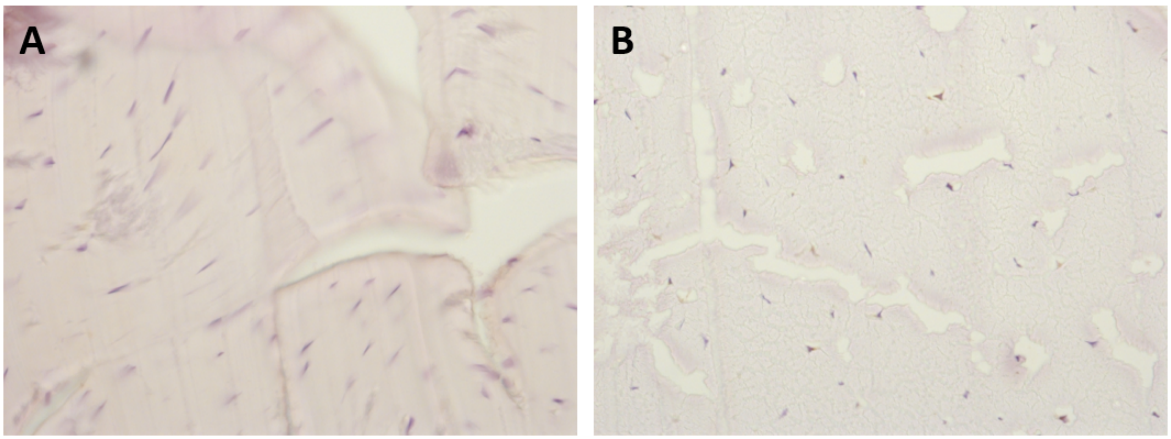

Figure 3.36: FOXO1A levels in diabetic vs. control rat tendon tissue cross sections. Control (A) and 16 week diabetic (B) rat tail tissue. Primary antibody FOXO1A was detected with DAB stain, while nuclear stain used was Hematoxylin. Magnification 400x. Photography courtesy of Assoc Prof Philippa Hulley.

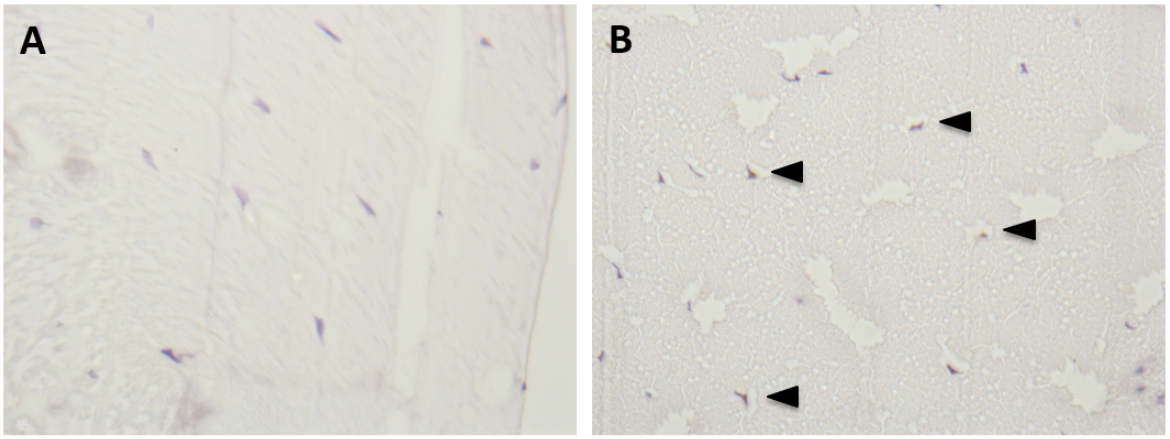

Figure 3.37: FOXO1A levels in diabetic vs. control rat tendon tissue cross sections. Control (A) and 16 week diabetic (B) rat tail tissue. Primary antibody FOXO1A was detected with DAB stain, while nuclear stain used was Hematoxylin. Magnification 600x. Arrows indicate cells with more pronounced FOXO1A stain. Photography courtesy of Assoc Prof Philippa Hulley.

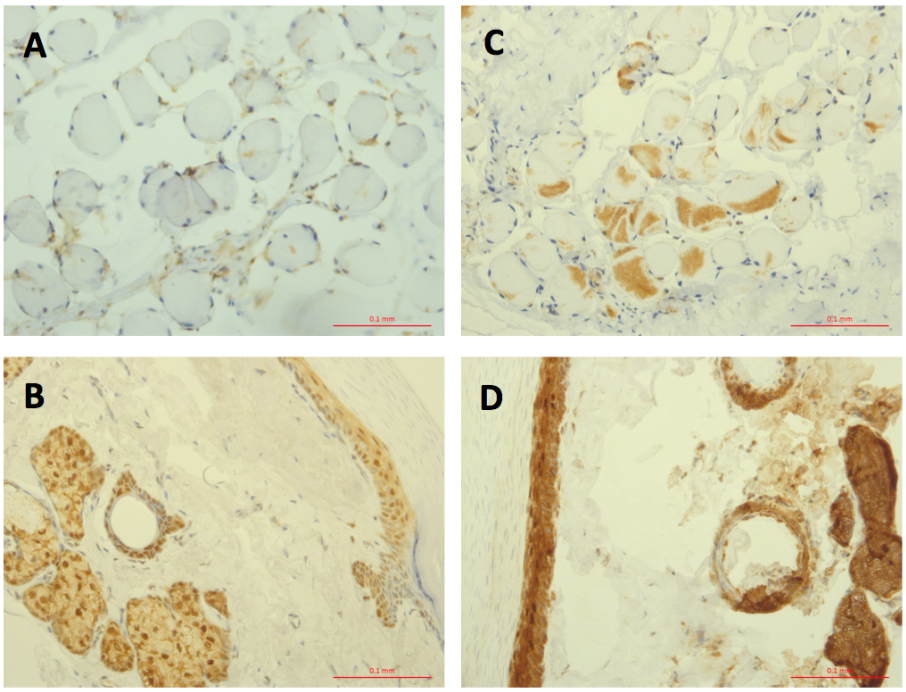

Figure 3.38: FOXO1A levels in diabetic vs. control rat tissue cross sections, assessed by Dako Autostainer Link 48. Control (A, B) and 16 week diabetic (C, D) rat tail tissue. Muscle A, C. Skin B, D. Primary antibody FOXO1A was detected with DAB stain, while nuclear stain used was Hematoxylin. Magnification 200x. Note that images are derived from 3 different rats (2 control and 1 diabetic).

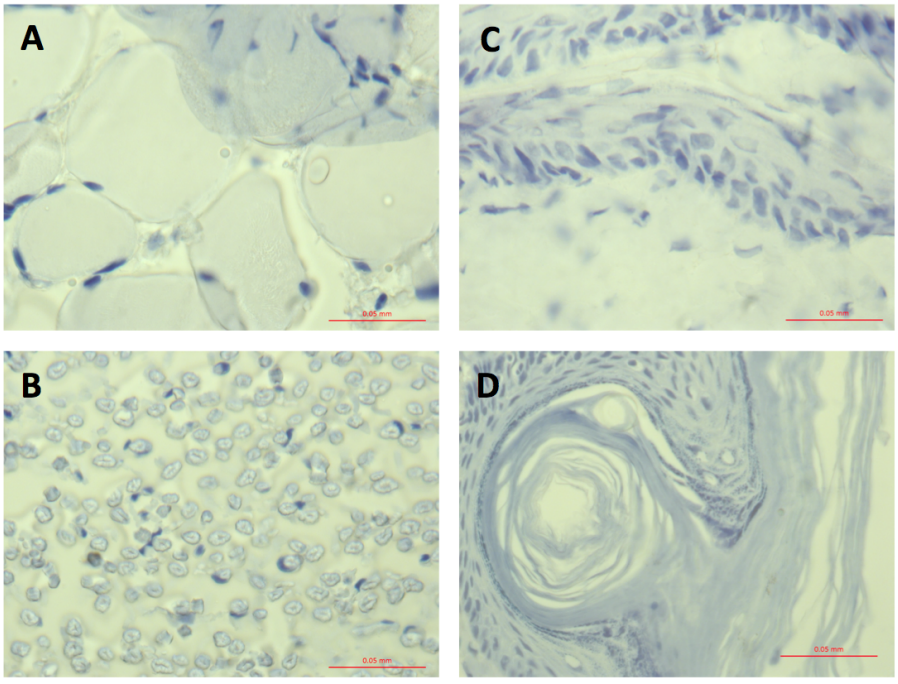

Figure 3.39: Negative isotype control (IgG rabbit) for FOXO1A IHC experiments, assessed by Dako Autostainer Link 48. Rat tail cross sections. A) muscle, B) nerve, C) adipose tissue, D) skin. Both DAB stain and nuclear stain (Hematoxylin) were applied. Magnification 400x.

3.4 Discussion

The null hypothesis of tenocyte physiology is rejected as it was shown that tenocyte physiology changes in multiple aspects in response to elevated glucose concentration.

When taking into account limitations of this project, one of them may be the method by which cells were derived from patient donors: the explant method was used on tendons that served in the former part of this project, while the collagenase method was used on tendons that served in the latter part. This may have had an effect on the cells that could have gone undisclosed. As with any primary cell culture, phenotypic drift constitutes a potential complication (141, 142). In our laboratory, tenocytes have been shown to be phenotypically stable up to cell passage P5 (114); therefore in this project tenocytes were not used beyond cell passage P4. Furthermore, 'contamination' by other cell types, such as smooth muscle cells, cannot be entirely ruled out and may have affected experimental results.

An interesting point to note is that often (but not always) the cells cultured in 17 mM glucose 'performed' the best: they were the most confluent of all conditions (figures 3.12, 3.13, 3.16). Collagen, asporin, biglycan and aggrecan genes were most upregulated in this condition (figures 3.21 and 3.23). Equally, these cells were also most able to upregulate the key oxidative stress gene: SOD-2 was the highest in 17 mM (figure 3.26). 17 mM glucose is precisely the glucose concentration in standard medium of choice for cell culture. However such concentration would be harmful (diabetic) to a human being. A healthy individual would have their glucose level below 7.8 mM 2 h after ingesting a meal. An untreated diabetic individual would be at 11.1 mM or above 2 h after ingesting a meal (116). Therefore the 17 mM glucose condition is very much in the diabetic range.

The most striking findings originate from chronic culture experiments, as opposed to acute glucose treatment experiment (figure 3.10). In this project I aimed to mimic chronically diabetic glucose levels, that an undiagnozed diabetic individual would have, and to evaluate their effect on the tendon tissue. I hypothesized that tendon tissue may be either more or less susceptible to glucose damage than other tissues, such as retinal, neural, kidney and vascular tissue.

Metabolic activity over time, as judged by Alamar Blue assay normalized to cell number, clearly indicates that 30/38 mM glucose cells are weakened (figures 3.4 to 3.9): their

total number is decreasing the most dramatically (figures 3.5 and 3.8) and their normalized metabolic activity is extremely low compared to the other glucose conditions (figure 3.9). Overall, the 30/38 mM glucose condition had been consistently shown as deleterious to viable cell number across multiple assays in this chapter.

Investigation of tenocyte number and proliferation rate uncovered a very interesting finding: tenocytes have a higher proliferation rate in 38 mM glucose medium however their net population number is reduced in this condition (figures 3.15 to 3.18). Perhaps tenocytes in the 38 mM glucose die at an increased rate and/or divide at an increased rate and thus reach senescence sooner. It was critical to follow up this finding and hence cell senescence was the first area for exploration. I show here that glucose dose-dependent morphological senescence is apparent (figures 3.19 and 3.20). QPCR markers p21 and p16 were uninformative. In the future, another attempt at qPCR of p21 and p16 should be made, while also evaluating their protein levels using Western Blot. Tenocyte senescence could be also evaluated by senescence-associated β-galactosidase assay which is the most widely used biomarker for determining cellular senescence (111, 143). Cell death was the second area of investigation and was explored by TUNEL assay, however a conclusion was not reached due to time constraints. Exploring cell apoptosis therefore constitutes one of possible future avenues: finishing the analysis of existing data, as well as evaluating the apoptotic markers p53 and Bim on gene expression gene using qPCR. In conclusion, a lesser number of cells and/or a higher ratio of senescent cells will invariably have a negative implication on tendon tissue integrity, possibly compromising physiological function of tendon.

Examination of selected key ECM components uncovered some being more sensitive to elevated glucose levels than other. Both *COL1A1* and *COL3A1* were dramatically upregulated in 17 mM glucose compared to 5 mM glucose on the mRNA level (figure 3.21), suggesting a possible anabolic response to glucose. Secreted soluble collagen, as measured by Sircol assay, was overall significantly lower in 38 mM glucose (figure 3.22). This would suggest rather a catabolic response to elevated glucose. A possible explanation might be that the collagen mRNA is being produced at a higher rate in 17 mM glucose but the protein is either not translated or secreted, or is being broken down at a higher rate. In the future, more research could be done on collagen in this experimental setting:

collagen ELISA might be informative in low versus high glucose conditions. Also, it might be worth investigating whether collagen secretion is impaired under elevated glucose conditions. Two of the enzymes involved in collagen synthesis are prolyl-4-hydroxylase and lysyl-hydroxylase which are responsible for collagen hydroxylation, and could be investigated using qPCR. Furthermore scleraxis, a biomarker that is extensively used for tendon characterization, regulates the expression of cola1a and col1a2 (140), and should be evaluated on the qPCR level in low versus high glucose.

The four investigated PGs were all shown to be upregulated in 17 and 30 mM glucose at the mRNA level (figure 3.23). Interestingly secreted PGs, as measured by the DMB assay, demonstrated no change across glucose conditions (figure 3.24). Other researchers report reduced proteoglycan levels in diabetic tendon (102). In a way my findings seem to repeat the collagen finding: a possible anabolic response at the mRNA level which is not observed at the secreted level. For this reason, it was critical to focus on ECM digestion. As collagen is the main component of the tendon ECM, the focus was on MMPs. In pilot investigation I looked at MMP-2 gene expression in response to different glucose conditions; no significant difference was recorded (figure 3.25). Future research for this section would therefore include a more detailed investigation of MMPs, as it was shown by other researchers that for example 25 mM glucose upregulates the expression of MMP-9 and MMP-13 in tendon cells of rat Achilles tendon (130). I would investigate MMP-2, -9 and -13 on the enzymatic activity level using zymography. Furthermore, the MMPs that have collagen I as substrate would be the ones to investigate using qPCR; those are MMP-1, -2, -7, -8, -12, -13, -14, -18, and -19 (31). Endogenous inhibitors of MMPs, TIMPs, would be also included (e.g. TIMP 1-4) as TIMP down-regulation has been demonstrated in both endothelial and retinal cells following high glucose treatment (126, 127). I would first suggest a qPCR study before proceeding with Western Blot / enzyme activity measure.

In conclusion, the fine balance between tendon ECM anabolism and catabolism may be disturbed in elevated glucose and here I show that, when considering the secreted level, it may be tipped toward excessive catabolism. More research is required to further support these findings.

In analysis of key oxidative stress response enzymes it was expected that oxidative

stress would be highest in 30 mM glucose and hence in 30 mM glucose there would be the most dramatic upregulation of all four selected enzymes. The data indicate that SOD-2 is dramatically increased in response to elevated glucose (12-fold increase in 17 mM glucose and 5-fold increase in 30 mM glucose, both compared to 5 mM glucose)(figure 3.26). SOD-1 did not reach significance threshold, while SOD-3 and catalase show a 2.5-fold upregulation in 30 mM and 17 mM glucose, respectively (figure 3.26). A possible explanation might be that cells in elevated (30 mM) glucose are compromised to such an extent that they are unable to properly respond to increased oxidative stress. The reported increase in SODs expression in the 17 mM glucose condition may be an adaptive response to increased ROS generation. As specifically SOD-2 is one of the most important enzymes in defence against oxidative stress, evaluating its protein level using Western Blot in low vs. high glucose would be important. Also, it would be informative to evaluate the 'basal' oxidative stress in the low vs. high glucose samples before focusing on the above mentioned enzymes: this would be done using the Cellular reactive oxygen species detection assay (DCFDA).

Scratch assay data showed that 38 mM glucose inhibits the cell migration rate at 72 h; with time the effect of glucose treatment is more apparent (figures 3.28 and 3.29). In patient 2 especially it is the 8 mM glucose that most benefits the cell migration. High error bars in these figures were inevitable with this crude assay. The analysis method includes a macro and a region of interest (ROI) which might both introduce a certain degree of error. Overall, the scratch assay data have meaning for tendon healing in diabetic patients. It is known that tendon healing is problematic in diabetic patients; this data adds to the evidence.

In general, cultured cells provide more quantitative data however they are altered by the culturing process (141, 142). Rat tissue was examined for effects of elevated glucose in addition to cultured tenocytes in order to achieve a more 'rounded' research approach. One of the advantages of the animal model is its 'controlled' nature, i.e. it differs only in the presence/absence of T1D. The null hypothesis of no difference between T1D and control rat tissues is rejected, as differences have been reported. Rats used in this project were *in vivo* T1D-induced, whereas cultured cells were *in vitro* T2D-mimicked (insulin was present in FCS). Therefore the two cannot be exactly compared, and should be

rather used in complement. Furthermore, rat control group had a mean plasma glucose value of 9.0 mM [1], while the control cells were cultured in 5.0 mM glucose. This should not interfere with the conclusion, as rat glucose levels are comparable to human values (144). The results indicate that skeletal muscle tissue is 3NT-positive to a high degree in diabetic vs. control condition. Tendon tissue also seems more 3NT-positive under diabetes (figure 3.32). Higher levels of FOXO1 would be expected under hyperglycemia, and the muscle tissue has been consistently shown to be dramatically FOXO1-positive in the diabetic condition as opposed to control. Skin was found highly FOXO1-positive in both conditions; perhaps FOXO1 is typically high in the skin. Overall, no differences in FOXO1 have been reported in tendon tissue (diabetic vs. control).

There are many targets which would deserve attention in future cell studies in low vs. high glucose and in IHC studies on rat tissue. SOD-1, -2 and -3 should be screened using IHC on rat tissue. Furthermore, FOXOs would constitute a substantial area of future research. The family of transcription factors FOXO is involved in ROS detoxification as their targets include SOD-2 and catalase (138, 139, 145, 146). FOXOs have also been hypothesized to play a role in the development of DM (hyperactive FOXO1 might lead to DM) (147). In mammals there are four FOXOs: FOXO1, 3, 4 and 6 (137, 139). Although FOXO1 has been investigated here in a pilot manner, I would suggest further investigation. FOXO1 is involved in regulating cell proliferation, aging and metabolic homeostasis in response to oxidative stress in a variety of cell types (148, 149): FOXO1 can regulate SOD-2 (140). Therefore, I would quantify the levels of FOXO1 in low vs. high glucose cells using qPCR. Next, focusing on insulin receptor might be worth: I would propose to evaluate the levels of insulin receptor by WB in order to answer whether tendon is an insulin-sensitive tissue. Sirtuins are the next area of future research. In mammalian cells sirtuin 1 (SIRT1) is involved in the regulation of glucose metabolism and insulin signaling, and it also regulates levels of ROS by deacetylating FOXO3 (SIRT1 and FOXO3 form a complex in cells in response to OS (139))(88, 138). In pancreatic beta-cells specifically SIRT1 positively regulates insulin secretion and protects cells from OS and inflammation (150). Perhaps SIRT1 can reduce ROS levels and in this manner protect tendon tissue against OS. Therefore my future targets would be both SIRT1 and FOXO3.

[1] Refer to Human & animal samples section in Chapter 2 for precise glucose values.

4

Effect of chronic glucose conditioning on hydrogen peroxide-induced oxidative stress response

4.1 Hypothesis & aims

Null hypothesis is as follows: *Glucose concentration in cell culture medium exerts no effect on the response of tenocytes to hydrogen peroxide (H_2O_2)-induced oxidative stress.*

This hypothesis will be tested by performing aim 1-5:

Aim 1: to determine an appropriate H_2O_2 concentration range for experiments on tenocytes;

Aim 2: to assess the effect of glucose and acute H_2O_2 treatment on tenocyte metabolic activity and viability;

Aim 3: to assess the effect of acute glucose and H_2O_2 treatment on tenocyte metabolic activity;

Aim 4: to quantify the effect of glucose and acute H_2O_2 on expression of selected genes;

Aim 5: to determine whether the glucose and H_2O_2-induced response can be attenuated by selected protective agents.

4.2 Experimental design

The overall research objective in this section was to assess the compounded effects of glucose and H_2O_2 on primary human tenocytes. Increased hyperglycemia-induced overproduction of superoxide by the mitochondrial electron transport chain is currently the leading hypothesis behind diabetes (57, 81, 151, 152, 153), and findings in the previous chapter (figure 3.26) support the fact that elevated glucose contributes to OS. In order to induce OS experimentally, one can either increase the radical load or inhibit the antioxidant deferences (74). Therefore, by adding additional H_2O_2 in this experimental chapter the effect of longer-term OS or a secondary oxidative load from infection and/or mechanical loading can be simulated and approximated.

H_2O_2 (figure 1.4) is one of the most abundant ROS in aerobic organisms including plants; it is being produced during catalytic breakdown of superoxide anions (which are produced by partial reduction of oxygen during aerobic respiration in mitochondria) (154). H_2O_2 is known for its cytotoxic effects but new evidence suggests it is also a regular of eukaryotic signal transduction (154). It appears that the physiological range of H_2O_2 concentration is conserved across species. Furthermore, H_2O_2 is the only ROS that is produced by several enzymes and this indicates its tight intracellular regulation (154, 155). In general, ROS levels must be buffered in order to maintain intracellular redox balance (72). However elevated concentrations of H_2O_2 may lead to balance disturbance and 'tip' it into cytotoxicity and thus be potentially damaging to a broad range of macromolecules, such as proteins, lipids and nucleic acids. Long-term increased levels of H_2O_2 in cells lead to OS and cause cellular damage, which is associated with many diseases, including DM (154). On the other hand, H_2O_2 in itself can act as a signaling molecule, and is involved in regulatation of many different cellular processes (154). For example, it can activate signaling pathways involved in mitogenic stimulation, cell cycle regulation, and apoptosis (156, 157) however its non-toxic levels must be maintained in a delicate balancing act between H_2O_2 production and its scavenging. Thus the role of H_2O_2 is two-fold, and depends on H_2O_2 level and the cell type (154).

Exogenous H_2O_2 can readily penetrate biological membranes and enhance formation of other ROS. H_2O_2 that is added directly into the cell culture medium will result in a rapidly diminishing concentration of H_2O_2 depending on cell population density and intracellular catalase contents (74). Treatment with extracellular H_2O_2 was used here, also for its ease of use in aqueous solution. Many experiments in this chapter were performed on two types of medium: "non-supplemented" and "supplemented". The non-supplemented medium is the standard medium of choice. The supplementation comprises addition of proline (50 g/ml) and L-ascorbic acid-2-P (50 g/ml) which is a standard supplementation used to support collagen production, but not explicitly designed to block ROS. In this thesis this medium is referred to as "pro-collagen medium". AA was also used at higher doses as part of the protective panel tested (Aim 5 in this Chapter).

4.3 Results

4.3.1 Aim 1: to determine an appropriate H_2O_2 concentration range for experiments on tenocytes

H_2O_2 dose response curve in 17 mM (standard) glucose medium

Different duration (3, 18 and 24 h) of H_2O_2 incubation was used at the beginning of this chapter in order to establish the optimal research design. Short (3 h) H_2O_2 treatment in 17 mM glucose shows that H_2O_2 lowers the metabolic activity of tenocytes, as measured by Alamar Blue assay (figure 4.1). However there is a partial protection from this effect in the supplemented medium. Dose-response to H_2O_2 is apparent in both types of media.

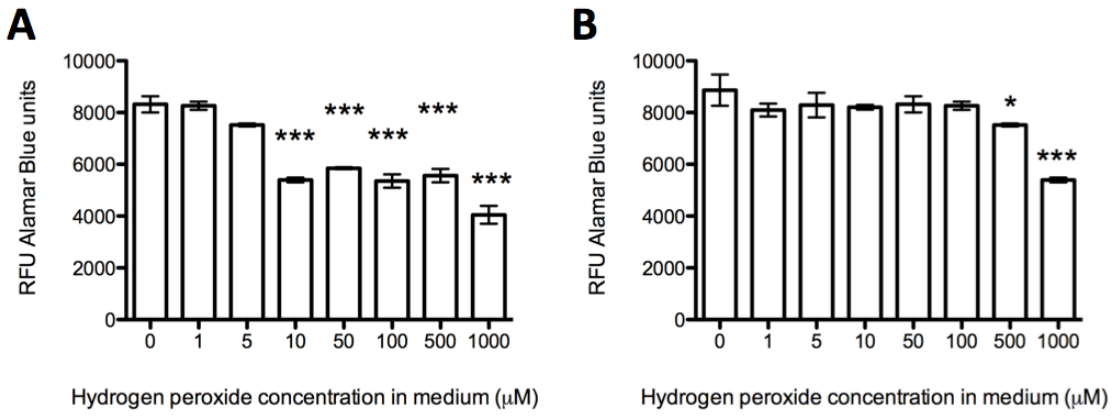

Figure 4.1: Tenocyte metabolic activity in response to varying H_2O_2 concentrations (0-1,000 μM), as quantified by Alamar Blue assay (n=1 patient). A) standard non-supplemented medium, B) medium supplemented with proline (50 μg/ml) and L-ascorbic acid-2-P (50 μg/ml). H_2O_2 treatment for 3 h. 17 mM glucose condition only, Lonza medium. Columns represent mean of 2 values, error bars are SD. One-way ANOVA, Tukey. Displayed statistical significance is compared to 0 μM H_2O_2.

Selected H_2O_2 concentrations were tested on samples obtained from 3 patients (figure 4.2); the dose-dependent response to H_2O_2 was confirmed for both types of media in the 17 mM glucose concentration. The figure shows that pro-collagen medium with 1,000 μM H_2O_2 treatment has a virtually identical percentage value (98.08%) of metabolic activity as the regular medium with 0 μM H_2O_2 (100%). This is to be expected as H_2O_2 should be scavenged by AA which is one of the two added supplements. It is worth noting that the baseline metabolic activity in the pro-collagen medium is higher than the baseline of standard medium; the supplements alone increase metabolic activity of cells.

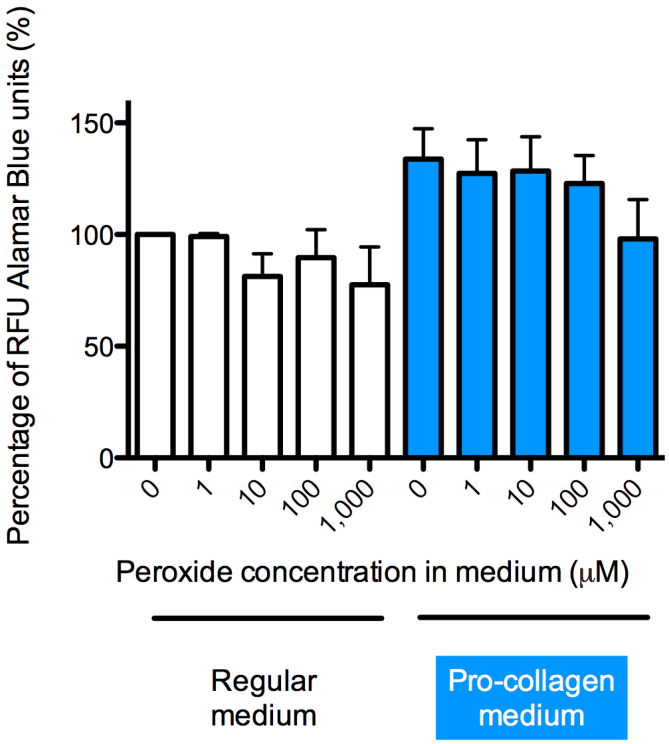

Figure 4.2: Tenocyte metabolic activity in response to varying H_2O_2 concentrations (0-1,000 μM) in regular vs. pro-collagen 17 mM glucose medium (n=3 patients). Lonza medium. Incubation with H_2O_2 for 3 h. 0 μM H_2O_2 of regular medium was set to 100%, all other values expressed relative, including pro-collagen medium values. Columns represent mean value of 3 data points, error bars represent SEM. N too small to determine normality (D'Agostino-Pearson test). One-way ANOVA (p value = 0.0377), Tukey all 'ns'.

4.3.2 Aim 2: to assess the effect of glucose and acute H_2O_2 treatment on cell metabolic activity and viability

Effect of 3 h and 18 h H_2O_2 treatment on tenocyte metabolic activity in different media compositions

Five different doses of H_2O_2 were tested in three glucose conditions (8, 17 and 38 mM) in both regular and pro-collagen medium. H_2O_2 incubation was for 3 h (figure 4.3) and 18 h (figure 4.4). In the 3 h data there is a significant drop in metabolic activity between 100 and 1,000 μM H_2O_2 in the 17 and 38 mM glucose condition. The 8 mM glucose condition has a lower metabolic activity overall. Figure 4.4 indicates that after 18 h of incubation with H_2O_2 the metabolic activity is not affected in 17 mM glucose, however is decreased in 38 mM glucose under 1,000 μM H_2O_2.

Ability of cells to withstand H_2O_2-induced oxidative stress decreases as glucose concentration rises: 8 mM glucose is most protective

24 h incubation with H_2O_2 was selected as better than 3 or 18 h for all future experiments in this chapter. Tenocytes were treated with H_2O_2 (doses as high as 2,000 μM) under varying media compositions. Following the treatment their metabolic activity was quantified by Alamar Blue assay, and cell viability was assessed using Live/Dead stain [1]. Alamar data (figure 4.5) indicates that the 5 mM glucose condition (A and B in the figure) did not protect cells under 1 mM and 2 mM H_2O_2 in neither regular nor pro-collagen medium, despite being expected to be the most protective. Later in this chapter the reasons behind Biosera medium problems were uncovered and will be discussed (figure 4.14). In the 8 mM glucose condition (C and D in 4.5) cells are protected from a decrease in metabolic activity under 1 mM H_2O_2 in both types of media (regular and pro-collagen). The 17 mM glucose condition (E, F in the figure) has a different range of H_2O_2 concentrations however demonstrates protection at all doses including 1 mM H_2O_2. Cells in 38 mM glucose (G, H in the figure) exhibit the most severe decrease in metabolic activity: in 1 mM H_2O_2 limited viability was detected only in pro-collagen medium. The protective response at lower doses of glucose (except for 5 mM Biosera medium) is striking: 8 mM

[1] Data presented in this section (figures 4.5, 4.6, 4.7, 4.8 and 4.9) are from multiple patients. The 5 mM glucose condition had a different brand of medium (Biosera, as opposed to Lonza for all else) and was conducted on patient T15. The 8 mM and 38 mM glucose conditions were conducted on patient T13. The 17 mM glucose condition was patient T17.

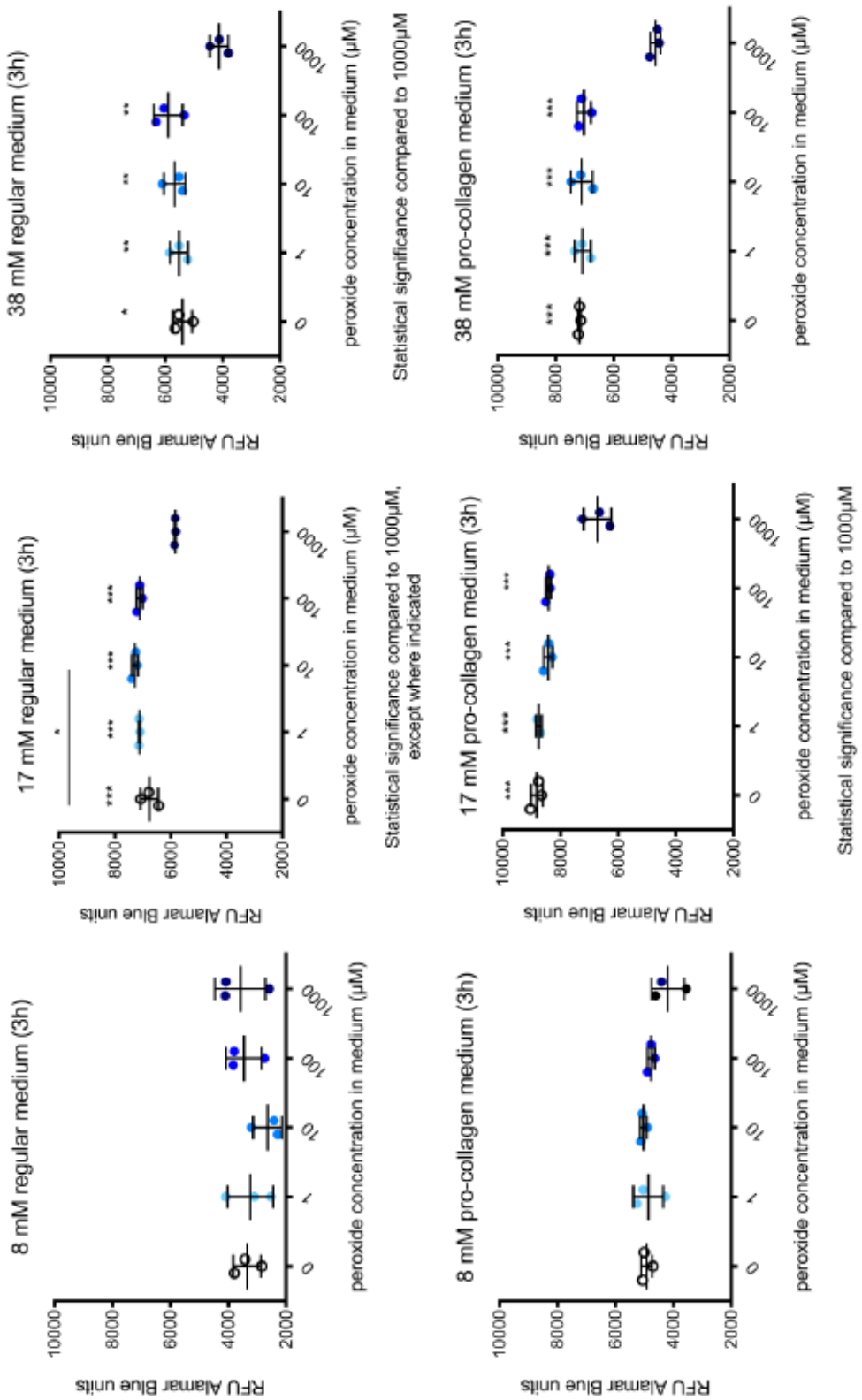

Figure 4.3: Tenocyte metabolic activity after 3 h incubation with H_2O_2, as determined by Alamar Blue assay (n=1 patient). 3 glucose conditions, regular and pro-collagen medium, Lonza brand. One-way ANOVA, Tukey. Note that statistics is performed within each graph only, not across graphs.

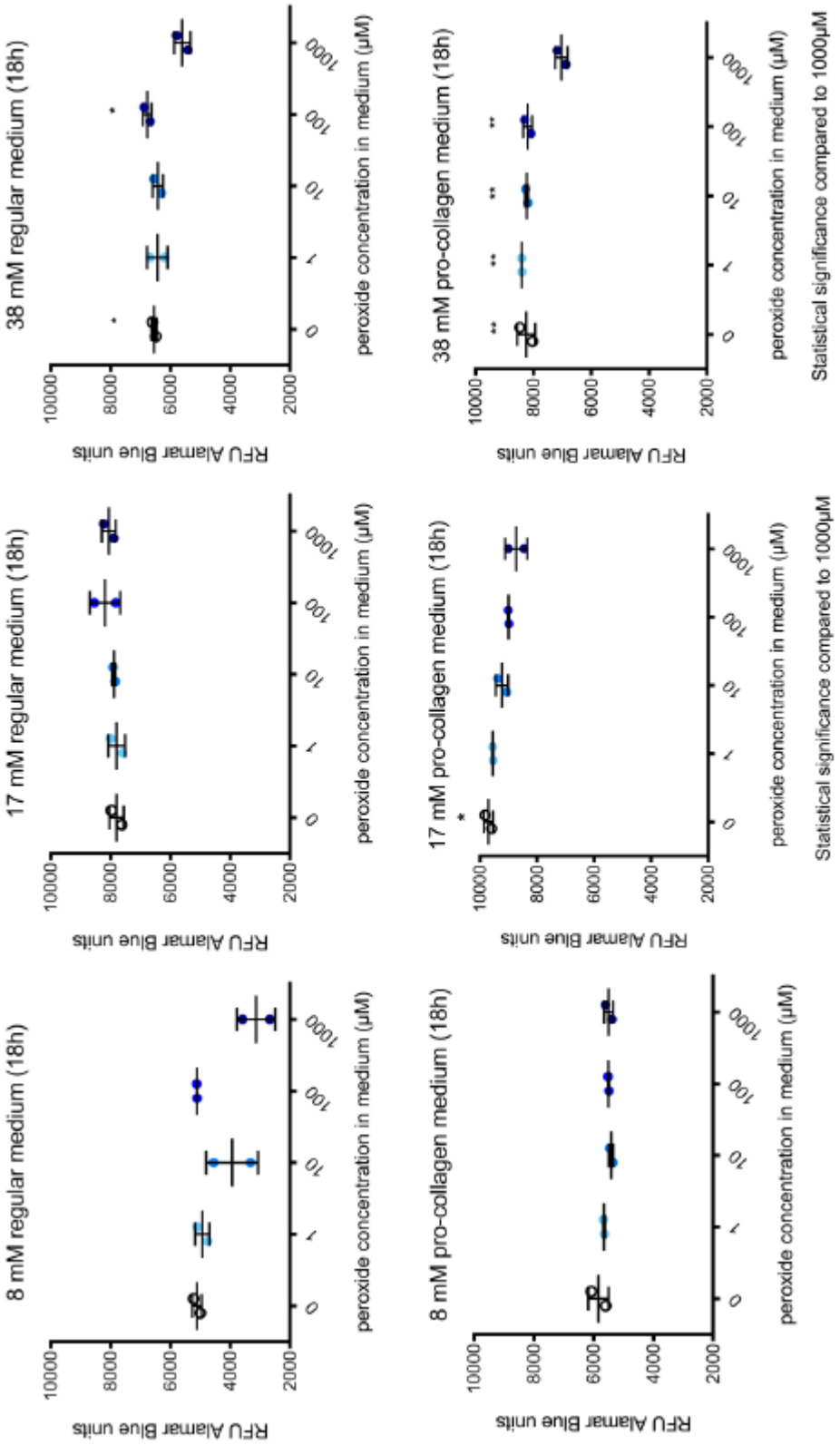

Figure 4.4: Tenocyte metabolic activity after 18 h incubation with H_2O_2, as determined by Alamar Blue assay (n=1 patient). 3 glucose conditions, regular and pro-collagen medium, Lonza brand. One-way ANOVA, Tukey. Note that statistics is performed within each graph only, not across graphs.

and 17mM glucose conditions offer more protection compared to 38 mM. Pro-collagen medium partially protected cells in all conditions except 5 mM Biosera, however 2 mM H_2O_2 severely compromised cell viability in all conditions.

Live/Dead data show that in the 5 mM glucose condition (figure 4.6) pro-collagen medium protects to a certain degree against 1 mM and 2 mM H_2O_2. Greater protection was expected in this condition; the 5 mM Biosera medium shortcomings will be explained later in this chapter (figure 4.14). In 1 mM H_2O_2 cells were protected from death in 8 mM glucose condition irrespective of supplementation (figure 4.7). 17 mM glucose condition (figure 4.8) shows increased vulnerability to H_2O_2 compared to 8 mM glucose; protection at 1 mM H_2O_2 takes place in pro-collagen medium only. Cells in 38 mM glucose (figure 4.9) did not survive under 1 mM H_2O_2 in regular medium which highlights the protective effects of 8 mM glucose medium. However pro-collagen supplements partially counteracted the oxidative stress-induced cell death even in 38 mM glucose. Tenocytes did not survive under 2 mM H_2O_2 in any media conditions.

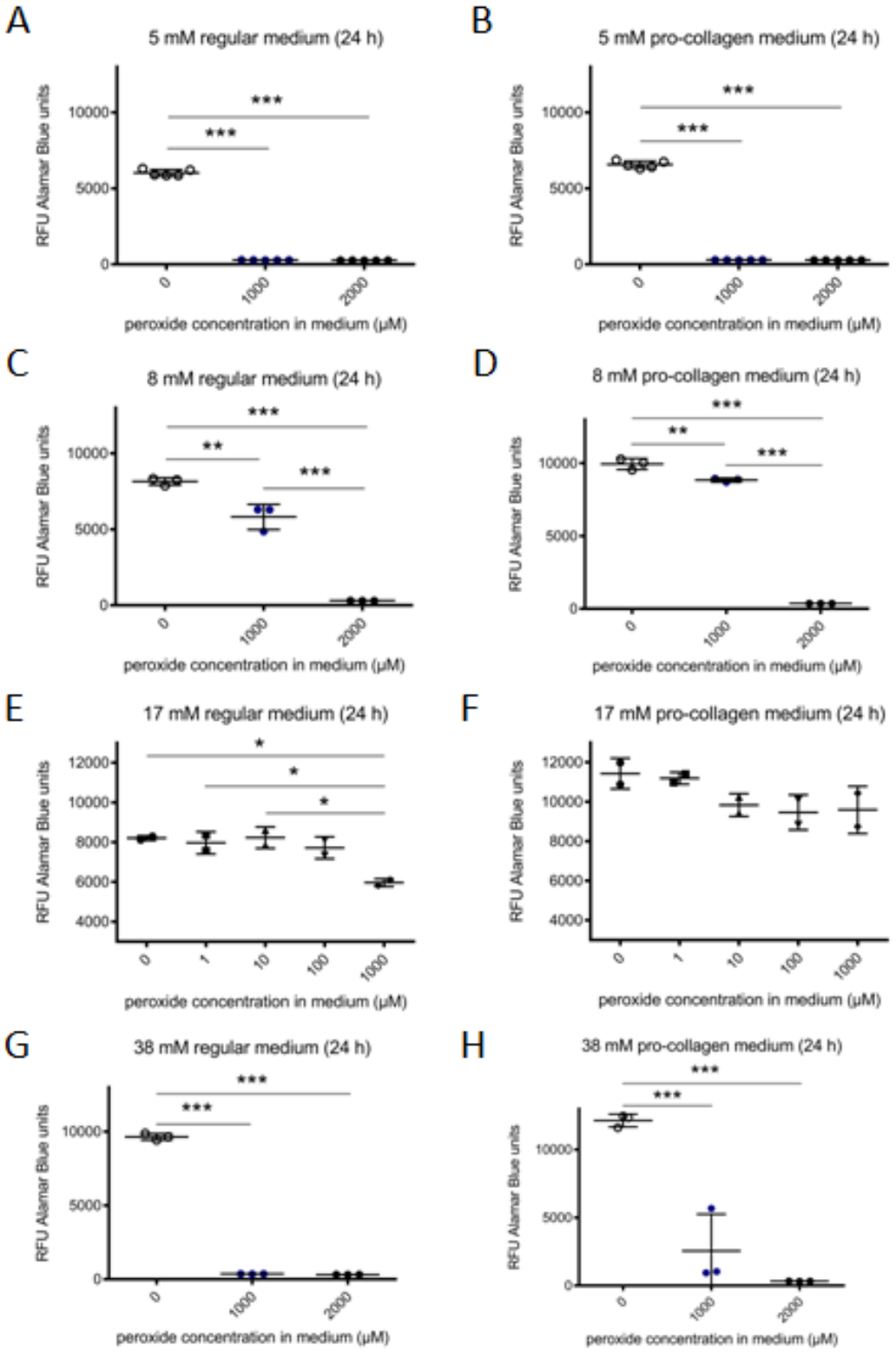

Figure 4.5: Tenocyte metabolic activity as quantified by Alamar Blue assay. H_2O_2 incubation for 24 h. Regular medium (A, C, E, G), pro-collagen medium (B, D, F, H). Data is not normalized to cell number, Alamar values are absolute. Note different patients: 5 mM T15, 8 mM and 38 mM T13, 17 mM glucose T17. Note that statistics is performed within each graph only, not across graphs. Prism significance intervals are defined as: not significant (ns) $P > 0.05$; * $P \leq 0.05$; ** $P \leq 0.01$; *** $P \leq 0.001$.

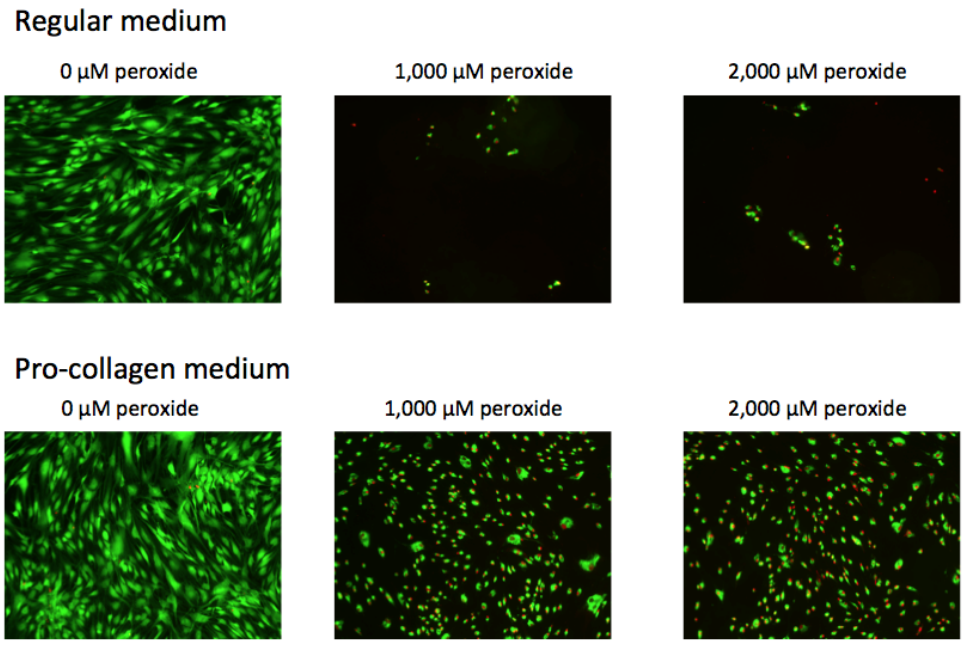

Figure 4.6: Effect of H_2O_2 on human tenocytes: Live/Dead stain microscopy images for 5 mM glucose condition after 24 h incubation with H_2O_2. 2 different media compositions (regular, pro-collagen). Composite images, magnification x100. Note patient is T15.

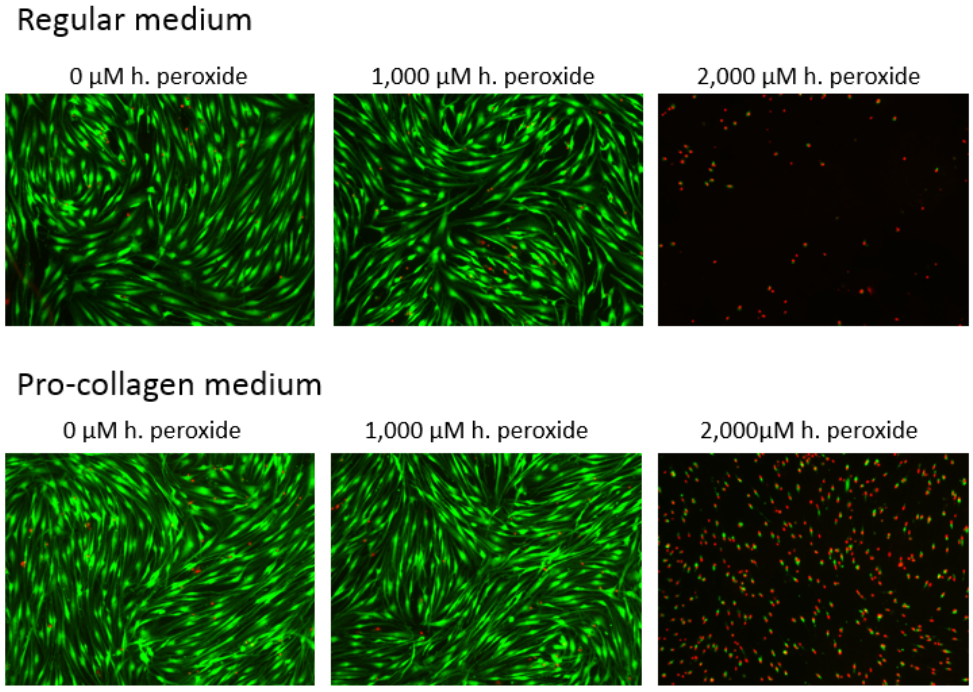

Figure 4.7: Effect of H_2O_2 on human tenocytes: Live/Dead stain microscopy images for 8 mM glucose condition after 24 h incubation with H_2O_2. 2 different media compositions (regular, pro-collagen). Composite images, magnification x100. Note patient is T13.

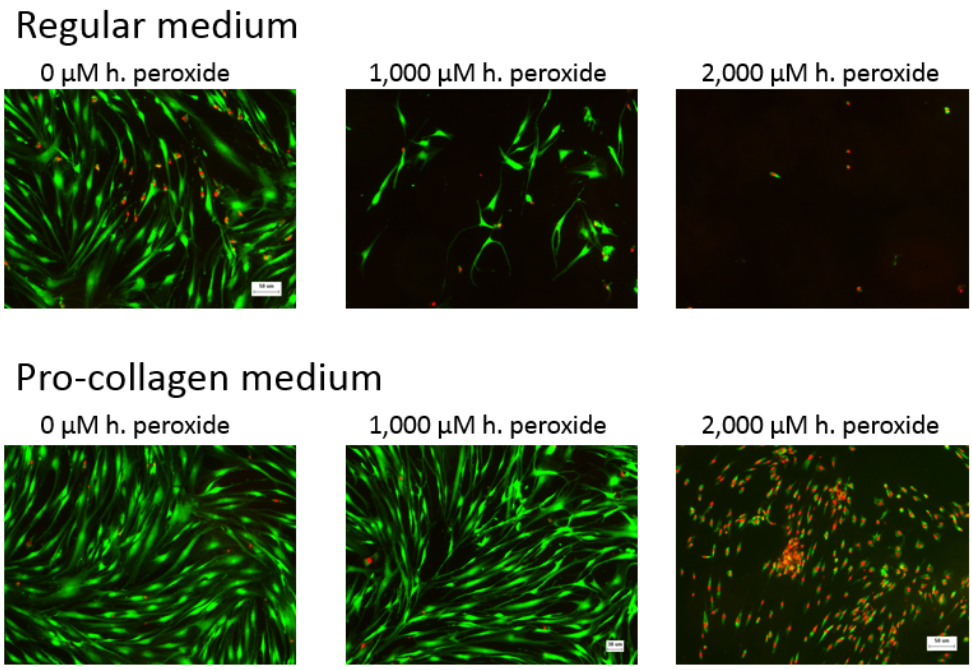

Figure 4.8: Effect of H_2O_2 on human tenocytes: Live/Dead stain microscopy images for 17 mM glucose condition after 24 h incubation with H_2O_2. 2 different media compositions (regular, pro-collagen). Composite images, magnification x100. Note patient is T17.

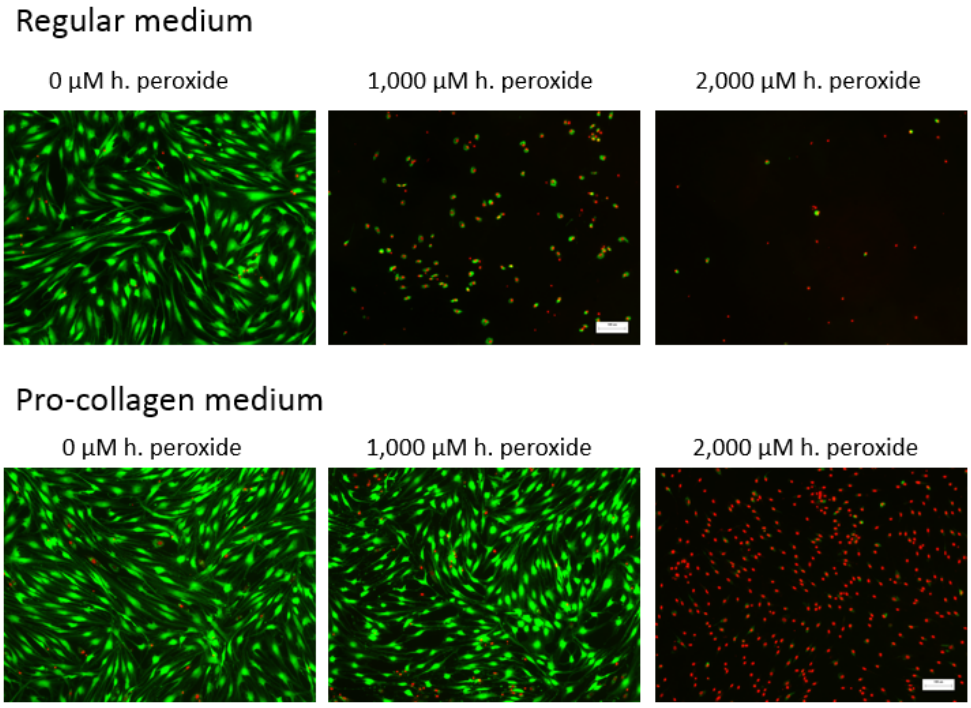

Figure 4.9: Effect of H_2O_2 on human tenocytes: Live/Dead stain microscopy images for 38 mM glucose condition after 24 h incubation with H_2O_2. 2 different media compositions (regular, pro-collagen). Composite images, magnification x100. Note patient is T13.

Metabolic activity and viability of cells that were chronically cultured in elevated glucose concentreations and acutely treated with H_2O_2

Because of the variability in response to very high doses of H_2O_2 in the initial experiments, tenocyte samples from 3 patients were subjected to an experiment with a similar but refined design: additional H_2O_2 doses were selected in the interval between 100 and 1,000 μM H_2O_2; 1,000 μM H_2O_2 was the maximum dose employed; only regular medium was used. Alamar Blue assay and L/D stain were employed, as previously.

Alamar data (figure 4.10) indicate that tenocyte metabolic activity drops extremely low between 500 and 800 μM H_2O_2 for all 3 patients in the 5 mM glucose condition. This suggests a 'threshold' of H_2O_2 toxicity to tenocytes cultured under the described conditions. The pattern is very similar in all 3 patients in the 30 mM glucose condition, too. The data for 17 mM glucose medium indicate that in this condition the significant metabolic drop takes place at a lower H_2O_2 concentration: between 100 and 500 μM H_2O_2.

Accompanying L/D data support the Alamar Blue findings. In the 5 mM glucose condition (figure 4.11) the capacity of tenocytes to survive under acute oxidative stress is severely impaired (i.e. cell death/detachment taking place) between 500 and 800 μM H_2O_2 in 2 patients. The third patient has a high proportion of morphologically senescent cells, as seen under microscopy, nevertheless still exhibits a very similar pattern to the other 2 patients. 17 mM glucose condition (figure 4.12) closely resembles its corresponding Alamar data: cells become severely compromised between 100 and 500 μM H_2O_2. Similar to cells in 5 M glucose, 30 mM glucose condition (figure 4.13) is very alike when one notices the higher baseline activity in Alamar Blue data; cell death/detachment takes place in the interval of 500 - 800 μM H_2O_2.

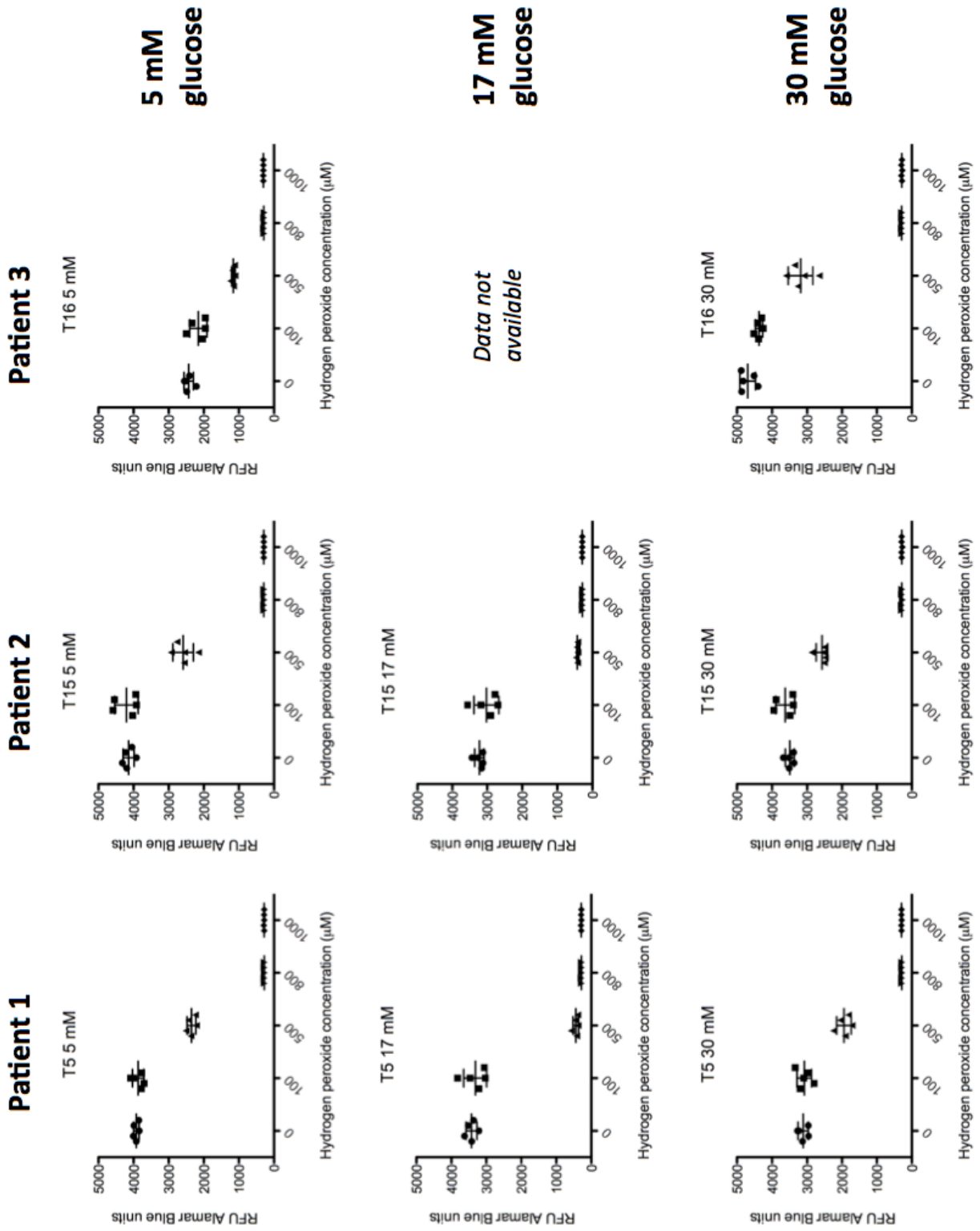

Figure 4.10: Tenocyte metabolic activity as quantified by Alamar Blue assay (n=3 patients). H_2O_2 incubation for 24 h. All regular Biosera medium. Cell passage P4. Data is not normalized to cell number, Alamar values are absolute. 5 data points in each cluster. Missing data where indicated due to technical issue, error bars represent SD. One-way ANOVA: all graphs $P < 0.0001$.

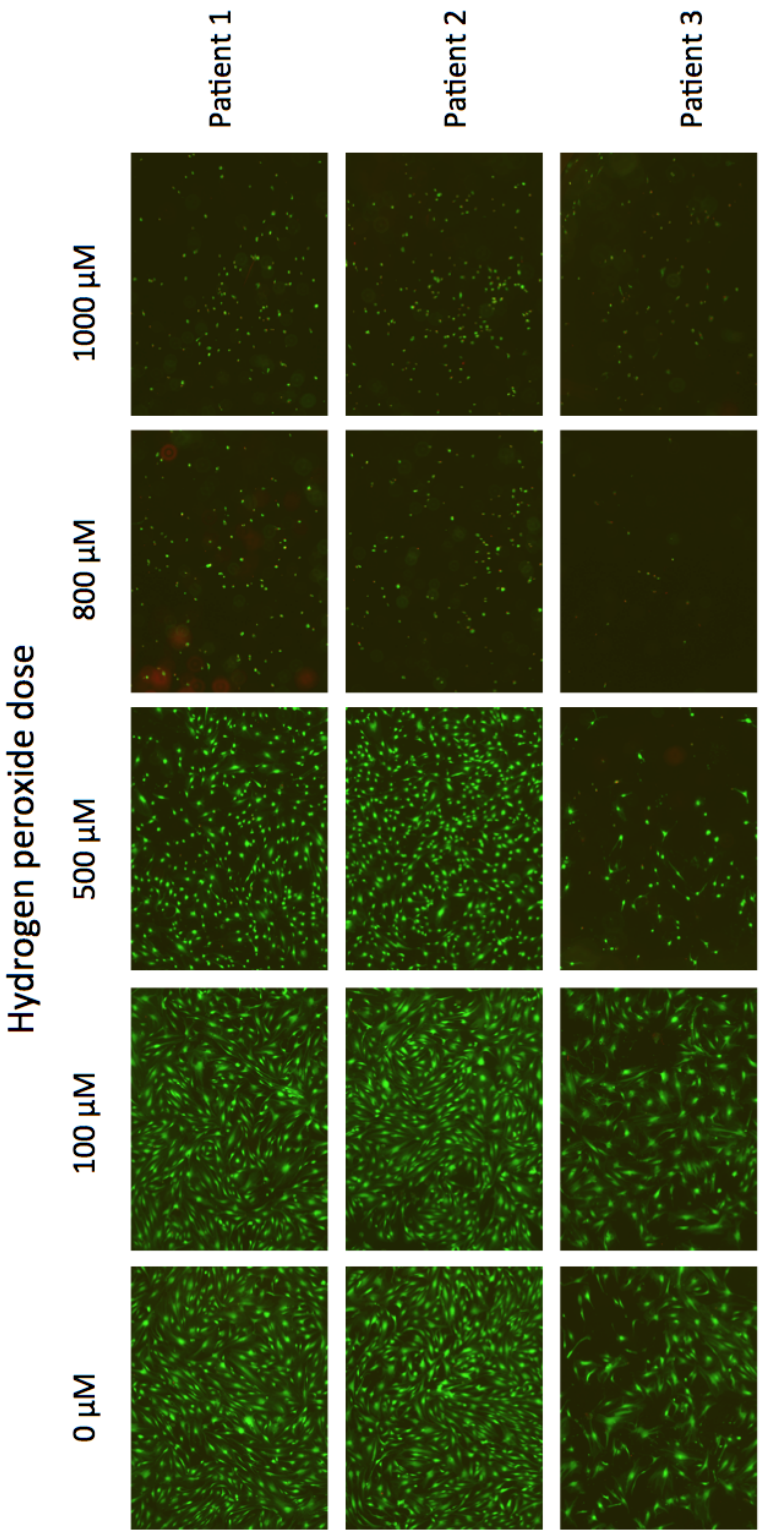

Figure 4.11: Effect of H_2O_2 on human tenocytes: Live/Dead stain microscopy images for 5 mM glucose-treated cells after 24 h incubation with H_2O_2. All regular Biosera medium, cell passage P4. Composite images, magnification x100.

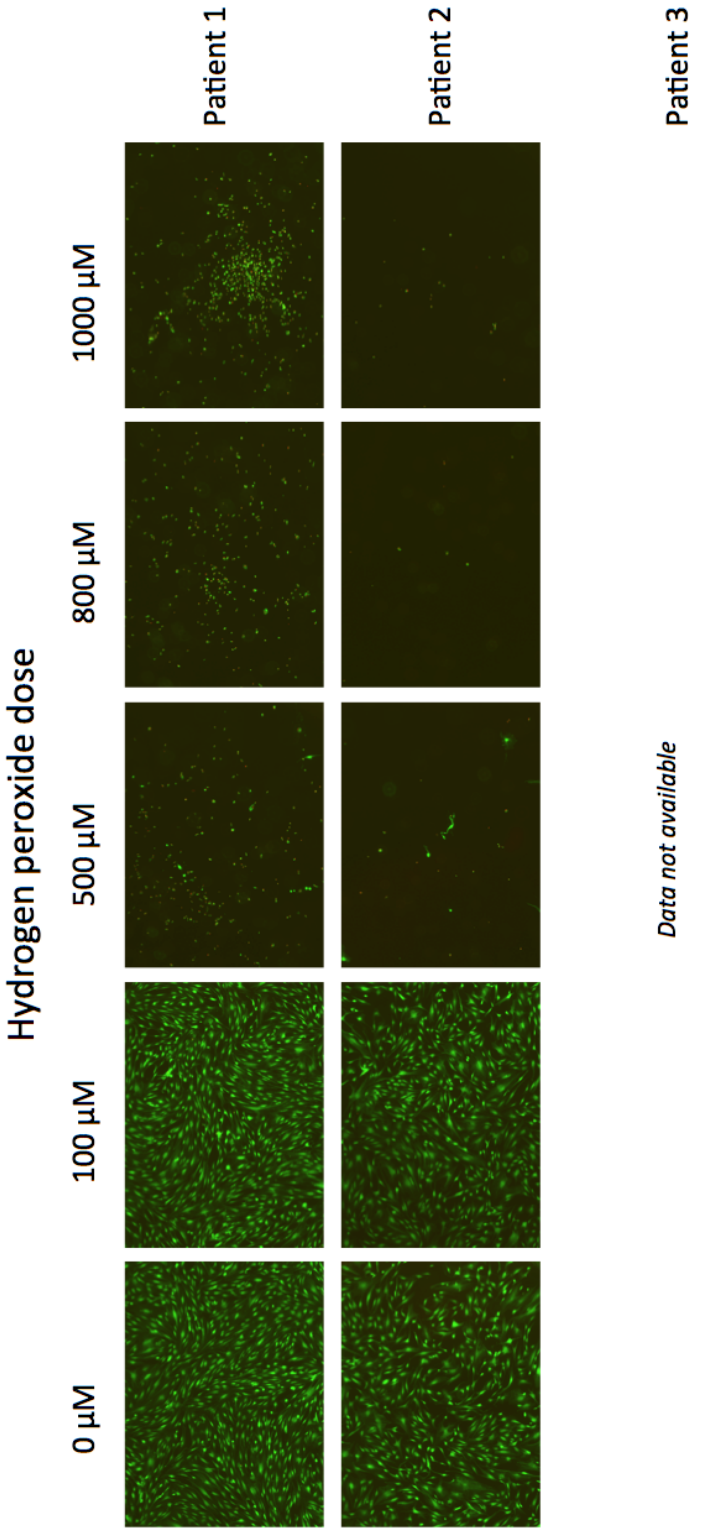

Figure 4.12: Effect of H_2O_2 on human tenocytes: Live/Dead stain microscopy images for 17 mM glucose-treated cells after 24 h incubation with H_2O_2. All regular Biosera medium, cell passage P4. Composite images, magnification x100. Missing data due to technical issue.

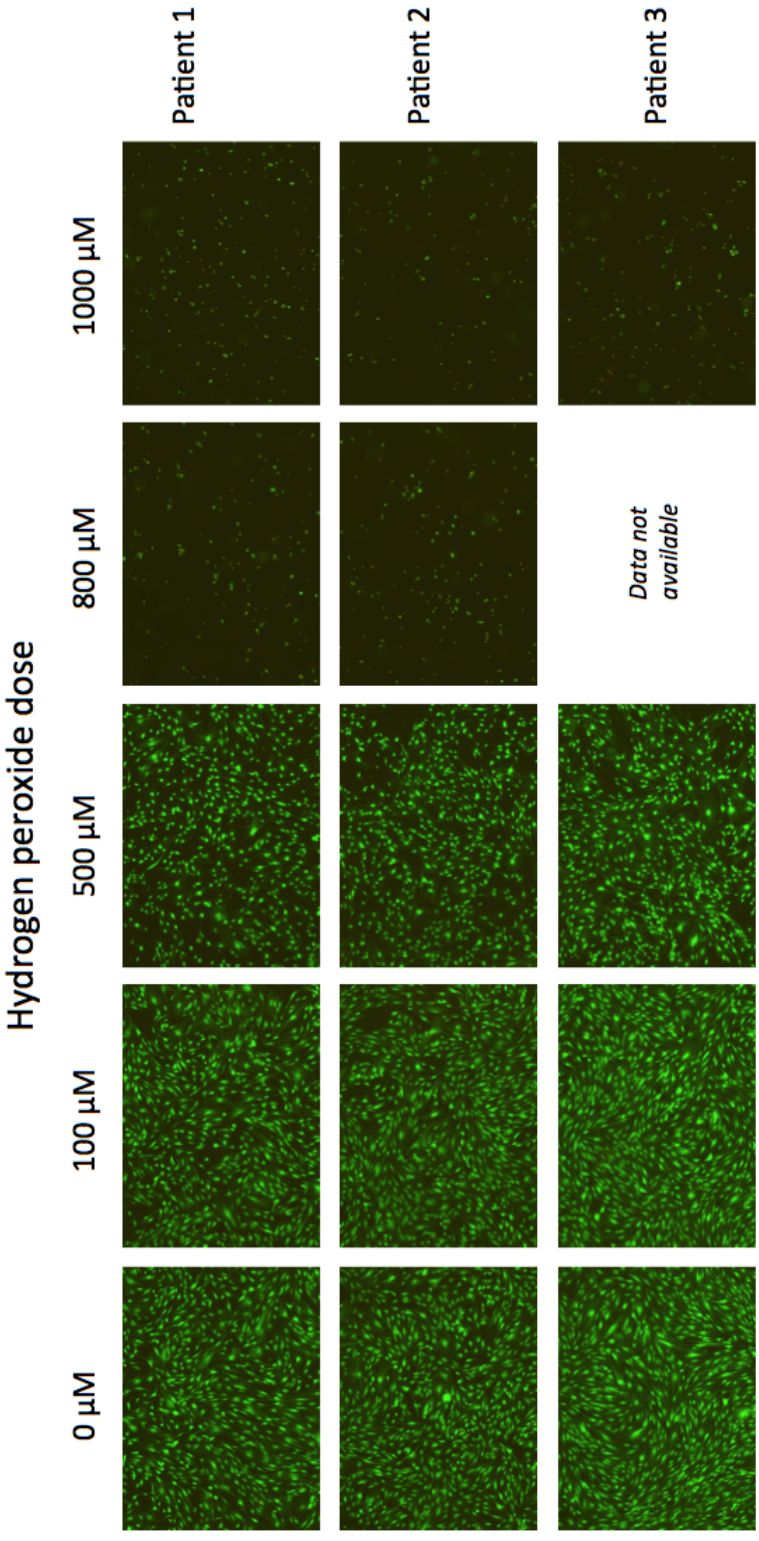

Figure 4.13: Effect of H_2O_2 on human tenocytes: Live/Dead stain microscopy images for 30 mM glucose-treated cells after 24 h incubation with H_2O_2. All regular Biosera medium, cell passage P4. Composite images, magnification x100. Missing data due to technical issue.

Sodium pyruvate is essential for cell protection against H_2O_2, and enables protection at low glucose concentrations

As described earlier, Biosera medium did not offer the expected H_2O_2 protection levels in low glucose concentrations. Further investigation uncovered the very likely reason: levels of sodium pyruvate in the Biosera medium were inadequately low. Biosera medium that was employed contained 0.055 g/l of sodium pyruvate, while the Lonza medium originally employed contained 0.110 g/l. The protective effect of low glucose did re-occur as soon as I used a pyruvate-rich medium (the original 8 mM glucose Lonza, B in figure 4.14) in the same experiment on an identical patient, however I did not supplement the Biosera medium with pyruvate specifically due to time constraints. In A, C and D of the figure 5, 17 and 30 mM glucose Biosera medium were used, respectively. Interestingly, even in Biosera media A and C in figure 4.14 show a difference at 500 μM H_2O_2 dose: cells cultured in 5 mM glucose exhibit a less dramatic drop in percentage metabolic activity than cells cultured in 17 mM glucose (drop to 39.9% and to 10.2%, respectively). Thus, low glucose protects cells from harmful effects of H_2O_2, although this is much weaker with lower sodium pyruvate levels.

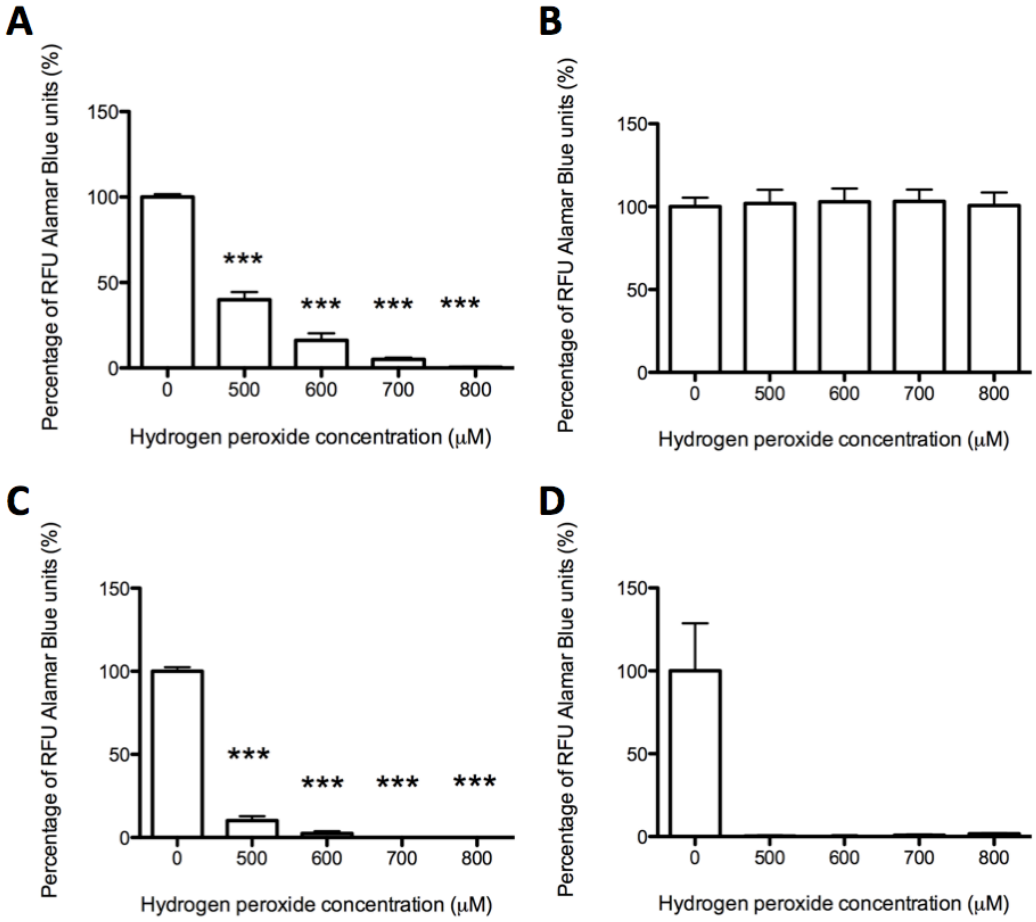

Figure 4.14: Tenocyte metabolic activity in different chronic media compositions (n=1 patient, all T27C P3, performed at same time). All 24 h H_2O_2 treatment. A) 5 mM glucose Biosera medium, B) 8 mM glucose *Lonza* medium (with 1:100 P-S), C) 17 mM glucose Biosera medium, D) 30 mM glucose Biosera medium. Baseline Alamar reading taken with medium alone as well, and incorporated into analysis. Each column represents mean of 5 data points, error bars represent SD. Note that all conditions were seeded at same original cell density, however 30 mM cells grew very little hence discounted from any conclusions (and statistics not performed). One-way ANOVA, Tukey. Displayed statistical significance is compared to 0 μM H_2O_2. 8 mM glucose condition was all 'ns'.

4.3.3 Aim 3: to assess the effect of acute glucose and H_2O_2 treatment on tenocyte metabolic activity

Based on the data in previous sections, it has been established that cells chronically cultured in the 30 mM glucose condition are more vulnerable to the toxic effects of H_2O_2. The next aim was to determine whether *acute* treatment with glucose would be sufficient to alter the observed metabolic activity of tenocytes following H_2O_2 treatment, as determined by Alamar Blue assay. Figure 4.15 shows that this is not the case in the following experiment: there is no difference in the response of tenocytes to H_2O_2 in either time point of acute glucose treatement (24 and 72 h), as measured by Alamar Blue assay. Metabolic activity of all glucose conditions drops to near zero after H_2O_2 insult. This might mean that the dose of H_2O_2 might be too high under these conditions to discern differences in the glucose-treated populations. It was noticed under microscope that cells in A (figure 4.15) were present under 800 μM H_2O_2, there was very little cell death apparent. Hence cells would be visible if L/D stain was performed, although Alamar values were approaching zero.

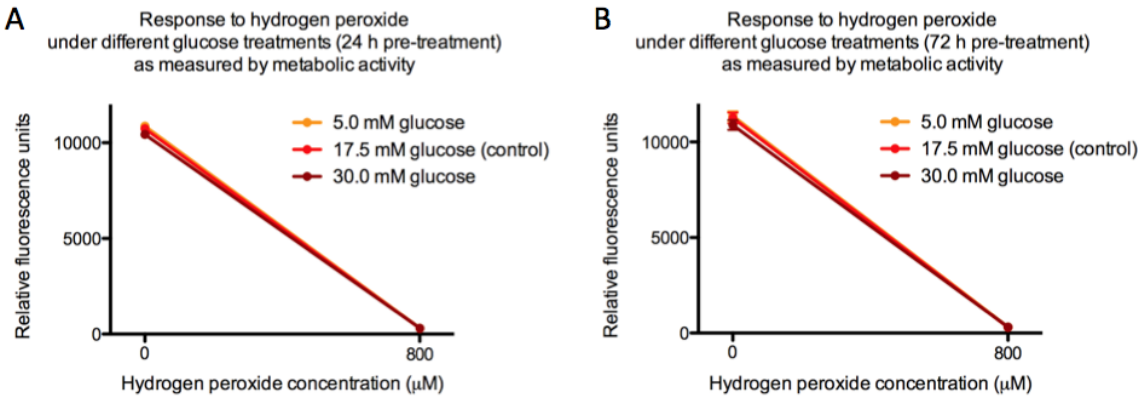

Figure 4.15: Tenocyte metabolic activity following treatments with *acute* glucose concentrations and with 800 μM H_2O_2, as determined by Alamar Blue assay (n=1 patient, Biosera medium). All cells chronically cultured in 17 mM glucose medium before being treated with 5, 17 and 30 mM glucose medium for (A) 24 h or (B) 72 h. Cells were then incubated with 0 or 800 μM H_2O_2 for 24 h in 5, 17 and 30 mM glucose conditions. Each point is a mean value of 5 data points, error bars represent SD (may not be visible due to SD small value). Also obtained DAPI microscope images for cell count (for no peroxide data only): appeared identical hence performed an initial count for the 3 glucose conditions: each group n=3; p=0.08 therefore concluded no differences in cell number.

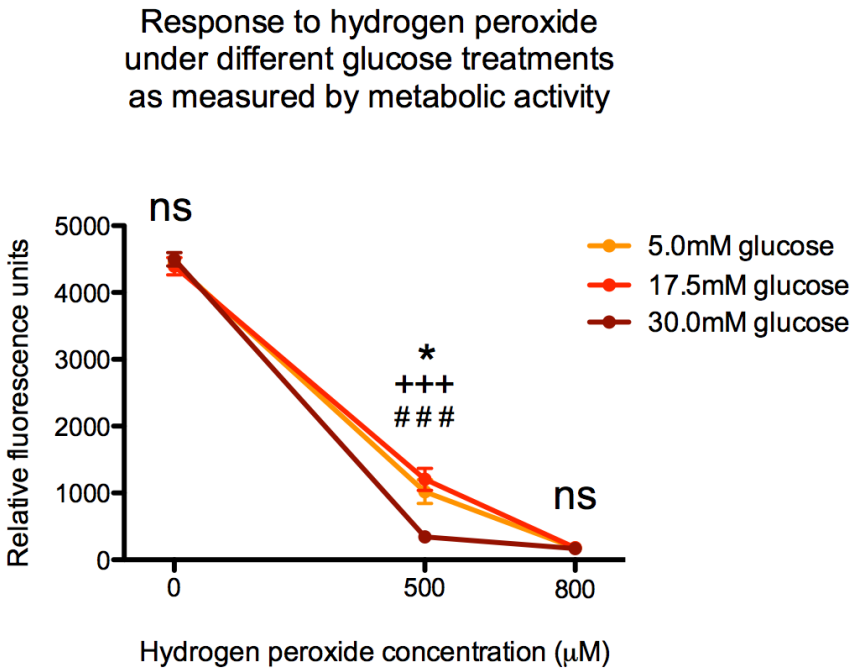

Figure 4.16: Tenocyte metabolic activity following treatment with *acute* glucose conditions and with 500 and 800 μM H_2O_2, as determined by Alamar Blue assay (n=1 patient, Biosera medium). All cells chronically cultured in 17 mM glucose medium before being treated with 5, 17 and 30 mM glucose medium for 72 h. Cells were then incubated with 0, 500 and 800 μM H_2O_2 for 24 h in 5, 17 and 30 mM glucose media. Each point is mean value of 5 data points, error bars represent SD (may not be visible due to small value). Data not normalized to cell number. Two-way ANOVA, Bonferroni *post hoc* test. $*$ is 5 vs. 17 mM, # is 5 vs. 30 mM, + is 17 vs. 30 mM.

In the subsequent experiment 500 μM H_2O_2 dose was included in order to address the issue that both H_2O_2 concentrations in the previous figure 4.15 yielded data that was indiscernible. Results in figure 4.16 indicate that cells that were acutely treated with 30 mM glucose for 72 h responded to 500 μM H_2O_2 with a lower metabolic activity compared to 5 and 17 mM glucose-treated cells. This is an important observation and may indicate that even acute exposure to elevated glucose levels may contribute to a reduced tolerance to H_2O_2-induced oxidative stress.

4.3.4 Aim 4: to quantify the effect of glucose and acute H_2O_2 on expression of selected genes

As mentioned previously, MMP-2, -9 and -13 were the targets selected among the human MMP family. These targets were chosen as high glucose concentrations have been shown to increase their expression in a variety of different cell types or cell lines, including primary neurons, endothelial cells, smooth muscle cells and adventitial fibroblasts (126, 127, 128, 129, 130). Rat tenocytes were tested in response to 25 mM glucose (130), however research has not yet been conducted to date on primary human tenocytes.

MMP-2 (*MMP2*) expression following glucose and H_2O_2 treatement

MMP-2 proved to be sensitive to H_2O_2 on the mRNA level (figure 4.17): under 100 μM H_2O_2 the expression of MMP-2 was significantly reduced in the 30 mM glucose condition compared to 5 mM glucose control. When considering the response to glucose alone, the data of this particular patient does not support the earlier findings in Chapter 3 (figure 3.25) where samples from 3 patients indicated rather MMP-2 upregulation in 30 mM glucose compared to 5 mM glucose control. Expression of MMP-9 and MMP-13 was tested without success. Since these MMPs have been reported in tendon by other researchers, we assume the primers have failed; a positive qPCR control was not available to check.

MMP-13 protein levels in response to glucose and H_2O_2

Tenocyte MMP-13 levels were evaluated after glucose and H_2O_2 incubation by quantitative western blotting (figure 4.18). Data that was not normalized to a housekeeper protein (B in the figure) would suggest a dose response to H_2O_2 in 17 mM glucose. Repeats of the experiment would resolve the absence of a housekeeping protein if time allowed.

mRNA expression in response to H_2O_2 treatment: collagen1α1, collagen1α2, collagen3α1, aggrecan, SOD-1, -2, -3, catalase and FOXO-1

The aim of this section was to see how H_2O_2 affects the gene expression of selected targets. H_2O_2 represents a method to increase cell oxidative stress. I hypothesized that oxidative stress impacts essential ECM components and therefore oxidative stress enzymes and FOXO1 should display a response to H_2O_2 treatment. A lower dose of H_2O_2 (100 μM) was selected from the literature and my viability experiments as mRNA expression is

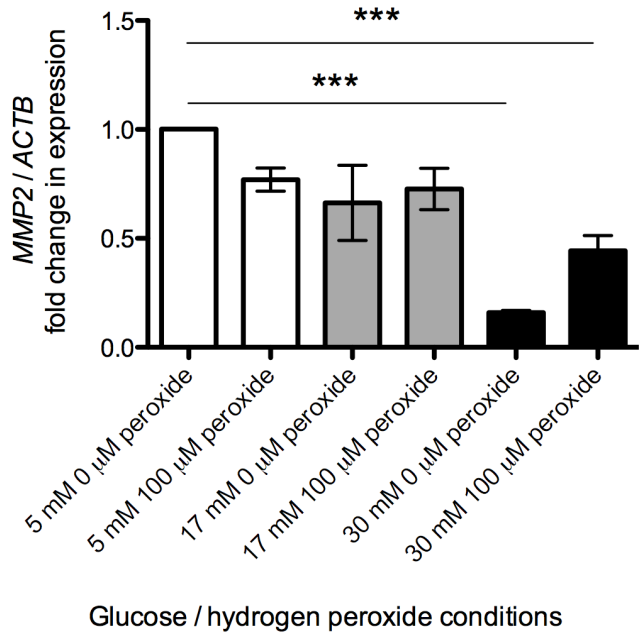

Figure 4.17: *MMP2* expression following culture in different glucose media and following H_2O_2 insult (n=1 patient, Biosera medium). Tenocytes were cultured in 5, 17 and 30 mM glucose media. For experiment, 100 μM H_2O_2 was applied for 18 h. At the end of the incubation RNA was extracted, converted to cDNA and qPCR was quantified using TaqMan. β-actin ($ACTB$) served as housekeeper gene. Each column is a mean of 3 technical replicates. Error bars represent SD. N too small to determine normality (D'Agostino & Pearson / Shapiro-Wilk normality tests). One-way ANOVA and Tukey as *post-hoc* test. ANOVA p-value < 0.0001. Significant results were reported for multiple comparisons, but only those < 0.5-fold were considered in order to follow standard qPCR practice (158).

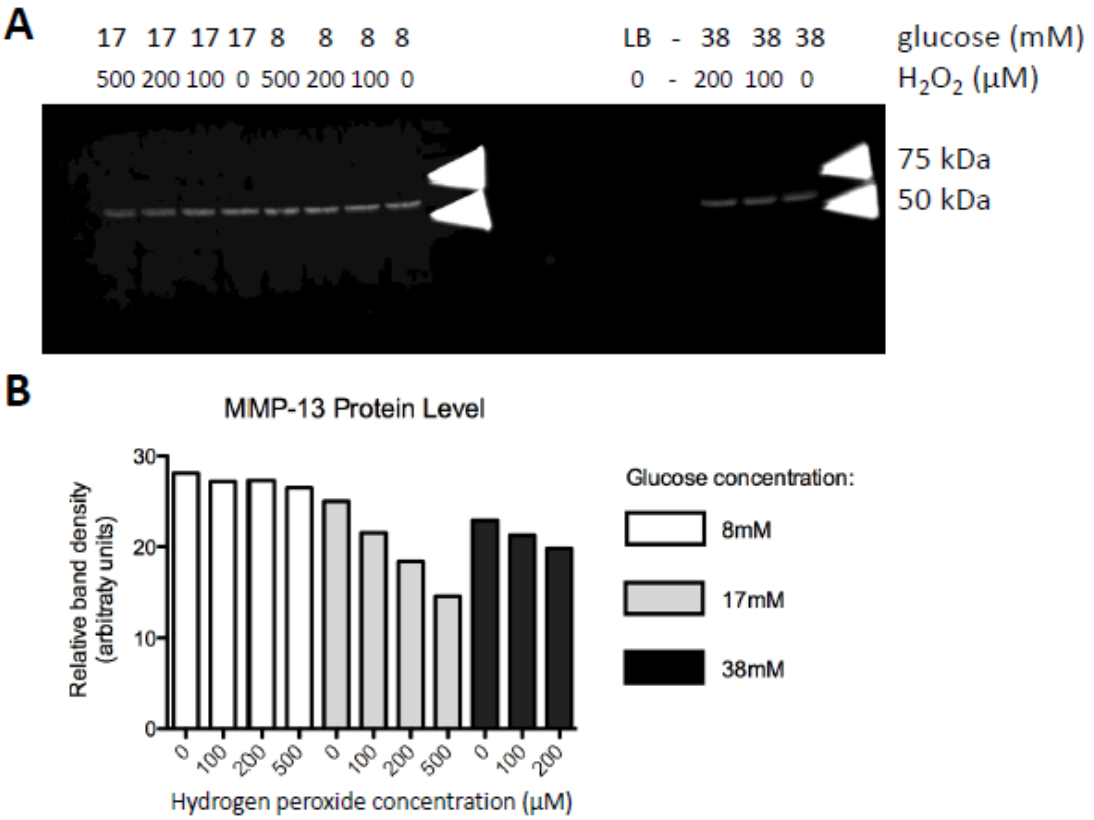

Figure 4.18: MMP-13 protein levels in response to glucose and H_2O_2, as determined by Western blot (n=1 patient, Lonza medium). A) MMP-13 immunublot. B) Heavier cleavage fragment of MMP-13. Tenocytes were chronically cultured in 8, 17 and 38 mM glucose media, and for experiment incubated with 0-500 μM H_2O_2 range for 24 h. Cells were harvested, and cell lysates were run using gel electrophoresis followed by transfer to a blotting membrane. Data for 38 mM glucose 500 μM H_2O_2 was not obtained due to cell death in this condition (confirmed by microscopy before cell harvest step). n=1 for each column (B). There was a technical issue with housekeeper β-actin immunoblot, therefore the data in B is not normalized. LB = loading buffer alone, used as control.

expected to be more sensitive to intracellular H_2O_2 concentration than whole cell responses such as death.

Response of collagen mRNA can be found in figure 4.19. It indicates that collagen1α1 is significantly downregulated in 5 mM glucose medium after H_2O_2 insult compared to the control condition (i.e. 5 mM glucose medium, no H_2O_2). In 30 mM glucose the H_2O_2-treated cells also show downregulation in collagen1α1 compared to cells grown in 30 mM glucose without H_2O_2 treatment. As for collagen1α2, the 30 mM glucose-treated cells would suggest a difference between H_2O_2 and no H_2O_2 treatment, however this difference is not statistically significant. The most significant results can be seen in collagen3α1: H_2O_2 treatment significantly reduces mRNA in both 5 and 17 mM glucose-treated cells, compared to 5 mM glucose no peroxide. The 30 mM data set for collagen3α1 was partially excluded due to technical issue. We have seen in Chapter 3 that collagen type I and collagen type III, encoded by *COL1A1* and *COL3A1* respectively, are both significantly upregulated in response to 17 mM and 30 mM glucose at the mRNA level (figure 3.21). The data here (figure 4.19) however does not confirm these findings. The data here is only 1 patient, whereas data in Chapter 3 was from 2-3 patients (as indicated in legend). Aggrecan shows a stronger response to H_2O_2: the expression did not change across glucose conditions alone, however H_2O_2 treatment significantly reduced the expression in all glucose conditions (figure 4.19). This is in agreement with the sulphated GAG assay results presented in figure 3.24 where no differences were observed across glucose conditions, but not in agreement with figure 3.23 where aggrecan responded with upregulation in both 17 and 30 mM glucose, compared to 5mM glucose.

Tested SOD enzymes responded to H_2O_2 in the following way (figure 4.20): SOD-1 was significantly ($\sim$ 2 to 2.5-fold) upregulated in all glucose conditions in response to H_2O_2 (although 30 mM glucose condition did not give statistical significance, the pattern was present). SOD-2 and SOD-3 exhibit a comparable pattern to SOD-1 (with up to 3.5-fold upregulation in SOD-2 in response to H_2O_2 under 17 mM glucose). Note that 30 mM condition was incomplete for SOD-3. In contrast, catalase 17 mM but not 5 mM glucose-treated cells indicated a borderline downregulation in response to H_2O_2 treatment (D in figure 4.20). Note that 30 mM condition was incomplete for catalase.

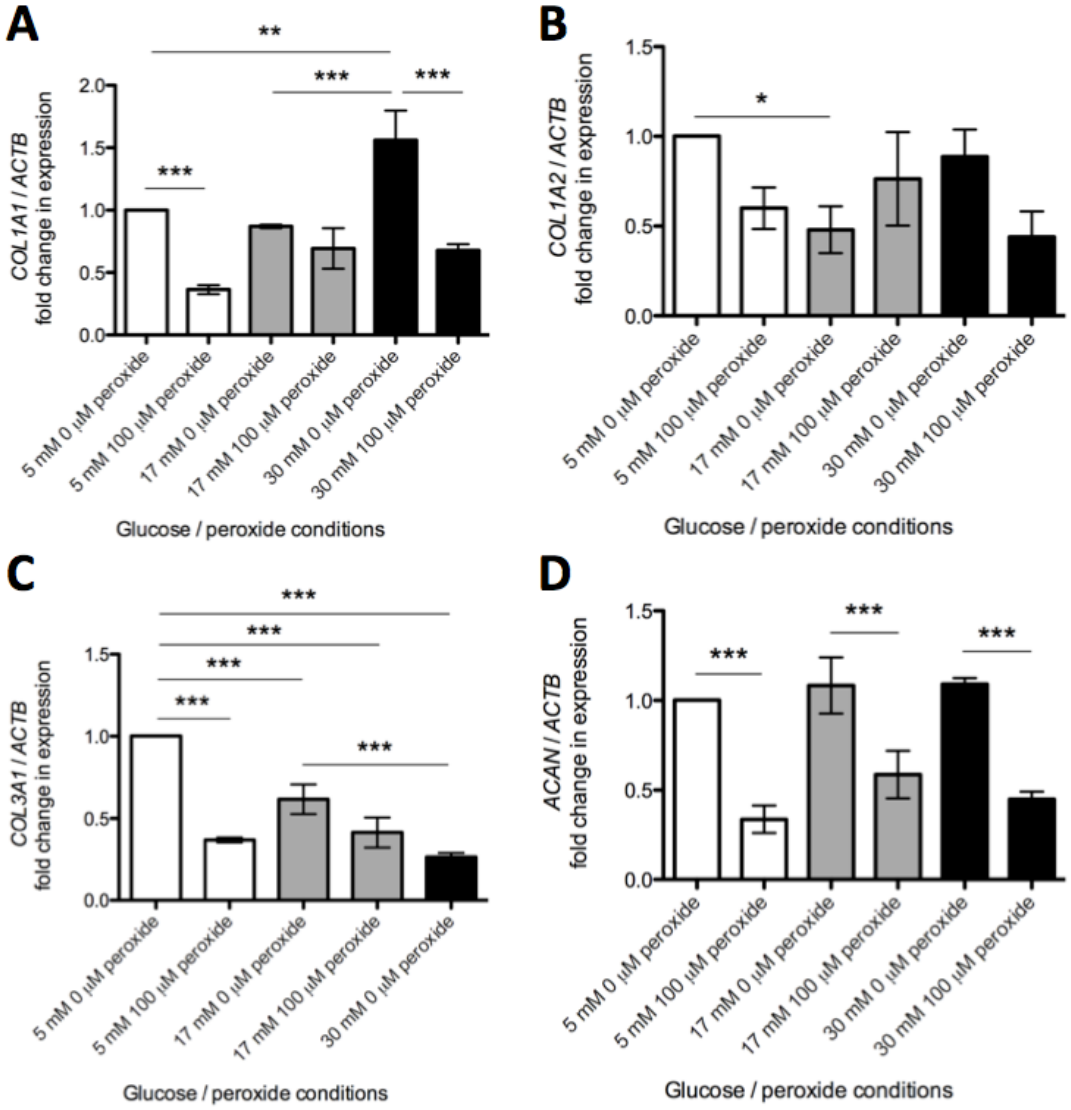

Figure 4.19: Gene expression following culture in different glucose media and H_2O_2 treatment (n=1 patient, Biosera medium). A) collagen type I alpha 1 chain *COL1A1*, B) collagen type I alpha 2 chain *COL1A2*, C) collagen type III alpha 1 chain *COL3A1*, D) aggrecan *ACAN*. Tenocytes were chronically cultured in 5, 17 and 30 mM glucose media. For experiment, a 100 μM H_2O_2 insult was applied for 18 h. RNA was then extracted, converted to cDNA and qPCR quantified using SYBR Green. β-actin (*ACTB*) served as housekeeper gene. Columns represent mean of 3 values, error bars are SD. N too small to determine normality (D'Agostino & Pearson / Shapiro-Wilk normality tests). One-way ANOVA and Tukey as *post hoc* test. A) ANOVA p-value < 0.0001, B) p-value $= 0.0072$, C) p-value < 0.0001, D) p-value < 0.0001. Only statistics of interest is shown. Technical information: all samples passed quality control on Nanodrop, except 30 mM samples. The 30 mM samples were very low in RNA yield to begin with. TapeStation data for sample 5 mM glucose no peroxide was borderline in terms of quality. In collagen3α1 one column was excluded.

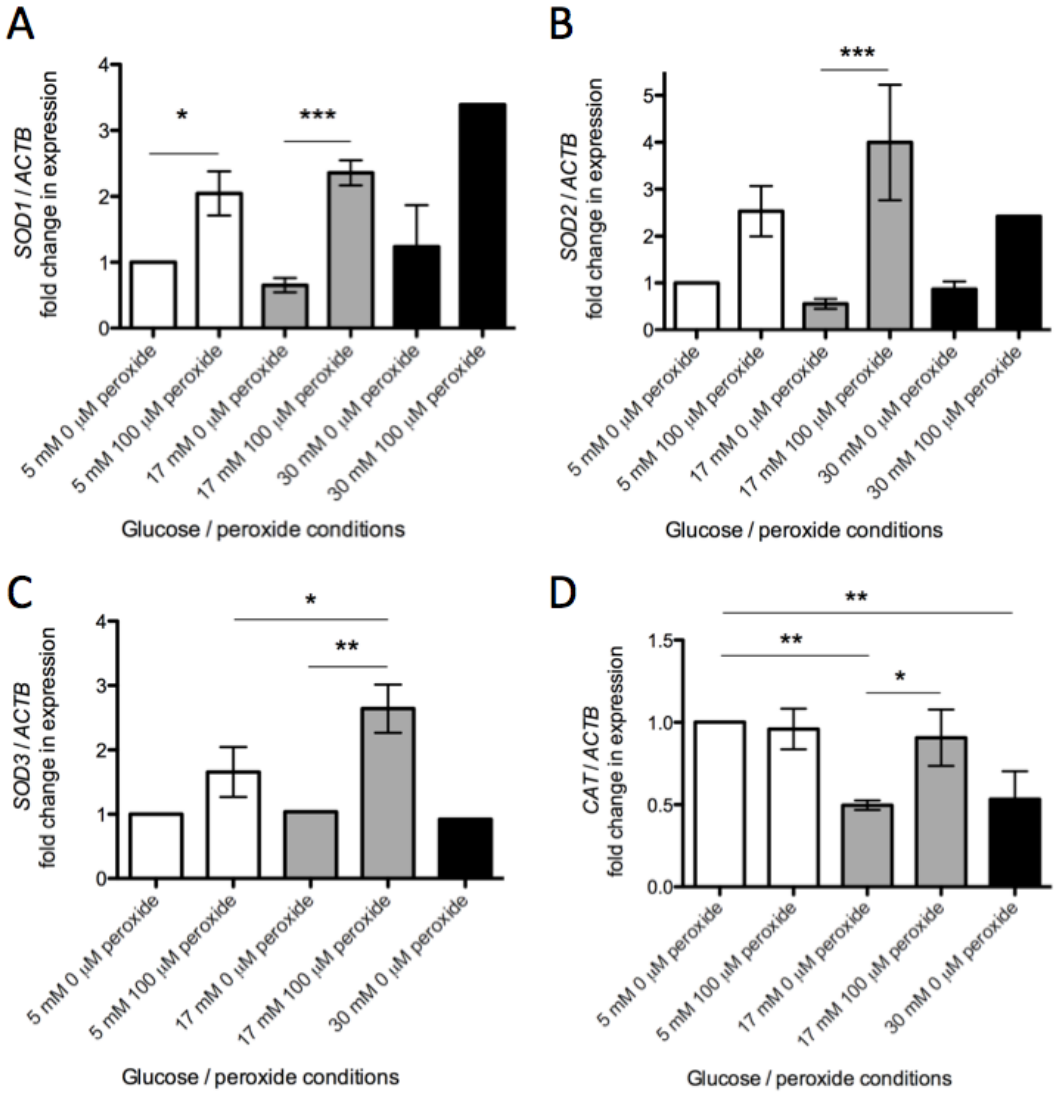

Figure 4.20: Gene expression following culture in different glucose media and H_2O_2 insult (n=1 patient, Biosera medium). A) SOD-1 *SOD1*, B) SOD-2 *SOD2*, C) SOD-3 *SOD3*, D) catalase *CAT*. Tenocytes were chronically cultured in 5, 17 and 30 mM glucose media. For experiment, a 100 μM H_2O_2 insult was applied for 18 h. RNA was then extracted, converted to cDNA and qPCR quantified using SYBR Green. β-actin (*ACTB*) served as housekeeper gene. Columns represent mean of 3 values except where otherwise indicated; error bars are SD. N too small to determine normality (D'Agostino & Pearson / Shapiro-Wilk normality tests). One-way ANOVA and Tukey as *post hoc* test: A) ANOVA p-value=0.0004, B) p-value=0.0002, C) p-value=0.0008, D) p-value=0.0008. Only statistics of interest is shown. Technical information: all samples passed quality control on Nanodrop, except 30 mM samples. The 30 mM samples were very low in RNA yield to begin with. TapeStation data for sample 5 mM glucose no peroxide was bordeline in terms of quality. Note about SODs: data with borderline CT values (only the case of 30 mM glucose that generated poor qPCR readings despite being adjusted to identical cDNA concentration) were included in order to visualize any potential expression pattern. Note about SOD-1 30 mM glucose 100 μM H_2O_2, SOD-2 30 mM glucose 100 μM H_2O_2, and SOD-3 30 mM glucose 0 μM H_2O_2: only 1 data point was available therefore no error bar is indicated, and had to be excluded from ANOVA analysis. Note that in C and D certain columns were excluded.

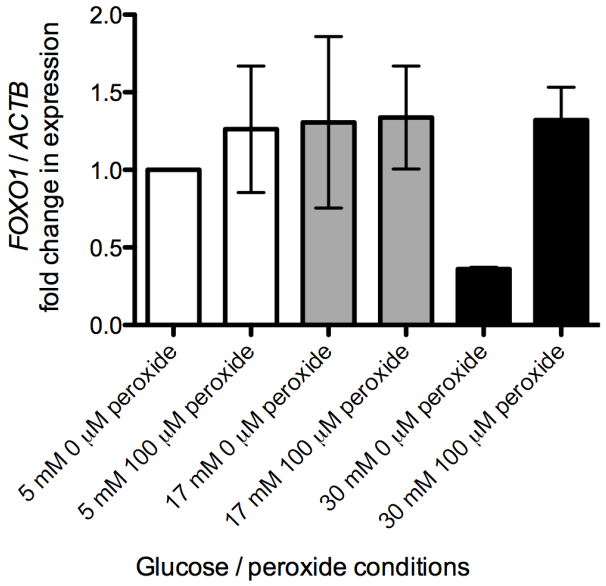

Figure 4.21: Forkhead box protein O1 (*FOXO1*) expression following culture in different glucose media and H_2O_2 insult (n=1 patient, Biosera medium). Tenocytes were chronically cultured in 5, 17 and 30 mM glucose medium. For experiment, a 100 μM H_2O_2 insult was applied for 18 h. RNA was then extracted, converted to cDNA and qPCR quantified using SYBR Green. β-actin (*ACTB*) served as housekeeper gene. Columns represent mean of 3 values, error bars are SD. *N* too small to determine normality (D'Agostino & Pearson / Shapiro-Wilk normality tests). One-way ANOVA and Tukey as *post hoc* test: ANOVA p-value=0.0918. Technical information: all samples passed quality control on Nanodrop, except 30 mM samples. The 30 mM samples were very low in RNA yield to begin with.

Given the involvement of FOXOs in the oxidative stress response, expression of FOXO-1 was evaluated in H_2O_2-treated cells (figure 4.21). No difference is seen in *FOXO1* expression in the tested conditions; 30 mM glucose condition had significant technical issues due to poor cell yield/senescence.

***CDKN1A* response to H_2O_2 in tenocytes from extended 30 mM glucose culture**

Phenotypic senescence was reported in Chapter 3 (Aim 3), especially in the 30 mM glucose condition. Senescent cells upregulate p21, p16 or both (depending on the type and level of stress the p21 pathway can either antagonize or synergize with p16), which are not commonly expressed by quiescent or terminally differentiated cells (112). Therefore the expression of P16 and P21 genes was examined in the 30 mM glucose condition to further evaluate the observed phenotype. Since the 30 mM glucose-treated cells generated very low RNA yield compared to 5 and 17 mM glucose-treated cells in previous

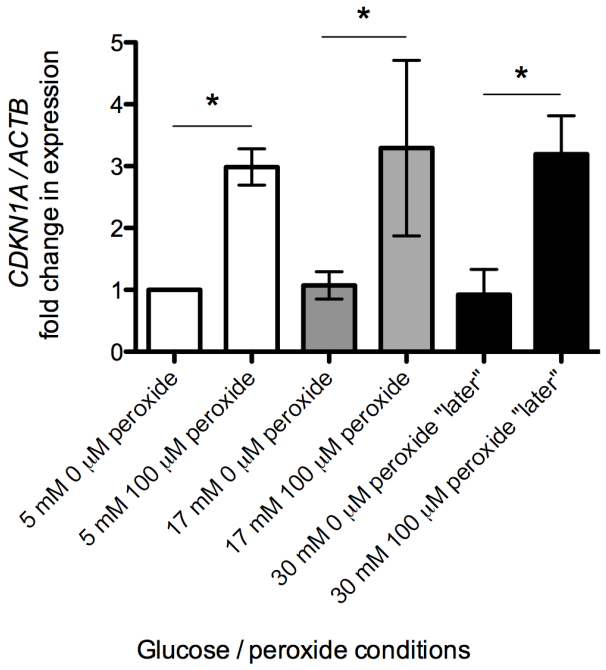

Figure 4.22: p21cip or cyclin dependent kinase inhibitor 1A (*CDKN1A*) expression following culture in different glucose media and H_2O_2 insult (n=1 patient, Biosera medium). Tenocytes were chronically cultured in 5, 17 and 30 mM glucose medium; the 30 mM glucose condition was kept growing for 9 days longer due to slow cell growth. For experiment cells were treated with 100 μM H_2O_2 for 18 h. RNA was extracted, converted to cDNA and qPCR quantified using SYBR Green. β-actin (*ACTB*) served as housekeeper gene. Columns represent mean of 3 values, error bars are SD. N too small to determine normality (D'Agostino & Pearson / Shapiro-Wilk normality tests). One-way ANOVA and Tukey as *post hoc* test: ANOVA p-value=0.0008. Technical information: all samples passed quality control on Nanodrop, except 30 mM samples. TapeStation analysis for the 30mM no peroxide "later" sample indicated high RNA degradation and failed quality control. Note that since 30 mM glucose-treated cells were cultured on its own for longer, any comparison between them and other conditions is not quantitative.

assays, solely for this experiment the 30 mM glucose-treated cells were cultured for an extended time (9 days longer) than 5 and 17 mM glucose-treated cells in an attempt to achieve confluency before RNA extraction. Data showed that the p16-targeted primer pair performed poorly in qPCR hence no data is available. Pro-senescence effector p21 (gene *CDKN1A*) data suggest that all glucose conditions respond to H_2O_2 with a 3-fold increase in p21 expression, however the magnitude of this response is independent of the glucose condition (figure 4.22).

4.3.5 Aim 5: to determine whether the glucose and H_2O_2-induced response can be attenuated by selected protective agents

Four potentially protective reagents were selected and applied under elevated glucose in order to determine whether any of these can protect tenocytes against toxic effects of H_2O_2. The tested reagents were AA (a non-enzymatic antioxidant), n-acetyl cysteine (NAC), resveratrol, and switching glucose concentration from low to high and *vice versa*. NAC is an effective scavenger of free radicals due to its interaction with ROS (e.g. hydroxyl radical and H_2O_2); it can in this way minimize the oxidative effect of ROS (159). Resveratrol is both a scavenger of free radicals (such as superoxide ion and hydroxyl radical) and a potent antioxidant due to its capacity to promote activities of antioxidant enzymes (160).

Initial toxicity screening (NAC, AA and resveratrol)

It was essential to first determine the appropriate treatment concentrations of three of the selected substances as their potential toxicity was unknown in this assay system. I aimed to select two doses for each substance from the literature and subsequently apply those in experiments. First experimental run is indicated in figure 4.23, second, complementary, run is in figure 4.24. Suitable doses for NAC were identified as 1 mM and 5 mM (other doses reduced metabolic activity compared to control). For AA [1] the appropriate doses were 0.5 mM and 1 mM since the dose curve plateaud after 1 mM AA. Finally, for resveratrol the doses of 10 μM and 30 μM were tolerated, however this was coupled with a substantial decrease in metabolic activity for all doses assessed.

Application of protective agents

Figure 4.25 reveals that both doses of **NAC** (1 and 5 mM) protect the metabolic activity of tenocytes that were treated with 800 μM H_2O_2 as opposed to controls. This experiment confirms previous observations that peroxide becomes toxic between 500 - 800 μM H_2O_2 where cell metabolic activity plummets dramatically. As cells in 17 mM glucose condition were seeded at different density (details in figure legend), it is advisable to compare percentage decrease in this figure. Percentage decrease for 5 mM and 17 mM conditions exhibits a very similar pattern, unlike in the 30 mM glucose condition.

[1] The composition of media employed in this project did not contain any AA (unless supplemented manually, as indicated).

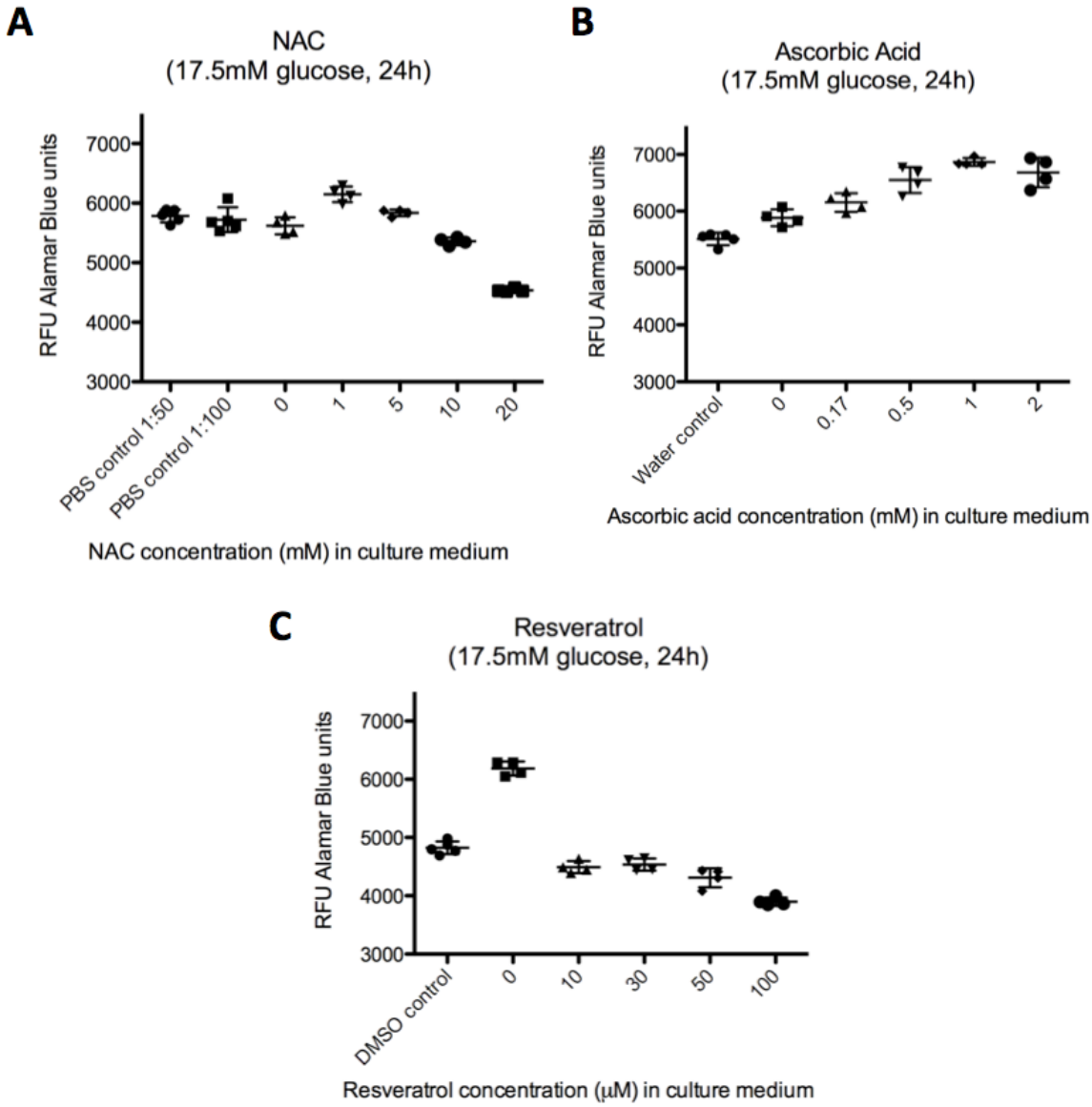

Figure 4.23: Toxicity screening as determined by tenocyte metabolic activity (n=1 patient, Biosera medium). A) NAC, B) AA, C) resveratrol. Substance incubation for 24 h, Alamar Blue for the last 3 h of the incubation. All experiments conducted in 17 mM glucose medium, cell passage was P5. Note resveratrol DMSO control was 1:1,000.

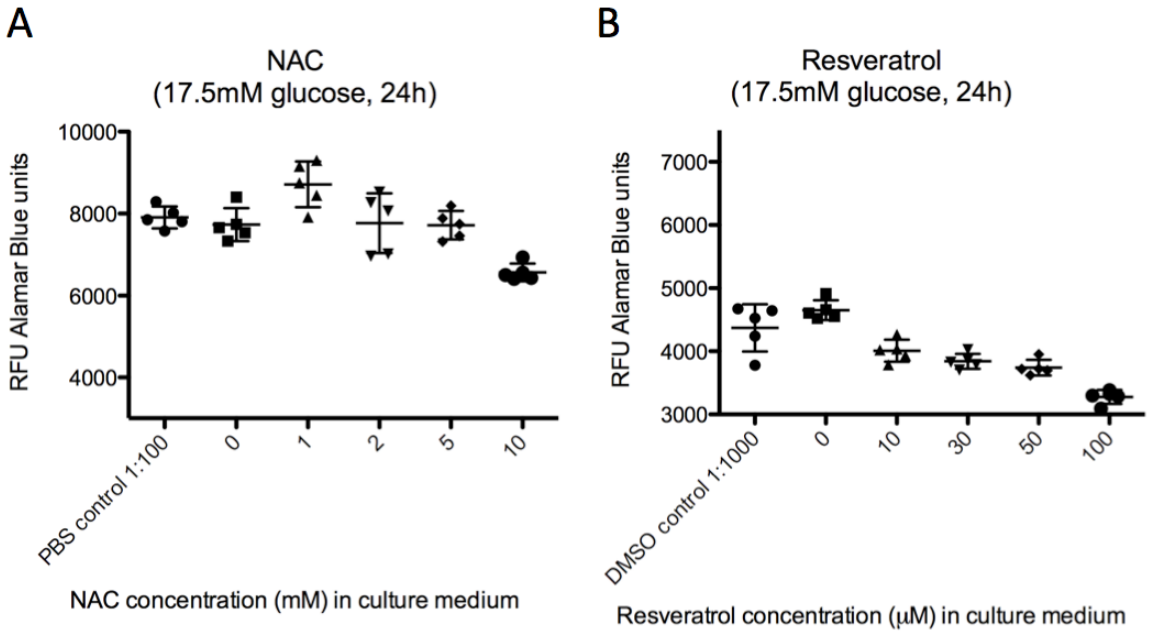

Figure 4.24: A supplementary experiment of toxicity screening, as determined by tenocyte metabolic activity (n=1 patient, Biosera medium). A) NAC, patient T15, B) resveratrol, patient T17. Substance incubation for 24 h, Alamar Blue for the last 3 h of the incubation. All experiments conducted in 17 mM glucose medium, cell passage was P5. Note different y axis scale. Technical note: seeding density for A and B was not identical.

Accompanying Live/Dead data for NAC treatment are in figures 4.26, 4.27 and 4.28. As hypothesized previously, threshold for H_2O_2 toxicity has been narrowed to the 500 - 800 μM H_2O_2 interval. The L/D data confirm this and indicate that cells are dead (and detached from the growth surface) in the 800 μM H_2O_2 treatment. However, as these figures show, both NAC doses (even the lower one of 1 mM) are able to protect cells in the damaging 800 μM H_2O_2 dose.

Figure 4.29 indicates that **AA** treatment alone increases cell metabolic activity compared to the control condition (no AA treatment 0 μM H_2O_2). As the cells had different initial seeding densities (details in figure legend), it is necessary to look at percentage decrease in metabolic activity. In 500 μM H_2O_2 dose, AA treatments do not offer any protective effect as it can be seen that they increase the cell metabolic activity independently. In 800 μM H_2O_2 dose, AA treatments are not protective: all cells in all conditions display a dramatic reduction in their metabolic activity. Altogether, no differences are seen across glucose conditions.

Accompanying Live/Dead data for AA treatment in 5 mM glucose-treated tenocytes

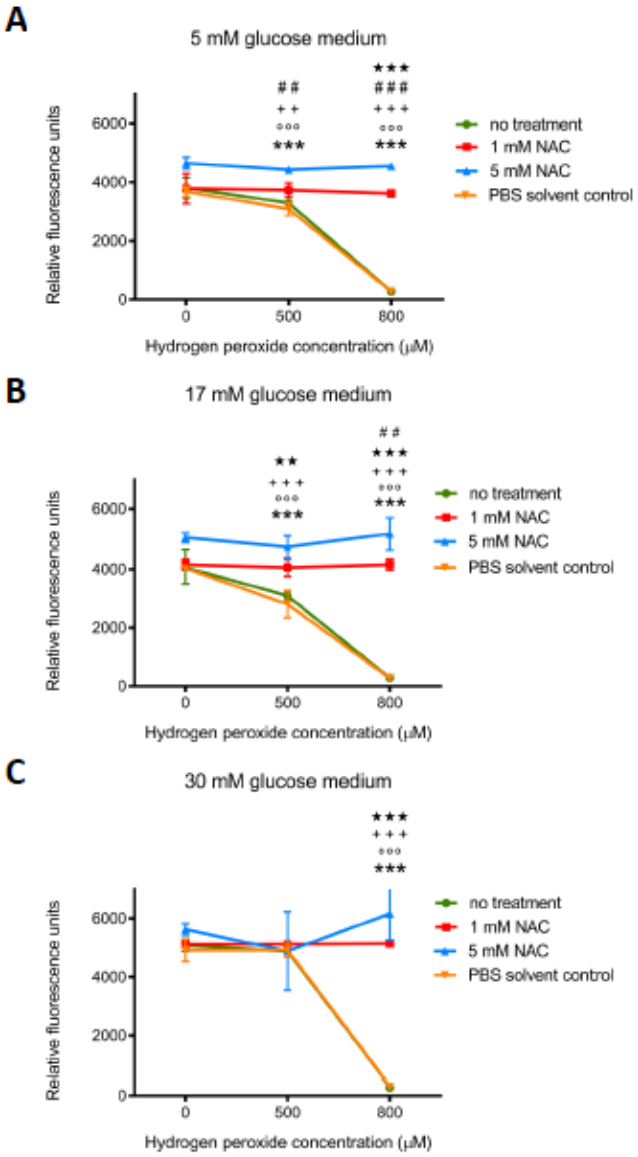

Figure 4.25: Tenocyte metabolic activity following H_2O_2 and NAC treatment (n=1 patient, Biosera medium). A) 5 mM glucose medium, B) 17 mM glucose medium, C) 30 mM glucose medium. Tenocytes were chronically cultured in 5, 17 and 30 mM glucose media, then seeded for experiment in 96-well dishes. Cells were treated with 0, 500 and 800 μM H_2O_2 for 24 h and at the same time with 0, 1 and 5 mM NAC (i.e. H_2O_2 and protective reagent were in same solution). 1:100 PBS solvent control. There was no pre-treatment with protective agent. Alamar Blue reagent was added for the last 4 h of incubation, then analyzed on Fluorstar Optima reader. Each point represents mean of 3 technical replicates, error bars represent SD. Note there was a difficulty with seeding: 5 mM cells were seeded at 2,900 cells/well, 17 mM at 1,500 cells/well, 30 mM cells at 2,900 cells/well density. Cells were seeded into experimental dishes 48 h before experiment however they were only 40% confluent (at most) at time of experiment. Two-way ANOVA with Bonferroni. Only statistical significance of interest is shown: results for statistics within the 500 μM and within the 800 μM H_2O_2 cluster are indicated with symbols above these clusters. Key to statistical symbols (comparisons made within clusters): $*$ compares no treatment vs. 5 NAC, # compares 1 NAC vs. 5 NAC, + compares 1 NAC vs. PBS, $^\circ$ compares 5 NAC vs. PBS, $\star$ compares no treatment vs. 1 NAC. Prism significance intervals are defined as: not significant (ns) $P > 0.05$; * $P \leq 0.05$; ** $P \leq 0.01$; *** $P \leq 0.001$.

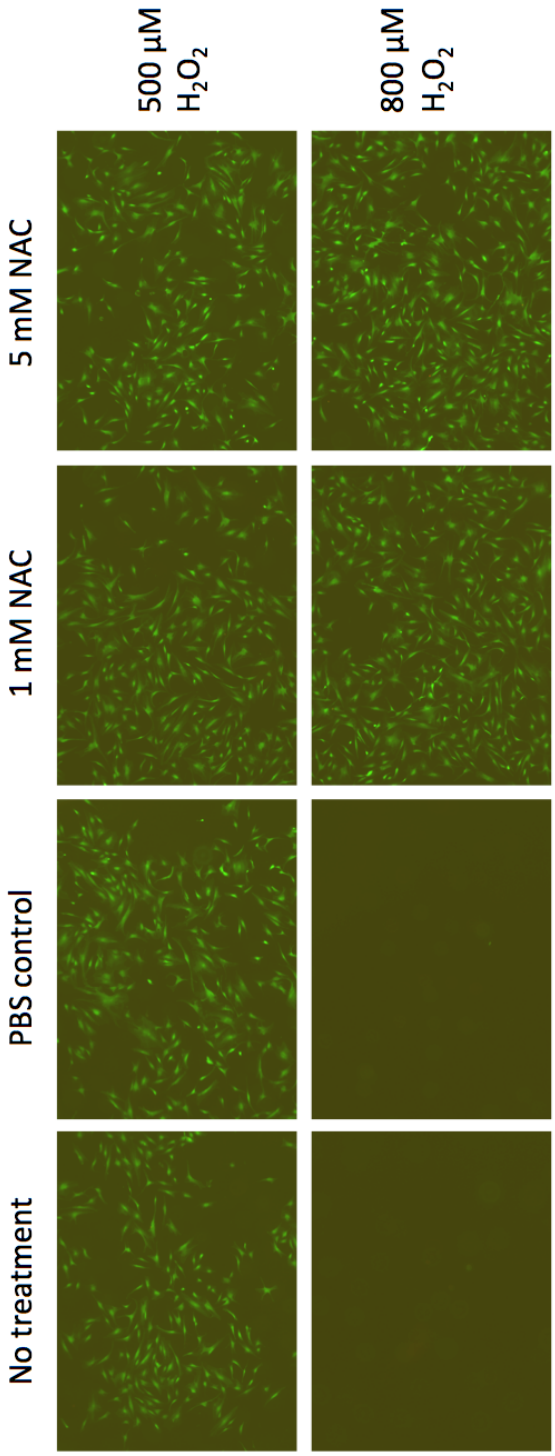

Figure 4.26: 5 mM glucose cell monolayer following NAC treatment, as visualized by L/D stain (n=1 patient, Biosera medium). Tenocytes were chronically cultured in 5 mM glucose medium. For experiment in 96-well plates they were treated for 24 h with 0, 500 and 800 μM H_2O_2, and simultaneously with 0, 1 and 5 mM NAC, in the same solution. Solvent control: 1:100 PBS. At end of 24 h treatment, cells were L/D stained and images taken under microscope. Composite images, magnification x100, only images of interest shown here. Note these 5 mM cells were seeded at 2,900 cells/well density.

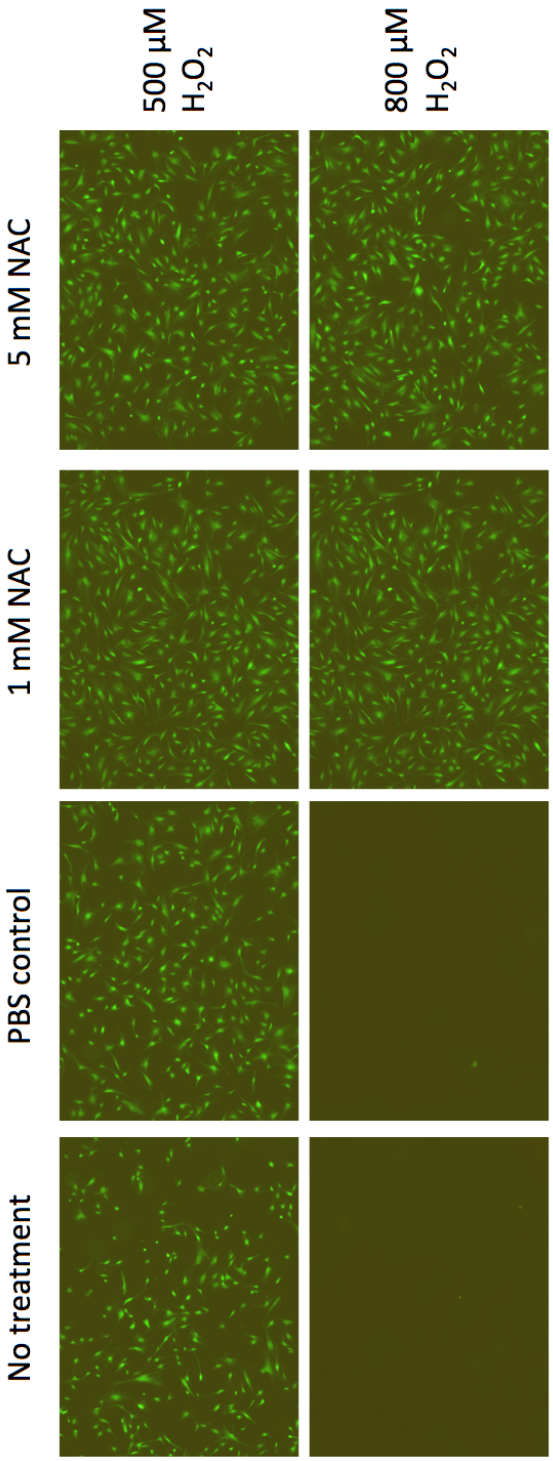

Figure 4.27: 17 mM glucose cell monolayer following NAC treatment, as visualized by L/D stain (n=1 patient, Biosera medium). Tenocytes were chronically cultured in 17 mM glucose. For experiment in 96-well plates they were treated for 24 h with 0, 500 and 800 μM H_2O_2, and simultaneously with 0, 1 and 5 mM NAC, in the same solution. Solvent control: 1:100 PBS. At end of 24 h treatment, cells were L/D stained and images taken under microscope. Composite images, magnification x100, only images of interest shown here. Note these 17 mM cells were seeded at 1,500 cells/well density.

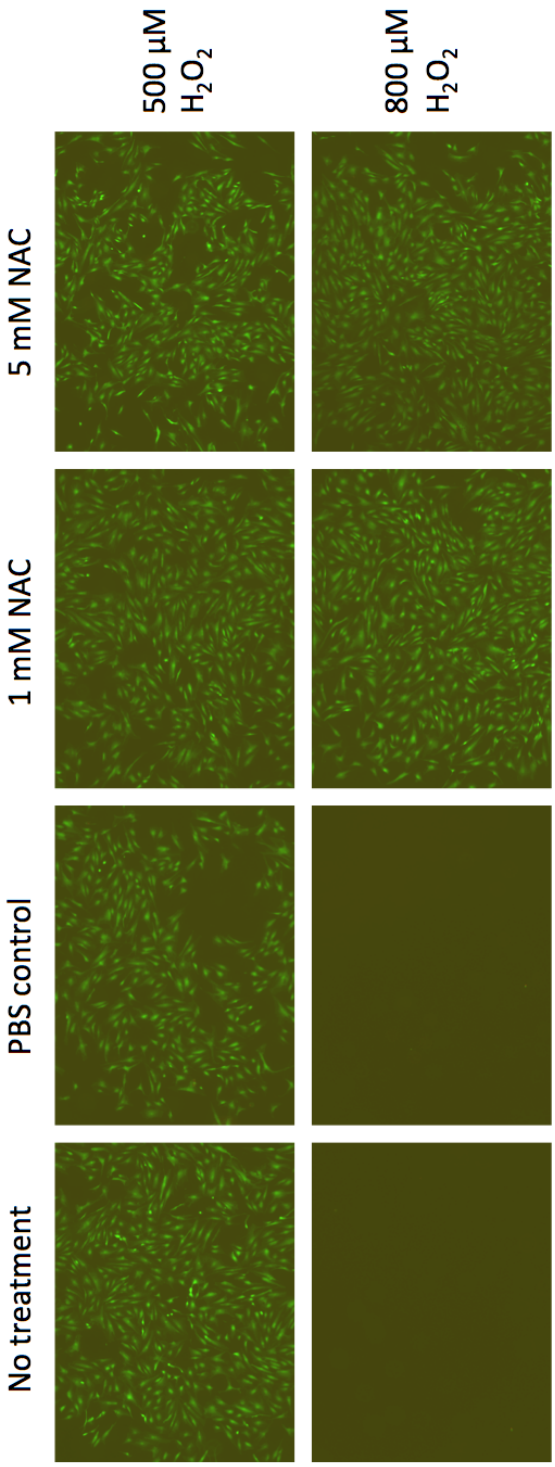

Figure 4.28: 30 mM glucose cell monolayer following NAC treatment, as visualized by L/D stain (n=1 patient, Biosera medium). Tenocytes were chronically cultured in 30 mM glucose. For experiment in 96-well plates they were treated for 24 h with 0, 500 and 800 μM H_2O_2, and simultaneously with 0, 1 and 5 mM NAC, in the same solution. Solvent control: 1:100 PBS. At end of 24 h treatment, cells were L/D stained and images taken under microscope. Composite images, magnification x100, only images of interest shown here. Note these 30 mM cells were seeded at 2,900 cells/well density.

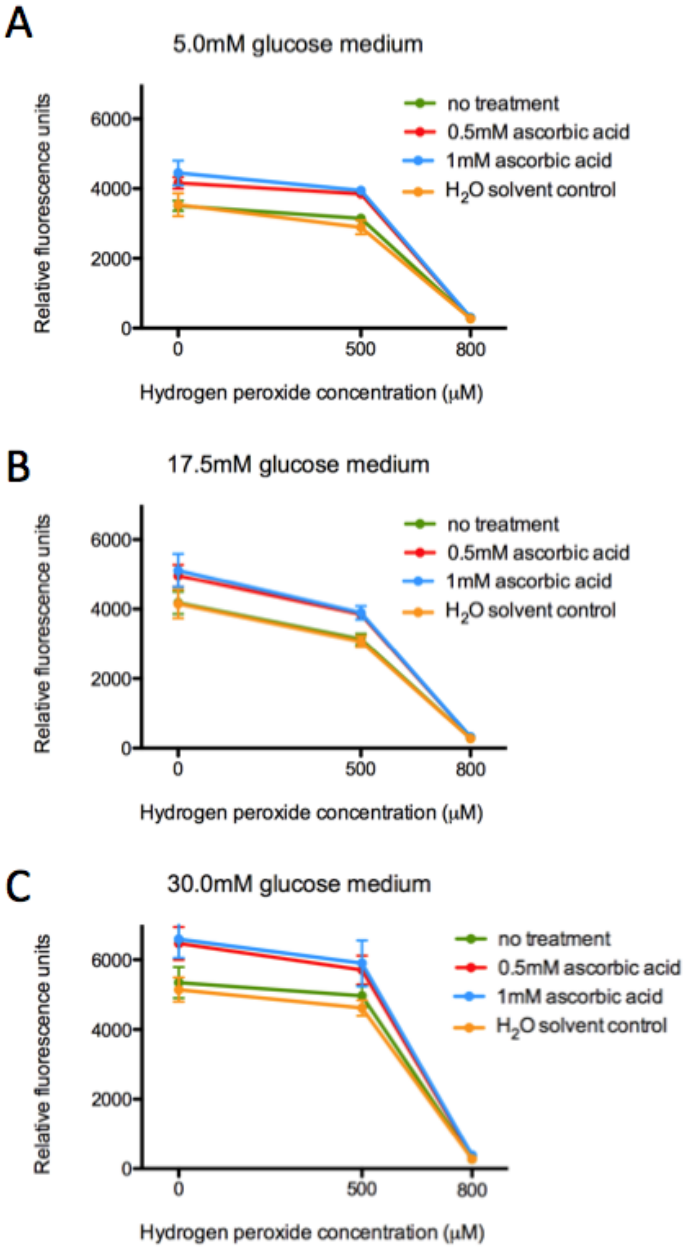

Figure 4.29: Tenocyte metabolic activity following H_2O_2 and AA treatment (n=1 patient, Biosera medium). A) 5 mM glucose medium, B) 17 mM glucose medium, C) 30 mM glucose medium. Tenocytes were chronically cultured in 5, 17 and 30 mM glucose media, then seeded for experiment in 96-well dishes. Cells were treated with 0, 500 and 800 μM H_2O_2 for 24 h, and simultaneously with 0, 0.5, 1.0 mM AA (i.e. H_2O_2 and protective reagent in same solution). 1:100 water solvent control. There was no pre-treatment with protective agent. Alamar Blue reagent was added for the last 4 h of incubation, then analyzed on Fluorstar Optima plate reader. Each point represents mean of 3 technical replicates, error bars represent SD. Note there was a difficulty with seeding: 5 mM cells were seeded at 2,900 cells/well, 17 mM at 1,500 cells/well, 30 mM cells at 2,900 cells/well density. Cells were seeded into experimental dishes 48 h before experiment however only 40% confluent (at most) at time of experiment.

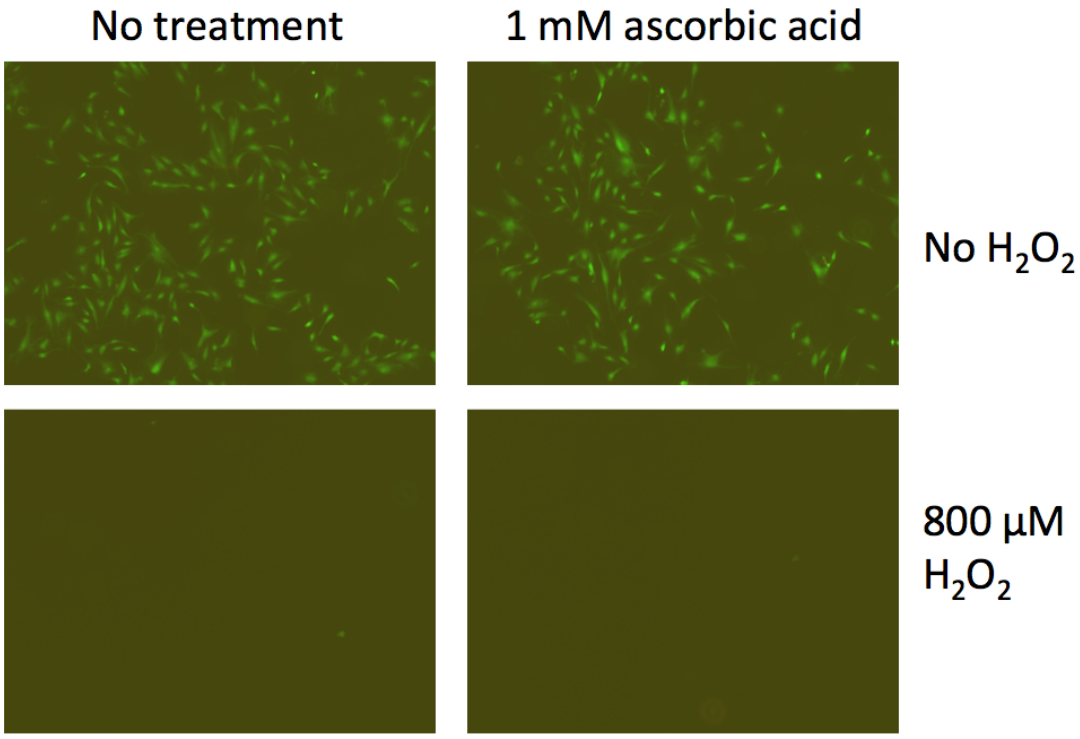

Figure 4.30: 5 mM glucose cell monolayer following AA treatment, as visualized by L/D stain (n=1 patient, Biosera medium). Tenocytes were chronically cultured in 5 mM glucose. For experiment in 96-well plates they were treated for 24 h with 0, 500 and 800 μM H_2O_2, and simultaneously with 0, 0.5 and 1.0 mM AA, in the same solution. Solvent control 1:100 water. At end of 24 h treatment, L/D stains were utilized and images taken under microscope. Composite images, magnification x100, only images of interest shown here. Note these 5 mM cells were seeded at 2,900 cells/well density.

is in figure 4.30, and confirms that tenocytes are dead (and detached from the growth surface) under 800 μM H_2O_2 dose.

Results of **resveratrol** treatment can be seen in figure 4.31: Alamar data indicate that in 5 and 17 mM glucose-treated cells there is no protective effect to be seen with either resveratrol dose in 500 μM H_2O_2. Resveratrol failed to protect cell metabolic activity in the 30 mM glucose condition. It is important to notice that the no treatment shows a higher metabolic activity than either of the resveratrol dose, especially in the 30 mM glucose condition. Altogether, the data suggest that resveratrol cannot be used as a protective agent in these experiments.

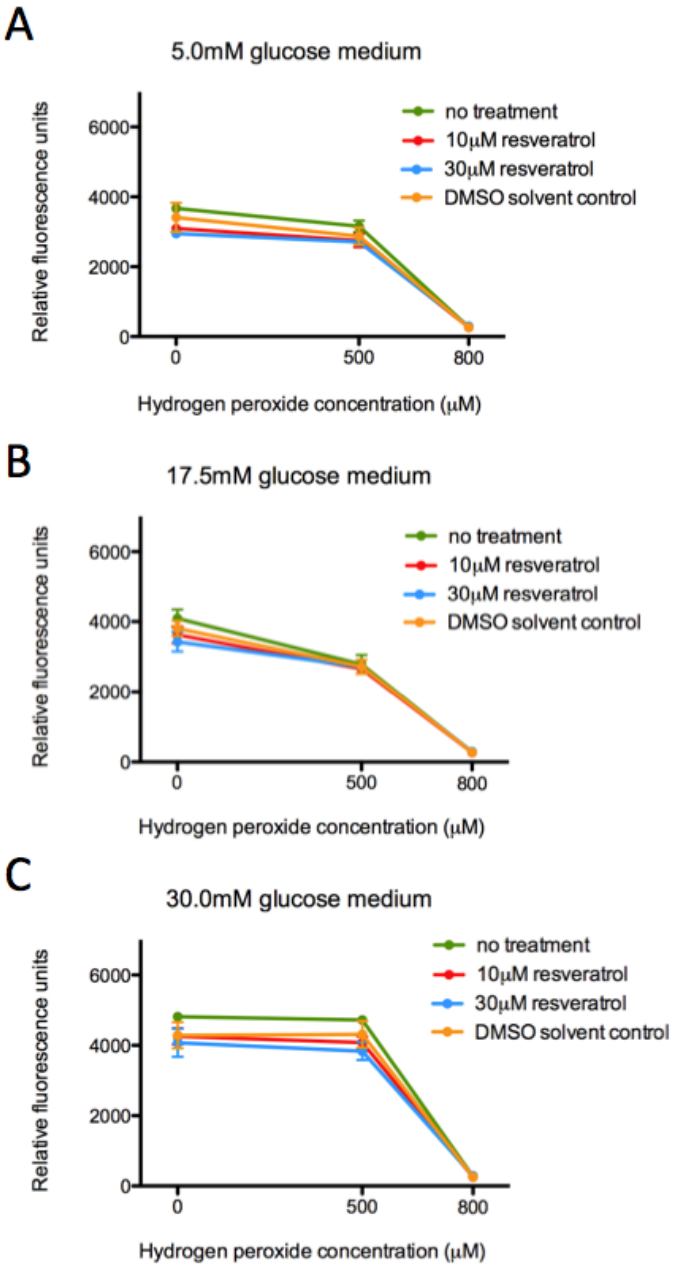

Figure 4.31: Tenocyte metabolic activity following H_2O_2 and resveratrol treatment (n=1 patient, Biosera medium). A) 5 mM glucose medium, B) 17 mM glucose medium, C) 30 mM glucose medium. Tenocytes were chronically cultured in 5, 17 and 30 mM glucose media, then seeded for experiment in 96-well dishes. Cells were treated with 0, 500 and 800 μM H_2O_2 for 24 h, and simultaneously with 0, 10 and 30 μM resveratrol (i.e. H_2O_2 and protective reagent in same solution). 1:1,000 DMSO solvent control. There was no pre-treatment with protective agent. Alamar Blue reagent was added for the last 4 h of incubation, then analyzed on Fluorstar Optima plate reader. Each point represents mean of 3 technical replicates, error bars represent SD. Note there was a difficulty with seeding: 5 mM cells were seeded at 2,900 cells/well, 17 mM at 1,500 cells/well, 30 mM cells at 2,900 cells/well density. Cells were seeded into experimental dishes 48 h before experiment however only 40% confluent (at most) at time of experiment.

Since we have seen that even short bursts of high glucose can be harmful (figure 4.16), and that low glucose can protect against H_2O_2 (figures 4.5 C and D, and 4.7), **low glucose** was tested as a protective agent in itself. Cells were chronically cultured in 5 mM and 30 mM glucose, then treated with H_2O_2 for 24 h and simultaneously switched into the opposite glucose concentration. Results indicate that glucose treatment with aim of protection was unsuccessful in this experimental design (figure 4.32).

Optimization of AA and resveratrol treatments

In figure 4.29 AA treatment did not protect under 500 nor 800 μM H_2O_2 as expected. Similarly, the resveratrol treatment (figure 4.31) exhibited shortcomings. For this reason further optimization was performed. The results (figure 4.33) indicate that AA works best in combination with proline, however even this does not protect the metabolic activity of cells under 800 μM H_2O_2. In B of the figure, it can be seen that resveratrol does not protect metabolic activity of cells as the absolute values of Alamar readings are very low in all tested conditions. It should be noted that in this particular experiment metabolic activity values were very low in 500 μM H_2O_2, a condition under which cells would previously not consistently exhibit lowered metabolic activity. A possible explanation might be that cells that were employed for this experiment were originally chronically cultured in 30 mM glucose, before being switched to 17 mM glucose as cell passage P3 for this optimization experiment. The chronic culture in 30 mM glucose might have rendered them more vulnerable.

Evaluation of proline as a potential synergistic protective agent

From figure 4.33 A it is clear that even lower dose of AA in combination with proline has a higher protective potential than a higher dose of AA alone. It was therefore hypothesized that addition of proline might improve the protective properties of AA against H_2O_2. Although differences were small and only evident at 500 μM H_2O_2, figure 4.34 confirms that the combination of AA and proline benefits protection of cell metabolic activity against H_2O_2. A dose of 1 mM AA combined with 50μg/ml proline results in the highest cell metabolic activity in 5 mM and 17 mM but not in 30 mM glucose conditions. Additionaly, it is apparent that proline alone as a treatment option does not offer as much protection as when combined with AA. As in previous experiments, 5 mM glucose condition seems to offer protection against 500 μM H_2O_2 compared to 17 mM glucose.

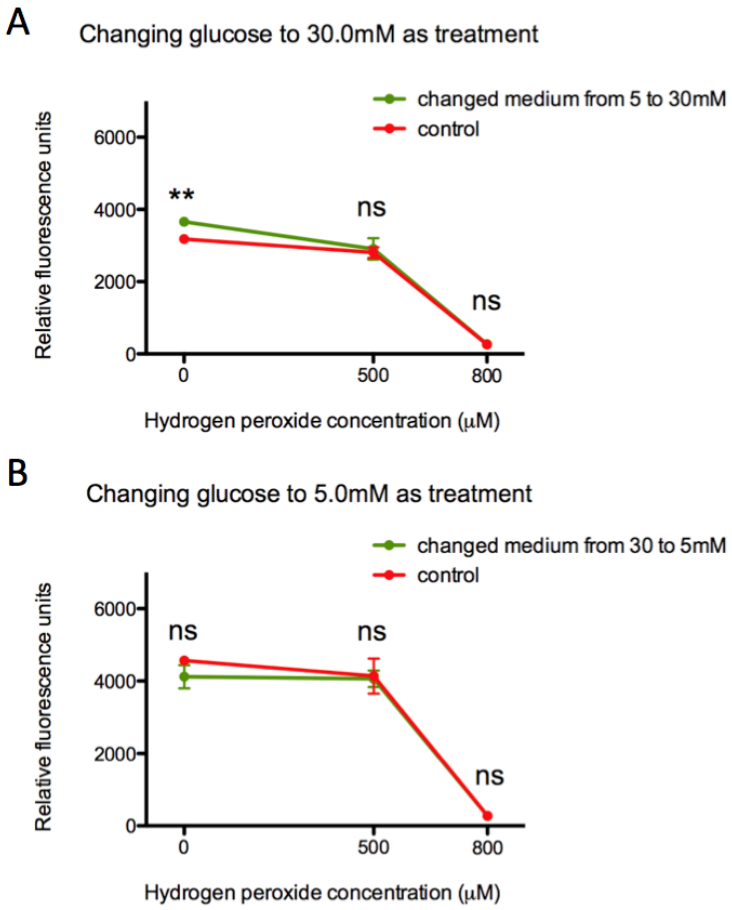

Figure 4.32: Tenocyte metabolic activity following H_2O_2 and glucose treatment (n=1 patient, Biosera medium). A) 5 mM glucose medium switched to 30 mM where control was 5 mM → 5 mM, B) 30 mM glucose medium switched to 5 mM where control was 30 mM → 30 mM. Tenocytes were chronically cultured in 5 and 30 mM glucose media, then seeded for experiment in 96-well dishes. Cells were incubated with 0, 500 and 800 μM H_2O_2 for 24 h, and simultaneously with 5 or 30 mM glucose as "protective treatment" (i.e. H_2O_2 and glucose in same solution). Alamar Blue reagent was added for the last 4 h of incubation, then analyzed on Fluorstar Optima plate reader. Each point represents mean of 3 technical replicates, error bars represent SD. Cells were seeded into experimental dishes 48 h before experiment however only 40% confluent (at most) at time of experiment. Two-way ANOVA with Bonferroni.

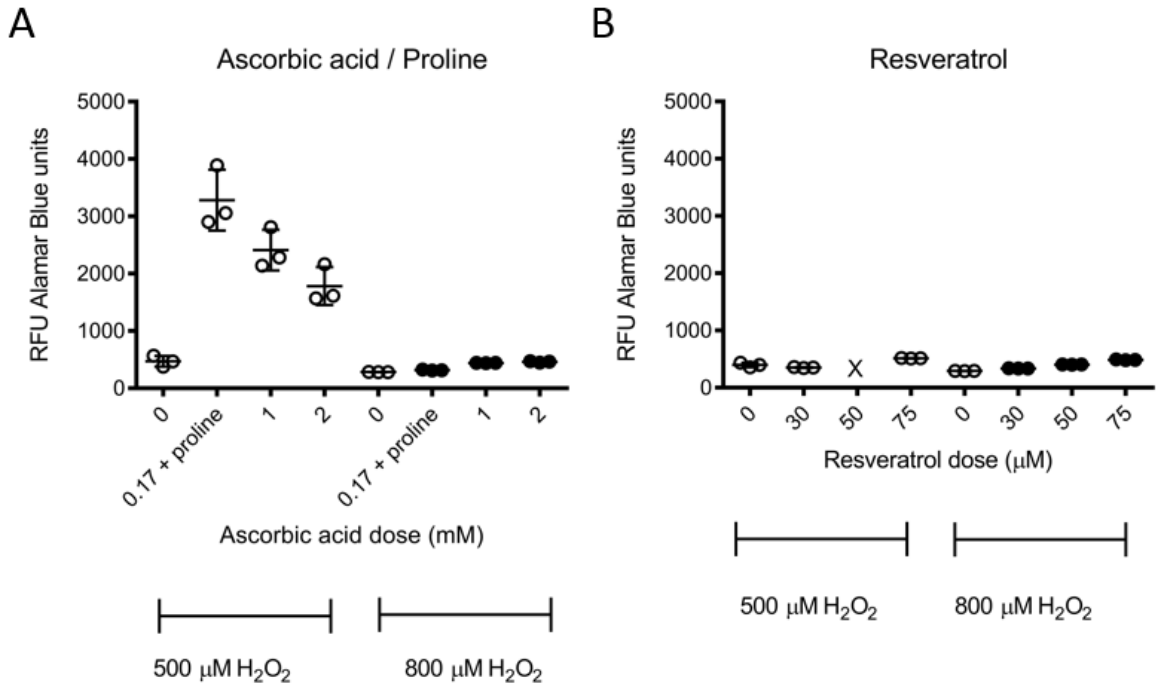

Figure 4.33: Optimisation of AA and resveratrol treatments. Tenocyte metabolic activity following 500 and 800 μM H_2O_2 treatment (n=1 patient, Biosera medium). A) AA treatments, B) resveratrol treatments. Tenocytes were cultured in 17 mM glucose medium, then seeded for experiment in 96-well dishes. Cells were treated with 0, 500 and 800 μM H_2O_2 for 24 h, and simultaneously with AA or resveratrol (i.e. H_2O_2 and protective agent in same solution). Alamar Blue reagent was added for the last 4 h of incubation, then analyzed on Fluorstar Optima plate reader. Each cluster of points contains 3 technical replicates, error bars represent SD. "X" in resveratrol figure represents absence of data due to technical issue.

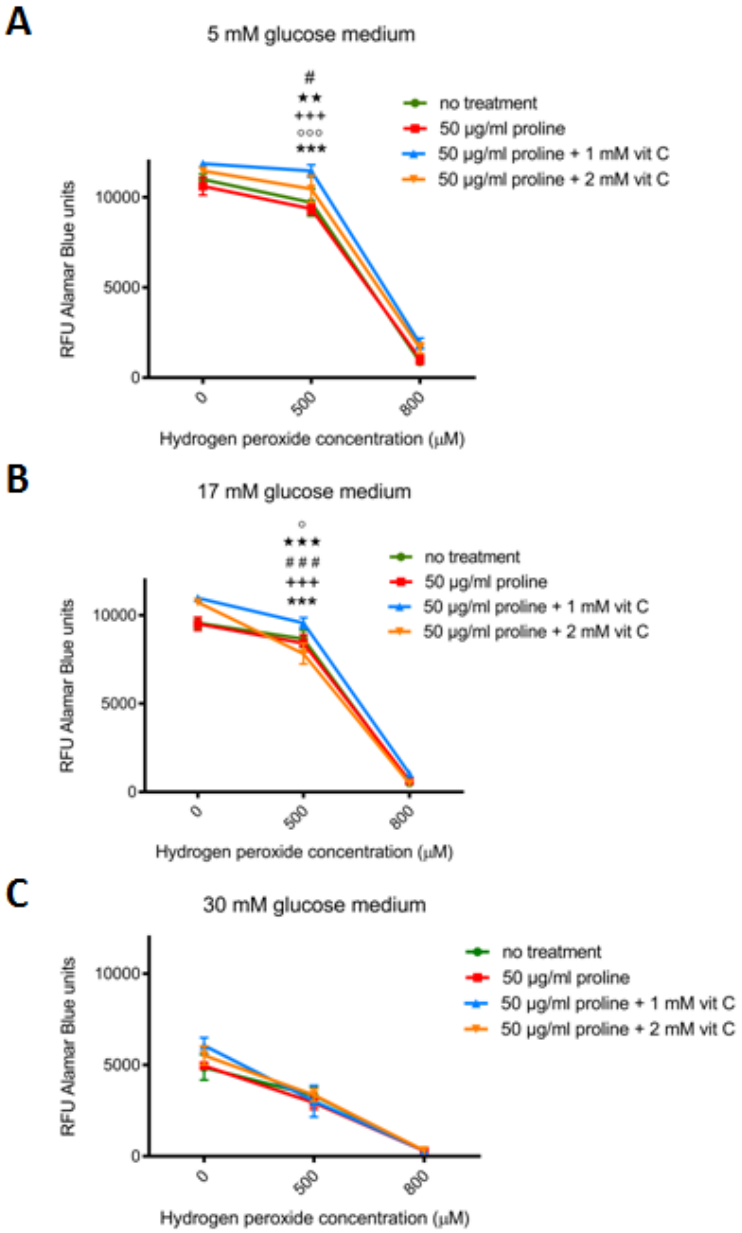

Figure 4.34: Tenocyte metabolic activity following H_2O_2 and AA/proline treatment (n=1 patient, Biosera medium). A) 5 mM glucose medium, B) 17 mM glucose medium, C) 30 mM glucose medium. Tenocytes were chronically cultured in 5, 17 and 30mM glucose media, then seeded for experiment in 96-well dishes. Cells were pre-conditioned with AA/proline treatment for 24 h, then treated with 0, 500 and 800 μM H_2O_2 and simultaneously with AA/proline (i.e. H_2O_2 and protective agent in same solution) for the subsequent 24 h. Alamar Blue reagent was added for the last 4 h of incubation, then analyzed on Fluorstar Optima plate reader. Values not normalized to cell number. Each point represents mean of 5 technical replicates, error bars represent SD. Note that 30 mM glucose-treated cells exhibited low confluency, as indicated by microscopy. These were therefore excluded from any conclusions. Two-way ANOVA with Bonferroni. Only statistical significance of interest is shown: results for statistics within the 500 μM H_2O_2 cluster are indicated with symbols above this cluster. Key to statistical symbols (comparisons made within clusters): $*$ compares no treatment vs. 50+1, # compares no treatment vs. 50+2, + compares 50 vs. 50+1, $^\circ$ compares 50 vs. 50+2, $\star$ compares 50+1 vs. 50+2. Prism significance intervals are defined as: not significant (ns) $P > 0.05$; * $P \leq 0.05$; ** $P \leq 0.01$; *** $P \leq 0.001$.

4.4 Discussion

In this chapter I aimed to determine if extracellular glucose levels alter the response of primary tenocytes to H_2O_2-induced oxidative stress. The null hypothesis is rejected since experimental data shown here reveal that glucose concentration in cell culture medium affects the response of tenocytes to H_2O_2. H_2O_2 is produced endogenously by several physiological processes, such as mitochondrial oxidative phosphorylation and inflammatory cell respiratory burst (161). It is necessary for many cell activities and is usually removed by the actions of catalase and superoxide dismutases. However when exogenously applied in excess, H_2O_2 acts to damage cells externally, for example by reacting with the lipid membrane or transmembrane proteins. H_2O_2 can freely diffuse through membrane lipid bilayers. In addition, there is evidence that selected aquaporin homologues from plants and mammals have the capacity to transport H_2O_2 across membranes (162). Channel proteins provide the possibility of transport regulation which can impact the intracellular H_2O_2 concentration. It has been demonstrated that exogenously added H_2O_2 is less effective at eliciting a signal response compared to endogenously produced H_2O_2 (163). Although this fact could be a potential limitation of this study we consistently observed H_2O_2-induced toxicity across a wide range of doses. It has been suggested that once inside the cell, excessive H_2O_2 can generate hydroxyl radicals when in presence of transition metal ions (such as iron or copper), and can also reach the nucleus to interact with DNA leading to single-strand breaks and base damage (74, 161).

When determining the appropriate experimental H_2O_2 doses for primary tenocytes in culture, it was immediately established that pro-collagen medium helps to offset the effect of H_2O_2 on metabolic activity of cells (figure 4.1). This was an expected finding as the pro-collagen medium contained both proline and AA, an antioxidant that scavenges ROS including H_2O_2. It was essential to determine H_2O_2 doses for primary tenocytes specifically. It is known that, for example, the concentration of H_2O_2 to cause apoptosis of mammalian cells can vary greatly depending on cell type; the mechanism regulating this phenomenon remains currently unclear (154). Cell population density also strongly affects dose response, with high density cultures being much less susceptible to the cytotoxic effect of H_2O_2, and able to metabolise and detoxify it more rapidly (74). On the other side of the spectrum, low doses of H_2O_2 can elicit anabolic response: in human tenocytes

significant *COL1A1* and *COL1A2* upregulation was observed after 18 h of 100 μM H_2O_2 incubation compared with untreated controls (140).

Figure 4.5 indicates that extracellular glucose has an effect on the cellular response to H_2O_2: 1 mM H_2O_2-treated tenocytes in 38 mM glucose media had their cell metabolic activity decreased significantly more than 1 mM H_2O_2-treated tenocytes in 8 mM glucose media. This finding was confirmed by L/D assay where regular 8 mM glucose medium protected cells against detachment and/or cell death in 1 mM H_2O_2, as opposed to regular 38 mM medium (figures 4.7 and 4.9). The combination of Alamar Blue assay with L/D is essential since Alamar Blue gives a quantitative effect on the population while L/D allows judgement of stress levels in single cells and can also display more subtle differences in grade of damage.

The data in figure 4.10 remains difficult to interpret. Under 500 μM H_2O_2, the metabolic activity is high in both 5 and 30 mM glucose media, however minimal in 17 mM glucose medium; this is an inexplicable pattern unless the cell density became lower in the 17 mM glucose cultures. The accompanying L/D data (figures 4.11, 4.12 and 4.13) present comparable pattern. Figure 4.11 clearly indicates that protection at 1 mM H_2O_2 was lost in low glucose though it was later explained: Biosera medium was used that contained only 50% of the concentration of sodium pyruvate compared to the originally used Lonza medium, and this proved to be likely critical in protecting cells. Sodium pyruvate is a common cell culture medium supplement; cells use the molecule as an easily accessible carbohydrate source in addition to glucose. Sodium pyruvate is effective at eliminating H_2O_2 by a decarboxylation reaction between the two (164). It has been noted by others that composition of media may modulate the effects of exogenously applied H_2O_2 (164); pyruvate is known to scavenge H_2O_2 (74). I strongly suspect the importance of sodium pyruvate in this study of H_2O_2 in tendon cell culture: the Alamar data in figure 4.14 suggest that one or more compounds that are present in the Lonza medium, likely the sodium pyruvate, protect from all tested doses of H_2O_2 (up to 800 μM in this experiment) in this 8 mM glucose condition. Sodium pyruvate concentration of 0.110 g/l is necessary in the culture medium for protection under low glucose against cytotoxic effects of H_2O_2 in this experimental setup (figure 4.14). This is in agreement with initial findings of this project where low glucose medium protected against harmful effects of H_2O_2 (figures 4.5

and 4.7).

The concentration threshold of H_2O_2 at which cytotoxic effect was consistently observed was determined to be in the interval of 500 and 800 μM. This was first noted in figures 4.10, 4.11 and 4.13; other figures that support this finding are: 4.16, 4.25, 4.26, 4.27, 4.28, 4.29, 4.31, 4.32 and 4.34. This is a useful finding for future cell culture work on tenocytes, although the effect of cell density will always play a role.

Acute treatment with glucose identified that even short (72 h) bursts of elevated glucose can aggravate the response of cells to H_2O_2 (more precisely 500 μM H_2O_2, figure 4.16). This finding might potentially imply that even brief periods of very high blood glucose levels might be damaging to tendons and other tissues.

Figure 4.17 indicates that high (30 mM) glucose alone significantly downregulates mRNA level of MMP-2 gelatinase as compared to the 5 mM glucose control. Altered transcriptional response could have profound effects on tendon ECM as MMP-2 substrates are numerous (table in (165)). Data of MMP-13 at the protein level needed experimental repeats to be certain of response pattern (figure 4.18).

In the previous chapter it was demonstrated that collagen *COL1A1* and *COL3A1* mRNA expression is significantly upregulated in both 17 and 30 mM glucose compared to the 5 mM glucose control condition (figure 3.21). In this chapter the gene expression data (figure 4.19) for *COL1A1* and *COL3A1* indicates - when considering glucose alone - stable expression across glucose conditions (*COL1A1*), and downregulation of expression in 30 mM glucose (*COL3A1*). It must be remembered that the qPCR collagen data in this chapter is derived from 1 patient, whereas the corresponding data in the previous chapter was derived from 3 independent patients, and hence should be perhaps trusted more. When considering the data (figure 4.19) in its entirety including H_2O_2 treatment, it can be seen that for *COL1A1* the H_2O_2 reduces expression in 5 and 30 mM glucose compared to glucose conditions alone. For *COL1A2* the data are difficult to interpret. For *COL3A1* H_2O_2 reduces expression in 5 mM glucose compared to no H_2O_2 in this condition. Altogether, H_2O_2 predominantly reduces all the tested collagen genes which is in agreement with data by other researchers who showed that *in vitro* H_2O_2-exposed cardiac fibroblasts exhibit decreased fibrillar collagen synthesis (166). Figure 4.19 also contains aggrecan expression data: a dramatic reduction of expression in H_2O_2-treated

samples can be seen regardless of the glucose condition.

I aimed to test whether any of the harmful H_2O_2 effects that are seen in the experiments can be reversed, i.e. biological function restored. In biological systems the anti-oxidative defence mechanisms include both enzymatic and non-enzymatic scavengers. Enzymes, such as catalase and SODs, and non-enzymatic compounds, such as AA, constantly regulate the level of ROS, including H_2O_2. Precise levels of H_2O_2 concentration are critical; the H_2O_2-detoxyfying antioxidant enzymes are tightly regulated (154). SOD enzymes possess H_2O_2 scavenging activity which is directed at reducing H_2O_2. Figure 4.20 demonstrates that mRNA concentrations for all 3 SODs increased in response to 100 μM H_2O_2. For the rat SOD-1 gene, it is known that H_2O_2 induces the gene through the hydrogen peroxide-responsive element (between nucleotides -533 and -520)(167). Data from previous chapter showed that it was especially SOD-2 that responded to glucose with increased mRNA expression: there was a 12-fold increase in 17 mM glucose condition compared to 5 mM glucose (figure 3.26). It is unfavorable that SOD-2 data in this chapter does not support the earlier finding: when glucose alone is considered (0 μM H_2O_2) there is no difference in expression of SOD-2 across glucose conditions (figure 4.20). It must be remembered that the qPCR SOD-2 data in this chapter is derived from 1 patient, whereas the corresponding data in the previous chapter was derived from 3 independent patients, and hence should be perhaps trusted more. Catalase data in this chapter (figure 4.20) shows a less pronounced pattern in comparison to SODs: only 17 mM glucose condition showed upregulation of the enzyme mRNA in response to H_2O_2.

It is appropriate to first consider what level of oxidative stress is created by glucose alone, i.e. the hyperglycemia-induced basal oxidative stress. Data for SOD enzymes and catalase (figures 3.26 and 4.20) provide some information. The former figure suggests that it is specifically SOD-2 that responds most dramatically to high (17 mM) glucose, while the latter figure suggests stability of mRNA expression of all four genes when considering glucose treatment alone. The former figure is representative of 3 patients hence is preferred. If SOD-2 is upregulated it might be that substrates for SOD-2 are more abundant in the 17 mM glucose condition. SOD-2 substrates are superoxide anions, just as for SOD-1 and SOD-3. These three SODs differ in their compartmentalization: SOD-1 is found almost exclusively in intracellular cytoplasmic spaces, SOD-2 belongs exclusively

to the mitochondrial spaces, while SOD-3 is directed exclusively to extracellular spaces (75). It could therefore be concluded from SOD-2 upregulation that high (17 mM) glucose first increased ROS levels in mitochondria of tenocytes. This is not unanticipated: glucose will be processed during oxidative prosphorylation, the pathway in which cells oxidize nutrients (the most common oxidizing agent or electron acceptor is molecular oxygen O_2) in order to form ATP. Oxidative phosphorylation is central to cellular metabolism however at the end of the pathway, in the electron transport system, premature electron leakage to oxygen takes place: it has been estimated that approximately 25% of oxygen passing through the mitochondrial electron transport chain results in superoxide (159). The ROS then propagate, potentially damaging cellular components. The more glucose that is oxidized into ATP, the more ROS will be produced as a by-product.

When considering technical aspects of qPCR data in this chapter, 30 mM glucose condition in figures 4.19 and 4.20 should be interpreted with caution, as the RNA quality of these samples was poor. Other limitation of qPCR work is such that positive controls were not available (also true for Chapter 3).

As cellular senescence is driven by sustained and robust activation of the p16Ink4a and/or the p53-p21 pathways (112), I aimed to examine P16 and P21 gene expression. However in general there is an absense of senescence-specific markers and both of these, even if present at high levels, are only semi-selective senescence markers (112). From the obtained data it was not possible to distinguish whether the observed morphological senescence in 30 mM glucose is driven via p16 or p21-dependent mechanism. The 3-fold increase in P21 mRNA in response to H_2O_2 which was seen in figure 4.22 was expected: oxidative stress is a known senescence-inducing stimulus (112). Unfortunately, the 30 mM glucose condition on its own did not exhibit any differences in mRNA expression (figure 4.22), although evidence has been published that links senescence with metabolic changes (168).

In the last section of this chapter, protective agents and their potential to attenuate the harmful effects of glucose and H_2O_2 were evaluated, using doses demonstrated to be effective in several other cell culture systems.

Alamar Blue data for NAC, AA and resveratrol (figures 4.25, 4.29 and 4.31, respectively) share one aspect: across these three sets the 5 and 17 mM glucose conditions are

similar in their pattern, while the 30 mM glucose condition was found to be more stable between 0 and 500 μM H_2O_2 and hence plummeting more between 500 and 800 μM H_2O_2. This is true especially for figures 4.29 and 4.31. Absolute Alamar Blue values were not used for comparison across 5-17-30 mM glucose conditions as cells were not seeded at identical seeding density, however these values can be reliably compared between 5 and 30 mM conditions (as same seeding density): baseline metabolic activity is higher in 30 mM than in 5 mM glucose across all 3 treatments (NAC, AA, resveratrol). Furthermore, it is apparent from the 3 sets that cells in 17 mM glucose condition eventually achieved the same apparent level of cell density as 5 and 30 mM cells despite being seeded at about 50% density: the Alamar Blue values are in the same range.

All in all, NAC was the sole treatment out of the four tested treatments that was effective to a certain degree. AA improved its protective effect following further optimization - which uncovered that combination with proline is preferred - to a modest level (figure 4.34) however the equivalent of NAC protection was never reached. What are the differences between NAC and AA? NAC is a well described acetylated cysteine residue that possesses potent antioxidant properties, but can also support the nitric oxide system as a vasodilator by facilitating the production and action of nitric oxide. NAC protects cells from oxidative stress by inhibiting H_2O_2 formation, as well as directly and effectively scavenging free radicals due to its interaction with ROS. And, notably, NAC serves as a major contributing source of cysteine to maintain levels of the key cellular antioxidant, glutathione (GSH). NAC can correct or prevent GSH depletion: the synthesis of GSH is limited by the level of its substrates, often cysteine. When NAC enters the cell it will be quickly hydrolyzed and will release cysteine (159, 169). In comparison, AA is a naturally-occuring antioxidant that is present in cells, body fluids and plasma; its coenzyme role in oxidative stress pathways makes it a ROS scavenger (170). Although AA is best known for its antioxidant character, it can also exert pro-oxidant properties under certain conditions: AA can stimulate free radical damage in the presence of metal ions. For example, a mixture consisting of copper ion-AA-H_2O_2 causes severe oxidative damage to the bases of DNA by generating hydroxyl radicals (171). As an antioxidant therapy, there is evidence that NAC might be favored over AA. For example, damage induced by methotrexate (a cytotoxic agent used in chemotherapy treatment) to hepatic structures likely involves OS

pathways. This damage can be alleviated significantly better by NAC than by AA (170). Another example is contrast medium-induced cytotoxicity (contrast agents for medical imaging can cause complications) which was reported to be significantly reduced by short duration pre-treatment with NAC however AA was unable to reduce cell death (172). Resveratrol, a natural plant polyphenol which is also a direct free radical scavenger as well as being able to activate multiple antioxidant pathways (160, 173, 174) and metabolic regulators sirtuins, proved to be ineffective in this experimental setting despite positive research findings of other groups (175, 176, 177, 178, 179). It is possible this was due to the DMSO solvent as there was low level toxicity with the solvent alone control (figure 4.23 however not 4.24). Acute lowering of glucose concentration to mimic normalized blood glucose was an important test as it would be a promising finding however low glucose did not prove to be effective in the evaluated conditions (figure 4.32).

Future experiments could include detailed examination of the response of MMPs to H_2O_2 (pilot data on MMP-2 and MMP-13 was performed here). DCFDA assay and/or MitoTracker assay could be employed to evaluate basal oxidative stress in glucose samples (i.e. glucose-generated ROS). Here I looked at mRNA levels of antioxidant enzymes that serve to counterbalance the ROS generated in the cell; the enzymes should reflect ROS levels. An additional approach would be to examine enzymatic activity. mRNA levels of other relevant markers such as as sirtuin 1, 4, 6 and scleraxis could be tested on tenocytes subjected to glucose and H_2O_2.

Overall the research in this chapter demonstrates that negative effects of H_2O_2 are more pronounced under elevated glucose condition in primary human tenocytes.

5 Discussion

Diabetes is becoming increasingly more prevalent in today's developed world. It leads to numerous secondary diseases, such as cardiovascular disease, renal failure, Charcot neuroarthropathy and chronic foot ulceration. Among these, diabetic foot ulcers represent a severe debilitating condition, and may lead to amputation (103). Diabetic foot ulcers incidence of up to 10% has been reported in the diabetic population, and foot amputation has reached as much as 2% of this population (103). Both nerve and tendon pathologic alterations are currently thought to be the main cause of diabetic foot injury, with altered gait and sensation leading to injuries which do not heal due to the compromised vasculature. Diabetic tendons are described as thicker and shorter, and possessing reduced elasticity and increased stiffness. Moreover, tendons of diabetic patients have increased packing density of collagen fibrils, decreased fibrillar diameter and abnormal fibril morphology on the microscopic level (91). Furthermore, diabetic tendons remodel and heal poorly compared to healthy tendons (98, 103, 178, 180). The mechanism of diabetic tendinopathy is currently insufficiently understood despite having an emerging morphological description. A deeper understanding of the mechanism would bring a potential improvement in the development of tendon treatments. This thesis is novel in two aspects. First, this thesis considers tendon cells in isolation - vascular and neural components are removed.

Second, effects of chronically elevated glucose are evaluated, as the majority of published experimental studies only considers acute glucose treatment. Chronic glucose treatment mimics diabetic physiology in a more accurate manner.

Human hamstring tendon used in anterior cruciate ligament reconstruction surgery was chosen as the tissue was not ruptured, diseased nor damaged in any way, and was derived from young patients. Furthermore, primary human cell culture is a robust experimental model. The nature of the animal model used in this thesis represents uncontrolled T1D (unfortunately not T2D) however the rats exhibited glucose concentrations (9 - 27.5 mM glucose) over 16 weeks corresponding to the range of my cell culture experiments. This animal model was not further challenged by e.g. wound healing or added oxidative stress from infection, ulceration or exercise beyond a contained cage. Human tendon cells were chronically maintained and cultured from explanting and throughout several weeks/months in 5, 17 and 30 mM glucose media, and experiments were also conducted in these conditions. 5 mM glucose represents physiological level of glucose in the blood stream of a healthy person, 17 mM represents standard tissue culture medium and diabetic levels for a human, while 30 mM glucose is an extreme diabetic level. Other researchers used comparable glucose concentrations: 5.5 and 30 mM glucose for 16 h (58), 5 and 50 mM (181), and 5 and 30mM for 3 weeks (89). However, this is an indication that long-term culture in elevated glucose has not been performed yet.

Key findings of this research project are as follows. Tenocytes proliferate at a higher rate in 38 mM glucose (compared to 8 mM glucose), but also detach or die at an increased rate in this condition. Senescence-like phenotype is observed in 30 mM glucose. The ECM components asporin, biglycan, aggrecan and decorin are all upregulated in 17 and 30 mM glucose at the mRNA level. Additionally, SOD-2 and catalase are both upregulated in response to the 17 mM glucose indicating oxidative stress. 38 mM glucose inhibits cell migration rate at 72 h, compared to 8 mM glucose. In the uncontrolled 16 week T1D animal model, cross sections of rat tails indicate that muscle tissue is more vulnerable to nitrosative and oxidative stress than tendon tissue, displaying elevated 3-nitrotyrosine and FOXO1. Viability of tenocytes is protected against H_2O_2 in 8 mM glucose providing

the culture medium contains sufficient sodium pyruvate. Short (72 h) episode of 30 mM glucose renders tenocytes more vulnerable to H_2O_2. The antioxidant NAC has shown protective properties against 800 μM H_2O_2. Other thesis findings are as follows. Metabolic activity of cells is increased in 17 and 38 mM glucose culture. Collagen 1a1 and 3a1 are both dramatically increased in 17 mM glucose on the mRNA level, and significantly increased in 30 mM glucose on the mRNA level. SOD-3 is upregulated in 30 mM glucose on the mRNA level. Pro-collagen medium exhibits protective effects compared to regular (standard) medium. H_2O_2 treatment clearly decreases aggrecan mRNA expression irrespective of glucose condition. 30 mM glucose decreases FOXO-1 on the mRNA level compared to 5 mM (control) glucose. 1 mM AA has protective properties against H_2O_2 when in combination with proline.

5.1 Effect of glucose on tendon cells

In order to maintain optimal tendon tissue integrity, healthy tenocytes are required to produce and remodel the ECM. Tenocytes were found to proliferate at an increased rate in 38 mM glucose medium, however cell numbers were always lower in these cultures, suggesting that they also detached and/or died at an increased rate in this condition. A TUNEL assay was used to assess apoptosis levels however an initial count suggested that differences were rather small so in the interest of time this was not completed. Senescence-like phenotype was observed in 30 mM glucose. Perhaps elevated glucose concentration induces tendon cell senescence *in vitro*. It would be vital to know whether senescence also happens *in vivo*, i.e. in tissues such as tendon in diabetic patients. There are morphological changes that can be observed in senescence (cell are larger, flat and vacuolized), but this is the case for *in vitro* cell culture. *In vivo* however there is normal cell physiology which would complicate investigating diabetic tissues *in vivo*. For this reason, in order to identify senescent cells in diabetic tissue *in vivo* I would employ a combination of approaches. The absence of proliferative markers (Ki67 protein or 5-bromodeoxyuridine incorporatation) together with the presence of senescence markers (p16, ARF, p53, p21, p15, p27 and hypophosphorylated RB) is accepted to define senescence (182). Senescence has its physiological role however an accumulation of senescent cells in tissue, whether tendon or other, could disrupt the milieu and lead to premature tissue degeneration

and/or tissue aging. Research into understanding senescence induction and maintance might pave new therapeutic avenues. Tenocytes overall "thrived" best in 17 mM glucose medium (the 5 mM and especially the 30 mM cell culture posed challenges). This was a surprising finding, as this level of glucose is considered diabetic for a patient. I had to elevate the glucose *in vitro* to as much as 30/38 mM to observe pathological behaviour of tenocytes. I would therefore conclude that 17 mM glucose medium remains optimal for tissue culture if one researches other areas than energy/glucose metabolism. This is in opposition with what was found to be true for cartilage: low (1 mM) glucose medium was found to be optimal (183).

5.2 Effect of glucose on tendon ECM

Tendon is 90% composed of ECM, therefore it was esssential to investigate the effects of glucose on the ECM. The changes of ECM components described above could severely impact the integrity of the tissue, and could have negative effects on its healing capacity. Could this explain, at least partially, the contracted and stiffened Achilles tendon that is observed in the clinic? Elevated glucose level decreased cell migration rate. Tendon healing follows the same set of principles as wound healing, therefore it is generally assumed that factors that improve or hinder wound healing could have comparable effects on the tendon healing process (178). The next research steps could be in the direction of more in depth investigation of MMPs, and also cross-linking of collagen, as an increase in advanced glycation end products (AGEs) has been reported in response to elevated glucose levels (184, 185). Very high levels of AGEs are observed in diabetes (186), since the chemical reaction that leads to AGE formation is enhanced in hyperglycemic environment (186, 187). The most commonly cross-linked targets are collagen, myelin and tubulin (186) and therefore this phenomenon is very relevant to tendon which is a collagen-rich tissue. I propose to evaluate the amount of AGEs in tendon tissue by IHC on control vs. T2D tendons from clinical samples. Furthermore, there are several receptors that bind AGEs: RAGE, AGE-R1, AGE-R2, and AGE-R3. RAGE is the one best described; it is a miltiligand member of the immunoglobulin superfamily (186, 187). AGE-modified proteins bind to RAGE and activate cell signaling pathways such as mitogen-activated

protein (MAP) kinase which can lead to cellular dysfunction (23, 69). I propose to investigate RAGE receptor in control vs. diabetic clinical tendon samples if AGEs prove to be upregulated in diabetic tendon.

5.3 Oxidative stress

Key antioxidant enzymes SOD-2 and catalase were dramatically upregulated in response to 30 mM glucose at the mRNA level; SOD-3 showed less dramatic upregulation. Next, H_2O_2 was used in this project as an additional source of oxidative stress, in addition to glucose-generated oxidative stress. Protection from H_2O_2-induced negative effects was observed under 8 mM glucose compared to 38 mM glucose, providing the culture medium contained sufficient sodium pyruvate. The protection extended to doses as high as 1 mM H_2O_2. This finding illustrates a potential beneficial effect of low glucose levels. Perhaps high glucose damages mitochondria. Mitochondria contain extensive antioxidant system to detoxify ROS (the enzymatic and nonenzymatic components were described earlier). If mitochondria are structurally and functionally intact then their capacity to counterbalance ROS generation remains sufficient. However, any mitochondrial damage will result in a decrease of effective antioxidant defences and hence in net ROS production. This is a vicious cycle where ROS further damage mitochondria in a positive feedback loop manner (188). It would be worth estimating the role of mitochondria in the observed decreased oxidative stress handling of high glucose cells to see whether mitochondria are damaged under high glucose conditions. Elevated glucose can be harmful when chronically present. Even transient (72 h) elevated glucose can change the response of tenocytes to H_2O_2. Replacing high glucose with low glucose was tested as a therapeutic approach and proved ineffective in the experiments. However, use of NAC proved to be effective in protecting tenocytes from harmful effects of H_2O_2. Equally, 1 mM AA was shown to have protective properties when administered in combination with proline. Furthermore, procollagen medium containing lower levels of AA also exhibited protective effects compared to regular non-supplemented medium. Negative effects of H_2O_2 treatment included a decrease in aggrecan mRNA expression (irrespective of glucose condition) and increased cell death under 38 mM glucose. Overall, cells that were chronically cultured in elevated

glucose were less able to oppose to H_2O_2 insult. Oxidative stress intervention (and cell migration described earlier) are particularly relevant to diabetic connective tissues.

5.4 Animal model

In my 16-week uncontrolled diabetic animal model, cross sections of rat tails uncovered that muscle tissue is more prone to effects of oxidative stress than tendon tissue. Could this imply that tendon is unaffected by diabetes in rats *in vivo*? This would be in agreement with some published literature (189), but not with other literature which demonstrated impaired tendon properties in diabetic animal models (96, 97). Perhaps the tendon changes take longer to develop, i.e. the rats used here would need to be T1 diabetic for a longer period of time. Could the initial muscle changes that we have seen in some way affect the tendon as well, since the two function as a unit? The rat tendon samples used here contain both tenocytes and the ECM, unlike the tissue culture cells that are devoid of ECM. A limitation of the rat model is that it represents T1D, whereas the data from the tissue culture experiments aim to mimic T2D.

5.5 Limitations of the study

There are a number of limitations of this study. First, the pH of the culture medium might have potentially contributed to the observed findings. The pH was 7.85 for the 8 mM glucose medium, 7.55 for the 17 mM glucose medium and 7.34 for the 38 mM glucose medium. Most normal mammalian cell lines grow well at pH 7.4, some normal fibroblast cell lines prefer slightly more basic environments (pH 7.4-7.7). Second, it would be vital to also always have the protein data available for all the targets that were screened on the mRNA level only using qPCR. It is unknown whether any corresponding variation occurred in absolute protein level as well. Third, the physiological significance of *in vitro* experiments might be questioned. This is a limitation true to any *in vitro* study. It is well known that *in vivo* micro-environment is complex hence mono-dimensional culture systems may be physiologically irrelevant (19). Cell culture is an artificial environment which is not identical to *in vivo* human tendon. On the other hand, primary cells are morphologically similar to parent tissue, and primary cell culture is the best experimental

model for *in vivo* studies, immediately after primary tissue culture and organ culture. Equally, extending observations from animal model to human tissue has its limitations. Moreover, my experiments were conducted on isolated cells, while the rats used in this study possessed both cells and the ECM. Fourth, it has been demonstrated that exogenously added H_2O_2 is less effective at eliciting a signal response compared to endogenously produced H_2O_2 (163) which might constitute a limitation of the method used here. Fifth, much of the data is conducted on n=1 or n=2, and needs more experimental repeats.

Ideal tendon therapeutic approaches would be systemic treatments that could be taken long-term with no or minimal side effects. For this reason, dietary supplements such as regulators of sirtuins (e.g. resveratrol) or green tea extract might be promising. Testing antioxidants in this project was an obvious choice, as for example AA is required during the process of collagen synthesis. However, the usage of classic dietary antioxidants in order to protect against oxidative stress damage has showed mixed success (81, 190, 191, 192, 193); it has been hypothesized that it might be due to difficulty of ensuring that the antioxidants reach the site of ROS generation (154). It has been suggested that current approach of mere scavenging of ROS might not be a sufficient strategy. Instead, a combination of ROS generation prevention together with their scavenging might be a more promising approach (81). A promising area of future research might be cellular senescence. Another potential avenue of future research might be in epigenetic approaches; initial research in this area has already showed great promise. An interesting concept, termed 'metabolic memory' or 'hyperglycemic memory', has been introduced in the hyperglycemia field (194, 195, 196). Transient hyperglycemia induces persistent activating epigenetic changes in the promoter of NFKB p65 subunit (57, 58). The persistent effects even after a restoration of glucose control could result in far-reaching clinical consequences, and it indicates potential long-term effect of glucose on gene expression (197). Furthermore, elevated glucose is thought to elicit genome-wide changes (64). Hence therapeutic strategies targeting epigenetic modification would be the avenue of the future, not only in tendon field, but in the biology field in general. Other areas of research could include a further probing into the witnessed differences between tendon and muscle tissue. Muscle is highly metabolic so it comes as a surprising finding that it did not deal with T1D as well as tendon. Hence,

could tendon potentially offer some answers for muscle? How is it possible that tenocytes are more resistant to high glucose effects than muscle? Perhaps insulin signaling is in some way different in tendon? Tenocytes express insulin and GLUT2 at both protein and mRNA level but the susceptibility to insulin resistance has not been fully defined in this cell type (198). Or perhaps do tenocytes use their ability to metabolically hibernate, as they normally do in heavy exercise, to evade damage? Is there a lesson that we can learn from tendon, and apply to other soft tissues? This research could lead to identification of new biomarkers for the diagnosis and/or progression of tendon disease.

Appendices

A

Conferences

Attended conferences:

- Epigenetics in matrix biology and disease. British society for matrix biology. Oxford, March 2013.
- 3rd epigenetics symposium on health and disease: neuropsychiatry and inflammation, epigenetic target discovery beyond oncology. Structural genomics consortium, University of Oxford. Oxford, March 2013.
- Frontiers in orthopaedic and plastic surgery research symposium. British orthopaedic association / NHS / RCS / University of Oxford. Oxford, May 2013.
- Under pressure: the cell's response. British society for matrix biology. Cardiff, September 2013. Awarded reporter bursary for compiling a meeting report together with another conference delegate (report later published in BSMB newsletter).
- Building the extracellular matrix: molecules, cells and evolution. Bristol, April 2014. Presented a poster.

- Slovak Oxford science 2014. Slovak Oxford science, Pian di Sco, Italy, May 2014. Gave a popular science talk on epigenetics.

- 3rd international scientific tendinopathy symposium. Oxford, September 2014. Assisted with organization, and presented a poster.

Conference abstracts:

Kalivodova Z, Ingram N, Tucker RP, Thompson MS, and Hulley PA. Effect of nutrition and mechanical loading on human tenocyte metabolism. International Journal of Experimental Pathology, 2014, 95, A18.

Kalivodova Z and Hulley PA. Effects of chronic high glucose on primary human tenocytes. British Journal of Sports Medicine. 2014;48(Suppl 2):A30-A31. doi:10.1136/bjsports-2014-094114.47

Miscellaneous:

I received the 'Primer Design Silver Award Student Sponsorship' from qPCR company Primer Design, UK. Two awards: 2013 & 2014.

B

Acquired training

- Laboratory and safety inductions (e.g. human tissue safety induction). NDORMS, University of Oxford. October 2012.
- Statistics: Designing clinical research and biostatistics. IT services, University of Oxford. 31 October & 1 November 2012.
- Research Skills Toolkit for Medical Sciences Division. IT services (Bodleain Libraries), University of Oxford. 29 November 2012.
- Endnote course. Medical Sciences Division Training, University of Oxford. 31 January 2013.
- Cryogenic gases safety. University Safety Office, University of Oxford. 13 March 2013.
- Transfer report writing course. Medical Sciences Division Training, University of Oxford. 8 May 2013.
- Cell culture techniques, good laboratory practise and safe use of microbiological cabinets. University Safety Office, University of Oxford. 29 May 2013.

- Grad Challenge. MPLS Division Graduate School, University of Oxford. 23-25 September 2013.
- Security and privacy online: Safe surfing. IT services, University of Oxford. 29 January 2014.
- LaTeX: An introduction to document preparation. IT services, University of Oxford. 31 January 2014.
- Career planning for DPhil students. Careers Service, University of Oxford. 17 February 2014.
- LaTeX: Further document preparation. IT services, University of Oxford. 28 February 2014.
- Networking skills for DPhils. Careers Service, University of Oxford. 13 may 2014.
- Writing skills - Papers and theses. Medical sciences teaching centre, University of Oxford. 18 june 2014.
- Viva preparation - Final viva. Medical Sciences Skills Training, University of Oxford. 29 January 2015.
- Scientific paper writing training course. NDORMS, University of Oxford. February-April 2016.
- Referencing: EndNote - Building your library (Mac). IT services, University of Oxford. 4 March 2016.
- Word: Charts, pictures and diagrams. IT services, University of Oxford. 7 March 2016.
- 7 secrets of highly successful research students. Medical Sciences Skills Training, University of Oxford. 9 March 2016.
- Security and privacy online: you are the target (extended session). IT services, University of Oxford. 10 March 2016.

- Referencing: EndNote - Citations and bibliographies (Mac). IT services, University of Oxford. 11 March 2016.
- Stata: An introduction to data access and management. IT services, University of Oxford. 26 May 2016.
- Presentation Skills. Medical Sciences Divisional Skills Training, University of Oxford. 9 June 9 2016.
- Stata: Statistical, survey and graphical analyses. IT services, University of Oxford. 16 June 2016.
- Statistics: Concepts of statistics for researchers. IT services, University of Oxford. 23 June 2016.

Bibliography

[1] A. S. Ahmed, N. Schizas, J. Li, M. Ahmed, C. G. Ostenson, P. Salo, C. Hewitt, D. A. Hart, and P. W. Ackermann. Type 2 diabetes impairs tendon repair after injury in a rat model. *J Appl Physiol (1985)*, 113(11):1784–91, 2012. 1, 17, 19, 20

[2] M. B. Silva and T. L. Skare. Musculoskeletal disorders in diabetes mellitus. *Rev Bras Reumatol*, 52(4):601–609, Aug 2012. 1, 17, 18, 19

[3] F. Ardic, F. Soyupek, Y. Kahraman, and R. Yorgancioglu. The musculoskeletal complications seen in type 2 diabetics: predominance of hand involvement. *Clin Rheumatol*, 22(3):229–33, 2003. 1, 17, 18

[4] H. Rafehi, A. El-Osta, and T. C. Karagiannis. Epigenetic mechanisms in the pathogenesis of diabetic foot ulcers. *Journal of Diabetes and its Complications*, 26(6):554–561, 2012. 1, 9, 18

[5] T. Nishikawa, D. Edelstein, X. L. Du, S. Yamagishi, T. Matsumura, Y. Kaneda, M. A. Yorek, D. Beebe, P. J. Oates, H. Hammes, et al. Normalizing mitochondrial superoxide production blocks three pathways of hyperglycaemic damage. *Nature*, 404(6779):787–790, 2000. 1, 12

[6] M. Kjaer. Role of extracellular matrix in adaptation of tendon and skeletal muscle to mechanical loading. *Physiol Rev*, 84(2):649–98, 2004. 2, 3, 4, 5, 7, 8, 19

[7] N. D. Murchison, B. A. Price, D. A. Conner, D. R. Keene, E. N. Olson, C. J. Tabin, and R. Schweitzer. Regulation of tendon differentiation by scleraxis distinguishes force-transmitting tendons from muscle-anchoring tendons. *Development*, 134(14):2697–2708, Jul 2007. 2

[8] R. James, G. Kesturu, G. Balian, and A. B. Chhabra. Tendon: biology, biomechanics, repair, growth factors, and evolving treatment options. *J Hand Surg Am*, 33(1):102–112, Jan 2008. 2, 6, 7, 9

[9] G. Riley. Tendinopathy–from basic science to treatment. *Nat Clin Pract Rheumatol*, 4(2):82–89, Feb 2008. 2, 3, 5, 7, 8, 9, 64

[10] H. R. Screen, D. E. Berk, K. E. Kadler, F. Ramirez, and M. F. Young. Tendon functional extracellular matrix. *J. Orthop. Res.*, 33(6):793–799, Jun 2015. 2, 3, 4, 5, 6

[11] P. D. Clegg, S. Strassburg, and R. K. Smith. Cell phenotypic variation in normal and damaged tendons. *Int J Exp Pathol*, 88(4):227–235, Aug 2007. 2, 3, 5

[12] C. T. Thorpe, H. L. Birch, P. D. Clegg, and H. R. Screen. The role of the non-collagenous matrix in tendon function. *Int J Exp Pathol*, 94(4):248–259, Aug 2013. 2

[13] P. Sharma and N. Maffulli. Biology of tendon injury: healing, modeling and remodeling. *J Musculoskelet Neuronal Interact*, 6(2):181–190, 2006. 2, 3, 5, 6, 7

[14] M. O'Brien. Structure and metabolism of tendons. *Scand J Med Sci Sports*, 7(2):55–61, Apr 1997. 2, 4, 5

[15] D. T. Kirkendall and W. E. Garrett. Function and biomechanics of tendons. *Scand J Med Sci Sports*, 7(2):62–66, Apr 1997. 2, 3

[16] G. Nourissat, F. Berenbaum, and D. Duprez. Tendon injury: from biology to tendon repair. *Nat Rev Rheumatol*, 11(4):223–233, Apr 2015. 3, 7

[17] C. Gungormus and D. Kolankaya. Gene expression of tendon collagens and tenocyte markers in long-term monolayer and high-density cultures of rat tenocytes. *Connect. Tissue Res.*, 53(6):485–491, 2012. 3

[18] M. Kuzma-Kuzniarska, C. Yapp, T. W. Pearson-Jones, A. K. Jones, and P. A. Hulley. Functional assessment of gap junctions in monolayer and three-dimensional cultures of human tendon cells using fluorescence recovery after photobleaching. *J Biomed Opt*, 19(1):15001, Jan 2014. 3

[19] K. Spanoudes, D. Gaspar, A. Pandit, and D. I. Zeugolis. The biophysical, biochemical, and biological toolbox for tenogenic phenotype maintenance in vitro. *Trends Biotechnol.*, 32(9):474–482, Sep 2014. 3, 4, 7, 143

[20] P. Kannus. Structure of the tendon connective tissue. *Scandinavian journal of medicine & science in sports*, 10(6):312–320, 2000. 4

[21] M. J. Peffers, Y. Fang, K. Cheung, T. K. Wei, P. D. Clegg, and H. L. Birch. Transcriptome analysis of ageing in uninjured human Achilles tendon. *Arthritis Res. Ther.*, 17:33, 2015. 4, 6

[22] K. E. Kadler, D. F. Holmes, J. A. Trotter, and J. A. Chapman. Collagen fibril formation. *Biochem. J.*, 316 (Pt 1):1–11, May 1996. 4

[23] J. G. Snedeker and A. Gautieri. The role of collagen crosslinks in ageing and diabetes - the good, the bad, and the ugly. *Muscles Ligaments Tendons J*, 4(3):303–308, Jul 2014. 4, 19, 142

[24] C. N. Ryan, A. Sorushanova, A. J. Lomas, A. M. Mullen, A. Pandit, and D. I. Zeugolis. Glycosaminoglycans in Tendon Physiology, Pathophysiology, and Therapy. *Bioconjug. Chem.*, 26(7):1237–1251, Jul 2015. 5

[25] The medical biochemistry page. glycosaminoglycans. 2016. `http://themedicalbiochemistrypage.org/glycans.php`. Accessed: 12-1-2017. 5

[26] R. Visse and H. Nagase. Matrix metalloproteinases and tissue inhibitors of metalloproteinases: structure, function, and biochemistry. *Circ. Res.*, 92(8):827–839, May 2003. 5

[27] M. E. Davis, J. P. Gumucio, K. B. Sugg, A. Bedi, and C. L. Mendias. MMP inhibition as a potential method to augment the healing of skeletal muscle and tendon extracellular matrix. *J. Appl. Physiol.*, 115(6):884–891, Sep 2013. 5

[28] J. D. Mott and Z. Werb. Regulation of matrix biology by matrix metalloproteinases. *Curr Opin Cell Biol*, 16(5):558–64, 2004. 5

[29] H. Nagase, R. Visse, and G. Murphy. Structure and function of matrix metalloproteinases and timps. *Cardiovasc Res*, 69(3):562–73, 2006. 5

[30] K. Brew, D. Dinakarpandian, and H. Nagase. Tissue inhibitors of metalloproteinases: evolution, structure and function. *Biochim. Biophys. Acta*, 1477(1-2):267–283, Mar 2000. 5

[31] M. D. Sternlicht and Z. Werb. How matrix metalloproteinases regulate cell behavior. *Annu. Rev. Cell Dev. Biol.*, 17:463–516, 2001. 5, 85

[32] H. Nagase and J. F. Woessner. Matrix metalloproteinases. *J. Biol. Chem.*, 274(31):21491–21494, Jul 1999. 5

[33] E. Karousou, M. Ronga, D. Vigetti, A. Passi, and N. Maffulli. Collagens, proteoglycans, MMP-2, MMP-9 and TIMPs in human achilles tendon rupture. *Clin. Orthop. Relat. Res.*, 466(7):1577–1582, Jul 2008. 5

[34] J. O. Ho, P. Sawadkar, and V. Mudera. A review on the use of cell therapy in the treatment of tendon disease and injuries. *J Tissue Eng*, 5:2041731414549678, 2014. 6, 7, 8, 9

[35] N. Andarawis-Puri, E. L. Flatow, and L. J. Soslowsky. Tendon basic science: Development, repair, regeneration, and healing. *J. Orthop. Res.*, 33(6):780–784, Jun 2015. 6, 7, 8

[36] L. M. Galatz, L. Gerstenfeld, E. Heber-Katz, and S. A. Rodeo. Tendon regeneration and scar formation: The concept of scarless healing. *J. Orthop. Res.*, 33(6):823–831, Jun 2015. 6, 7, 8

[37] M. Kjaer, H. Langberg, K. Heinemeier, M. L. Bayer, M. Hansen, L. Holm, S. Doessing, M. Kongsgaard, M. R. Krogsgaard, and S. P. Magnusson. From mechanical loading to collagen synthesis, structural changes and function in human tendon. *Scandinavian journal of medicine & science in sports*, 19(4):500–510, 2009. 6, 7

[38] T. Y. Yu, J. H. Pang, K. P. Wu, M. J. Chen, C. H. Chen, and W. C. Tsai. Aging is associated with increased activities of matrix metalloproteinase-2 and -9 in tenocytes. *BMC Musculoskelet Disord*, 14:2, Jan 2013. 6

[39] G. P. Riley, V. Curry, J. DeGroot, B. van El, N. Verzijl, B. L. Hazleman, and R. A. Bank. Matrix metalloproteinase activities and their relationship with collagen remodelling in tendon pathology. *Matrix Biol.*, 21(2):185–195, Mar 2002. 6

[40] C. Franceschi, M. Bonafe, S. Valensin, F. Olivieri, M. De Luca, E. Ottaviani, and G. De Benedictis. Inflamm-aging. An evolutionary perspective on immunosenescence. *Ann. N. Y. Acad. Sci.*, 908:244–254, Jun 2000. 6

[41] M. Magra and N. Maffulli. Genetic aspects of tendinopathy. *J Sci Med Sport*, 11(3):243–247, Jun 2008. 6

[42] J. D. Rees, M. Stride, and A. Scott. Tendons–time to revisit inflammation. *Br J Sports Med*, 48(21):1553–1557, Nov 2014. 6

[43] G. Riley. The pathogenesis of tendinopathy. A molecular perspective. *Rheumatology (Oxford)*, 43(2):131–142, Feb 2004. 6

[44] P. B. Voleti, M. R. Buckley, and L. J. Soslowsky. Tendon healing: repair and regeneration. *Annu Rev Biomed Eng*, 14:47–71, 2012. 7

[45] P. W. Ackermann, E. Domeij-Arverud, P. Leclerc, P. Amoudrouz, and G. A. Nader. Anti-inflammatory cytokine profile in early human tendon repair. *Knee Surg Sports Traumatol Arthrosc*, 21(8):1801–1806, Aug 2013. 7

[46] B. R. Freedman, J. A. Gordon, and L. J. Soslowsky. The Achilles tendon: fundamental properties and mechanisms governing healing. *Muscles Ligaments Tendons J*, 4(2):245–255, Apr 2014. 7, 8

[47] E. Shapiro, D. Grande, and M. Drakos. Biologics in Achilles tendon healing and repair: a review. *Curr Rev Musculoskelet Med*, 8(1):9–17, Mar 2015. 7

[48] B. M. Andres and G. A. Murrell. Treatment of tendinopathy: what works, what does not, and what is on the horizon. *Clin. Orthop. Relat. Res.*, 466(7):1539–1554, Jul 2008. 7, 8

[49] L. M. Galatz, C. M. Ball, S. A. Teefey, W. D. Middleton, and K. Yamaguchi. The outcome and repair integrity of completely arthroscopically repaired large and massive rotator cuff tears. *J Bone Joint Surg Am*, 86-A(2):219–224, Feb 2004. 8

[50] W. S. Khan, A. Malik, U. G. Longo, and V. Denaro. Editorial: (thematic issue: bench to bedside: ligament and tendon tissue engineering). *Curr Stem Cell Res Ther*, 10(1):2–4, 2015. 8, 9

[51] D. Gaspar, K. Spanoudes, C. Holladay, A. Pandit, and D. Zeugolis. Progress in cell-based therapies for tendon repair. *Adv. Drug Deliv. Rev.*, 84:240–256, Apr 2015. 8

[52] R. Bullough, T. Finnigan, A. Kay, N. Maffulli, and N. R. Forsyth. Tendon repair through stem cell intervention: cellular and molecular approaches. *Disabil Rehabil*, 30(20-22):1746–1751, 2008. 8, 9

[53] P. Zimmet, K. G. Alberti, and J. Shaw. Global and societal implications of the diabetes epidemic. *Nature*, 414(6865):782–787, Dec 2001. 9

[54] Diabetes uk: Facts and stats. `https://www.diabetes.org.uk/Documents/Position%20statements/Diabetes%20UK%20Facts%20and%20Stats_Dec%202015.pdf`. Accessed: 28-11-2016. 9

[55] Diabetes uk: What is diabetes? `https://www.diabetes.org.uk/Guide-to-diabetes/What-is-diabetes/`. Accessed: 28-11-2016. 9

[56] World health organization: Global report on diabetes. geneva, 2016. `http://apps.who.int/iris/bitstream/10665/204871/1/9789241565257_eng.pdf`. Accessed: 28-11-2016. 9

[57] F. Giacco and M. Brownlee. Oxidative stress and diabetic complications. *Circulation research*, 107(9):1058–1070, 2010. 9, 11, 15, 89, 144

[58] D. El-Osta, A.and Brasacchio, D. Yao, A. Pocai, P. L. Jones, R. G. Roeder, M. E. Cooper, and M. Brownlee. Transient high glucose causes persistent epigenetic changes and altered gene expression during subsequent normoglycemia. *The Journal of experimental medicine*, 205(10):2409–2417, 2008. 9, 16, 139, 144

[59] A. El-Osta. Redox mediating epigenetic changes confer metabolic memories. *Circulation research*, 111(3):262–264, 2012. 9, 11

[60] S. T. Keating and A. El-Osta. Epigenetic changes in diabetes. *Clinical genetics*, 84(1):1–10, 2013. 9

[61] Diabetes.org.uk. Diabetes in the uk 2012. key statistics on diabetes. 2012. 10

[62] International diabetes federation: Diabetes facts and figures. `http://www.idf.org/about-diabetes/facts-figures`. Accessed: 28-11-2016. 10

[63] D. Daneman. Type 1 diabetes. *The Lancet*, 367(9513):847–858, 2006. 10

[64] L. Pirola, A. Balcerczyk, J. Okabe, and A. El-Osta. Epigenetic phenomena linked to diabetic complications. *Nat Rev Endocrinol*, 6(12):665–75, 2010. 10, 144

[65] M. Abate, C. Schiavone, V. Salini, and I. Andia. Occurrence of tendon pathologies in metabolic disorders. *Rheumatology*, 52(4):599–608, 2013. 10, 17, 18, 19

[66] M. Brownlee. Biochemistry and molecular cell biology of diabetic complications. *Nature*, 414(6865):813–820, 2001. 12, 15

[67] National institute on alcohol abuse and alcoholism. energy availability and alcoholrelated liver pathology. october 2004. `https://pubs.niaaa.nih.gov/publications/arh27-4/291-299.htm`. Accessed: 30-3-2017. 12

[68] N. Calcutt, M. Cooper, T. Kern, and A. Schmidt. Therapies for hyperglycaemia-induced diabetic complications: from animal models to clinical trials. *Nature Reviews Drug Discovery*, (8):417–430, 2009. 11, 13

[69] M. J. Sheetz and G. L. King. Molecular understanding of hyperglycemia's adverse effects for diabetic complications. *Jama*, 288(20):2579–2588, 2002. 11, 142

[70] D. Harman. The aging process. *Proc. Natl. Acad. Sci. U.S.A.*, 78(11):7124–7128, Nov 1981. 13

[71] T. Finkel and N. J. Holbrook. Oxidants, oxidative stress and the biology of ageing. *Nature*, 408(6809):239–247, Nov 2000. 13, 15

[72] T. Finkel. Oxidant signals and oxidative stress. *Curr. Opin. Cell Biol.*, 15(2):247–254, Apr 2003. 13, 15, 89

[73] P. Charitou and B. M. Burgering. Forkhead box(o) in control of reactive oxygen species and genomic stability to ensure healthy lifespan. *Antioxid Redox Signal*, 19(12):1400–19, 2013. 13, 77

[74] J. J. Gille and H. Joenje. Cell culture models for oxidative stress: superoxide and hydrogen peroxide versus normobaric hyperoxia. *Mutat. Res.*, 275(3-6):405–414, Sep 1992. 13, 89, 90, 131, 132

[75] I. N. Zelko, T. J. Mariani, and R. J. Folz. Superoxide dismutase multigene family: a comparison of the CuZn-SOD (SOD1), Mn-SOD (SOD2), and EC-SOD (SOD3) gene structures, evolution, and expression. *Free Radic. Biol. Med.*, 33(3):337–349, Aug 2002. 13, 15, 16, 66, 135

[76] B. Halliwell and M. Whiteman. Measuring reactive species and oxidative damage in vivo and in cell culture: how should you do it and what do the results mean? *Br. J. Pharmacol.*, 142(2):231–255, May 2004. 14

[77] Biotek.com. an introduction to reactive oxygen species - measurement of ros in cells. 26 jan 2014. `http://www.biotek.com/resources/articles/reactive-oxygen-species.html`. Accessed: 4-3-2017. 14

[78] B. Halliwell. Reactive species and antioxidants. redox biology is a fundamental theme of aerobic life. *Plant Physiol*, 141(2):312–22, 2006. 13

[79] M. P. Murphy, A. Holmgren, N. G. Larsson, B. Halliwell, C. J. Chang, B. Kalyanaraman, S. G. Rhee, P. J. Thornalley, L. Partridge, D. Gems, T. Nystrom, V. Belousov, P. T. Schumacker, and C. C. Winterbourn. Unraveling the biological roles of reactive oxygen species. *Cell Metab.*, 13(4):361–366, Apr 2011. 13

[80] J. L. Martindale and N. J. Holbrook. Cellular response to oxidative stress: signaling for suicide and survival. *J. Cell. Physiol.*, 192(1):1–15, Jul 2002. 13

[81] J. S. Johansen, A. K. Harris, D. J. Rychly, and A. Ergul. Oxidative stress and the use of antioxidants in diabetes: linking basic science to clinical practice. *Cardiovasc Diabetol*, 4:5, 2005. 13, 16, 89, 144

[82] J. Chandra, A. Samali, and S. Orrenius. Triggering and modulation of apoptosis by oxidative stress. *Free Radic. Biol. Med.*, 29(3-4):323–333, Aug 2000. 13

[83] D. H. Lee, J. G. Rhee, and Y. J. Lee. Reactive oxygen species up-regulate p53 and Puma; a possible mechanism for apoptosis during combined treatment with TRAIL and wogonin. *Br. J. Pharmacol.*, 157(7):1189–1202, Aug 2009. 13

[84] T. von Zglinicki. Oxidative stress shortens telomeres. *Trends Biochem. Sci.*, 27(7):339–344, Jul 2002. 15

[85] F. Johnson and C. Giulivi. Superoxide dismutases and their impact upon human health. *Mol. Aspects Med.*, 26(4-5):340–352, 2005. 15

[86] I. Giardino, D. Edelstein, and M. Brownlee. Bcl-2 expression or antioxidants prevent hyperglycemia-induced formation of intracellular advanced glycation endproducts in bovine endothelial cells. *Journal of Clinical Investigation*, 97(6):1422, 1996. 15

[87] S. Tonna, A. El-Osta, M. E. Cooper, and C. Tikellis. Metabolic memory and diabetic nephropathy: potential role for epigenetic mechanisms. *Nature Reviews Nephrology*, 6(6):332–341, 2010. 16

[88] F. Liang, S. Kume, and D. Koya. SIRT1 and insulin resistance. *Nat Rev Endocrinol*, 5(7):367–373, Jul 2009. 16, 87

[89] M. A. Ihnat, J. E. Thorpe, C. D. Kamat, C. Szabo, D. E. Green, L. A. Warnke, Z. Lacza, A. Cselenyak, K. Ross, S. Shakir, et al. Reactive oxygen species mediate a cellular memory of high glucose stress signalling. *Diabetologia*, 50(7):1523–1531, 2007. 16, 139

[90] E. Cagliero, W. Apruzzese, G. S. Perlmutter, and D. M. Nathan. Musculoskeletal disorders of the hand and shoulder in patients with diabetes mellitus. *Am. J. Med.*, 112(6):487–490, Apr 2002. 17

[91] W. P. Grant, R. Sullivan, D. E. Sonenshine, M. Adam, J. H. Slusser, K. A. Carson, and A. I. Vinik. Electron microscopic investigation of the effects of diabetes mellitus on the Achilles tendon. *J Foot Ankle Surg*, 36(4):272–278, 1997. 17, 18, 20, 138

[92] L. Smith, S. Burnet, and J. McNeil. Musculoskeletal manifestations of diabetes mellitus. *British journal of sports medicine*, 37(1):30, 2003. 17, 18

[93] L. C. Ramirez and P. Raskin. Diabetic foot tendinopathy: abnormalities in the flexor plantar tendons in patients with diabetes mellitus. *J. Diabetes Complicat.*, 12(6):337–339, 1998. 18

[94] National institute for health and clinical excellence (nice). diabetic foot problems: Inpatient management of diabetic foot problems. 2010. `https://www.nice.org.uk/guidance/cg119/documents/`. Accessed: 5-12-2016. 18

[95] U. G. Longo, F. Franceschi, L. Ruzzini, F. Spiezia, N. Maffulli, and V. Denaro. Higher fasting plasma glucose levels within the normoglycaemic range and rotator cuff tears. *British journal of sports medicine*, 43(4):284–287, 2009. 19

[96] A. J. Fox, A. Bedi, X. H. Deng, L. Ying, P. E. Harris, R. F. Warren, and S. A. Rodeo. Diabetes mellitus alters the mechanical properties of the native tendon in an experimental rat model. *J Orthop Res*, 29(6):880–5, 2011. 19, 143

[97] R. R. de Oliveira, K. D. de Lira, P. V. Silveira, M. P. Coutinho, M. N. Medeiros, M. F. Teixeira, and S. R. de Moraes. Mechanical properties of achilles tendon in rats induced to experimental diabetes. *Ann Biomed Eng*, 39(5):1528–1534, May 2011. 19, 143

[98] N. Chbinou and J. Frenette. Insulin-dependent diabetes impairs the inflammatory response and delays angiogenesis following Achilles tendon injury. *Am. J. Physiol. Regul. Integr. Comp. Physiol.*, 286(5):R952–957, May 2004. 19, 68, 138

[99] A. Bedi, A. J. S. Fox, P. E. Harris, X. Deng, L. Ying, R. F. Warren, and S. A. Rodeo. Diabetes mellitus impairs tendon-bone healing after rotator cuff repair. *Journal of shoulder and elbow surgery*, 19(7):978–988, 2010. 19

[100] A. D. Gonzalez, M. A. Gallant, D. B. Burr, and J. M. Wallace. Multiscale analysis of morphology and mechanics in tail tendon from the ZDSD rat model of type 2 diabetes. *J Biomech*, 47(3):681–686, Feb 2014. 19

[101] O. Egemen, O. Ozkaya, M. B. Ozturk, E. Sen, M. Akan, D. Sakiz, and C. Aygit. The biomechanical and histological effects of diabetes on tendon healing: experimental study in rats. *J Hand Microsurg*, 4(2):60–64, Dec 2012. 19

[102] T. Burner, C. Gohr, E. Mitton-Fitzgerald, and A. K. Rosenthal. Hyperglycemia reduces proteoglycan levels in tendons. *Connect. Tissue Res.*, 53(6):535–541, 2012. 19, 85

[103] G. P. Boivin, E. Y. Elenes, A. K. Schultze, H. Chodavarapu, S. A. Hunter, and K. M. Elased. Biomechanical properties and histology of db/db diabetic mouse Achilles tendon. *Muscles Ligaments Tendons J*, 4(3):280–284, Jul 2014. 19, 138

[104] M. Akturk, S. Karaahmetoglu, M. Kacar, and O. Muftuoglu. Thickness of the supraspinatus and biceps tendons in diabetic patients. *Diabetes care*, 25(2):408–408, 2002. 20

[105] S. de Jonge, R. Rozenberg, B. Vieyra, H. J. Stam, H. J. Aanstoot, H. Weinans, H. T. van Schie, and S. F. Praet. Achilles tendons in people with type 2 diabetes show mildly compromised structure: an ultrasound tissue characterisation study. *Br J Sports Med*, 49(15):995–999, Aug 2015. 20

[106] R. R. De Oliveira, A. Lemos, P. V. de Castro Silveira, R. J. Da Silva, and S. R. A. De Moraes. Alterations of tendons in patients with diabetes mellitus: a systematic review. *Diabetic Medicine*, 28(8):886–895, 2011. 20

[107] S. T. Keating and A. El-Osta. Glycemic memories and the epigenetic component of diabetic nephropathy. *Current diabetes reports*, 13(4):574–581, 2013. 20

[108] M. Althubiti, L. Lezina, S. Carrera, R. Jukes-Jones, S. M. Giblett, A. Antonov, N. Barlev, G. S. Saldanha, C. A. Pritchard, K. Cain, and S. Macip. Characterization of novel markers of senescence and their prognostic potential in cancer. *Cell Death Dis*, 5:e1528, 2014. 20

[109] H. B. Sun, C. Schaniel, D. J. Leong, and J. H. Wang. Biology and mechano-response of tendon cells: Progress overview and perspectives. *J Orthop Res*, 33(6):785–92, 2015. 20

[110] J. Campisi and F. d'Adda di Fagagna. Cellular senescence: when bad things happen to good cells. *Nat Rev Mol Cell Biol*, 8(9):729–40, 2007. 20

[111] M. Muller. Cellular senescence: molecular mechanisms, in vivo significance, and redox considerations. *Antioxid Redox Signal*, 11(1):59–98, 2009. 20, 84

[112] J. M. van Deursen. The role of senescent cells in ageing. *Nature*, 509(7501):439–46, 2014. 20, 57, 115, 135

[113] R. C. Poulsen, A. J. Carr, and P. A. Hulley. Protection against glucocorticoid-induced damage in human tenocytes by modulation of erk, akt, and forkhead signaling. *Endocrinology*, 152(2):503–514, 2011. 23

[114] M. Liang, H. R. Cornell, N. Zargar Baboldashti, M. S. Thompson, A. J. Carr, and P. A. Hulley. Regulation of hypoxia-induced cell death in human tenocytes. *Advances in orthopedics*, 2012, 2012. 24, 83

[115] World Health Organization et al. Definition and diagnosis of diabetes mellitus and intermediate hyperglycaemia: report of a who/idf consultation. 2006. 25

[116] Diabetes.co.uk. blood sugar level ranges. 2016. `http://www.diabetes.co.uk/diabetes_care/blood-sugar-level-ranges.html`. Accessed: 29-12-2016. 25, 83

[117] K. J. Livak and T. D. Schmittgen. Analysis of relative gene expression data using real-time quantitative pcr and the 2(-delta delta c(t)) method. *Methods*, 25(4):402–8, 2001. 30

[118] R. W. Farndale, C. A. Sayers, and A. J. Barrett. A direct spectrophotometric microassay for sulfated glycosaminoglycans in cartilage cultures. *Connective tissue research*, 9(4):247–248, 1982. 32

[119] R. W. Farndale, D. J. Buttle, and A. J. Barrett. Improved quantitation and discrimination of sulphated glycosaminoglycans by use of dimethylmethylene blue. *Biochimica et Biophysica Acta (BBA)-General Subjects*, 883(2):173–177, 1986. 32

[120] M. P. Barde and P. J. Barde. What to use to express the variability of data: Standard deviation or standard error of mean? *Perspect Clin Res*, 3(3):113–116, Jul 2012. 38

[121] M. Abercrombie and J. E. Heaysman. Observations on the social behaviour of cells in tissue culture. I. Speed of movement of chick heart fibroblasts in relation to their mutual contacts. *Exp. Cell Res.*, 5(1):111–131, Sep 1953. 41

[122] M. Abercrombie and J. E. Heaysman. Observations on the social behaviour of cells in tissue culture. II. Monolayering of fibroblasts. *Exp. Cell Res.*, 6(2):293–306, May 1954. 41

[123] S. Chen and D. E. Birk. The regulatory roles of small leucine-rich proteoglycans in extracellular matrix assembly. *FEBS J.*, 280(10):2120–2137, May 2013. 63

[124] S. C. Juneja and C. Veillette. Defects in tendon, ligament, and enthesis in response to genetic alterations in key proteoglycans and glycoproteins: a review. *Arthritis*, 2013:154812, 2013. 63

[125] L. Xu, Z. Li, S. Y. Liu, S. Y. Xu, and G. X. Ni. Asporin and osteoarthritis. *Osteoarthr. Cartil.*, 23(6):933–939, Jun 2015. 63

[126] D. Lee, J. S. Kim, H. K. Cho, and J. H. Lee. The effects of glucose on the expression of MMP and TIMP in cultured retinal pigment epithelial cells. *Korean J Ophthalmol*, 18(2):132–140, Dec 2004. 64, 85, 109

[127] F. M. Ho, S. H. Liu, W. W. Lin, and C. S. Liau. Opposite effects of high glucose on MMP-2 and TIMP-2 in human endothelial cells. *J. Cell. Biochem.*, 101(2):442–450, May 2007. 64, 85, 109

[128] S. J. Lee, S. S. Bae, K. H. Kim, W. S. Lee, B. Y. Rhim, K. W. Hong, and C. D. Kim. High glucose enhances MMP-2 production in adventitial fibroblasts via Akt1-dependent NF-kappaB pathway. *FEBS Lett.*, 581(22):4189–4194, Sep 2007. 64, 109

[129] H. L. Hsieh, C. C. Lin, L. D. Hsiao, and C. M. Yang. High glucose induces reactive oxygen species-dependent matrix metalloproteinase-9 expression and cell migration in brain astrocytes. *Mol. Neurobiol.*, 48(3):601–614, Dec 2013. 64, 109

[130] W. Tsai, F. Liang, J. Cheng, L. Lin, S. Chang, H. Chen, and J. Pang. High glucose concentration up-regulates the expression of matrix metalloproteinase-9 and -13 in tendon cells. *BMC Musculoskeletal Disorders*, 14(1):1–7, 2013. 64, 85, 109

[131] Y. H. Xuan, B. B. Huang, H. S. Tian, L. S. Chi, Y. M. Duan, X. Wang, Z. X. Zhu, W. H. Cai, Y. T. Zhu, T. M. Wei, H. B. Ye, W. T. Cong, and L. T. Jin. High-glucose inhibits human fibroblast cell migration in wound healing via repression of bFGF-regulating JNK phosphorylation. *PLoS ONE*, 9(9):e108182, 2014. 68

[132] P. Pacher, I. G. Obrosova, J. G. Mabley, and C. Szabo. Role of nitrosative stress and peroxynitrite in the pathogenesis of diabetic complications. Emerging new therapeutical strategies. *Curr. Med. Chem.*, 12(3):267–275, 2005. 75

[133] E. M. Horvath, R. Magenheim, E. Kugler, G. Vacz, A. Szigethy, F. Levardi, M. Kollai, C. Szabo, and Z. Lacza. Nitrative stress and poly(ADP-ribose) polymerase activation in healthy and gestational diabetic pregnancies. *Diabetologia*, 52(9):1935–1943, Sep 2009. 75

[134] J. R. Lancaster. Nitroxidative, nitrosative, and nitrative stress: kinetic predictions of reactive nitrogen species chemistry under biological conditions. *Chem. Res. Toxicol.*, 19(9):1160–1174, Sep 2006. 75

[135] A. Ceriello, F. Mercuri, L. Quagliaro, R. Assaloni, E. Motz, L. Tonutti, and C. Taboga. Detection of nitrotyrosine in the diabetic plasma: evidence of oxidative stress. *Diabetologia*, 44(7):834–838, Jul 2001. 75

[136] V. R. Drel and N. Sybirna. Protective effects of polyphenolics in red wine on diabetes associated oxidative/nitrative stress in streptozotocin-diabetic rats. *Cell Biol. Int.*, 34(12):1147–1153, Dec 2010. 75

[137] D. R. Calnan and A. Brunet. The foxo code. *Oncogene*, 27(16):2276–88, 2008. 77, 87

[138] A. Eijkelenboom and B. M. Burgering. Foxos: signalling integrators for homeostasis maintenance. *Nat Rev Mol Cell Biol*, 14(2):83–97, 2013. 77, 87

[139] A. Brunet, L. B. Sweeney, J. F. Sturgill, K. F. Chua, P. L. Greer, Y. Lin, H. Tran, S. E. Ross, R. Mostoslavsky, H. Y. Cohen, L. S. Hu, H. L. Cheng, M. P. Jedrychowski, S. P. Gygi, D. A. Sinclair, F. W. Alt, and M. E. Greenberg. Stress-dependent regulation of FOXO transcription factors by the SIRT1 deacetylase. *Science*, 303(5666):2011–2015, Mar 2004. 77, 87

[140] R. C. Poulsen, H. J. Knowles, A. J. Carr, and P. A. Hulley. Cell differentiation versus cell death: extracellular glucose is a key determinant of cell fate following oxidative stress exposure. *Cell death & disease*, 5(2):e1074, 2014. 77, 85, 87, 132

[141] L. Yao, C. S. Bestwick, L. A. Bestwick, N. Maffulli, and R. M. Aspden. Phenotypic drift in human tenocyte culture. *Tissue engineering*, 12(7):1843–1849, 2006. 83, 86

[142] A. D. Mazzocca, D. Chowaniec, M. B. McCarthy, K. Beitzel, M. P. Cote, W. McKinnon, and R. Arciero. In vitro changes in human tenocyte cultures obtained from proximal biceps tendon: multiple passages result in changes in routine cell markers. *Knee Surg Sports Traumatol Arthrosc*, 20(9):1666–1672, Sep 2012. 83, 86

[143] F. Debacq-Chainiaux, J. D. Erusalimsky, J. Campisi, and O. Toussaint. Protocols to detect senescence-associated beta-galactosidase (SA-betagal) activity, a biomarker of senescent cells in culture and in vivo. *Nat Protoc*, 4(12):1798–1806, 2009. 84

[144] A. Akbarzadeh, D. Norouzian, M. R. Mehrabi, S. h. Jamshidi, A. Farhangi, A. A. Verdi, S. M. Mofidian, and B. L. Rad. Induction of diabetes by Streptozotocin in rats. *Indian J Clin Biochem*, 22(2):60–64, Sep 2007. 87

[145] G. J. Kops, T. B. Dansen, P. E. Polderman, I. Saarloos, K. W. Wirtz, P. J. Coffer, T. T. Huang, J. L. Bos, R. H. Medema, and B. M. Burgering. Forkhead transcription factor FOXO3a protects quiescent cells from oxidative stress. *Nature*, 419(6904):316–321, Sep 2002. 87

[146] S. Nemoto and T. Finkel. Redox regulation of forkhead proteins through a p66shc-dependent signaling pathway. *Science*, 295(5564):2450–2452, Mar 2002. 87

[147] J. Nakae, W. H. Biggs, T. Kitamura, W. K. Cavenee, C. V. Wright, K. C. Arden, and D. Accili. Regulation of insulin action and pancreatic beta-cell function by

mutated alleles of the gene encoding forkhead transcription factor Foxo1. *Nat. Genet.*, 32(2):245–253, Oct 2002. 87

[148] A. van der Horst and B. M. Burgering. Stressing the role of FoxO proteins in lifespan and disease. *Nat. Rev. Mol. Cell Biol.*, 8(6):440–450, Jun 2007. 87

[149] H. Huang and D. J. Tindall. Dynamic FoxO transcription factors. *J. Cell. Sci.*, 120(Pt 15):2479–2487, Aug 2007. 87

[150] M. Kitada and D. Koya. SIRT1 in Type 2 Diabetes: Mechanisms and Therapeutic Potential. *Diabetes Metab J*, 37(5):315–325, Oct 2013. 87

[151] A. C. Maritim, R. A. Sanders, and J. B. Watkins. Diabetes, oxidative stress, and antioxidants: a review. *J. Biochem. Mol. Toxicol.*, 17(1):24–38, 2003. 89

[152] M. Brownlee. The pathobiology of diabetic complications: a unifying mechanism. *Diabetes*, 54(6):1615–1625, 2005. 89

[153] E. Wright, J. L. Scism-Bacon, and L. C. Glass. Oxidative stress in type 2 diabetes: the role of fasting and postprandial glycaemia. *Int. J. Clin. Pract.*, 60(3):308–314, Mar 2006. 89

[154] E. A. Veal, A. M. Day, and B. A. Morgan. Hydrogen peroxide sensing and signaling. *Mol Cell*, 26(1):1–14, 2007. 89, 131, 134, 144

[155] M. Giorgio, M. Trinei, E. Migliaccio, and P. G. Pelicci. Hydrogen peroxide: a metabolic by-product or a common mediator of ageing signals? *Nat. Rev. Mol. Cell Biol.*, 8(9):722–728, Sep 2007. 89

[156] J. Foreman, V. Demidchik, J. H. Bothwell, P. Mylona, H. Miedema, M. A. Torres, P. Linstead, S. Costa, C. Brownlee, J. D. Jones, J. M. Davies, and L. Dolan. Reactive oxygen species produced by NADPH oxidase regulate plant cell growth. *Nature*, 422(6930):442–446, Mar 2003. 89

[157] T. S. Gechev and J. Hille. Hydrogen peroxide as a signal controlling plant programmed cell death. *J. Cell Biol.*, 168(1):17–20, Jan 2005. 89

[158] S. A. Bustin, V. Benes, J. A. Garson, J. Hellemans, J. Huggett, M. Kubista, R. Mueller, T. Nolan, M. W. Pfaffl, G. L. Shipley, J. Vandesompele, and C. T. Wittwer. The MIQE guidelines: minimum information for publication of quantitative real-time PCR experiments. *Clin. Chem.*, 55(4):611–622, Apr 2009. 110

[159] R. Bavarsad Shahripour, M. R. Harrigan, and A. V. Alexandrov. N-acetylcysteine (NAC) in neurological disorders: mechanisms of action and therapeutic opportunities. *Brain Behav*, 4(2):108–122, Mar 2014. 117, 135, 136

[160] C. A. de la Lastra and I. Villegas. Resveratrol as an antioxidant and pro-oxidant agent: mechanisms and clinical implications. *Biochem. Soc. Trans.*, 35(Pt 5):1156–1160, Nov 2007. 117, 137

[161] D. H. Lee, T. R. O'Connor, and G. P. Pfeifer. Oxidative DNA damage induced by copper and hydrogen peroxide promotes CG–>TT tandem mutations at methylated CpG dinucleotides in nucleotide excision repair-deficient cells. *Nucleic Acids Res.*, 30(16):3566–3573, Aug 2002. 131

[162] G. P. Bienert, J. K. Schjoerring, and T. P. Jahn. Membrane transport of hydrogen peroxide. *Biochim Biophys Acta*, 1758(8):994–1003, 2006. 131

[163] M. H. Choi, I. K. Lee, G. W. Kim, B. U. Kim, Y. H. Han, D. Y. Yu, H. S. Park, K. Y. Kim, J. S. Lee, C. Choi, Y. S. Bae, B. I. Lee, S. G. Rhee, and S. W. Kang. Regulation of PDGF signalling and vascular remodelling by peroxiredoxin II. *Nature*, 435(7040):347–353, May 2005. 131, 144

[164] A. R. Giandomenico, G. E. Cerniglia, J. E. Biaglow, C. W. Stevens, and C. J. Koch. The importance of sodium pyruvate in assessing damage produced by hydrogen peroxide. *Free Radic. Biol. Med.*, 23(3):426–434, 1997. 132

[165] A. DeCoux, M. L. Lindsey, F. Villarreal, R. A. Garcia, and R. Schulz. Myocardial matrix metalloproteinase-2: inside out and upside down. *J Mol Cell Cardiol*, 77:64–72, 2014. 133

[166] D. A. Siwik, P. J. Pagano, and W. S. Colucci. Oxidative stress regulates collagen synthesis and matrix metalloproteinase activity in cardiac fibroblasts. *Am. J. Physiol., Cell Physiol.*, 280(1):53–60, Jan 2001. 133

[167] H. Y. Yoo, M. S. Chang, and H. M. Rho. The activation of the rat copper/zinc superoxide dismutase gene by hydrogen peroxide through the hydrogen peroxide-responsive element and by paraquat and heat shock through the same heat shock element. *J. Biol. Chem.*, 274(34):23887–23892, Aug 1999. 134

[168] J. R. Dorr, Y. Yu, M. Milanovic, G. Beuster, C. Zasada, J. H. Dabritz, J. Lisec, D. Lenze, A. Gerhardt, K. Schleicher, S. Kratzat, B. Purfurst, S. Walenta, W. Mueller-Klieser, M. Graler, M. Hummel, U. Keller, A. K. Buck, B. Dorken, L. Willmitzer, M. Reimann, S. Kempa, S. Lee, and C. A. Schmitt. Synthetic lethal metabolic targeting of cellular senescence in cancer therapy. *Nature*, 501(7467):421–425, Sep 2013. 135

[169] H. Kahraman, E. Kurutas, M. Tokur, S. Bozkurt, H. Ciralik, B. Kabakci, N. Koksal, and V. Balkan. Protective effects of erythropoietin and n-acetylcysteine on methotrexate-induced lung injury in rats. *Balkan Med J*, 30(1):99–104, 2013. 136

[170] S. Akbulut, H. Elbe, C. Eris, Z. Dogan, G. Toprak, E. Otan, E. Erdemli, and Y. Turkoz. Cytoprotective effects of amifostine, ascorbic acid and n-acetylcysteine against methotrexate-induced hepatotoxicity in rats. *World J Gastroenterol*, 20(29):10158–65, 2014. 136, 137

[171] B. Halliwell. Vitamin C: antioxidant or pro-oxidant in vivo? *Free Radic. Res.*, 25(5):439–454, Nov 1996. 136

[172] H. C. Lee, S. H. Sheu, I. H. Liu, C. C. Lee, C. C. Hsieh, H. W. Yen, W. T. Lai, and J. G. Chang. Impact of short-duration administration of n-acetylcysteine, probucol and ascorbic acid on contrast-induced cytotoxicity. *J Nephrol*, 25(1):56–62, 2012. 137

[173] H. Zhang, B. Morgan, B. J. Potter, L. Ma, K. C. Dellsperger, Z. Ungvari, and C. Zhang. Resveratrol improves left ventricular diastolic relaxation in type 2 diabetes by inhibiting oxidative/nitrative stress: in vivo demonstration with magnetic

resonance imaging. *Am. J. Physiol. Heart Circ. Physiol.*, 299(4):H985–994, Oct 2010. 137

[174] H. X. Zhang, G. L. Duan, C. N. Wang, Y. Q. Zhang, X. Y. Zhu, and Y. J. Liu. Protective effect of resveratrol against endotoxemia-induced lung injury involves the reduction of oxidative/nitrative stress. *Pulm Pharmacol Ther*, 27(2):150–155, Apr 2014. 137

[175] K. T. Howitz, K. J. Bitterman, H. Y. Cohen, D. W. Lamming, S. Lavu, J. G. Wood, R. E. Zipkin, P. Chung, A. Kisielewski, L. L. Zhang, B. Scherer, and D. A. Sinclair. Small molecule activators of sirtuins extend Saccharomyces cerevisiae lifespan. *Nature*, 425(6954):191–196, Sep 2003. 137

[176] L. Rivera, R. Moron, A. Zarzuelo, and M. Galisteo. Long-term resveratrol administration reduces metabolic disturbances and lowers blood pressure in obese zucker rats. *Biochem Pharmacol*, 77(6):1053–63, 2009. 137

[177] H. Zhang, J. Zhang, Z. Ungvari, and C. Zhang. Resveratrol improves endothelial function: role of tnf-alpha and vascular oxidative stress. *Arterioscler Thromb Vasc Biol*, 29(8):1164–71, 2009. 137

[178] K. Zeytin, N. S. Ciloglu, F. Ates, F. Vardar Aker, and F. Ercan. The effects of resveratrol on tendon healing of diabetic rats. *Acta Orthop Traumatol Turc*, 48(3):355–362, 2014. 137, 138, 141

[179] D. Bonnefont-Rousselot. Resveratrol and cardiovascular diseases. *Nutrients*, 8(5), 2016. 137

[180] P. J. Kim, J. S. Steinberg, M. Kikuchi, and C. E. Attinger. Tibialis anterior tendon lengthening: Adjunctive treatment of plantar lateral column diabetic foot ulcers. *J Foot Ankle Surg*, 54(4):686–91, 2015. 138

[181] S. Roy, R. Sala, E. Cagliero, and M. Lorenzi. Overexpression of fibronectin induced by diabetes or high glucose: phenomenon with a memory. *Proc. Natl. Acad. Sci. U.S.A.*, 87(1):404–408, Jan 1990. 139

[182] D. Munoz-Espin and M. Serrano. Cellular senescence: from physiology to pathology. *Nat Rev Mol Cell Biol*, 15(7):482–96, 2014. 140

[183] H. K. Heywood, G. Nalesso, D. A. Lee, and F. Dell'accio. Culture expansion in low-glucose conditions preserves chondrocyte differentiation and enhances their subsequent capacity to form cartilage tissue in three-dimensional culture. *Biores Open Access*, 3(1):9–18, 2014. 141

[184] A. Elgawish, M. Glomb, M. Friedlander, and V. M. Monnier. Involvement of hydrogen peroxide in collagen cross-linking by high glucose in vitro and in vivo. *Journal of Biological Chemistry*, 271(22):12964–12971, 1996. 141

[185] C. J. Mentink, M. Hendriks, A. A. Levels, and B. H. Wolffenbuttel. Glucose-mediated cross-linking of collagen in rat tendon and skin. *Clin. Chim. Acta*, 321(1-2):69–76, Jul 2002. 141

[186] R. Singh, A. Barden, T. Mori, and L. Beilin. Advanced glycation end-products: a review. *Diabetologia*, 44(2):129–146, Feb 2001. 141

[187] A. Goldin, J. A. Beckman, A. M. Schmidt, and M. A. Creager. Advanced glycation end products: sparking the development of diabetic vascular injury. *Circulation*, 114(6):597–605, 2006. 141

[188] M. T. Lin and M. F. Beal. Mitochondrial dysfunction and oxidative stress in neurodegenerative diseases. *Nature*, 443(7113):787–795, Oct 2006. 142

[189] B. D. Volper, R. T. Huynh, K. A. Arthur, J. Noone, B. D. Gordon, E. W. Zacherle, E. Munoz, M. A. Srensen, R. B. Svensson, T. L. Broderick, S. P. Magnusson, R. Howden, T. M. Hale, and C. C. Carroll. Influence of acute and chronic streptozotocin-induced diabetes on the rat tendon extracellular matrix and mechanical properties. *Am. J. Physiol. Regul. Integr. Comp. Physiol.*, 309(9):R1135–1143, Nov 2015. 143

[190] D. Ziegler, M. Hanefeld, K. J. Ruhnau, H. Hasche, M. Lobisch, K. Schutte, G. Kerum, and R. Malessa. Treatment of symptomatic diabetic polyneuropathy

with the antioxidant alpha-lipoic acid: a 7-month multicenter randomized controlled trial (ALADIN III Study). ALADIN III Study Group. Alpha-Lipoic Acid in Diabetic Neuropathy. *Diabetes Care*, 22(8):1296–1301, Aug 1999. 144

[191] M. G. Cinar, S. Ulker, G. Alper, and A. Evinc. Effect of dietary vitamin E supplementation on vascular reactivity of thoracic aorta in streptozotocin-diabetic rats. *Pharmacology*, 62(1):56–64, Jan 2001. 144

[192] A. Ceriello and R. Testa. Antioxidant anti-inflammatory treatment in type 2 diabetes. *Diabetes Care*, 32 Suppl 2:S232–6, 2009. 144

[193] B. Lipinski. Hydroxyl radical and its scavengers in health and disease. *Oxid Med Cell Longev*, 2011:809696, 2011. 144

[194] M. E. Cooper and A. El-Osta. Epigenetics: mechanisms and implications for diabetic complications. *Circ. Res.*, 107(12):1403–1413, Dec 2010. 144

[195] A. L. Siebel, A. Z. Fernandez, and A. El-Osta. Glycemic memory associated epigenetic changes. *Biochemical pharmacology*, 80(12):1853–1859, 2010. 144

[196] A. El-Osta. Glycemic memory. *Current opinion in lipidology*, 23(1):24–29, 2012. 144

[197] D. Brasacchio, J. Okabe, C. Tikellis, A. Balcerczyk, P. George, E. K. Baker, A. C. Calkin, M. Brownlee, M. E. Cooper, and A. El-Osta. Hyperglycemia induces a dynamic cooperativity of histone methylase and demethylase enzymes associated with gene-activating epigenetic marks that coexist on the lysine tail. *Diabetes*, 58(5):1229–36, 2009. 144

[198] C. Lehner, R. Gehwolf, A. Wagner, H. Resch, C. Hirzinger, P. Augat, D. Stephan, L. Aigner, F. J. Rivera, H. C. Bauer, and H. Tempfer. Tendons from non-diabetic humans and rats harbor a population of insulin-producing, pancreatic beta cell-like cells. *Horm. Metab. Res.*, 44(7):506–510, Jun 2012. 145